

University of Alberta

**QUANTIFICATION OF RESERVOIR UNCERTAINTY FOR
OPTIMAL DECISION MAKING**

by

Alshehri, Naeem Salem

A thesis submitted to the Faculty of Graduate Studies and Research
in partial fulfillment of the requirements for the degree of

Doctor of Philosophy

in

Petroleum Engineering

Civil and Environmental Engineering

©Alshehri, Naeem Salem

Spring 2010

Edmonton, Alberta

Permission is hereby granted to the University of Alberta Libraries to reproduce single copies of this thesis and to lend or sell such copies for private, scholarly or scientific research purposes only. Where the thesis is converted to, or otherwise made available in digital form, the University of Alberta will advise potential users of the thesis of these terms.

The author reserves all other publication and other rights in association with the copyright in the thesis and, except as herein before provided, neither the thesis nor any substantial portion thereof may be printed or otherwise reproduced in any material form whatsoever without the author's prior written permission.

Examining Committee

Clayton V. Deutsch, Civil and Environmental Engineering

Jose Carlos Cunha, Petrobras America Inc.

Oy Leuangthong, Civil and Environmental Engineering

Hooman Askari-Nasab, Civil and Environmental Engineering

Michael Lipsett, Mechanical Engineering

Ezeddin Shirif, Engineering and Applied Science, University of Regina

To my mom: your love, pray, and encouragement helped me to find my way.

To my father: Thanks a lot for giving me the courage and strength to set and reach goals and providing a better life for me. I wish that you were here to see your eyes. I miss you so much.

To my wife, Wasmia: your patience, encouragement, and love mean the world to me. Your presence in my life means more than anything.

To my daughter Sadeem, my son Rakan, and my son Bassam: you are a constant source of joy and happiness in my life and with you, all is possible

ABSTRACT

A reliable estimate of the amount of oil or gas in a reservoir is required for development decisions. Uncertainty in reserve estimates affects resource/reserve classification, investment decisions, and development decisions. There is a need to make the best decisions with an appropriate level of technical analysis considering all available data. Current methods of estimating resource uncertainty use spreadsheets or Monte Carlo simulation software with specified probability distributions for each variable. 3-D models may be constructed, but they rarely consider uncertainty in all variables. This research develops an appropriate 2-D model of heterogeneity and uncertainty by integrating 2-D model methodology to account for parameter uncertainty in the mean, which is of primary importance in the input histograms. This research improves reserve evaluation in the presence of geologic uncertainty. Guidelines are developed to: a) select the best modeling scale for making decisions by comparing 2-D vs. 0-D and 3-D models, b) understand parameters that play a key role in reserve estimates, c) investigate how to reduce uncertainties, and d) show the importance of accounting for parameter uncertainty in reserves assessment to get fair global uncertainty by comparing results of Hydrocarbon Initially-in-Place (HIIP) with/without parameter uncertainty. The parameters addressed in this research are those required in the assessment of uncertainty including statistical and geological parameters. This research shows that fixed parameters seriously underestimate the actual uncertainty in resources. A complete setup of

methodology for the assessment of uncertainty in the structural surfaces of a reservoir, fluid contacts levels, and petrophysical properties is developed with accounting for parameter uncertainty in order to get fair global uncertainty. Parameter uncertainty can be quantified by several approaches such as the conventional bootstrap (BS), spatial bootstrap (SBS), and conditional-finite-domain (CFD). Real data from a large North Sea reservoir dataset is used to compare those approaches. The CFD approach produced more realistic uncertainty in distributions of the HIIP than those obtained from the BS or SBS approaches. 0-D modeling was used for estimating uncertainty in HIIP with different source of thickness. 2-D is based on geological mapping and can be presented in 2-D maps and checked locally.

Acknowledgments

I would like to express my deep gratitude and appreciation to Dr. Clayton V. Deutsch for being an excellent co-supervisor and outstanding professor, for giving me the chance to work on a research of parameter uncertainty quantification, and for his constant guidance and supervision of this research work. Without his guidance, the dissertation would not exist.

I would like to thank Dr. J.C. Cunha for being my co-supervisor and for his time, encouragement, and support, especially in the first two years of my program. I would also like to thank my committee members Dr. Hooman Askari-Nasab, Dr. Oy Leuangthong, Dr. Micael Lipsett, and Dr. Ezeddin Shirif, for their time and effort in reviewing this work.

I must also thank all the students of Centre for Computational Geostatistics for their friendship. I want to thank Saudi Aramco who grant me the permission and support me to pursue my education. Finally, I thank everyone supported me along the way.

Table of Contents

1. Introduction	1
1.1. Overview	2
1.1.1. Gross Rock Volume (GRV)	2
1.1.2. Net-to-Gross (NTG)	4
1.1.3. Porosity (ϕ)	5
1.1.4. Residual Saturation (S_w)	5
1.1.5. Formation Volume Factor (B_o)	5
1.2. Problem Statement	6
1.3. Literature Review	7
1.4. Dissertation Outline	9
2. Hierarchical Reservoir Modeling and Uncertainty Quantification ...	10
2.1. 0-D Modeling	10
2.2. 2-D Modeling	11
2.3. 3-D Modeling	12
2.4. Remarks	13
3. Parameter Uncertainty	15
3.1. Bootstrap	15
3.2. Spatial Bootstrap	17
3.3. Conditional Finite Domain	20
3.4. Remarks	24
4. Uncertainty Management	25
4.1. Presenting and Understanding Uncertainty	26
4.1.1. Distribution and Quantiles	27
4.1.2. Sensitivity Analysis	28
4.1.3. Tornado Chart and Spider Plot	28
4.1.4. Merging Uncertainty	29
4.1.5. Local Uncertainty vs. Global Uncertainty	30
4.2. Decision Making in Presence of Uncertainty	31
4.2.1. Robust Decisions	32
4.2.2. Decide to Reduce Uncertainty	32
4.2.3. Value of Information	32
4.2.4. Transferring Uncertainty Through Economics/ Performance Forecasting	33
4.2.5. Design for Fixed Production Rate	34
5. Methodology	35
5.1. Simulating Realizations without Parameter Uncertainty	36
5.1.1. Sequential Gaussian Simulation (SGS)	37

5.1.2.	Monte Carlo Simulation (MCS)	41
5.1.3.	Cosimulation with Super Secondary Data	43
5.2.	Simulating Realizations with Parameter Uncertainty	44
5.2.1.	Multivariate Parameter Uncertainty (MVPU)	45
5.2.2.	Sequential Gaussian Simulation (SGS) with Parameter Uncertainty	48
5.2.3.	Monte Carlo Simulation (MCS)	51
5.2.4.	Cosimulation with Super Secondary Data with Parameter Uncertainty	52
5.3.	Work Flow	55
6.	Case Study	66
6.1.	Input Data	66
6.2.	HIIP without Parameter Uncertainty	79
6.2.1.	HIIP with Uncertainty in Structural Surfaces	79
6.2.2.	HIIP with Uncertainty in Fluid Contacts Level	85
6.2.3.	HIIP with Uncertainty in Petrophysical Properties	85
6.2.4.	HIIP with Full Uncertainty	91
6.3.	HIIP with Parameter Uncertainty	92
6.3.1.	Parameter Uncertainty Distributions	92
6.3.2.	HIIP with Uncertainty in Structural Surfaces	102
6.3.3.	HIIP with Uncertainty in Fluid Contacts Level	107
6.3.4.	HIIP with Uncertainty in Petrophysical Properties	108
6.3.5.	HIIP with Full Uncertainty	113
6.3.6.	HIIP with Uncertainty in Petrophysical Properties Using High Variogram Ranges	116
6.3.7.	HIIP with Full Uncertainty Using High Variogram Ranges	120
6.4.	Comparing Results and Discussion	120
6.4.1.	Comparing Uncertainty Effects of Individual Parameters in Each Scenario	124
6.4.2.	Comparing Effects of Uncertainty in Individual Parameters from Different Scenarios	133
6.4.3.	Comparing Effects of Full Parameter Uncertainty Using Different Approaches	142
7.	2-D vs. 0-D and 3-D Modeling	147
7.1.	Comparison between 2-D and 0-D Modeling	147
7.1.1.	0-D Modeling with Thickness Data obtained from Seismic	148
7.1.2.	0-D Modeling with Thickness Data obtained from Well Logs	153
7.2.	Comparison between 2-D and 3-D Modeling	159
8.	Conclusions and Future Work	165
8.1.	Summary of Contributions	165
8.2.	Future Work	169

Bibliography	170
Appendix A	174
Appendix B	180
Appendix C	182

LIST OF TABLES

Table 2-1: Hierarchical-Geostatistical models and their application	11
Table 2-2: Hierarchical-Geostatistical modeling comparison	14
Table 4-1: A schematic to calculate HIIP uncertainty	30
Table 5-1: Techniques for sampling realizations of HIIP	36
Table 6-1: Summary of reservoir grids	67
Table 6-2: Summary of well locations, depths of top structures, and thicknesses of H1 and H2 layers	73
Table 6-3: Summary of thickness, net pay, net-to-gross, and average porosity	75
Table 6-4: Comparison of parameter uncertainty approaches	102
Table 6-5: Statistical analysis for all HIIP distributions	123
Table 6-6: Order of parameters affecting HIIP distribution	132
Table 6-7: Order of parameter uncertainty approaches affecting HIIP uncertainty	141

LIST OF FIGURES

Figure 1-1:	The components of the hydrocarbon resource base	3
Figure 1-2:	Reservoir cross-section	3
Figure 3-1:	Configuring new data combinations in CFD approach	21
Figure 3-2:	Schematic representation of the calculations performed in one step of the CFD algorithm	22
Figure 4-1:	Terms relating to reserves uncertainty	27
Figure 5-1:	Uncertainty in surfaces and layer thickness without parameter uncertainty	39
Figure 5-2:	Uncertainty in fluid contacts levels without parameter uncertainty	42
Figure 5-3:	Uncertainty in surfaces and layer thickness with parameter uncertainty	49
Figure 5-4:	Uncertainty in fluid contacts levels with parameter uncertainty	51
Figure 5-5:	Work Flow 5.1: Quantifying HIIP uncertainty without parameter uncertainty in The Mean	56
Figure 5-6:	Work Flow 5.2: Sampling realizations for structural surfaces without parameter uncertainty	57
Figure 5-7:	Work Flow 5.3: Sampling realizations for fluid contacts levels without parameter uncertainty	58
Figure 5-8:	Work Flow 5.4: Sampling realizations for petrophysical properties without parameter uncertainty	59

Figure 5-9:	Work Flow 5.5: Quantifying HIIP uncertainty with parameter uncertainty	60
Figure 5-10:	Work Flow 5.6: Multivariate Parameter Uncertainty	61
Figure 5-11:	Work Flow 5.7: Sampling realizations for structural surfaces with parameter uncertainty	62
Figure 5-12:	Work Flow 5.8: Sampling realizations for fluid contacts levels with parameter uncertainty	63
Figure 5-13:	Work Flow 5.9: Preparing different reference distributions by shifting the original data	64
Figure 5-14:	Work Flow 5.10: Sampling realizations for petrophysical properties with parameter uncertainty	65
Figure 6-1:	2D map view of top surface of H1 layer in Hekla field	67
Figure 6-2:	3D map view of H1 layer top structure in Hekla field	68
Figure 6-3:	Contour map of H1 layer depth in Hekla field	68
Figure 6-4:	Contour map of H2 layer depth in Hekla field	69
Figure 6-5:	Contour map of H1 layer thickness in Hekla field	69
Figure 6-6:	Contour map of H2 layer thickness in Hekla field	70
Figure 6-7:	Cross sectional views along Y-axes at different X values ...	71
Figure 6-8:	Cross sectional views along X-axes at different Y values ...	72
Figure 6-9:	Histograms for surface structure depths	74
Figure 6-10:	Histograms of NTG and porosity from well logs	75
Figure 6-11:	Net pay data at well locations	76
Figure 6-12:	Net-to-gross data at well locations	76

Figure 6-13: Porosity data at well locations	77
Figure 6-14: Correlation coefficient matrix for some parameters in the two layers	78
Figure 6-15: Case-1: Experimental variograms and best fitted model for top surface of H1 layer	80
Figure 6-16: Case-1: The effect of uncertainty in the top and bottom surfaces on HIIP without parameter uncertainty	81
Figure 6-17: Case-2: Experimental variograms for thickness of H1 layer	82
Figure 6-18: Case-2: The effect of uncertainty in the H1 layer thickness on HIIP without parameter uncertainty	83
Figure 6-19: Case-3: Experimental variograms and best fitted model for H2 layer thickness	84
Figure 6-20: Case-3: The effect of uncertainty in the H2 layer thickness on HIIP without parameter uncertainty	84
Figure 6-21: Case-4: The effect of uncertainty in the OWC on HIIP without parameter uncertainty	85
Figure 6-22: Case-5: Experimental variograms and best fitted model for NTG of H1 layer	86
Figure 6-23: Case-7: Experimental variograms and best fitted model for porosity of H1 layer	87
Figure 6-24: Case-5: The effect of uncertainty in the H1 layer NTG on the HIIP without parameter uncertainty	88
Figure 6-25: Case-7: The effect of uncertainty in the H1 layer porosity on the HIIP without parameter uncertainty	88
Figure 6-26: Case-6: Experimental variograms for NTG of H2 Layer ...	89

Figure 6-27: Case-8: Experimental variograms and best fitted model for porosity of H2 Layer	90
Figure 6-28: Case-6: The effect of uncertainty in the H2 layer NTG on the HIIP without parameter uncertainty	90
Figure 6-29: Case-8: The effect of uncertainty in the H2 layer porosity on the HIIP without parameter uncertainty	91
Figure 6-30: Case-9: The effect of uncertainty in all variables on the HIIP without parameter uncertainty	92
Figure 6-31: Case-1: Parameter uncertainty distributions for H1 layer top surface	93
Figure 6-32: Case-2: Parameter uncertainty distributions for H1 layer thickness	94
Figure 6-33: Case-3: Parameter uncertainty distributions for H2 layer thickness	95
Figure 6-34: Case-5: Parameter uncertainty distributions for H1 layer NTG	96
Figure 6-35: Case-6: Parameter uncertainty distributions for H2 layer NTG	97
Figure 6-36: Case-7: Parameter uncertainty distributions for H1 layer porosity	98
Figure 6-37: Case-8: Parameter uncertainty distributions for H2 layer porosity	99
Figure 6-38: Cases 5 & 6: Parameter uncertainty quantification with high arbitrary range	100
Figure 6-39: Cases 7 & 8: Parameter uncertainty quantification with high arbitrary range	101
Figure 6-40: Case-1: The effect of uncertainty in the top and bottom surfaces on the HIIP with parameter uncertainty	104

Figure 6-41: Case 2: The effect of uncertainty in the H1 layer thickness on the HIIP with parameter uncertainty	105
Figure 6-42: Case-3: The effect of uncertainty in the H2 layer thickness on the HIIP with parameter uncertainty	106
Figure 6-43: Case-4: The effect of uncertainty in the OWC levels on the HIIP with parameter uncertainty	107
Figure 6-44: Case-5: The effect of the uncertainty in the H1 layer NTG on the HIIP with parameter uncertainty	109
Figure 6-45: Case-6: The effect of uncertainty in the H2 layer NTG on the HIIP with parameter uncertainty	110
Figure 6-46: Case-7: The effect of uncertainty in the H1 layer porosity on the HIIP with parameter uncertainty	111
Figure 6-47: Case-8: The effect of uncertainty in the H2 layer porosity on the HIIP with parameter uncertainty	112
Figure 6-48: Correlation coefficient matrix between the mean values obtained from MVPU technique	114
Figure 6-49: Case-9: The effect of full uncertainty in all parameters on the HIIP with parameter uncertainty	115
Figure 6-50: Case-5: The effect of uncertainty in the H1 layer NTG on the HIIP with parameter uncertainty	117
Figure 6-51: Case-6: The effect of uncertainty in the H2 layer NTG on the HIIP with parameter uncertainty	118
Figure 6-52: Case-7: The effect of uncertainty in the H1 layer porosity on the HIIP with parameter uncertainty	119
Figure 6-53: Case-8: The effect of uncertainty in the H2 layer porosity on the HIIP with parameter uncertainty	121

Figure 6-54: Case-9: The effect of full uncertainty in all parameters on the HIIP with parameter uncertainty	122
Figure 6-55: Sensitivity analysis for quantifying HIIP without parameter uncertainty	125
Figure 6-56: Sensitivity analysis for quantifying HIIP with parameter uncertainty using BS approach	126
Figure 6-57: Sensitivity analysis for quantifying HIIP with parameter uncertainty using SBS approach	127
Figure 6-58: Sensitivity analysis for quantifying HIIP with parameter uncertainty using CFD approach	128
Figure 6-59: Sensitivity analysis for quantifying HIIP with parameter uncertainty using BS approach and high arbitrary variogram range	130
Figure 6-60: Sensitivity analysis for quantifying HIIP with parameter uncertainty using SBS approach and high arbitrary variogram range	131
Figure 6-61: Sensitivity analysis for quantifying HIIP with parameter uncertainty using CFD approach and high arbitrary variogram range	132
Figure 6-62: Case-1: Sensitivity analysis to compare different parameter uncertainty approaches with uncertainty in Top/Bottom Structure Surfaces	133
Figure 6-63: Case-2: Sensitivity analysis to compare different parameter uncertainty approaches with uncertainty in the thickness of H1 layer	134
Figure 6-64: Case-3: Sensitivity analysis to compare different parameter uncertainty approaches with uncertainty in the thickness of H1 layer	135

Figure 6-65:	Case-4: Sensitivity analysis to compare effects of OWC in the OOIP with/without parameter uncertainty	136
Figure 6-66:	Case-5: Sensitivity analysis to compare different parameter uncertainty approaches with uncertainty in the NTG of H1 layer	137
Figure 6-67:	Case-6: Sensitivity analysis to compare different parameter uncertainty approaches with uncertainty in the NTG of H2 layer	138
Figure 6-68:	Case-7: Sensitivity analysis to compare different parameter uncertainty approaches with uncertainty in the porosity of H1 layer	139
Figure 6-69:	Case-8: Sensitivity analysis to compare different parameter uncertainty approaches with uncertainty in the porosity of H2 layer	140
Figure 6-70:	Case-9: Sensitivity analysis to compare different parameter uncertainty approaches with full uncertainty	143
Figure 6-71:	Case-9: A comparison of probability distributions for OOIP with full uncertainty using different parameter uncertainty approaches	144
Figure 6-72:	Case-9: A comparison of cumulative probability distributions for OOIP with full uncertainty using different parameter uncertainty approaches	145
Figure 7-1:	Histograms for H1 and H2 layer thickness obtained from Seismic data	149
Figure 7-2:	Parameter Uncertainty in the means of H1 and H2 layer thicknesses obtained from Seismic Data	150
Figure 7-3:	Parameter Uncertainty in the means of NTG and porosity of H1 and H2 layers using BS approach	151

Figure 7-4:	HIIP using 0-D modeling with thickness obtained from seismic data	152
Figure 7-5:	Parameter Uncertainty in Thickness of H1 and H2 layers using BS approach	153
Figure 7-6:	HIIP using 0-D modeling with thickness obtained from well data	155
Figure 7-7:	2-D vs. 0-D modeling: a spider plot and tornado chart ...	156
Figure 7-8:	2-D vs. 0-D modeling: a comparison between the probability and cumulative distribution frequencies of HIIP volumes estimated	157
Figure 7-9:	2-D HIIP Maps for different realizations	158
Figure 7-10:	Proportional Stratigraphic Coordinate	160
Figure 7-11:	3-D Experimental variograms for H1 layer porosity	162
Figure 7-12:	Parameter uncertainty in H1 layer porosity using 3-D modeling	162
Figure 7-13:	2-D vs. 3-D Modeling: Parameter uncertainty in H1 layer porosity	163

Chapter 1

INTRODUCTION

An accurate estimate of the reservoir volume is important for selecting number of wells to be drilled, deciding their locations, and making other reservoir development decisions. The first choice to make in any geostatistical study is the modeling scale. High resolution 3-D models are appropriate for modeling heterogeneity and providing input to flow simulation; however, they cannot be used effectively for uncertainty quantification. Global statistical analysis is appropriate for checking and providing input to parameter uncertainty, but it does not permit uncertainty assessment for specific locations or well patterns. Reserves estimations may be undertaken with 2-D modeling, which can be used in early stages of reservoir development and account for uncertainty in structural surfaces.

Hydrocarbon resources are calculated as the product of gross rock volume, net/gross ratio, porosity, hydrocarbon saturation, and formation volume factor, while hydrocarbon reserves are calculated by multiplying resources volumes by recovery factor. This study focuses more on resource volumes, although the proposed methodology can be extended to estimate the reserve volumes. A single resource/reserve figure (deterministic case) can be computed if the value of each parameter is well known. It is more realistic to represent individual parameters by a range of values, or a probability distribution. This leads to a probability distribution for the resources and improves decisions. It is important to have a narrow and fair estimate of uncertainty at the early stages of field life; otherwise, designed production facilities might be underestimated or overestimated.

The uncertainty is due to limited data, measurement errors, and an imperfect model. Limited data leads to incomplete knowledge of the complex subsurface structure, petrophysical properties, and fluid properties. Errors in the measured data lead to increased error. It is difficult to generate a model that represents the real reservoir. With all these sources of uncertainty, a reasonable numerical model is needed to relate available data and understand the subsurface.

1.1. Overview

For each reservoir, management requires a volumetric estimate of discovered resources (HIIP) calculated based on gross reservoir volume (GRV), petrophysical properties including net-to-gross (NTG), porosity (ϕ), and fluid saturations, and hydrocarbon properties such as formation volume factor. The reserve volumes depend on the economic feasibility and the confidence in the resource. Figure 1.1 shows the components of the hydrocarbon resource base. The structure for this chart comes from SPE publications. The resources can be categorized to undiscovered and discovered resources (HIIP) where the discovered resources can be divided into economically unrecoverable resources and economically recoverable resources (ultimate recovery). The Ultimate Recovery can be classified into three levels, P-90, P-50, and P-10, based on level of confidence. These probability hurdles are applied by both Society of Petroleum Engineers (SPE) and Canadian Institute of Mining, Metallurgy and Petroleum (CIM) (Etherington et. al., 2005).

1.1.1. Gross Rock Volume (GRV)

Reservoirs consist of stratigraphic layers constrained by a top seal. GRV is the volume of a reservoir trapped between stratigraphic surfaces and/or hydrocarbon-water contacts. A reservoir is sometimes bounded by stratigraphic pinch-outs or faults, see Figure 1-2. The uncertainty in GRV is due to sparse well

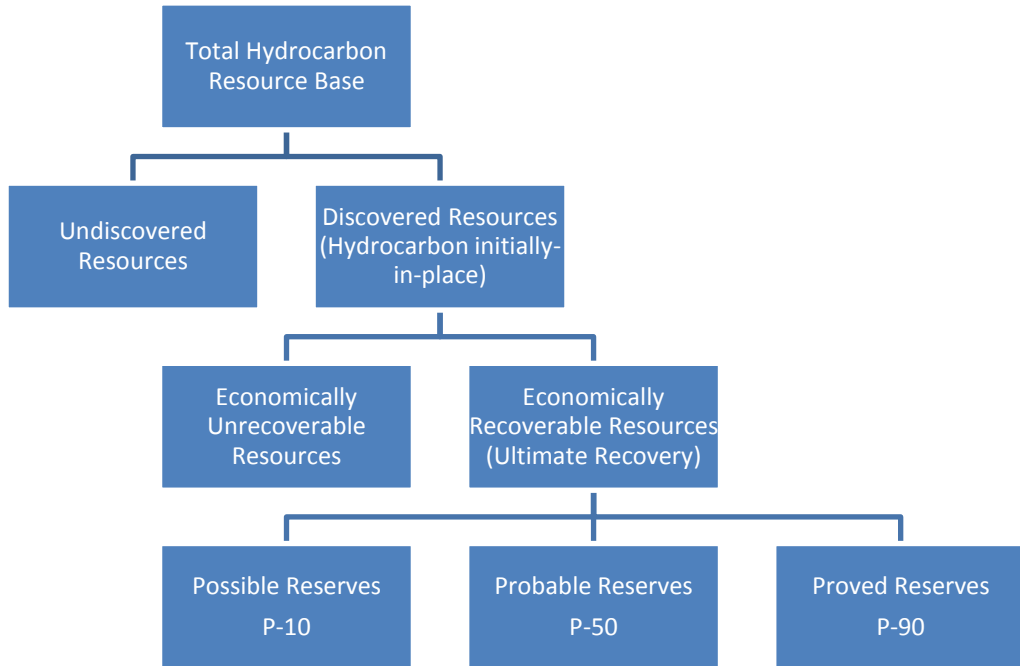


Figure 1-1: The components of the hydrocarbon resource base (from: SPE website accessed March 2007)⁴.

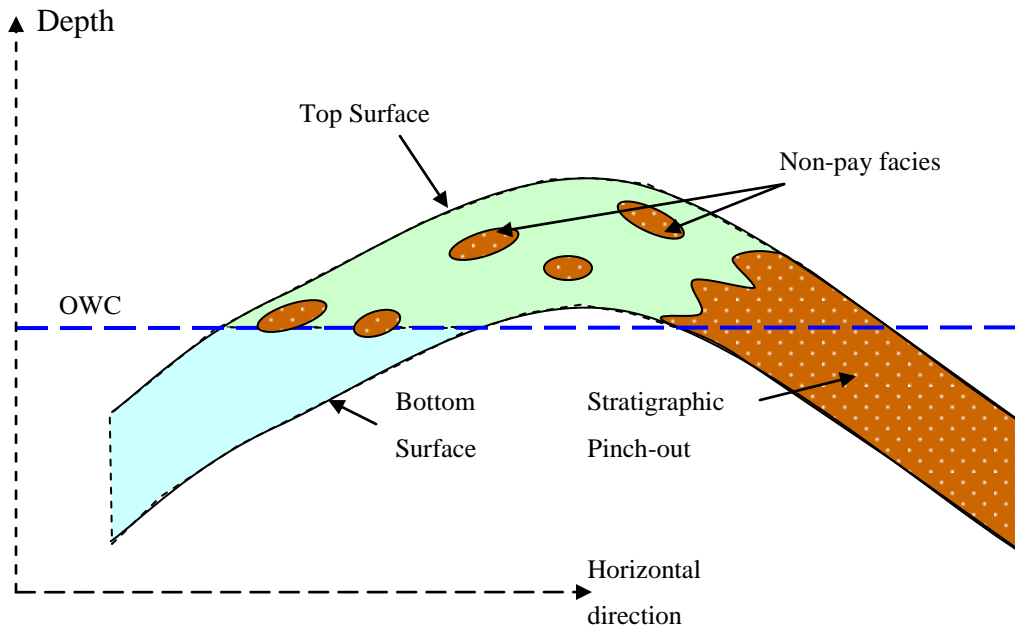


Figure 1-2: Reservoir Cross-section: The reservoir is bounded by top and bottom structure surfaces and above OWC level as shown in the green area above and excluding the non-pay facies.

data and uncertainty in structural surfaces interpreted from seismic data. Generally, the top and bottom structure surfaces and faults are obtained from seismic interpretation, while the oil-water contact (OWC) can be estimated from the available wells. The depth of these surfaces is never exactly known and the OWC depth may also be uncertain. Monte Carlo approaches are widely used to quantify this uncertainty.

Seismic interpretation is performed in the time domain and transferred to depth with a time-to-depth conversion using some type of velocity model. There is no unique surface in units of depth because of uncertainties in the interpretation (in time) and uncertainties in the time-to-depth conversion. In general, the further away from the well locations, the larger the uncertainties in the surfaces. Therefore, the calculated GRV is uncertain. This uncertainty is often recognized but not always quantified.

1.1.2. Net-to-Gross (NTG)

The net-to-gross ratio (NTG) or Net Pay (NP) is a major element in estimating a reservoir volume. Procedures to estimate NTG or NP tend to be subjective. The thickness of the pay zone can be calculated by summing the vertical samples where the rock and fluid properties meet specified criteria within the given layer. The Net-to-Gross ratio can be calculated by dividing the thickness of the NP estimate by the gross thickness of the layer. The remaining/excluded zone from gross thickness has non-net facies, very low porosity, or high water saturation to be considered noncommercial. Figure-1.2 shows the non-net facies inside the reservoir layer. There is often significant dependency between porosity, water saturation, and net-to-gross ratio, which must be accounted for in geostatistical models. Models that ignore the correlation between those variables may lead to wrong estimates of volumes and suboptimal decisions.

1.1.3. Porosity (ϕ)

The third element affecting reserve volume estimation is the effective porosity, which refers to the interconnected pore volume that contributes to fluid flow in a reservoir excluding dead-end or isolated pores. Porosity can be determined from logs or measured from cores in the lab. These measurements are local samples and do not represent the whole reservoir. Porosity is important for two reasons: to estimate hydrocarbon volume and to model permeability due to the high correlation between porosity and permeability.

1.1.4. Residual Saturation

Another variable affecting reserve volume estimation is residual saturation, which is saturation level below which fluid drainage will not occur. It is also called immobile saturation or connate water saturation (S_{wi}). Residual saturation is affected by several factors such as fluid viscosity, pore sizes, and rock wettability if it is oil-wet or water-wet. Residual saturation estimates are used to estimate the volume of recoverable hydrocarbon of concern in the reservoir. Its values can be measured by running logs or collecting a representative core sample and saturating it with the hydrocarbon of concern, followed by allowing the sample to drain for several days and then measuring the volume of hydrocarbon retained by the core sample.

1.1.5. Formation Volume Factor (B_o)

Most measurements of oil and gas production are made at the surface, which is known as standard conditions. Therefore, volume factors are needed to convert measured surface volumes to reservoir conditions and vice versa. Oil formation volume factor (B_o) is a measure of the shrinkage or reduction in the volume of crude oil as it is produced. B_o can be calculated by dividing oil and dissolved gas volume at reservoir conditions by oil volume at standard conditions.

It is almost always greater than 1.0 because the oil in the formation usually contains dissolved gas that comes out of solution in the wellbore with dropping pressure. B_o is measured in PVT labs. Accurate evaluation of B_o is of prime importance as it relates directly to the calculation of the reserve and oil in place under stock tank conditions.

1.2. Problem Statement

Decision-makers need to make the best decisions with an appropriate level of technical analysis with the acquisition of appropriate data. The definition of “appropriate” in the context of uncertainty management is important to this dissertation. This research will compare 0-D, 2-D, and 3-D approaches to quantify uncertainty.

Reserves volumes have significant uncertainty due to sparse well data and uncertainty in structural surfaces. In this dissertation, reservoir data are used to develop a geostatistical approach to surface simulation and uncertainty assessment. The top surface structure of a reservoir, subsequent layer thickness, and oil water contact depths are uncertain. The main controls on the uncertainty assessment are (1) the possible deviations from the base case seismic predicted surfaces, that is, a distribution of the possible deviations from the base case, and (2) a variogram that specifies how fast the uncertainty increases away from the well locations. Careful assessment of parameter uncertainty is an important aspect of this research.

The current methods of estimating reserves are spreadsheet or Monte Carlo simulation (MCS) software using somewhat arbitrary distributions for the variables. 3D models may be constructed, but they do not consider uncertainty in all variables. Experimental Design could be used in multiple deterministic (or scenario) modeling to quantify the uncertainties in some variables. Ignoring

structural uncertainties can lead to wrong estimates of volumes and bad decisions. Underestimating could lead to lost opportunities while overestimating could give high-risk exposure.

The proposed methodology consists of four main steps: (1) assess uncertainty in gross rock volumes with uncertainty in structural surfaces using conditional sequential simulation with conditioning data at well locations to be equal to certain values; (2) assess uncertainty in reserves volumes with uncertainty in fluid contacts using MCS; (3) assess uncertainty in reserves volumes with uncertainty in petrophysical properties using cosimulation with super secondary data obtained from seismic data; and (4) assess full uncertainty in reserves volumes by combining uncertainty in all previous parameters properly. This scenario will be conducted twice, one without accounting for parameter uncertainty and one with parameter uncertainty.

1.3. Literature Review

Many papers have been published about using MCS to estimate reserve volumes and quantify parameter uncertainty especially in the early reservoir life (Behrenbruch *et al.*, 1985; Murtha, 1997; Berteig *et al.*, 1988). Conditional simulations were proposed instead of single or multiple deterministic scenarios to assess uncertainty of hydrocarbon pore volume associated with structural parameters, NTG, porosity, and permeability. The methodology in their paper was based on simulating structural surfaces with conditioning data at well locations to match available data. None of those papers mentioned varying the mean of the variable of interest to assess its uncertainty.

Samson *et al.* (1996) proposed a method to assess the uncertainty in the position of the top structure by assuming that maps of uncertainty on the time pick and on the average velocity have been produced, and they evaluated the impact of

these uncertainty maps on GRV uncertainties. Their proposed method consists of generating possible error maps that are all within the range provided by uncertainty maps. A possible depth map is obtained by adding an error map to the reference case. A simulated GRV can then be computed between the simulated top of the reservoir, the base of the reservoir and the OWC. By iterating many times, histograms and expectation curves of the GRV can be derived. This paper focused on uncertainty due to structural surfaces and fluids contacts levels but not petrophysical properties. It also did not account for parameter uncertainty in the mean for structural deviation.

Abrahamsen *et al.* (1998) proposed a stochastic model to assess the uncertainty in estimating the reserve volumes, based on the uncertainties in cap rock geometry and the depth to the hydrocarbon contact determined by a spill point detection algorithm. First, the geometry of the cap rock is simulated using established MCS techniques for surfaces based on Gaussian random field models. Second, a new algorithm finds location of spill points and trapping areas of the simulated structures. Then, GRV of the traps can be calculated and volume distributions can be quantified in terms of histograms and quantiles.

There are many papers published about constructing a deterministic 3D geological model. This is easily accomplished with commercial software. Multiple deterministic (or scenario) models can be generated (perhaps using experimental design) to quantify the uncertainties in some variables. This methodology might give an idea about the limits of global uncertainty but it will not give a full picture of uncertainty (or a distribution) plus it does not consider for local uncertainty (Peng and Gupta, 2003).

1.4. Dissertation Outline

This research aims to improve reserve evaluation in the presence of geologic uncertainty accounting for parameter uncertainty using 2-D models. The second chapter presents the hierarchical-geostatistical modeling and shows how to select the best modeling scale for making decisions. Chapter 3 introduces three different approaches to quantify parameter uncertainty and discusses their implementation details. The fourth chapter focuses on uncertainty management. It discusses how it can be presented and understood to know parameters that play a key role in reserve estimations in order to reduce their uncertainty. Chapter 5 explains the proposed methodology and how to assess uncertainty of HIIP associated with structure such as top and bottom surfaces, layer thicknesses, and fluid contact levels and petro-physical properties such as net-to-gross, porosity, and oil saturation. It also presents the methodology with and without accounting for parameter uncertainty. A case study of real data from Hekla Field, a portion of a large North Sea reservoir is presented in the sixth Chapter to compare using different parameter uncertainty approaches. Chapter 7 presents 2-D vs. 0-D and 3-D modeling using the same real data from Hekla Field. The last chapter presents some remarks on the developed methodology including future research directions.

HIERARCHICAL RESERVOIR MODELING AND UNCERTAINTY QUANTIFICATION

Different modeling scales are discussed with their applications, benefits and disadvantages. An accurate estimate of reservoir volume is important for optimal decision making. The first decision to make in any geostatistical study is the modeling scale.

Modeling scale can be categorized into three groups as shown in Table-2.1. Selecting the appropriate modeling scale depends on the goals of the study and the stage in the lifecycle of a reservoir. Another factor affecting the modeling scale selection is time sensitivity; sometimes quick decisions must be made based on preliminary modeling results. One of the difficulties in modeling is getting a reliable distribution for all variables.

2.1. 0-D Modeling

In general, 0-D methods are used at the prospect evaluation stage, whereas 2-D and 3-D methods are used during appraisal through to development and production. There are several fast and friendly programs using Monte Carlo Simulations of this method (Murtha, 1997 and Garb, 1988). These programs use the probability distributions for each of the parameters used in the calculation where values are drawn according to the specified probability distributions. MCS

Geostatistical Modeling	Reservoir Life				
	Exploration	Appraisal	Development	Production	Secondary development
0D	←————→				
2D		←————→			
3D				←————→	

Table 2-1: Hierarchical-Geostatistical models and their application through reservoir life.

is used when the distributions of each of the independent variables can be reasonably quantified. These methods may ignore the interdependencies among input parameters. The input uncertainty ranges for a given parameter are often subjective. In addition, this method is used for global statistical analysis; it does not permit uncertainty assessment for specific locations or development areas.

Using a 0-D MCS approach offers several advantages (Mishra, 1996) for propagating uncertainty in reservoir engineering problems. First of these is that the full range of each uncertain input parameter is sampled and used in generating the probabilistic model outcome. A second advantage is the ease of implementation. Finally, the Monte-Carlo approach is conceptually simple, widely used and easy to explain.

2.2. 2-D Modeling

Reserves estimates can be undertaken with 2-D modeling of parameters such as structural elevation, thickness (h), net-to-gross (NTG), average porosity (ϕ), average water saturation (S_w), and oil formation volume factor (B_o).

Neither 0-D nor 3-D modeling considers local uncertainties in structural surfaces. The 2-D modeling method uses 2-D and 3-D data and combines them to investigate uncertainties in estimating reserves or resources globally and locally.

The 2-D methods map reservoir parameters and use their spatial relationship rather than simply averaging. The parameter values for the 2-D grids can be either structural position or some other reservoir property. These methods are not as fast as 0-D methods but can give a better base for making decisions.

Structural uncertainties can be modeled by 2-D geostatistical tools such as GSLIB software (Deutsch and Journal, 1998) that take into account the spatial correlation between data points for a given surface. Stochastic models are created with such a program. Multiple equally probable realizations of the structure can be produced. Then, a range in GRV can be calculated by combining the uncertainty range for fluid contacts with each of the simulated depth maps. Hydrocarbon-in-place volumes can then be calculated by combining GRV uncertainties with the uncertainty in petrophysical parameters using Monte Carlo simulation.

2.3. 3-D Modeling

High resolution 3-D models are appropriate for modeling heterogeneity and providing input to flow simulation. They are not necessarily the most efficient for uncertainty quantification. In addition, they are not appropriate to make time sensitive decisions since detailed 3-D modeling will take significant professional and CPU time.

3-D modeling involves the construction of a geological framework grid using the mapped structural horizons and fault surfaces together with the individual reservoir layers. This framework is then merged with the sedimentary

building blocks, or lithofacies, and their associated petrophysical characteristics. 3-D models allow for the population of the sparsely sampled space (between wells) with the individual building blocks of a reservoir and their reservoir properties. Multiple realizations of a reservoir can be produced from which quantitative models for uncertainty analysis can be derived.

The procedures and the geostatistical tools used in 3-D modeling are dependent on the data, time available, and particular reservoir or problem to be investigated. The models also provide for full integration of subsurface data, but they also require geostatistical specialists to keep them updated.

Peng *et al.* (2003) investigated the feasibility of using Experimental Design and Analysis EDA methods with multiple deterministic scenarios to study the hydrocarbon in-place volume (HIIP) of a reservoir. This may be important during the exploration or early appraisal stage, where the amount of data is not sufficient for meaningful 3-D numerical reservoir simulations. Multiple deterministic models are being used more frequently as higher-risk marginal fields are developed. This may be better than a probabilistic approach using 0-D model in the investigation of HIIP because this method is based on a geological representation of the reservoir that can be used for field development planning. However, it may not be practical because a large number of models must be built to generate the volume distribution curve (similar to that derived from the probabilistic approach).

2.4. Remarks

0-D modeling is fast and used in the early stages of the reservoir life cycle with few or no well data. Table 2-1 shows the hierarchical-geostatistical models and their application through reservoir life. 2-D modeling is better than 0-D

modeling in the investigation of HIIP in the appraisal stage of reservoir life because it is based on a geological representation of the reservoir.

Table 2-2 shows a comparison between hierarchical-geostatistical modeling based on speed, purpose, required input data, advantages, and disadvantages. It shows that 0-D modeling is the best for quick decisions. 2-D modeling is the best to quantify local and global uncertainties.

Gaussian-based techniques can be used without concern for non-linear averaging. Converting data to 2-D summaries further simplifies multiscale modeling. 2-D mapping is the most common approach to large scale modeling, and used for estimating resources, quantifying, and accounting for parameter uncertainty.

Detailed 3-D models are useful for flow simulation but not necessary for resource estimation. They have many disaggregated components, take significant time, and are not appropriate to make quick decisions; but they are used more to make specific local decisions in mature reservoirs or to evaluate areas of interest.

Parameters	Hierarchical-Geostatistical Modeling		
	0-D	2-D	3-D
High Speed	Yes	Maybe	No
Purpose	Mainly to estimate the GRV for rush decisions	Mapping	More detailed modeling
Input data	Probability distribution of each element	2D maps	All data available
Advantages	Fast.	Good for local and global uncertainties.	Good for local uncertainties.
Disadvantages	- Ignoring dependencies among input parameters. - Subjectivity.	- Not suitable for flow simulation.	- Needs a lot of time.

Table 2-2: Hierarchical-Geostatistical modeling comparison.

PARAMETER UNCERTAINTY

It is important to account for uncertainty in input histogram parameters to geostatistical modeling. The input histogram parameters are almost always assumed fixed, but they have some uncertainty that should be assessed. There is uncertainty in the mean, standard deviation, and sample range of the input histogram. Uncertainty in the mean is of primary importance; the details of the histogram are of second order importance compared to mean. The mean of the variables of interest was considered to be the statistic of interest in this study. Different methods were developed to quantify parameter uncertainty in such parameters of statistic. In this chapter, three different methods are discussed: conventional Bootstrap method (BS), spatial Bootstrap method (SBS), and Conditional Finite Domain (CFD). Each of these three methods will be described with a comparison and recommendation for practical reservoir uncertainty quantification.

3.1. Bootstrap

A first method for assessing uncertainty in the input histogram parameters to geostatistical modeling is a bootstrap method (BS) developed by Efron (1979). It is a useful application of Monte Carlo simulation to quantify uncertainty in statistical parameters. There are two important assumptions implicit to the use of the bootstrap: (1) the data are representative of the entire population and (2) the data are independent, which is acceptable in early reservoir appraisal with widely spaced wells.

The bootstrap is a statistical resampling technique that permits the quantification of uncertainty in any calculated statistics by resampling from the original data. This method makes no assumption about the data distribution. In other words, it is applicable regardless of the form of the data probability density function.

Consider n data values of a single variable ($z_i, i=1, \dots, n$) and a calculated statistic, say, the experimental mean m_z . The bootstrap can be used to calculate the uncertainty in the statistic of interest (the mean) by the following simple procedure:

- 1) Assemble the representative distribution of the Z random variable using declustering and debiasing techniques if appropriate: $F_Z(z)$. This distribution could simply be the equal weighted histogram of the n data; so each point will have a probability of $1/n$.
- 2) Draw n values from the representative distribution, that is, generate n uniformly distributed random numbers $p_i, i=1, \dots, n$ and read the corresponding quantiles:

$$z_{s,i} = F_Z^{-1}(p_i), \quad 3.1$$

where $i=1, \dots, n$.

The number of data drawn is typically equal to the number of data available in the first place. The distribution of simulated values is not identical to the initial data distribution because they are drawn randomly and with replacement.

- 3) Calculate the statistic of interest (such as the experimental mean, m_{sz}) from the resampled set of data.
- 4) Return to steps 2-3 and repeat L times, where L is a large number, in order to create L resamples. Typically, L is at least equal to 1000.
- 5) Assemble the distribution of uncertainty in the calculated statistic. This distribution can now be used to make inferences about the parameter.

A GSLIB-like code called *boot_avg* was developed by Deutsch (Neufeld and Deutsch; 2007) based on a resampling technique. The bootstrap technique is reasonable if the data are independent, but reservoir data are often correlated to some extent. This correlation does not satisfy the independency assumption of this technique as more data are collected.

3.2. Spatial Bootstrap

Data from a spatial region usually have a correlation structure. These correlations are ignored in the conventional bootstrap. The bootstrap has been extended to resample dependent data. Hall (1985); Kunsch (1989); Liu & Singh (1992) have independently proposed a block resampling scheme. This method termed also the moving blocks method. It is a common method of the block bootstrap where blocks of the spatial data are sampled at random, then joined together to form a new sample. The block bootstrap takes care of the dependence structure within the blocks, but not the correlation between blocks. Hall et al. (1995) pointed out that the bias and the variance of a block bootstrap estimator are seriously affected by the block length.

Andy Solow (1985) proposed the spatial Bootstrap method (SBS) by adding spatial dependency specified by a covariance matrix to the bootstrap. In the spatial bootstrap method (Journel, 1993; Norris et.al., 1993), alternative sets of data are resampled from whole simulated fields. This resampling method accounts for any prior model of spatial dependency between the data, and allows for integration of secondary information.

A GSLIB-like code, based on an efficient matrix simulation approach, was presented by Deutsch (2004). It resamples with correlation, which relaxes the assumption of independence. A LU simulation algorithm is used to simulate values under a multivariate Gaussian model. The simulated values are

unconditional and are only required at the data locations. The method of the SBS is simple and efficient for a large number of realizations. The number of data has a limit of 10000. The covariance values between each pair of data are established based on an input of a 3-D variogram model.

n values are simulated from the deemed representative histogram $Fz(z)$ following the variogram of the normal scores of the Z variable, which can be represented by a 3-D variogram model $\gamma(h)$. The algorithm is to perform an LU decomposition of the n by n covariance matrix:

$$\mathbf{C} = \mathbf{L}\mathbf{U} \quad 3.2$$

where \mathbf{C} , \mathbf{L} , and \mathbf{U} are n by n matrices. The variogram model is used to build \mathbf{C} . A Cholesky LU decomposition is used to calculate the lower and upper triangular matrices \mathbf{L} and \mathbf{U} . Unconditional Gaussian simulations are calculated by a simple matrix multiplication:

$$\mathbf{y}^{(l)} = \mathbf{L}\mathbf{w}^{(l)}, \quad l = 1, \dots, L \quad 3.3$$

where \mathbf{w} and \mathbf{y} are n by 1 vectors and L is the number of realizations.

The \mathbf{w} vector consists of independent Gaussian values and the \mathbf{y} vector consists of the resulting unconditionally simulated values with the correct covariance. Then the Gaussian values are converted to probability values to draw from the representative distribution.

$$\mathbf{p}^{(l)} = \mathbf{G}(\mathbf{y}^{(l)}), \quad l = 1, \dots, L \quad 3.4$$

where \mathbf{G}^{-1} is the inverse of the standard normal distribution and \mathbf{p} is an n by 1 vector of probability values [0,1]. The drawn z -values are calculated as:

$$\mathbf{z}^{(l)} = Fz^{-1}(\mathbf{p}^{(l)}), \quad l = 1, \dots, L \quad 3.5$$

Performing the LU decomposition is required only once to generate the simulated realizations by the following equation:

$$\mathbf{z}^{(l)} = Fz^{-1}(\mathbf{G}(\mathbf{L}\mathbf{w}^{(l)})), \quad l = 1, \dots, L \quad 3.5$$

The distribution of the results can be used to calculate any parameter of statistic using from each set of simulated values.

The uncertainty is larger when the data are more correlated. The effective number of data can be calculated as:

$$n_{eff} = \frac{\sigma_Z^2}{\sigma_{\bar{Z}}^2} \quad 3.6$$

where σ_Z^2 is the variance of the data values.

$\sigma_{\bar{Z}}^2$ is the variance of the average values.

The following steps describe the methodology to perform the spatial bootstrap:

- 1) Assemble the representative data.
- 2) Calculate the 3-D variogram for the data set.
- 3) Perform the LU simulation at the data locations.
- 4) Calculate the statistic of interest.
- 5) Return to step 3 and repeat many times.
- 6) Assemble the distribution of uncertainty in the statistic.

There are two apparent limitations of the SBS. The first limitation is that it allows only quantifications of uncertainty of order one in the histogram. The second limitation is that SBS does not account for all possible data in the area of interest. It is always the case, especially in the early reservoir life, that some lower and higher values of the variable of interest than those previously sampled are obtained with collecting more samples. Ignoring such possibility in the uncertainty assessment process can lead to underestimation/overestimation of uncertainty.

A major problem with the spatial bootstrap approach is that increased spatial correlation leads to greater uncertainty than if the data are more random. The SBS does not consider the affect of conditioning data or the finite reservoir domain. Directly accounting for size of domain and local conditioning data is likely to be quite important.

3.3. Conditional Finite Domain

The Conditional Finite Domain technique (CFD) is a new stochastic approach that is based on a multivariate Gaussian distribution and used to assess uncertainty in the input histogram (Babak and Deutsch, 2006).

The CFD approach has many advantages over the SBS approach. First, SBS allows only quantification of uncertainty of order one in the histogram, while CFD quantify uncertainty of any order in the histogram. CFD is also the first approach that accounts for the size of the domain and the local conditioning data. A disadvantage of the SBS is that it does not account for all possible data in the area of interest. Some lower and higher values of the variables of interest can be observed with additional sampling compared to those previously sampled; therefore, CFD approach determines the possible higher and lower values of the variable of interest.

This approach does not work directly with original data but with the standard normal distribution after transforming the data prior to simulation. After simulating the full grid in the area of interest, uncertainty assessment is based not on the full grids of the simulated values, but rather on the sub samples of it. It is assumed that every set of simulated data which have the same configuration as the original data can be considered as an observation from the same underlying distribution as the original data. Then the data are back transformed to the original data.

Any desired number of data combinations, K can be chosen using translation and/or rotation with respect to some centre of the original data, which have the same configuration as the original data and belong to the study domain, see Figure 3-1. The same K simulated data combinations can be found for all other $L-1$ simulated realizations. Then the uncertainty in the statistic of interest is quantified from the results of these K combinations obtained from L simulations.

The reference distribution in the first realization is obtained from the original data then the realization results used in the next simulated realization and so on. Figure 3-2 shows schematic representation of the calculations performed in one step.

Babak and Deutsch (2006) proved in their work that the “correct” starting reference distribution has no effect on the limiting uncertainty but the lower and upper tail values have a major effect on the limiting uncertainty value. The effect of the number of data and the variogram range on the limiting uncertainty was investigated. It was found that the uncertainty decreases as the number of data increases. With respect to the change in range of correlation, it was observed that the uncertainty in the statistic of interest decreases as the range of correlation increases due to the fact that the conditioning data are more correlated with each other and more correlated to the locations being simulated. This impact is reversed with using the SBS approach, that is, the uncertainty decreases if the range of correlation decreases. The variogram uncertainty was also investigated

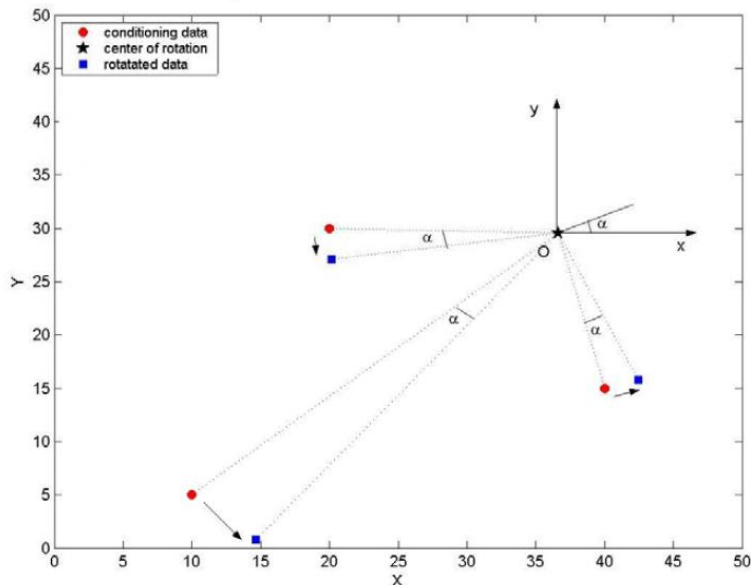
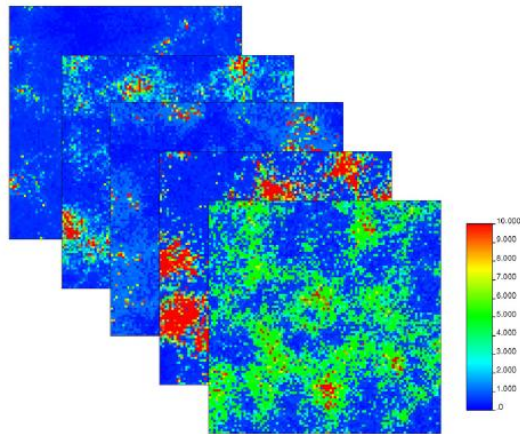
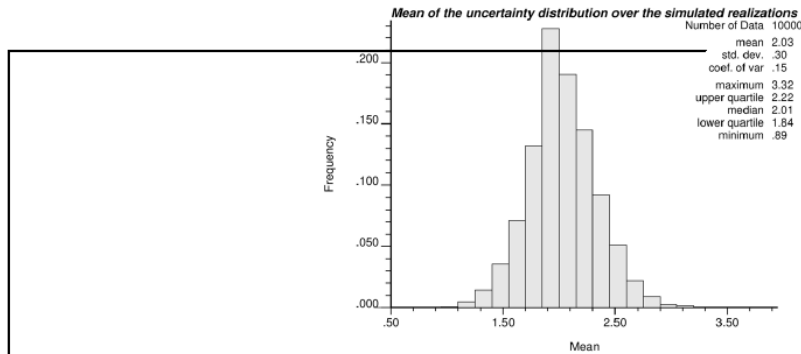


Figure 3-1: Use of centroid and angle in determining new data combination: Conditioning data (circles) is rotated on angle α anticlockwise around the centre in point O to obtain a new data combination (squares). (Babak and Deutsch; 2006).

Sequential Gaussian Simulation



Assessment of uncertainty in the statistic of interest over the simulated realizations (rotations)



Uncertainty in the statistic of interest as a standard deviation of the distribution of uncertainty in the mean over the simulated realizations

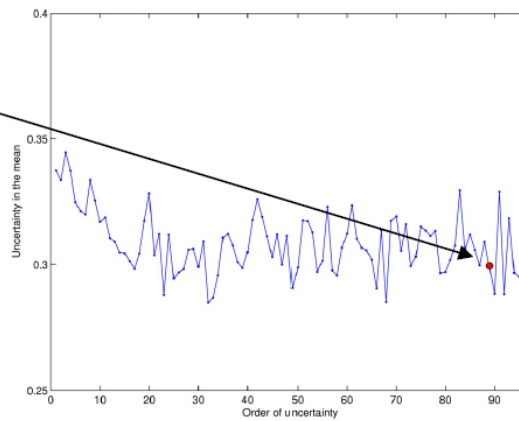


Figure 3-2: Schematic representation of the calculations performed in one step of the CFD algorithm (Babak and Deutsch; 2006).

for the real geological data. It was shown that the variogram of the reference distribution can be very different from the input variogram to sequential Gaussian simulation. Their recommendation was that variogram uncertainty also be incorporated in the limiting uncertainty assessment by applying SGS each time not only with a different reference distribution, but also with a different input variogram corresponding to that reference distribution.

The CFD procedure is summarized in the following steps:

- 1) apply SGS to create L realizations of the variable of interest using an input reference distribution.
- 2) calculate and quantify the uncertainty of order 1 in the statistic of interest and establish the reference distributions to be used in the subsequent assessment of uncertainty in the statistic of interest.
- 3) select desired number of data combinations, say K, using translation and/or rotation with respect to some centre of the original data, which have the same configuration as the original data and belong to the study domain.
- 4) use the reference distribution obtained in step 2 to create L realizations of SGS using available conditioning data and calculate and quantify uncertainty of order k in the statistic of interest.
- 5) establish the reference distributions to be used in the subsequent assessment of uncertainty in the statistic of interest.
- 6) repeat generating K number of data combinations, create L realizations using updated reference distribution obtained from last uncertainty order, calculate uncertainty of order k, and obtain new reference distribution for the next order of uncertainty.

Where $k = 2, \dots, \infty$.

The CFD has shown to be convergent in the sense of limiting uncertainty calculation, design independent, and parameterization invariant. It is expected that the uncertainty in the parameter of interest will increase/decrease to a point where

the parameter uncertainty stabilizes. The “stabilization” phase corresponds to the fluctuation of the limiting parameter uncertainty around some constant value, which defines the limiting parameter uncertainty.

3.4. Remarks

It is important to know which approach is the best to be used in any case study. It might depend on input data if they are correlated or not and how much these approaches can be reliable.

In the early stage of reservoir life, using BS is more recommended because it is simple and easy to use. Even though, all three approaches might give the same results, especially if all data are independent. Conventional bootstrap can be used till more data are collected and their correlation can be noticed.

SBS and CFD can be used if there is correlation between the input data. SBS is expected to give more uncertainty in the statistic of interest since CFD accounts for the conditioning data and size of the domain, which reduces uncertainty caused by correlation between the input data. CFD is the first approach that accounts for those two factors.

The good thing about SBS is that it is more popular and has been used more; even though, it might overestimate the uncertainty in the statistic of interest. It is recommended to conduct another study on a mature reservoir that has more well data and investigate the sensitivity of the uncertainty in the statistic of interest for a variable of interest with increasing input well data by adding them in steps.

Chapter 4

UNCERTAINTY MANAGEMENT

There are a lot of variables that play key factors in reserve estimations. The variables and their sources should be known to do more investigations in order to reduce uncertainties. Measuring the uncertainty of variables is easy to account for in 0-D modeling but difficult in 3-D modeling. Those variables affecting reserve estimates can be categorized into three major types:

- Geologic factors such as Gross rock volume, Net to Gross ratios, Porosity, Water saturation, Cutoff values, Contacts, and Facies distribution.
- Economic conditions such as Hydrocarbon prices, Development costs, Operating costs, and Marketing uncertainty.
- Engineering factors involve Formation Volume Factors, Hydrocarbon fluid properties, Well productivity, Well spacing, Recovery Factors, Drive Mechanisms, and Secondary and tertiary projects.

A complete study often studies the effects of more than 20 factors. Hydrocarbon resources or reserves are calculated as a combination of these factors. In this research, only geologic factors will be considered, even though the procedure might be extended in the future to study the effects of other ones. All geologic factors, economic conditions, and some of engineering factors are uncontrollable factors in estimating reserves, while some of engineering factors (such as well spacing, drive mechanisms sometimes, secondary projects, etc) are controllable.

Uncertainty of parameters of any distribution is important, especially uncertainty in the mean of the variable of interest, which is of primary importance. The remaining parameters of the histogram are of second-order importance compared to the mean. Uncertainty in the mean of any variable of interest can be quantified with any of the three techniques described in Chapter 3.

In this chapter, uncertainty management will be discussed from two aspects: how uncertainty can be presented and understood and how it is important to improve decision making.

4.1. Presenting and Understanding Uncertainty

Uncertainty is an essential and inescapable part of life not only oil business. There are a lot of decisions made under uncertainty, which causes bad consequences. Therefore, it is really important to make the decisions with a full picture of uncertainty. Uncertainty is caused by incomplete knowledge regarding relevant geological, geophysical, and reservoir engineering parameters of the subsurface formation. Estimating HIIP in the appraisal stage of a reservoir is often most critical because of the large financial risk. Sometimes there is no time to consider uncertainty in all parameters; so, important parameters have to be investigated and presented in a good manner.

In estimating resources or reserves volumes, if the uncertainty was not fully captured and presented in a good manner then it might underestimate or overestimate the volumes and cause unwanted avoidable consequences. Even though, uncertainty is affected by the methodology of estimating HIIP too.

4.1.1. Distribution and Quantiles

A single reserves figure or deterministic case can be computed if the value of each parameter is certain. Because of uncertainty, individual parameters are better represented by a probability distribution or different realizations, which then leads to a probability distribution for reserves, which can be summarized in a few numbers, for ease of reporting or comparison, such as minimum, maximum, mode, median, and mean, see Figure 4-1. According to SPE and CIM (Etherington, J. *et.al.*; 2005), P90, P50, and P10 can be applied in reporting reserves or HIIP using probabilistic methods to represent proved, probable, and possible reserves, respectively or low estimate, best estimate, and high estimate for resources.

P90, P50, and P10 means that the quantities actually recovered will equal or exceed the estimate with a probability of at least a 90%, 50%, and 10%, respectively.

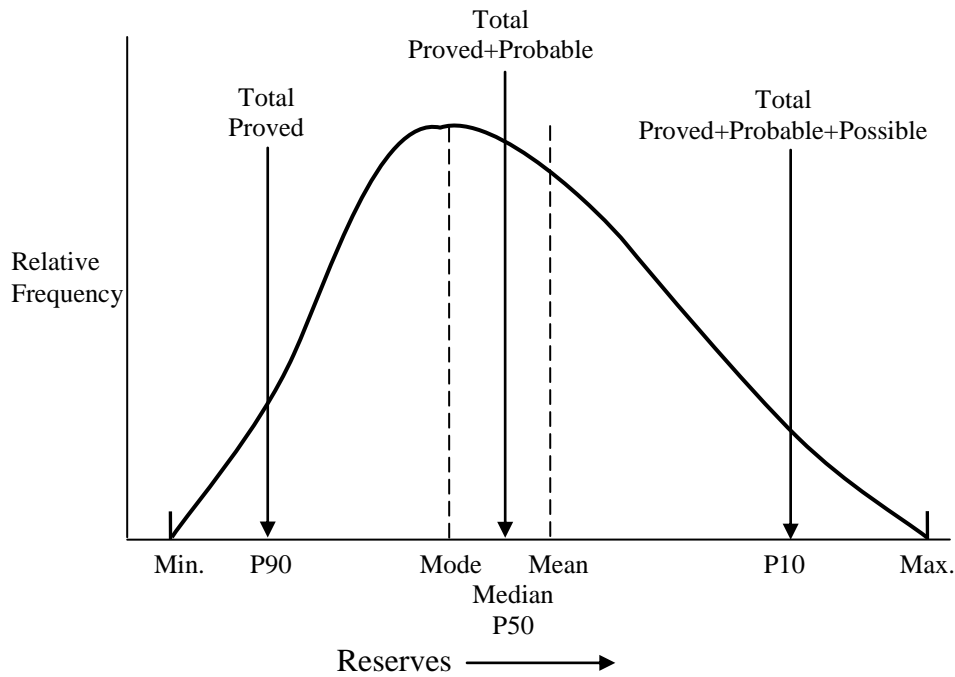


Figure 4-1: Terms Relating to Reserves Uncertainty.

4.1.2. Sensitivity Analysis

It is important to have sensitivity analysis in reserve estimations. Sensitivity Analysis studies the manner how the most optimal target solution or output would be affected by changing one parameter or more of inputs at the time with keeping all the other parameters unchanged at the base case value. For most parameters, at least two runs are required, with an optimistic and a pessimistic setting, respectively. The analysis can be used to know the important or most critical variables since reducing the number of variables is the most effective way to reduce computational cost in a risk analysis process. In addition, once the key uncertainties have been identified, attention can be focused on appropriate contingency plans to reduce their impact.

It is easy to conduct sensitivity analysis in 0-D models but difficult in 3-D models. The difficulty in conducting sensitivity analysis in 3-D models is because of not having one parameter value due to heterogeneity. Also, the interdependence between some parameters has some constraints on uncertainty. The procedure to analyze the parameters' uncertainty has to be repeatable, robust, consistent between reservoirs, and as independent as possible.

To conduct sensitivity analysis in this research, different realizations for a variable of interest will be used to investigate its effect on HIIP while using fixed realizations for other variables.

4.1.3. Tornado Chart and Spider diagram

A tornado chart is often used to compare distributions, in the form of back-to-back histograms. It is particularly popular for comparing closely related populations. It also ranks input parameters in terms of their impact on the output from the most effective to the least effective one, where the greater the

corresponding bar in the tornado chart, the greater the sensitivity and importance of that parameter to generate output.

Each parameter will vary by generating different realizations and using them to calculate different HIIP output. From the HIIP distribution, some statistic parameters can be used to evaluate the uncertainty in the HIIP. For example, the difference between the mean and P90 and P10 (“P90 – Mean” and “P10 – Mean”) can be calculated and compared using a tornado chart. Another way of the comparison is to compare P90/P50 and P10/P50 or the standard deviation of the output results using a tornado chart.

Spider diagram is another way of the comparison between the results, where the more inclined a parameter’s line is to the horizontal line, the more significant the change in the value of the target optimal solution or function is whenever the parameter’s value changes. This type of diagrams was used to compare the results of changing input realizations of interest variables by plotting “P90 – Mean”, “P50 – Mean”, and “P10 – Mean”.

4.1.4. Merging Uncertainty

The uncertainty in derived variables such as HIIP involves a combination of the uncertainty in multiple variables:

$$\text{HIIP} = \text{GRV} * \text{NTG} * \phi * \text{So} \quad (4-1)$$

Simulation is required to combine the correlated uncertainty in basic variables into uncertainty in HIIP variable. Multiple realizations of basic variables are simulated as shown in the yellow shaded squares in Table 4-1. Then HIIP is calculated with each set of realizations as shown in the last column. The uncertainty in the HIIP (or any derived property) can be assembled from the realizations. The uncertainty in HIIP might become less than uncertainty of some

Realization Number	GRV	NTG	ϕ	So	Calculated HIIP
1	95	0.55	0.22	0.80	9.20 MMbbl
2	105	0.60	0.23	0.79	11.44 MMbbl
...
100	100	0.59	0.24	0.77	10.90 MMbbl

Table 4-1: A schematic table to calculate HIIP and obtain the histogram and the uncertainty in HIIP.

basic variables due to merging some variables uncertainties while calculating HIIP uncertainty (Ren, W. *et.al.*; 2004).

4.1.5. Local Uncertainty vs. Global Uncertainty

Uncertainty can be quantified on a variety of scales. It is important to understand the scale of the calculation and the results. It might be local or global uncertainty (Neufeld and Leuangthong, 2005).

Global uncertainty relates to some calculated statistic that involves many locations simultaneously. It is difficult to check global uncertainty. To assess global uncertainty or merged uncertainty in a derived variable, a common approach is to construct alternative realizations of the spatially distributed variables. Then these realizations are used to calculate resources or reserves, where uncertainty in the global response is assembled as a histogram of the responses. The realizations would not be the same; there would be local uncertainty, which is obtained from differences between the realizations at each location.

On the other hand, local uncertainty relates rock properties at specific locations that can be potentially sampled in the future. It can be assessed by using

2-D models and checked by cross validation or new drilling where the proportions of true values falling within specified probability intervals are checked against the width of the intervals. P10, P50, and P90 maps can be used not only to summarize uncertainty but also to identify the high/low valued areas, where the high P10 values reflect areas that are surely high and the low P90 values reflect areas that are surely low.

4.2. Decision Making in Presence of Uncertainty

The more uncertainty is available, the harder decision can be taken. Specially, at the early life of reservoir, when the data is sparse and decisions have to be taken. Therefore, it is important to quantify uncertainty available in estimations to optimize the decisions.

Resources/reserves volumes might be underestimated or overestimated in the presence of uncertainty. The decisions made based on the estimated volumes might lead to a huge loss due to not quantifying the uncertainty in a proper way.

Designing new production facilities is one of the most important decisions made in the life of a producing reservoir since it is made usually in the early stage of the reservoir life when there is a lack of information and sparse well data. Quantifying uncertainty of reserves volumes and estimated fixed production rates might help in planning to have a flexible design that can be changed in the future depends on the future reserves estimates when more data are collected and analyzed. Several options should be explored, and strategies should be devised that allow for quick de-constructing and re-establishing of production facilities.

4.2.1. Robust Decisions

Getting a fair reserve distribution will help to make better decisions such as selecting best area for field development, optimum number of wells needed to be drilled, best strategic production plan, and optimum production facilities.

Decisions made have to be robust and flexible, where robustness means the absence of a need to change or react and flexibility means the ability to change or react when necessary. It is important to seek for robust and flexible alternatives. The idea is that picking a single optimum choice as the alternative for a given decision may be flawed, if the uncertainties are large and the outcomes are sensitive to the uncertainties. In that case, it is better to seek alternatives that are expected to perform reasonably well over a wide range of futures (i.e., are robust to key uncertainties) and can be changed over time as new data is gathered and experience is gained.

4.2.2. Decide to Reduce Uncertainty

Conducting sensitivity analysis in reserve estimations is really helpful in order to reduce uncertainty or better understand the nature and source of the uncertainty. Then the attention can be focused on appropriate contingency plans to reduce their impact.

4.2.3. Value of Information

Sometimes economics play a role on the value of information, it might be too expensive to get a value of a variables at unsampled location than getting the value of another less important whether in the same location or another one.

The information is not only valuable as it reduces uncertainty in estimating resources/reserves volumes, but also because other unfeasible alternatives can become possible.

4.2.4. Transforming of Uncertainty Through Economics/ Performance Forecast

Geological uncertainty is an unavoidable reality for any reservoir recovery project. Therefore, production performance is also always uncertain since production performance is significantly related to reservoir geology. Geostatistical simulation provides a model of geological uncertainty through multiple realizations of geological variables such as facies type, porosity, water saturation, and permeability. These geological realizations can be used to calculate various production performance measures by way of transfer functions such as flow simulation.

A flow simulator is used to evaluate the responses of parameters governing fluid flow through heterogeneous reservoirs and make reservoir management decisions based on predicted dynamic reservoir responses to production. Normally, only one deterministic set of parameters is considered and no uncertainty is associated with the responses or taken into account for the decisions.

Predicting future reservoir performance is an important goal of reservoir flow models. Performance forecasting permits optimization of the economic recovery of the oil and gas resources. It is important to transform uncertainty in resources/reserves volumes estimates through Economics/Performance forecast to optimize decision making.

In this dissertation, a methodology to estimate HIIP with uncertain in geological parameters is set up. Even though, it can be developed in the future to transform this uncertainty through Economics/Performance Forecast.

4.2.5. Design for Fixed Production Rate

It is common to simulate reservoir performance to estimate reservoir recovery within a certain period or a reservoir life. This step is needed to design production facilities and consider any future modifications in production facilities or changes in reservoir management such as shifting from primary to secondary production scheme.

Chapter 5

METHODOLOGY

The Hydrocarbon Initially in Place (HIIP) of a resource can be calculated by multiplying the GRV by NTG by net porosity by net hydrocarbon saturation. An economic feasibility study has to be conducted to provide a level of confidence and an estimate of reserves. In this research, HIIP uncertainty will be assessed by conducting sensitivity analysis to investigate the effects of uncertainty of each variable of interest individually. Then HIIP will be estimated in the end with full uncertainty in all variables of interest.

Two scenarios will be considered in this research. The first scenario describes the traditional approach of simulating multiple realizations for uncertainty in variables of interest without parameter uncertainty. The second scenario presents the main contribution of this research, which is a procedure to simulate realizations for uncertainty in variables of interest with parameter uncertainty in the mean. The second scenario will be conducted three times, where different parameter uncertainty distribution will be incorporated each time. The different approaches used will be compared and discussed in Chapter 6, where a case study will be conducted. The results of the case study will be compared with each other and ended by some comments and recommendations.

All techniques required in assessing uncertainty in variables of interest will be described in this chapter with the required changes to incorporate parameter uncertainty. Table 5-1 shows a summary of the techniques that will be used in a traditional scenario without parameter uncertainty and in the proposed

Parameters to be considered		To quantify the Uncertainty	
		Without PU	With PU
Structural Surfaces	<ul style="list-style-type: none"> • Top/Bottom Surface • Layer Thickness 	Conditional Sequential Gaussian Simulation	Conditional Sequential Gaussian Simulation
Fluids Contacts Levels	<ul style="list-style-type: none"> • GOC • GWC • OWC 	Monte Carlo Simulation	Monte Carlo Simulation
Petrophysical Properties	<ul style="list-style-type: none"> • Net-to-Gross • Porosity • Oil Saturation 	Cosimulating with Super Secondary data	Cosimulating with Super Secondary data
Full Uncertainty	<ul style="list-style-type: none"> • Full Uncertainty 	Combining all realizations randomly	Multivariate Parameter Uncertainty

Table 5-1: Techniques for sampling realizations to quantify uncertainty in estimating HIIP without/with Parameter Uncertainty.

scenario with parameter uncertainty. All techniques mentioned in the table will be explained below.

5.1. Sampling Realizations without Parameter Uncertainty

The traditional scenario of simulating realizations of uncertainty in variables of interest without Parameter Uncertainty is described. It is assumed that the mean of the variables of interest is fixed and has no uncertainty in it. For example, the deviations from the reference surfaces for the structural parameters are assumed to follow a normal distribution with a mean of zero and some standard deviation.

Three different techniques are used to sample realizations for quantifying HIIP uncertainty without parameter uncertainty. Sequential Gaussian simulation (SGS) is used to quantify uncertainty in structural surfaces variables such as top and bottom surfaces and layer thickness (Xie and Deutsch, 1999), while Monte Carlo simulation (MCS) is used to quantify uncertainty in fluid contacts levels such as Gas-Oil contact (GOC), Gas-Water contact (GWC), or Oil-Water contact

(OWC). The third method used is a cosimulation approach with a super secondary data using the Ultimate SGSIM program (Deutsch and Zanon, 2002). This method quantifies uncertainty in petrophysical properties such as NTG, porosity, and oil saturation.

5.1.1. Sequential Gaussian Simulation (SGS)

Sequential Gaussian Simulation (SGS) approach is a common approach used for reservoir modeling applications. SGS creates multiple equiprobable numerical models based on some conditioning data and global statistical parameters. SGS became a practical approach in the last two decades because it is simple, flexible, and reasonably efficient (Zanon and Leuangthong, 2003).

SGS is a simulation algorithm based on kriging. Locations are assigned property values sequentially using previously simulated values as conditioning data. It is necessary to use Gaussian values in the SGS method; therefore, the data are transformed into Gaussian space. The SGS work-flow can be summarized in the following basic steps:

1. Assemble the histogram of raw data and statistical parameters.
2. Transform data into Gaussian units.
3. Establish grid network and coordinate system (Z_{rel} -space).
4. Decide whether to assign data to the nearest grid node or keep separate.
5. Determine a random path to visit all grid nodes.
6. At each location:
 - a) search to find nearby data and previously simulated grid nodes.
 - b) construct the conditional distribution by kriging.
 - c) draw a random value from Gaussian distribution which known as simulated value.
7. Repeat step 6 until every location has been visited.

8. Transform the data and all simulated values back to their original distribution and check results (by this step a realization is generated).
9. Create any number of realizations by repeating steps 1-8 with a change of the random number seed.

Conditional SGS was used in this research to assess HIIP uncertainty with uncertainty in structural surfaces variables such as top and bottom surfaces and layer thickness. In this approach, the top and bottom surfaces from seismic interpretation were considered as reference surfaces that have been fitted to the well data. Away from the well locations, there exist uncertainties in the surfaces. The deviations from the reference surfaces are assumed to follow a known distribution. The deviation will be zero at the well locations and fluctuate away from the well locations. Such deviations can be simulated by SGS with conditioning data at the well locations. The deviations can then be added to the reference surfaces/layer thicknesses. Such simulation provides alternative realizations that quantify the uncertainty in the GRV and provides us with a distribution of GRV, see Figure 5-1.

Different standard deviations should be used in the undulation generation for the top and bottom surfaces. The standard deviations used need to be determined based on knowledge of the uncertainty in the seismic interpretation of the surfaces and the mismatch between seismic interpretation and well observations. In the seismic interpretation process, the first surface captures uncertainty from the present day surface down to the depth of the reservoir; subsequent surface uncertainty is the incremental uncertainty due to the distance between the reservoir layers. Usually, surfaces are interpreted with seismic data and then calibrated with well observations to remove the mismatch between seismic interpretation and well observations. However, the mismatch information provides us valuable hints of the uncertainties on the top and bottom surfaces.

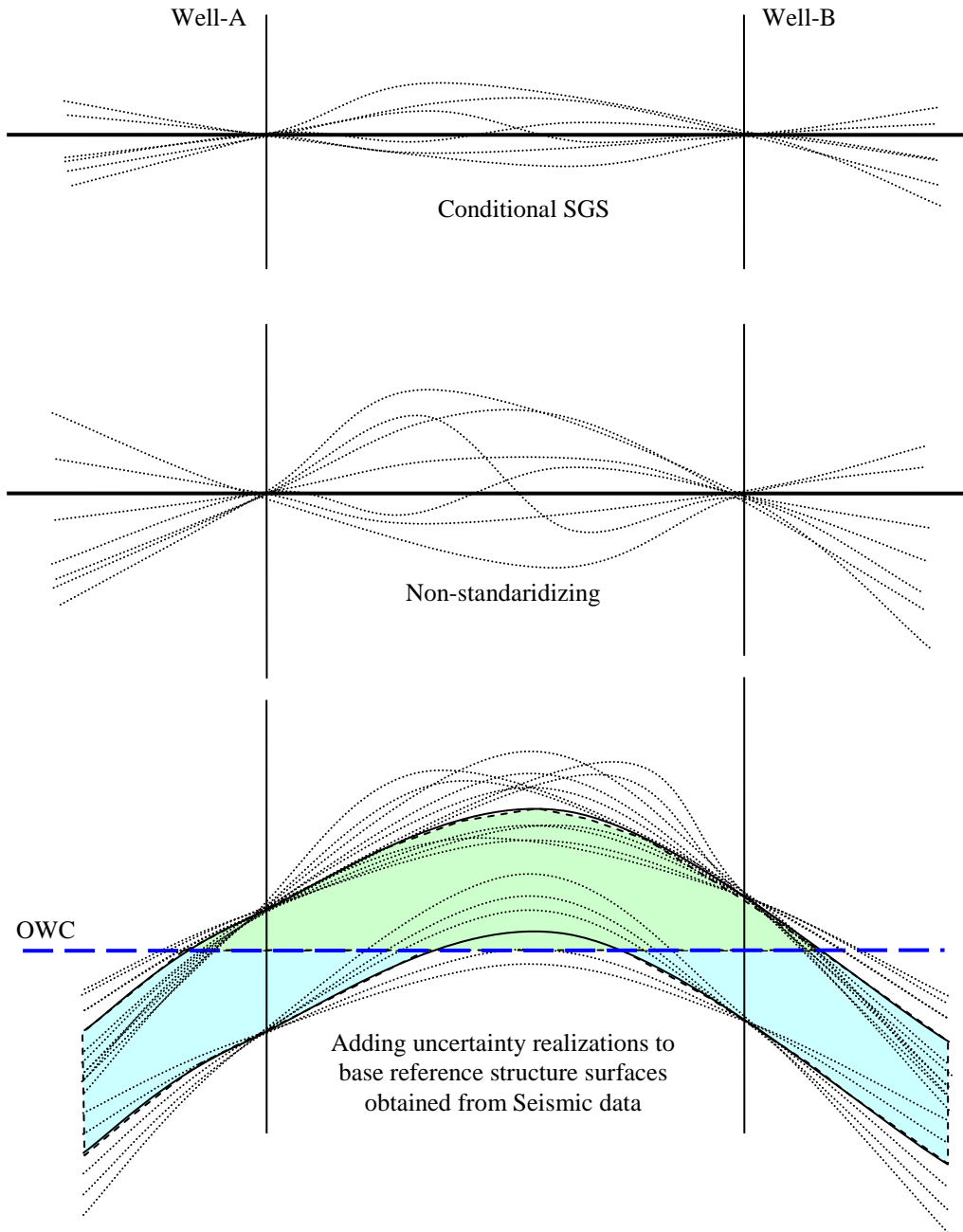


Figure 5-1: Uncertainty in top and bottom surfaces and layer thickness without PU can be simulated by using SGS with conditioning data to be zeros at well locations.

The following are required parameters in the conditional SGS procedure to simulate realizations without parameter uncertainty for the structural variables:

- 1) The base case value (structure or thickness): $(z_b(\mathbf{u}), \mathbf{u}$ in A) a 2-D grid of values coming from the seismic. In general these values are fitted to the well data.
- 2) A global estimate of the uncertainty in the base case surface σ_Δ – a single number established from time interpretation uncertainty and time to depth uncertainty. It could be calculated from:

$$\sigma_\Delta = \sqrt{\sigma_{TI}^2 + \sigma_{TD}^2} \quad (5.1)$$

Where TI refers to the time interpretation standard deviation and TD refers to the time-to-depth standard deviation and obtained from the mismatch between seismic interpretation and well observations. These would be based on a review of the seismic data and, perhaps, differences between different interpretations. The former equation is based on two assumptions: the deviations have a normal distribution shape and errors in TI and TD are independent.

These two parameters must be established from the available reservoir data. The simulation proceeds by establishing a target mean, that could be different from 0.0, simulating the deviations and adding them to the base case surface. The procedure for simulation can be summarized by the following steps:

- 1) obtain the best variogram model fitting the experimental variogram result for Structure Surfaces or Layer Thickness.
- 2) simulate y^l uncertainty realizations using SGS with conditioning values at well locations to be zeros. The realizations will have a mean of zero and a standard deviation of one. Different random numbers should be used at each step to avoid unwanted correlations.
- 3) non-standardize the realizations by multiplying them with some standard deviations σ_Δ (referring from seismic data).

$$\Delta^l(\mathbf{u}_i) = y^l(\mathbf{u}_i) * \sigma_\Delta \quad (5-2)$$

- 4) add the results to the base reference surfaces obtained from seismic data (to the top and bottom surfaces to quantify uncertainty in top and bottom surfaces and only to the bottom surface to quantify uncertainty in layer thickness).

$$\begin{aligned} z^l(\mathbf{u}_i) &= z_b(\mathbf{u}_i) + \Delta^l \\ &= z_b(\mathbf{u}_i) + y^l(\mathbf{u}_i) * \sigma_\Delta \end{aligned} \quad (5-3)$$

where $i = 1, \dots, n$ grid nodes

- 5) calculate HIIP by calculating HIIP of each realization using equation (4-1) and generating a distribution plot.

SGS with conditioning data can be used to quantify uncertainties in the structural parameters, the top and bottom surfaces and the layers thickness. For assessing the uncertainty in the top and bottom surfaces, the uncertainty realizations are added to the reference top and bottom structure obtained from the seismic. On the other hand, the uncertainty realizations are added to the bottom surface to assess the uncertainty in a layer thickness and in case of cross-over, the thickness will be zero since it cannot be negative.

5.1.2. Monte Carlo Simulation (MCS)

Monte Carlo simulation (MCS) relies on repeated random or pseudo-random sampling to compute results. It tends to be used when it is unfeasible or impossible to compute an exact result with a deterministic algorithm. For example, the depths of the fluids contact levels are uncertain in many cases.

Typically, when the fluid contacts level is not clearly measured, a minimum, most-likely and maximum location can be identified. In such a case, the location of the contact can be simulated using a triangular distribution, see Figure 5-2. The mean and standard deviation of a triangular distribution can be defined by the following equations:

$$\text{Mean} = (a+m+b)/3 \quad (5-4)$$

$$\sigma^2 = (a^2 + m^2 + b^2 - am - ab - mb)/18 \quad (5-5)$$

Where: a = minimum

m = mode

b = maximum

The following steps can be followed to simulate the fluid contacts levels:

1. generate deviations randomly assuming a triangular distribution (minimum, mode, and maximum).
2. run L realizations with different seed numbers.
3. calculate HIIP for each realization and get a HIIP distribution.

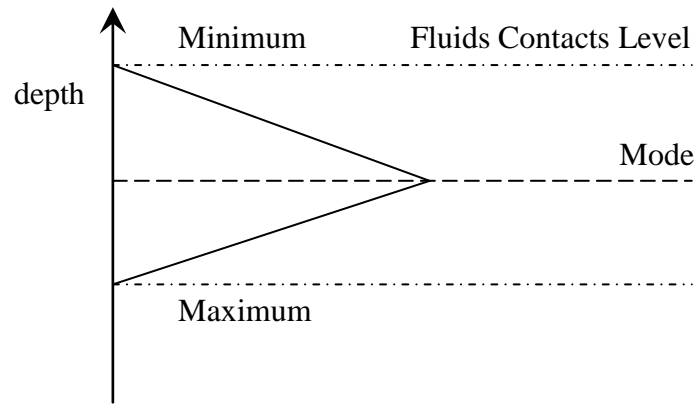


Figure 5-2: Uncertainty in Fluids Contacts Level without PU can be simulated by using MCS with assuming a triangular distribution.

MCS technique can be used to generate realizations for depths of fluid contacts such as gas-oil contact (GOC), gas-water contact (GWC), and oil-water contact (OWC). Different distributions, such as double triangular distributions (Behrenbruch et.al., 1985) and uniform distributions, might be assumed to represent fluid contacts levels. Uniform distribution can be used in the early

stages of reservoir life with the absence of data because it is a convenient and well understood source of random variation. Sometimes it is used to represent a worst case scenario for variation when doing sensitivity analysis.

As the most likely outcome can be determined, then the triangular distribution might be the best choice. Another advantage for the triangular distribution is that it is used for a variable not suitable for a normal distribution, because it is either bounded or not symmetrical.

5.1.3. Cosimulation with Super Secondary Data

An important consideration when calculating reserve volumes is the correlation between some parameters. For example, NTG, ϕ , and Sw have some relationship with thickness and may have a relation between each other. Another consideration is correlation to other data types such as seismic and sparse well data. These correlations must be resolved by a different technique than SGS.

A cosimulation technique with super secondary data is used to quantify the uncertainty in petrophysical properties such as NTG, ϕ , and Sw. Many realizations of those petrophysical properties can be generated simultaneously by using an *ultimate_sgsim* program. This program was generated by CCG Group for collocated cokriging using a super secondary variable (Babak and Deutsch, 2007).

First, NP or NTG can be inferred from well logs. Generally, the procedure involves exclusion of log intervals judged to be noncommercial, the remainder being considered net pay. The relationship between the NTG and porosity has to be considered in the simulation. Then, the minimum cutoff porosity usually selected based on a correlation between permeability and porosity, where the cutoff porosity corresponds to the minimum permeability judged to be commercial.

The following steps are required to quantify uncertainty in petrophysical properties using cosimulation with a super secondary data, that is, thickness obtained from seismic data:

- 1) calculate variables of interest (such as NTG, porosity, and Sw) at well locations.
- 2) obtain the best variogram model fitting the experimental variogram result for variables of interest.
- 3) generate correlation matrix among variables of interest.
- 4) cosimulate variables of interest with super secondary data (thickness obtained from seismic data) using the *ultimate_sgsim* program.
- 5) calculate HIIP using different realizations and get its distribution.

To simulate different realizations using cosimulating technique with super secondary data without parameter uncertainty, the reference distribution, obtained from well data, for the variable of interest was fixed and used as an input for generating all realizations of the variable of interest.

5.2. Sampling Realizations with Parameter Uncertainty

The second scenario that is novel to this research will incorporate parameter uncertainty distributions obtained from using parameter uncertainty approaches described in Chapter 3. This scenario will be conducted three times to compare the results of using different parameter uncertainty methods, BS, SBS, and CFD. In each run, four techniques will be used to assess HIIP uncertainty with parameter uncertainty. The four techniques are SGS, MCS, Cosimulating with Super Secondary data, and Multivariate Parameter Uncertainty, where the first three techniques will have some changes from those conducted without parameter uncertainty and the fourth technique will be conducted to assess HIIP uncertainty with parameter uncertainty in all variables of interest. Parameter

uncertainty in the means of variables means that the uncertainty realizations have variable means for those variables of interest.

The Multivariate Parameter Uncertainty technique is used when full uncertainty HIIP with parameter uncertainty is quantified. It is based on incorporating the correlation coefficients among variables of interest to determine the means of parameter uncertainty to eliminate the aggregation problem.

5.2.1. Multivariate Parameter Uncertainty (MVPU)

As mentioned before, this research is mainly to quantify the uncertainties in estimating the reserve/resource volumes with parameter uncertainty. The techniques described in Sections 5.1.1 through 5.1.3 needs slight changes to incorporate the parameter uncertainty distribution. To assess full uncertainty, Multivariate Parameter Uncertainty technique (MVPU) has to be used prior applying other techniques, conditional SGS, MCS, and cosimulation with super secondary data. MVPU is a stochastic approach that helps to determine the values of target means for parameter uncertainty instead of selecting the means randomly, in descending or in ascending order by incorporating the correlation coefficient among variables of interest. GSLIB-like code is used for this purpose. The code is called *correlate* created by (Neufeld and Deutsch, 2007). MVPU technique can be summarized by the following steps (followed by more details description):

- 1) Generate normal scores distributions for all variables of interest such as Top, Thickness, NTG, Porosity, and Sw. (using *n_score* code).
- 2) Generate random (independent) normal score values (w_i) (using Excel or *mcs* code). The output should have a column for each variable means:

$$w_i = w_1, \dots, w_n \quad (5-6)$$

where n = number of variables of interest.

- 3) Multiply w_i values by L where $C = LU$ (using *correlate* code).

$$Y=Lw_i \quad (5-7)$$

$$\text{Cov}\{y y^+\} = C \quad (5-8)$$

- 4) Back transform y_i to mean values for variables of interest using transformation tables from step 1 and *backtr* code.

Where $y_i = y_1, \dots, y_n$

n = number of variables of interest.

- 5) Check the correlation.

The Multivariate Parameter Uncertainty can be described in more detail in the following steps:

- 1) clean the data and calculate 2D data for variables of interest (such as NTG, porosity, and Sw) at well locations;
- 2) obtain the best variogram model fitting the experimental variogram result for variables of interest;
- 3) generate correlation coefficients matrix among variables of interest;
- 4) get a distribution of parameter uncertainty in the mean for all variables of interest using a bootstrap method;
- 5) get the transformation tables for PU distributions of all variables of interest by normal scoring their PU distributions using *nscore* code;
- 6) generate random values for means using MCS. The output will have columns of values w_i where $i = 1, \dots, n$ (n = number of interest variables). It is recommended to have each column in a separate file. The number of data should be equal to number of realizations.
- 7) Multiply w values by L where $C = LU$ (using *correlate* code).
 - i. $Y=Lw$
 - ii. $\text{Cov}\{y y^+\} = C$
- 8) back transform the results y_1, \dots, y_n to values of variables means such as Top, Thickness, NTG, Porosity, and Sw using transformation tables obtained from Step 5;

- 9) check the correlation among the back transformed values (using *corrmat* code) and compare the results to the input correlation coefficients used in step 7.
- 10) use correlated mean values in calculating uncertainty in variables of interest (such as Structure Surfaces and Petrophysical properties) using the same procedures described earlier in Sections 5.2.1 through 5.2.3; in other words, use the first value of back transformed y_1 as a Top mean and generate first realization of Top, use first value of back transformed y_2 as a Thickness mean, use first value of back transformed y_3 as a NTG mean to generate first realization of NTG, and so on. Then repeat the step for the second values to generate the second realizations for all variables of interest. Do the same process for all values of back transformed y_i (L realizations).
- 11) combine all realizations generated to quantify uncertainty in all variables of interest then calculate HIIP and get its distribution.
- 12) repeat the procedure from step 1 for a different PU method (Spatial Bootstrap and Conditional Finite Domain).

MVPU technique is important if resource/reserve volumes are estimated with full uncertainty since it accounts for correlation coefficient between all variables of interest. It is not needed if a sensitivity analysis is conducted. In case of conducting a sensitivity analysis, different realizations of a variable of interest will be used with one fixed realization (selected randomly) of the remaining variables of interest, while in case of full uncertainty, all realizations of all variables of interest will be used to calculate HIIP and get its distribution.

5.2.2. Sequential Gaussian simulation (SGS) with Parameter Uncertainty

As mentioned in Section 5.1.1, SGS is a stochastic approach that can be used to quantify uncertainty in structural surfaces. In this section, it will be modified to account for parameter uncertainty in the mean of the variable of interest. The methodology will be modified to have the uncertainty realizations shifted by a mean other than zero since there is uncertainty in the means of the variables of interest. To generate such realizations, realizations are simulated by SGS with conditioning data at well locations to be a non-zero value that is based on the mean and standard deviation of the variable of interest obtained from well data a mean of the variable of interest drawn randomly from parameter uncertainty distribution. Figure 5-3 shows illustration of sampling realizations using SGS with parameter uncertainty.

Three parameters must be established from the available reservoir data. Two of them, the base case value (structure or thickness) and a global estimate of the uncertainty in the base case surface (σ_A), were mentioned in Section 5.1.1, while the third parameter is uncertainty distribution in the mean calculated from the conventional bootstrap, the spatial bootstrap, or the conditional finite domain.

The procedure for simulating realizations using conditional SGS with parameter uncertainty can be summarized by the following steps:

- 1) generate a histogram for the data obtained at well locations;
- 2) obtain a variogram model fit to the experimental variogram result for the variable of interest (such as top and bottom surfaces and layer thickness);
- 3) calculate a distribution of parameter uncertainty in the mean for the variables of interest using a bootstrap method;

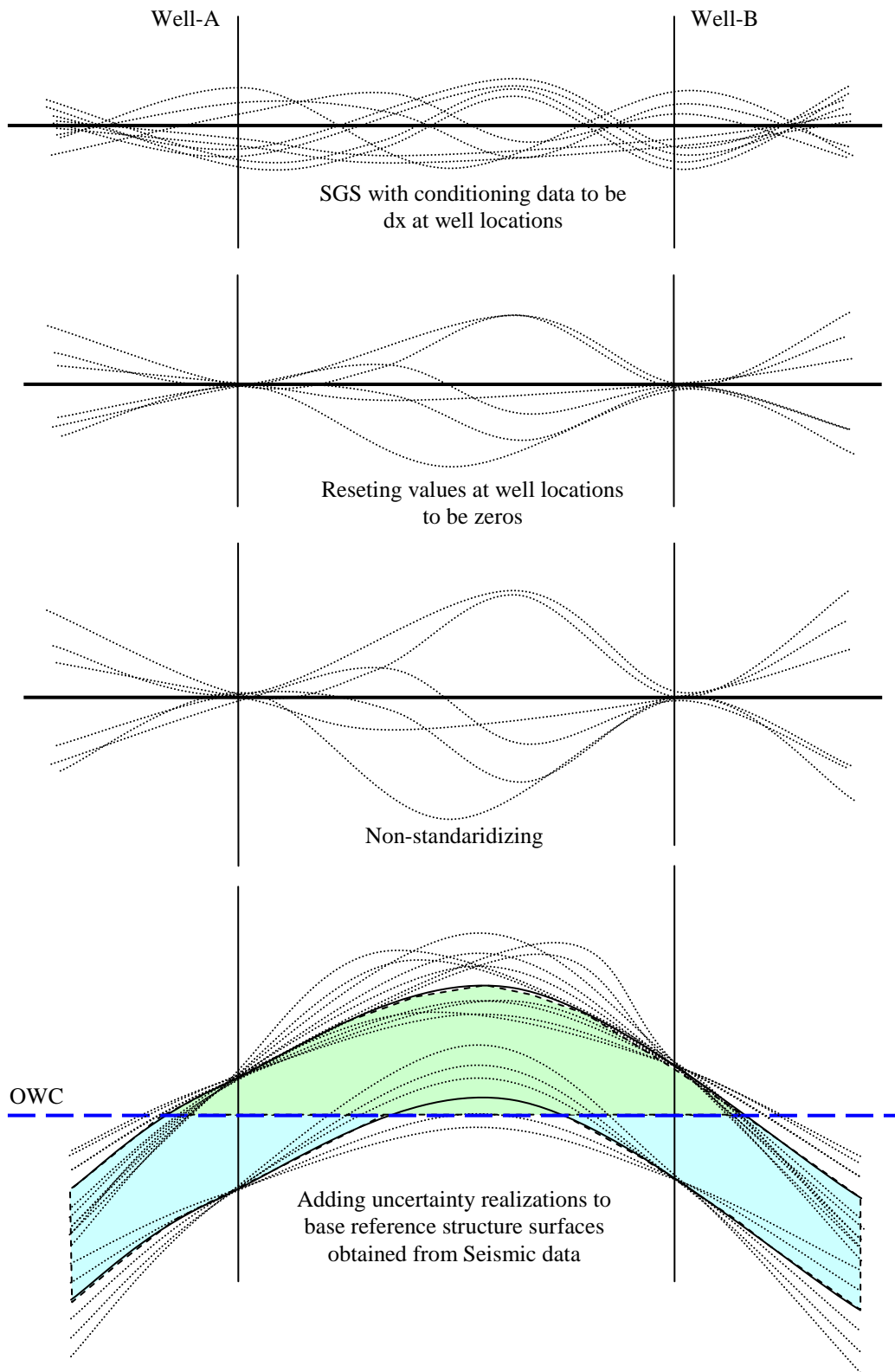


Figure 5-3: Uncertainty in top and bottom surfaces and layer thickness with PU can be simulated by using SGS with conditioning data to be non-zeros at well locations.

- 4) run SGS to generate L realizations with a mean of zero and standard deviation of one, and conditioning values at well locations to be dx;

$$dx^l = \frac{m_p^l - m_o}{\sigma_o} \quad (5-9)$$

where, $l = 1, \dots, L$

m_p^l = parameter mean drawn from parameter uncertainty distribution for the variable of interest;

m_o = a mean obtained from 2D original data for the variable of interest;

σ_o = a standard deviation obtained from 2D original data for the variable of interest;

- 5) reset values at well locations to be zero by adding (-dx) to the results of step 4;

- 6) To non-standardize the realizations by multiplying them with some standard deviations σ_Δ (referring from seismic data), then add the new results to the reference data;

$$\Delta^l(\mathbf{u}_i) = y^l(\mathbf{u}_i) * \sigma_\Delta \quad (5-10)$$

- 7) To add the results to the base reference surfaces obtained from seismic data (to the top and bottom surfaces to quantify uncertainty in top and bottom surfaces and only to the bottom surface to quantify uncertainty in layer thickness).

$$\begin{aligned} z^l(\mathbf{u}_i) &= z_b(\mathbf{u}_i) + \Delta^l(\mathbf{u}_i) \\ &= z_b(\mathbf{u}_i) + y^l(\mathbf{u}_i) * \sigma_\Delta \end{aligned} \quad (5-11)$$

- 8) To calculate the uncertainty in HIIP by calculating HIIP of each realization and generating a distribution plot.

- 9) Repeat steps 3 to 8 for PU distributions obtained from Spatial Bootstrap and Conditional Finite Domain methods.

Different random numbers can be used at each step in the simulation to avoid unwanted correlations. Care should be taken to ensure data conditioning and reasonable standard deviations at each step since determining uncertainty in

the base case surface needs a good experience of a geostatistician to calculate the standard deviations of the uncertainty in the structural parameters. The results are sensitive to those standard deviations and might underestimate or overestimate the uncertainty in resources estimations.

5.2.3. Monte Carlo Simulation (MCS)

In case of simulating fluid contacts levels with parameter uncertainty, almost the same procedure described when assessing uncertainty in fluid contacts levels without parameter uncertainty, as in Section 5.1.2, but the distribution mode has to be a variable in each realization, see Figure 5-4. The following steps summarized the procedure to simulate realizations for fluid contacts levels with parameter uncertainty in the mode:

- 1) To generate deviations randomly assuming a triangular distribution (minimum, mode, and maximum);
- 2) To run L realizations with different mode values in each realization;
- 3) To calculate HIIP for each realization and get a HIIP distribution plot.

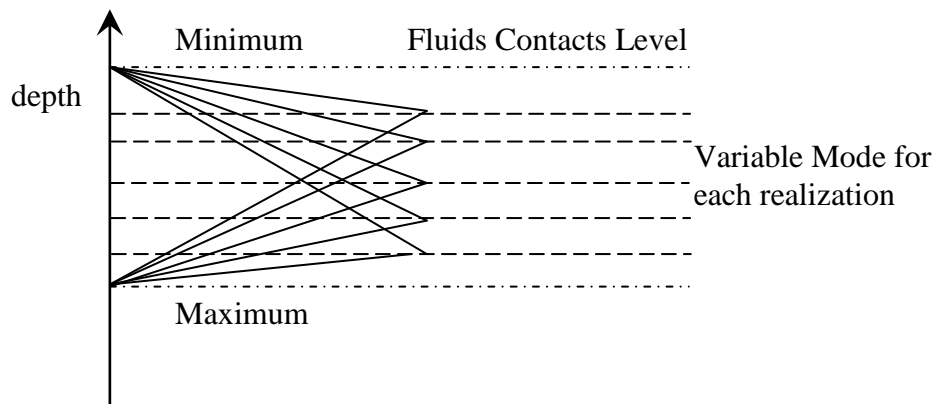


Figure 5-4: Uncertainty in Fluids Contacts Level with PU can be simulated by using MCS with assuming a variable mode triangular distribution.

The fluid contacts levels uncertainty might be also in the limits of the fluid contacts levels, the minimum and maximum, but they are assumed to be fixed in this procedure. The uncertainty in the mode of fluid contacts levels is used instead of the mean uncertainty for simplicity in calculation. Even though, the mean can be easily calculated for a triangular distribution as in equation 5-4.

5.2.4. Cosimulation with Super Secondary Data

To assess HIIP uncertainty with uncertainty in petrophysical properties, cosimulation with super secondary data is a suitable technique to be used since it incorporates the correlation among the variables of interest and the secondary data. Some changes to the steps described in Section 5.1.3 are required to incorporate the parameter uncertainty distribution.

Petrophysical properties such as NTG, ϕ , and Sw can be simulated sequentially or simultaneously. To account for parameter uncertainty, the changes to the methodology will be the input reference histogram used in the cosimulation. It has to be different in each realization based on shifting the original reference histogram to a new mean drawn from parameter uncertainty distribution.

In case of assessing resource volumes with full uncertainty, MVPU technique, as mentioned in Section 5.2.1, is used to determine the mean values for the petrophysical properties, where those mean values have to be used to generate different reference distributions. To shift the reference distribution, there are two approaches can be applied, addition and multiplication approaches. The addition approach is based on shifting the original data mean to a new mean by adding the difference between those two means to all original data as shown in the following equations:

$$\Delta m = m_o - m_p \quad (5-12)$$

$$xn_l = \Delta m + x_l \quad (5-13)$$

Where m_o = the mean of original data.

m_p = the parameter mean obtained from parameter distribution.

Δm = the difference between original data mean and parameter mean.

x_l = a value of variable of interest at l sampled location.

xn_l = the new shifted value of variable of interest at l sampled location.

This approach has a disadvantage that the data might be assigned to values out of its real limits from the two sides, over or below the limits. For example a porosity value can not be zero or negative. Also, NTG is always between 0 and 1 and can not out of this range.

On the other hand, the multiplication approach is based on using the following equations to shift the reference distribution:

$$xn_l = x_l * \frac{m_p}{m_o} \quad (5-14)$$

where m_o = the mean of original data.

m_p = the parameter mean obtained from parameter distribution.

x_l = a value of variable of interest at l sampled location.

xn_l = the new shifted value of variable of interest at l sampled location.

The multiplication approach might cause some values of the variable of interest exceeding the trimming limits as the addition approach does. In addition, the multiplication approach changes the standard deviation of the original data. Regardless of which approach is used, all data exceeding the limits are deleted

from the distribution and the mean of the remaining data has to be recalculated then shifted again to the parameter mean (iterative process).

Next step is to use those different reference distributions as input in the cosimulation process to simulate different realizations for petrophysical properties with parameter uncertainty. The required steps are as follows:

- 1) calculate 2D data for variables of interest (such as NTG, porosity, and Sw) at well locations;
- 2) obtain the best variogram model fitting the experimental variogram result for variables of interest;
- 3) generate correlation matrix among variables of interest;
- 4) get a distribution of parameter uncertainty in the mean using a bootstrap method;
- 5) use L reference files obtained from original data file by shifting its distribution to a new mean, which is drawn from parameter uncertainty distribution;
- 6) generate L realizations by cosimulating variables of interest with supersecondary data (thickness obtained from seismic data) using an *ultimate_sgsm* code with changing the reference file for each realization;
- 7) calculate HIIP using different realizations and get its distribution.
- 8) repeat the procedure from step 4 for a different parameter uncertainty method (Spatial Bootstrap and Conditional Finite Domain).

All realizations of all variables of interest are used in the calculations to assess full uncertainty in resource/reserve estimations, but there is no base scenario in simulating realizations for petrophysical properties. Therefore, different realizations of the variable of interest will be used with one fixed realization selected randomly for each of the remaining variables to conduct a sensitivity analysis.

5.3. Work Flow

Figure 5-5 illustrates a work flow for quantifying HIIP uncertainty without parameter uncertainty in the mean.

Figure 5-6 illustrates a work flow for sampling realizations for structural surfaces without parameter uncertainty in the mean.

Figure 5-7 illustrates a work flow for sampling realizations for fluids contacts levels without parameter uncertainty in the mode.

Figure 5-8 illustrates a work flow for sampling realizations for Petrophysical Properties without parameter uncertainty in the mean.

Figure 5-9 illustrates a work flow for quantifying HIIP uncertainty with parameter uncertainty in the mean.

Figure 5-10 illustrates a work flow for Multivariate Parameter Uncertainty.

Figure 5-11 illustrates a work flow for sampling realizations for structural surfaces with parameter uncertainty in the mean.

Figure 5-12 illustrates a work flow for sampling realizations for fluids contacts levels with parameter uncertainty in the mode.

Figure 5-13 illustrates a work flow for preparing different reference distributions by shifting the original data.

Figure 5-14 illustrates a work flow for sampling realizations for Petrophysical Properties with parameter uncertainty in the mean.

Quantifying HIIP uncertainty without Parameter Uncertainty in The Mean (5.1)

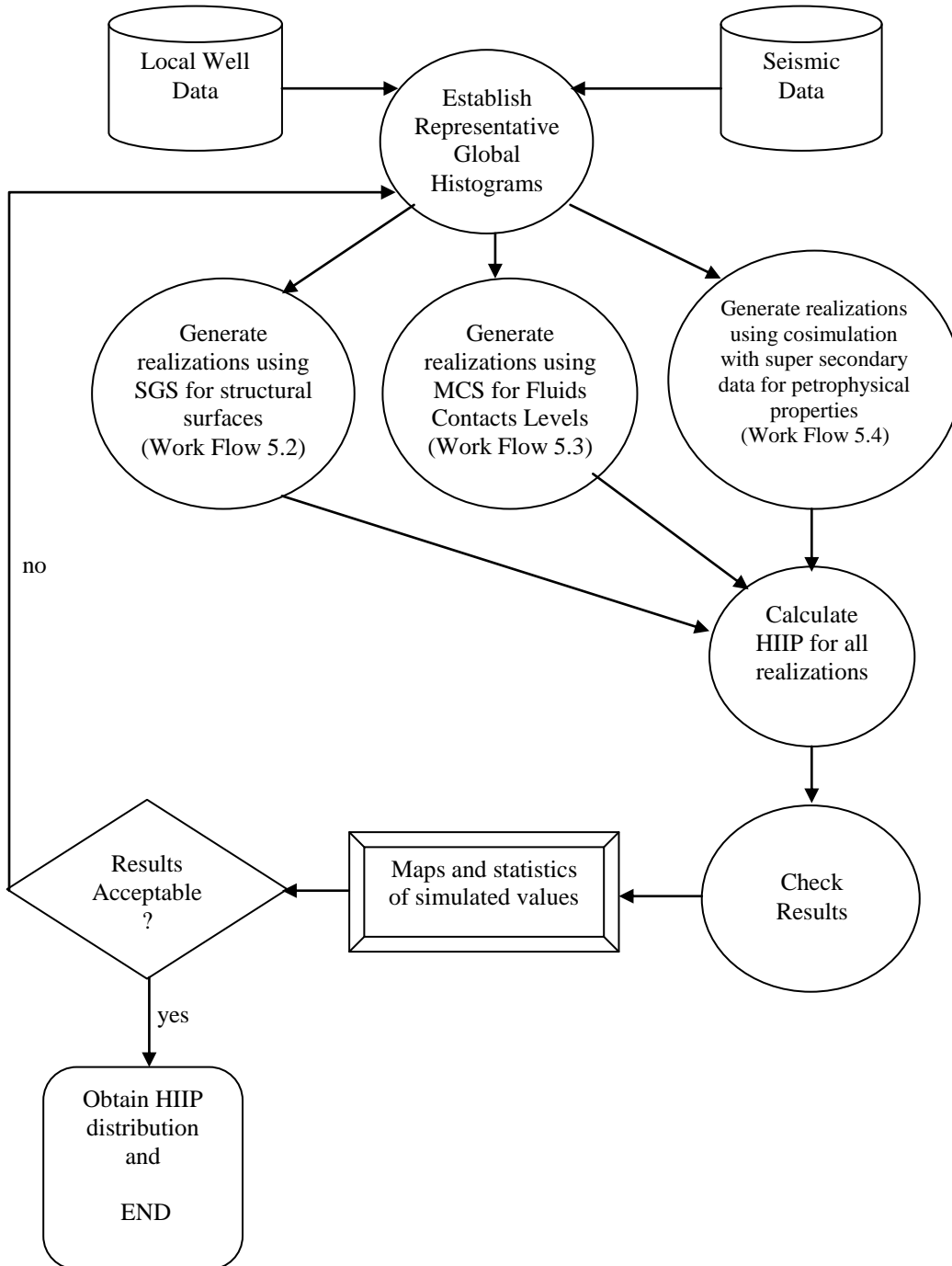


Figure 5-5: Work Flow 5.1: Quantifying HIIP uncertainty without Parameter Uncertainty in The Mean.

Sampling Realizations for Structural Surfaces without Parameter Uncertainty (5.2)

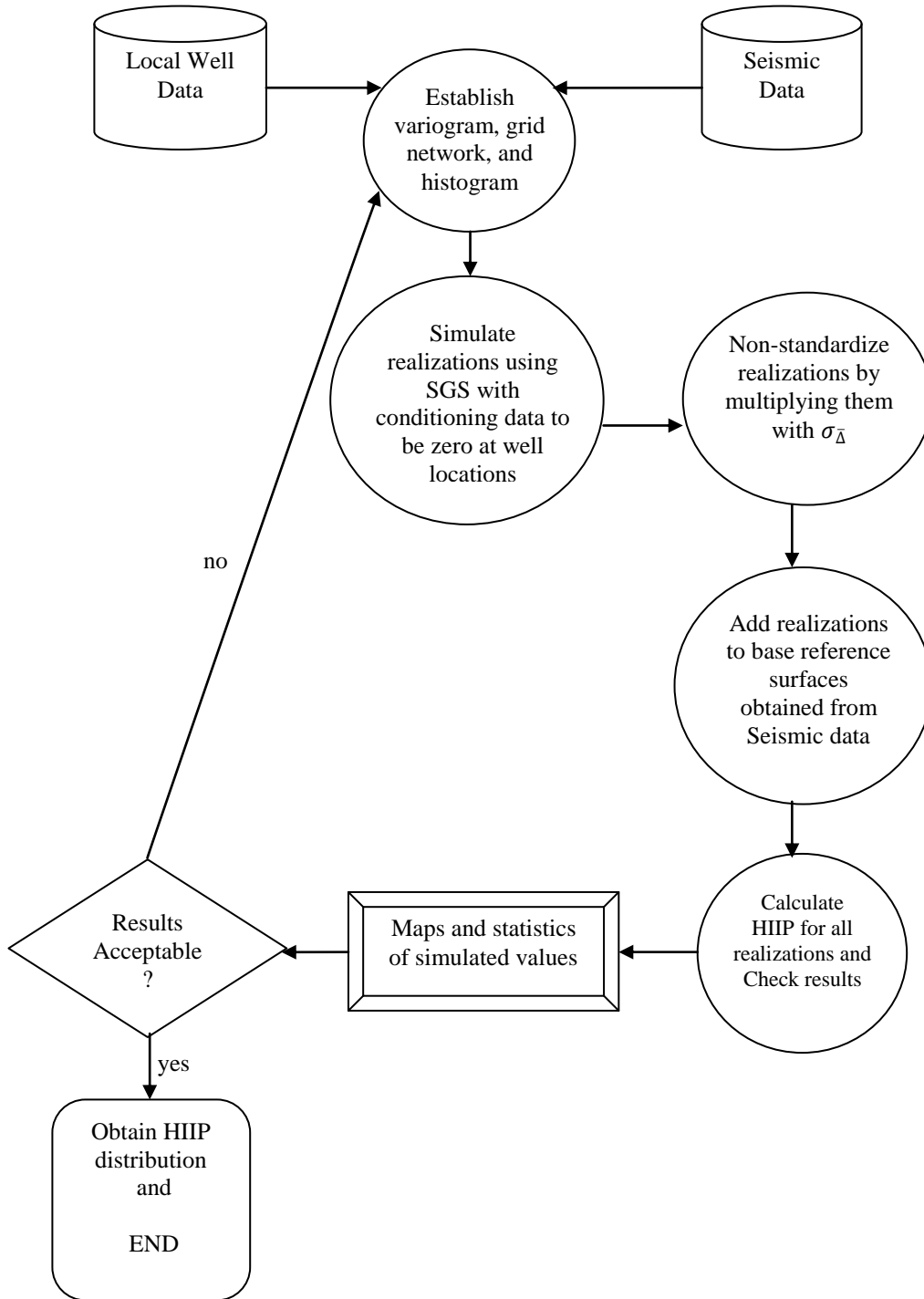


Figure 5-6: Work Flow 5.2: Sampling Realizations for Structural Surfaces without Parameter Uncertainty.

Sampling Realizations for Fluid Contacts Levels without Parameter Uncertainty (5.3)

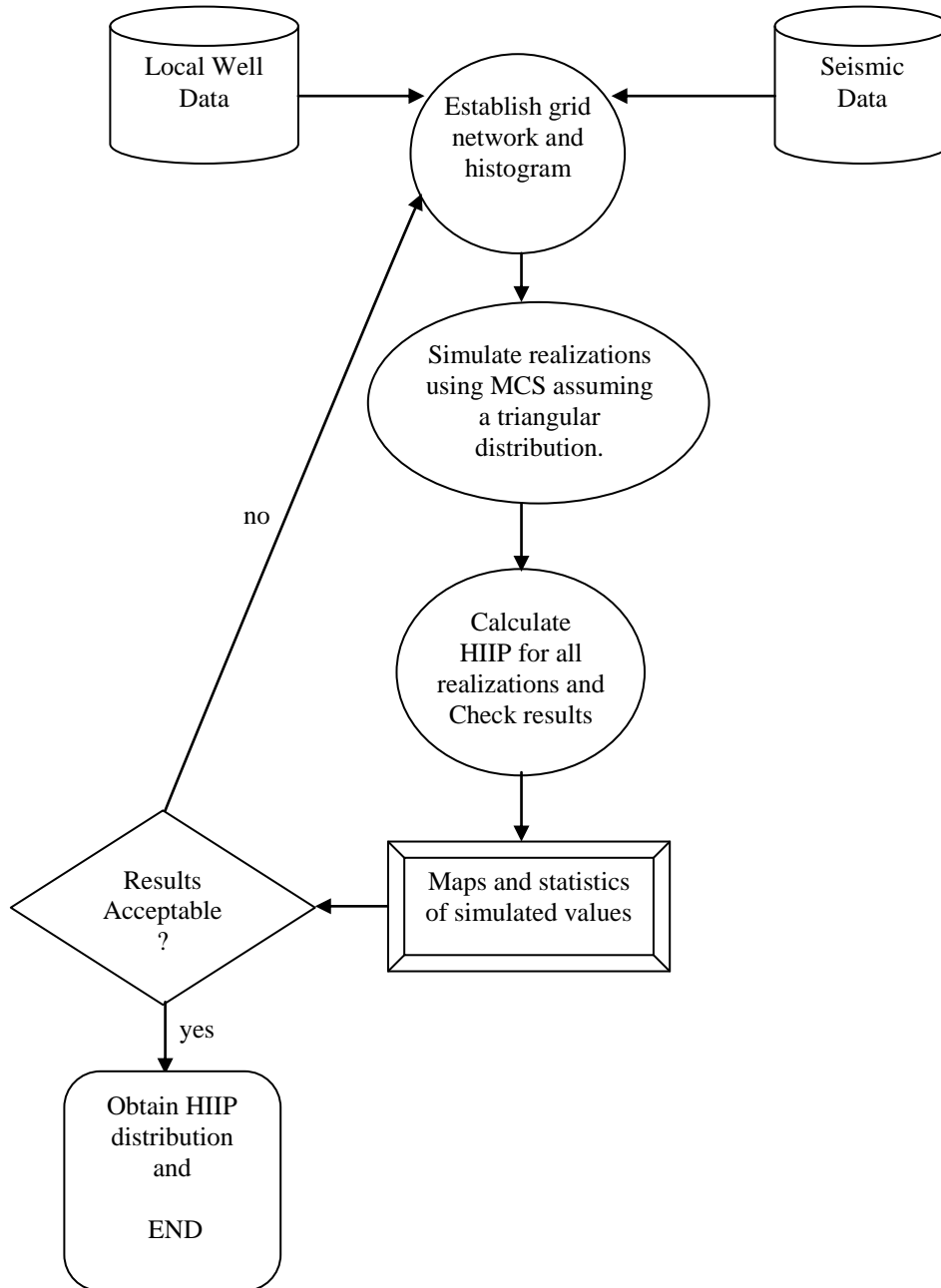


Figure 5-7: Work Flow 5.3: Sampling Realizations for Fluids Contacts Levels without Parameter Uncertainty.

Sampling Realizations for Petrophysical Properties without Parameter Uncertainty (5.4)

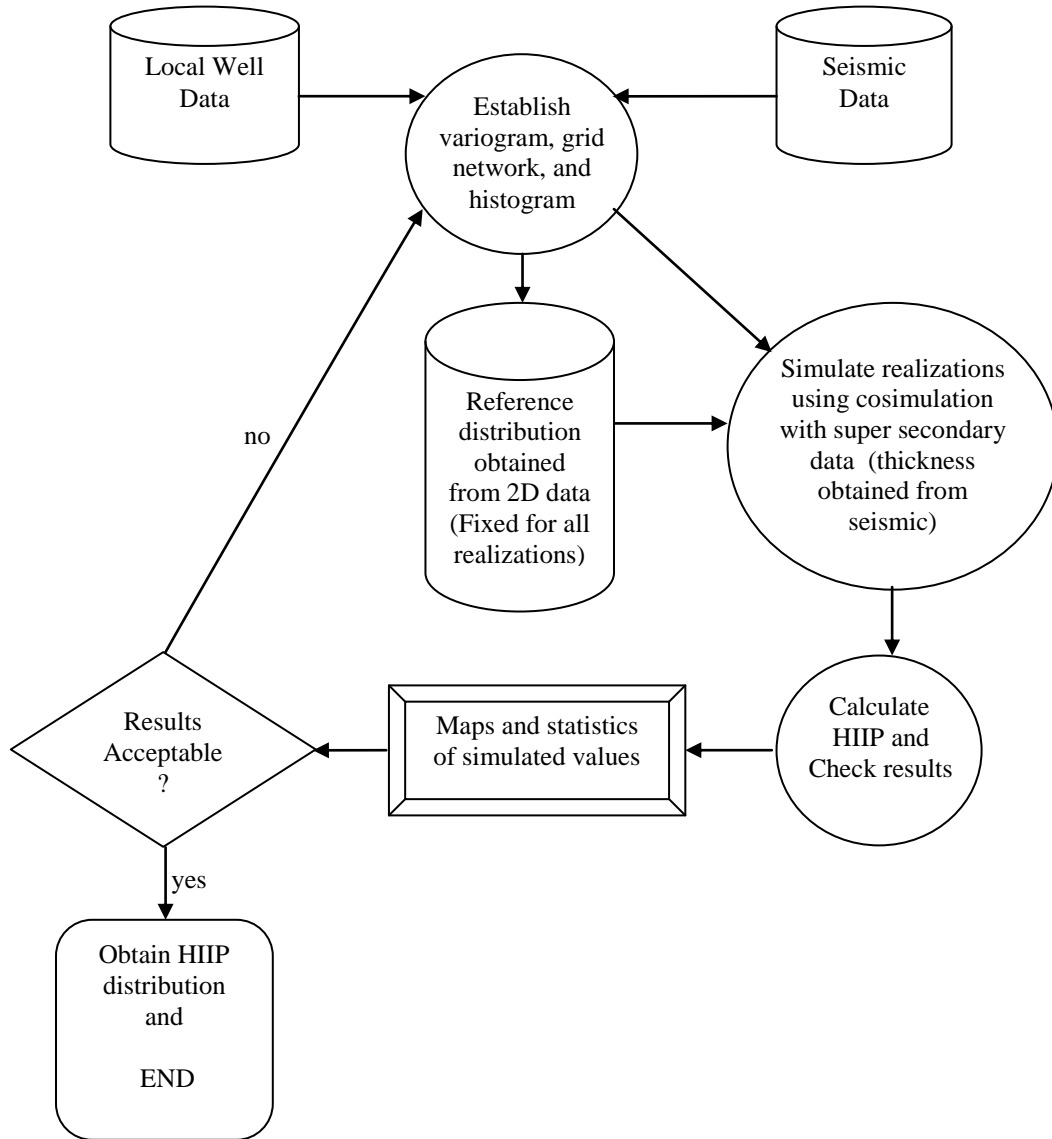


Figure 5-8: Work Flow 5.4: Sampling Realizations for Petrophysical Properties without Parameter Uncertainty.

Quantifying HIIP uncertainty with Parameter Uncertainty (5.5)

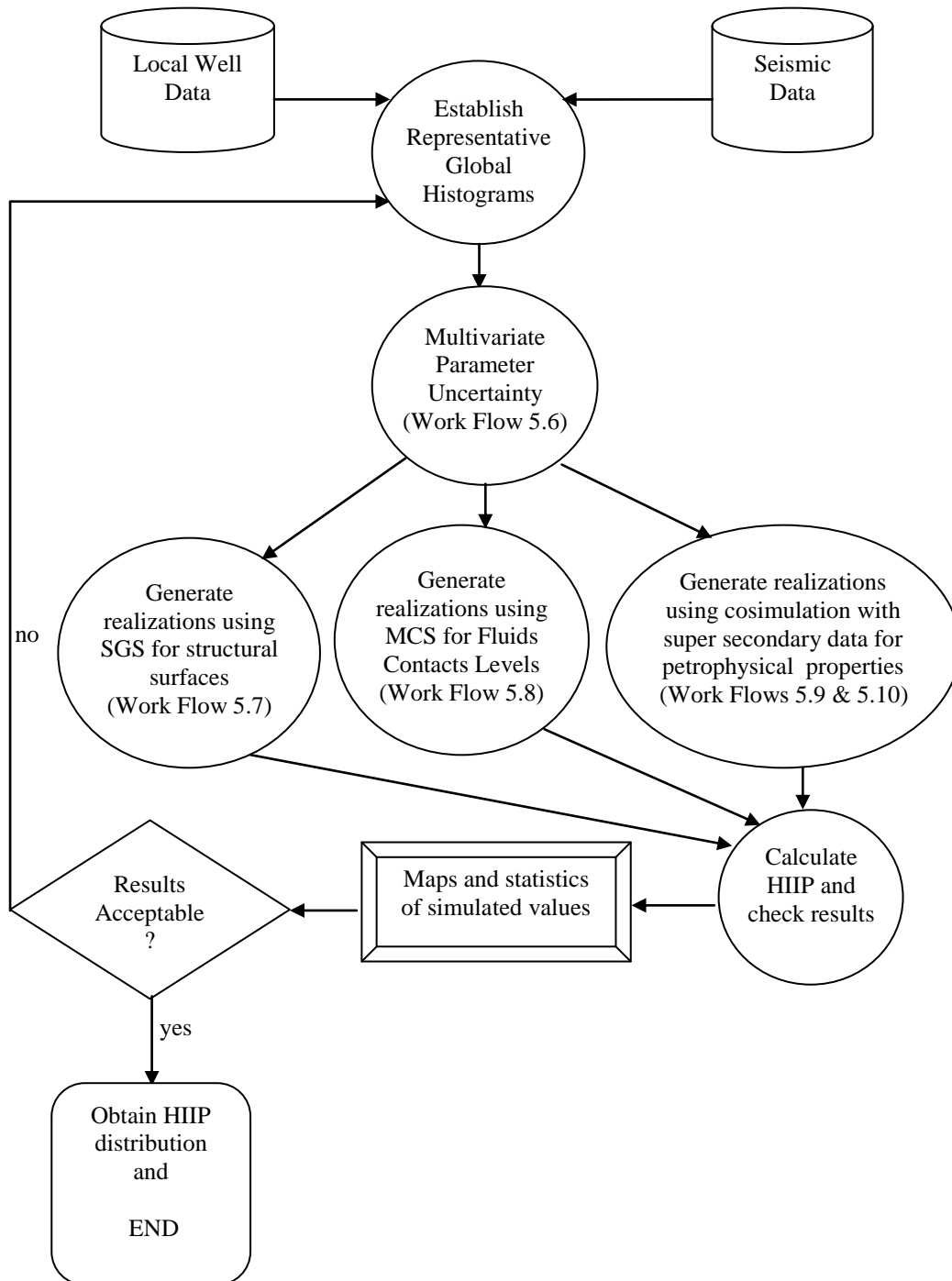


Figure 5-9: Work Flow 5.5: Quantifying HIIP uncertainty with Parameter Uncertainty.

Multivariate Parameter Uncertainty (5.6)

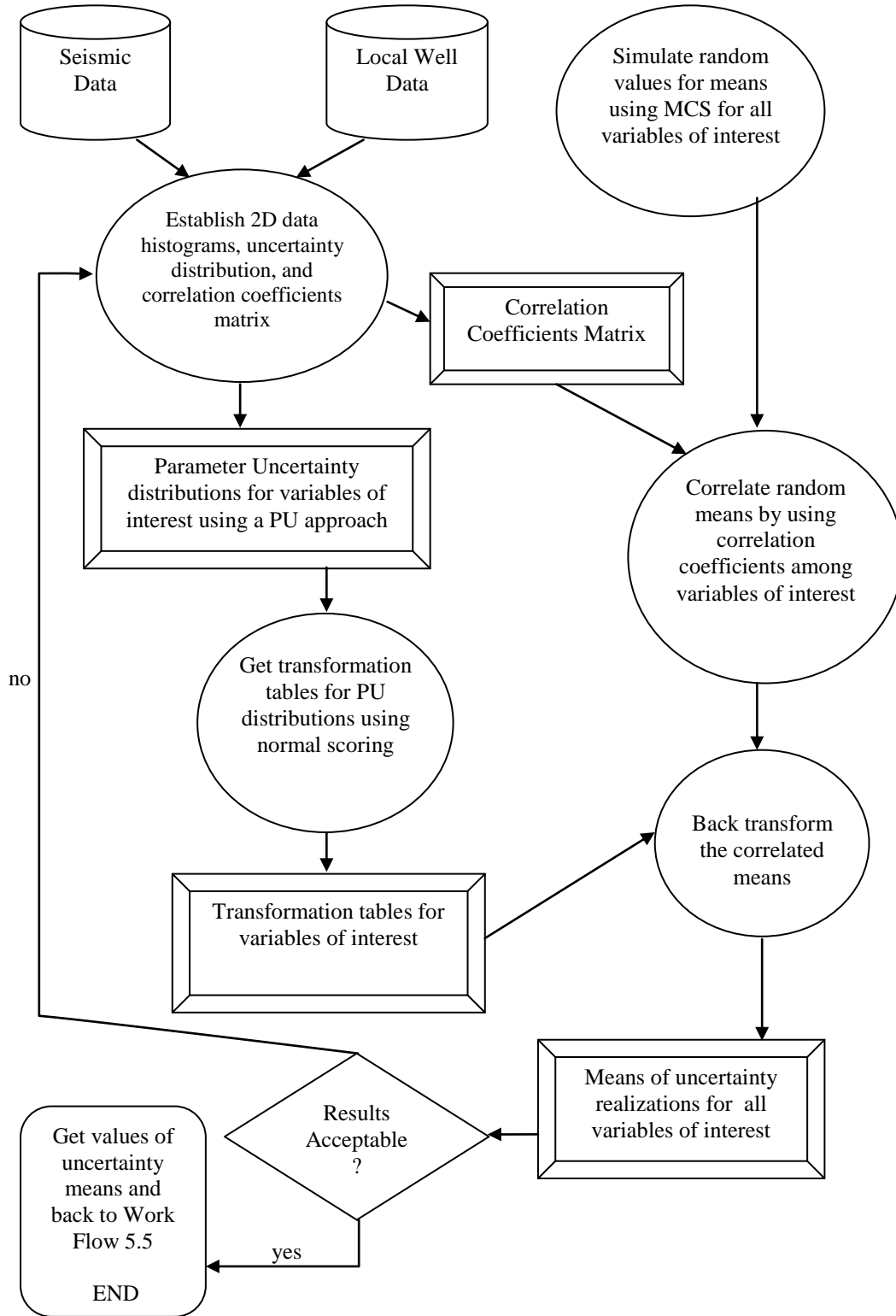


Figure 5-10: Work Flow 5.6: Multivariate Parameter Uncertainty.

Sampling Realizations for Structural Surfaces with Parameter Uncertainty (5.7)

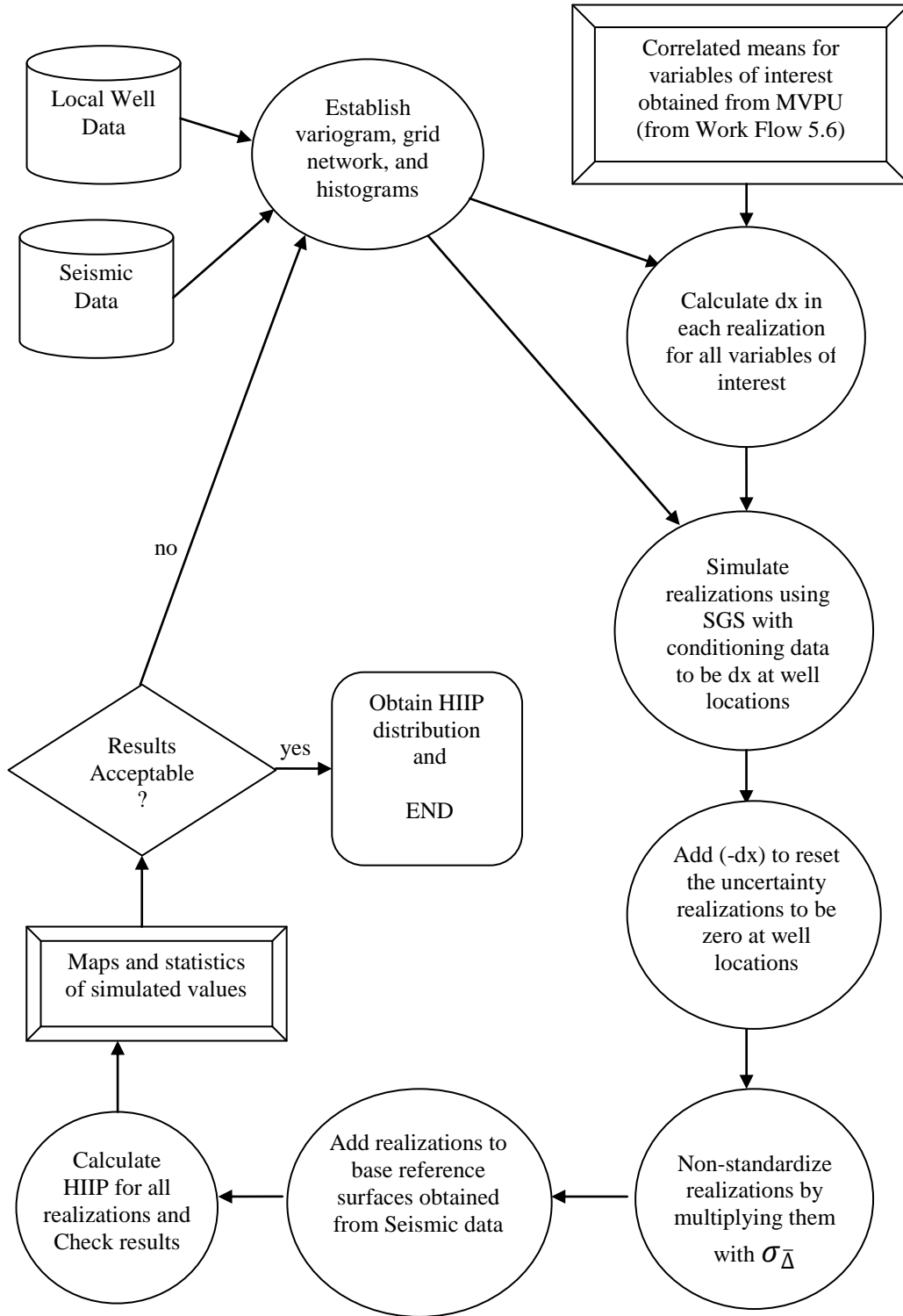


Figure 5-11: Work Flow 5.7: Sampling Realizations for Structural Surfaces with Parameter Uncertainty.

Sampling Realizations for Fluid Contacts Levels with Parameter Uncertainty (5.8)

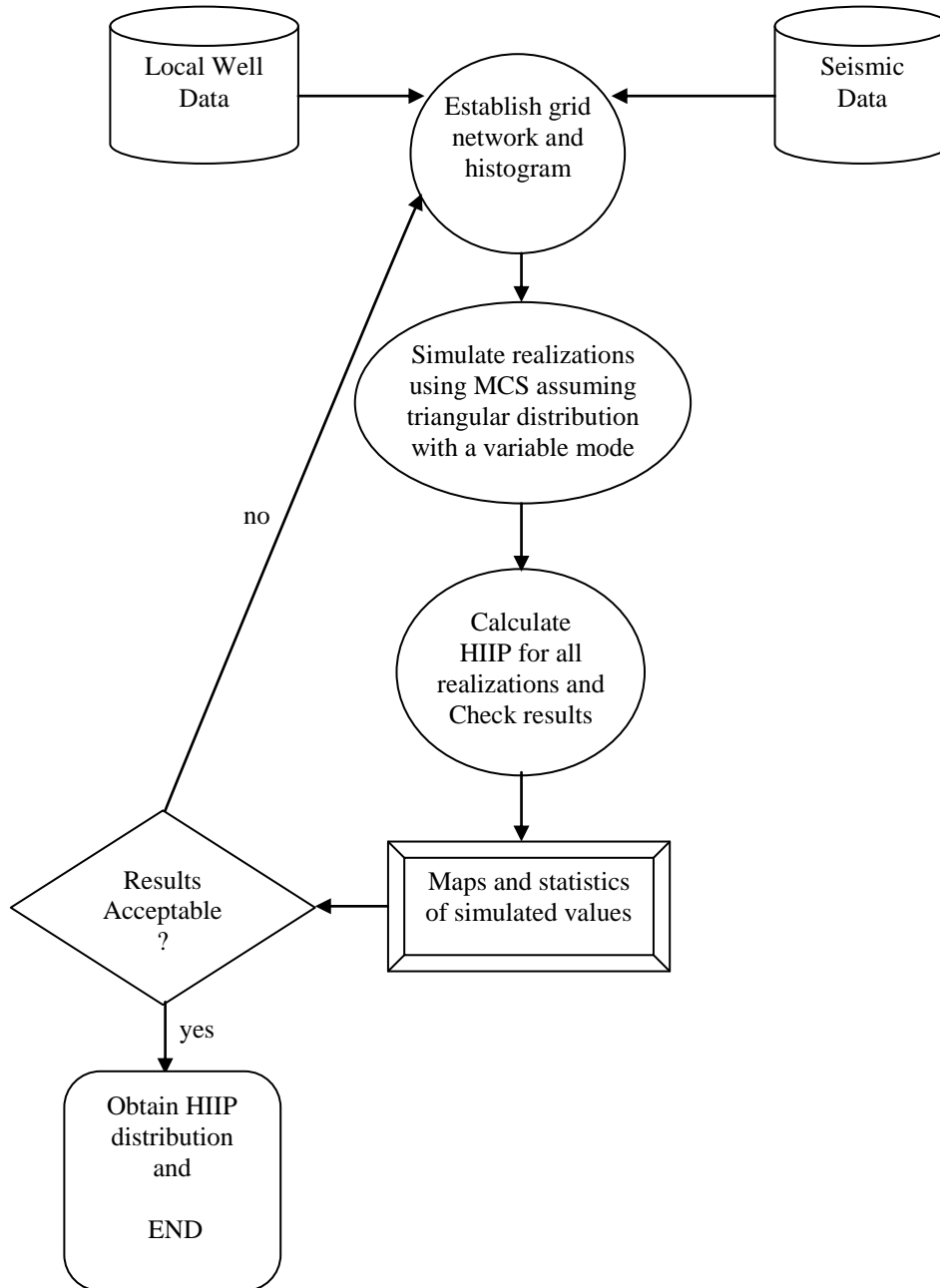


Figure 5-12: Work Flow 5.8: Sampling Realizations for Fluids Contacts Levels with Parameter Uncertainty.

Preparing Different Reference Distributions by Shifting the Original Data (5.9)

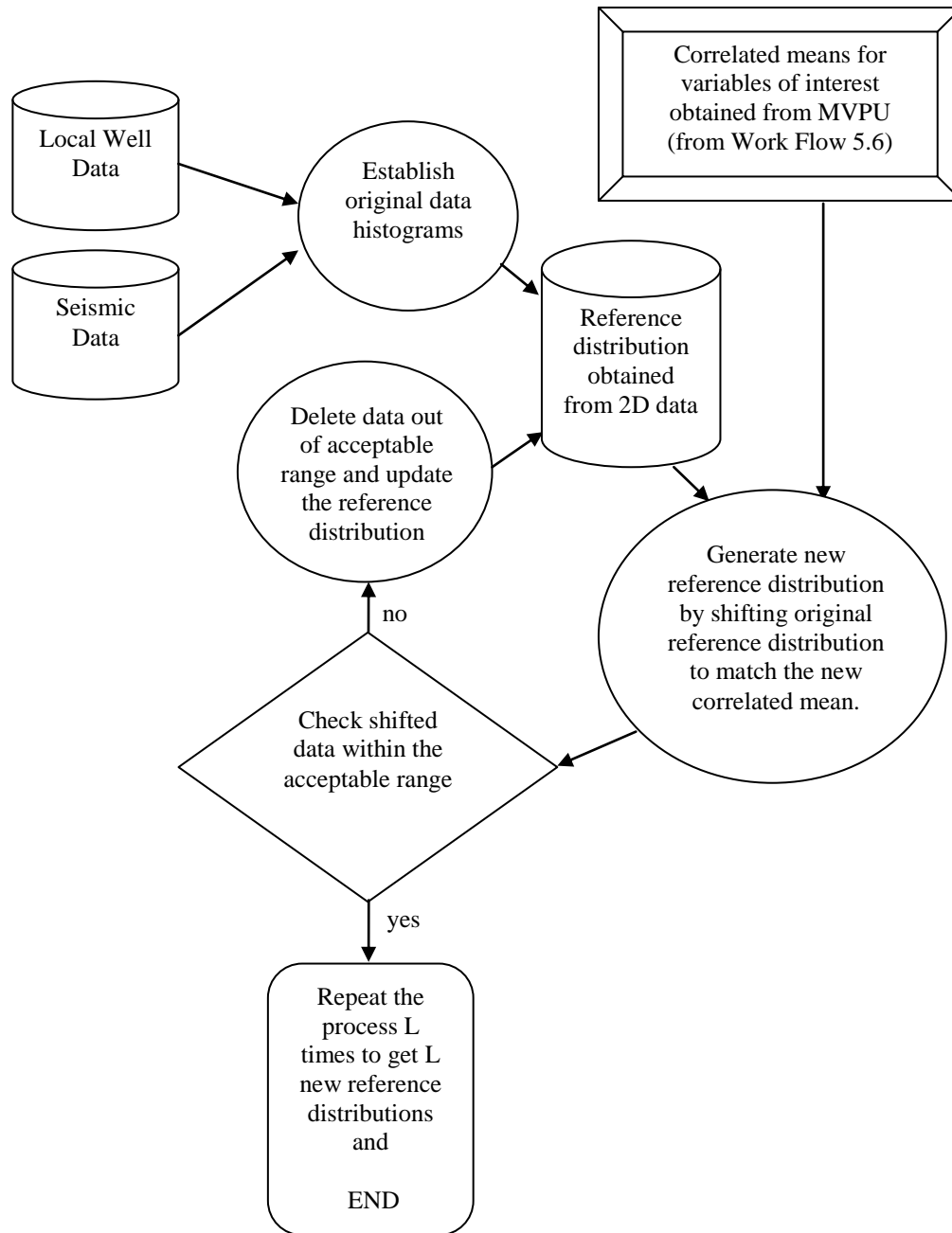


Figure 5-13: Work Flow 5.9: Preparing Different Reference Distributions by Shifting the Original Data.

Sampling Realizations for Petrophysical Properties with Parameter Uncertainty (5.10)

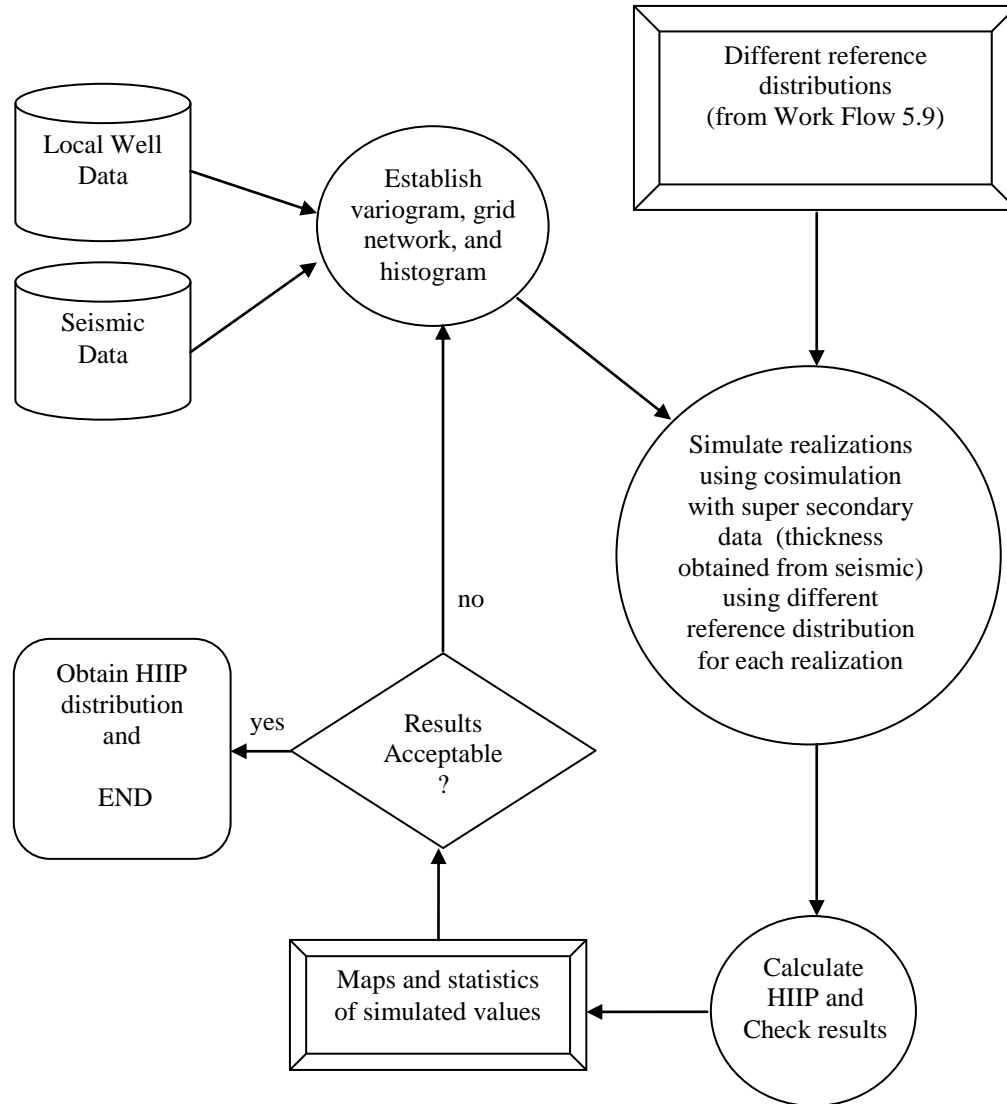


Figure 5-14: Work Flow 5.10: Sampling Realizations for Petrophysical Properties with Parameter Uncertainty.

Chapter 6

CASE STUDY

In this part, a real case will be presented using Hekla data. The Hekla reservoir is a portion of a large North Sea fluvial deposit offshore Norway. The Hekla data set is suitable for demonstrating the proposed approach described in chapter 5. The data set includes 20 wells containing petrophysical properties and seismic data defining reservoir geometry. The reservoir consists of two major layers, H1 and H2. From the seismic data, there are major faults crossing the fields diagonally as in Figures 6-1 and 6-2, which show the 2D and 3D views of H1 layer top structure of Hekla field.

6.1. Input Data

The following case study is based on data set of Hekla reservoir. The data are available in two data files. The first file contains seismic data defining reservoir geometry. It contains 8 columns about seismic data defining reservoir geometry (X-Coordinate, Y-Coordinate, H1 Top depth, H2 Top depth, H3 Top depth, H1 Impedance, H2 Impedance, H3 Impedance). The second file contains 20 well data. It includes 12 columns of well data (Well ID, X-Coordinate, Y-Coordinate, Depth, Acoustic Impedance, Facies, Core Porosity, Core Horizontal Permeability, Core Vertical Permeability, Log Porosity, Log Permeability). Not all data in the input files were used in this research.

By analyzing the seismic data, it is obvious that the reservoir consists of two major layers, H1 and H2. It is also gridded horizontally into a 101 x 131 cells,

	Minimum	Maximum	Cell Size (meters)	No. of Cells
X-Coordinate	0	5000	50	101
Y-Coordinate	0	6500	50	131

Table 6-1: Summary of Reservoir Grids

and each cell represents 50 meters in two directions, X and Y (see Table 6-1), where X axis represents the horizontal direction from West to East and Y axis represents the vertical direction from South to North. From the seismic data, 2D and 3D views of H1 top surface are shown in Figures 6-1 and 6-2 to give an idea about the field structures and trends. Figures 6-3 and 6-4 show the contour maps for the top surface depth of both H1 and H2 layers with the distribution of the twenty well locations. Also, Figures 6-5 and 6-6 show the contour maps for H1 and H2 layer thickness with the wells distribution in the field. From all those six maps view, it was noticed that the low thickness-thin areas crossing the field have

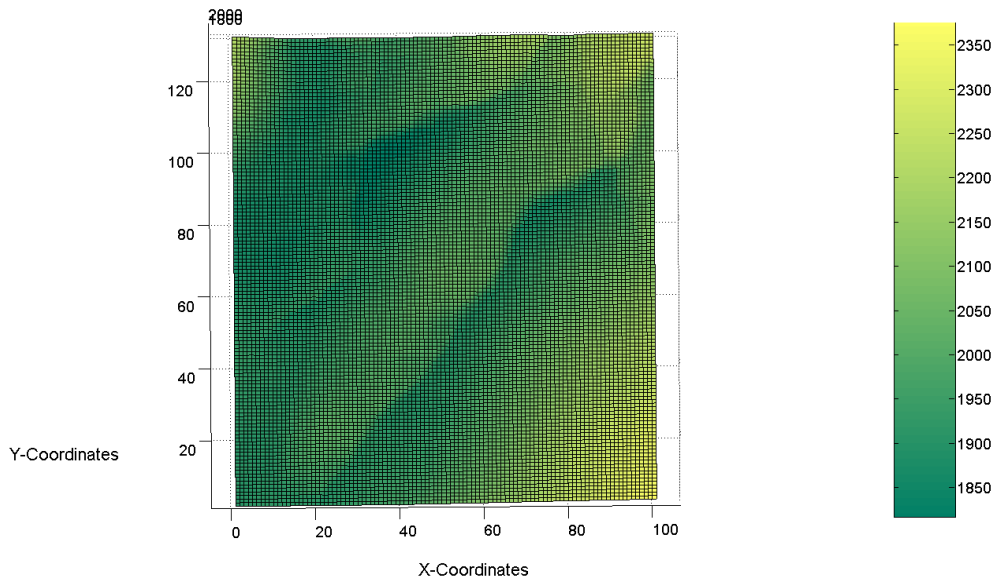


Figure 6-1: 2D map view of Top Surface of H1 Layer in Hekla field. There are two faults in the field structure as shown in the map. The depths are in meters.

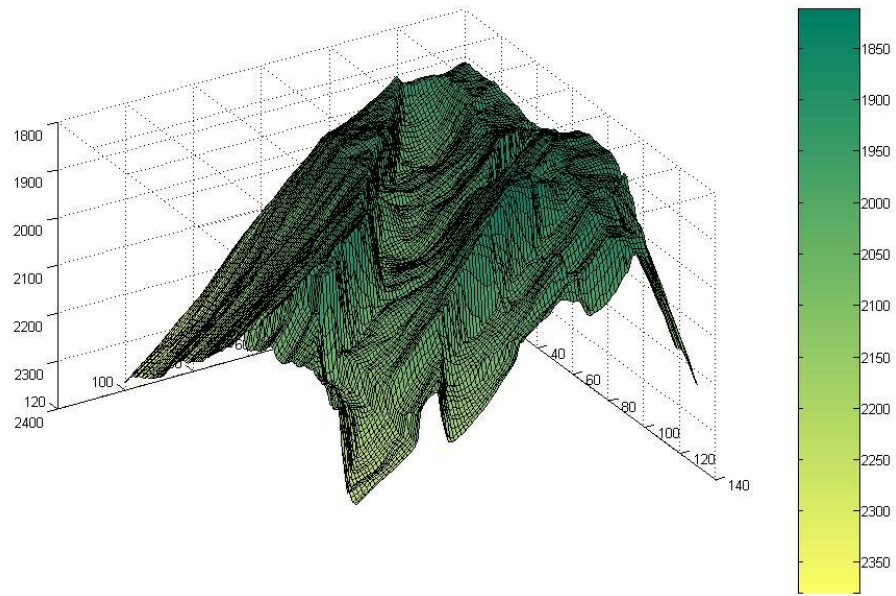


Figure 6-2: 3D map view of H1 layer top structure in Hekla field. The depths are in meters.

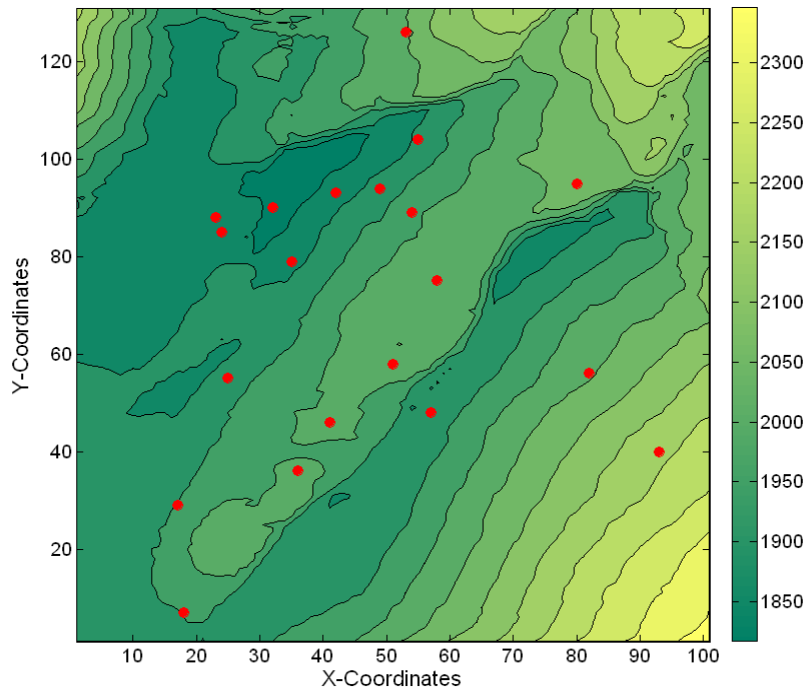


Figure 6-3: Contour map of H1 layer depth in Hekla field with showing the distribution of twenty well locations. The depths are in meters.

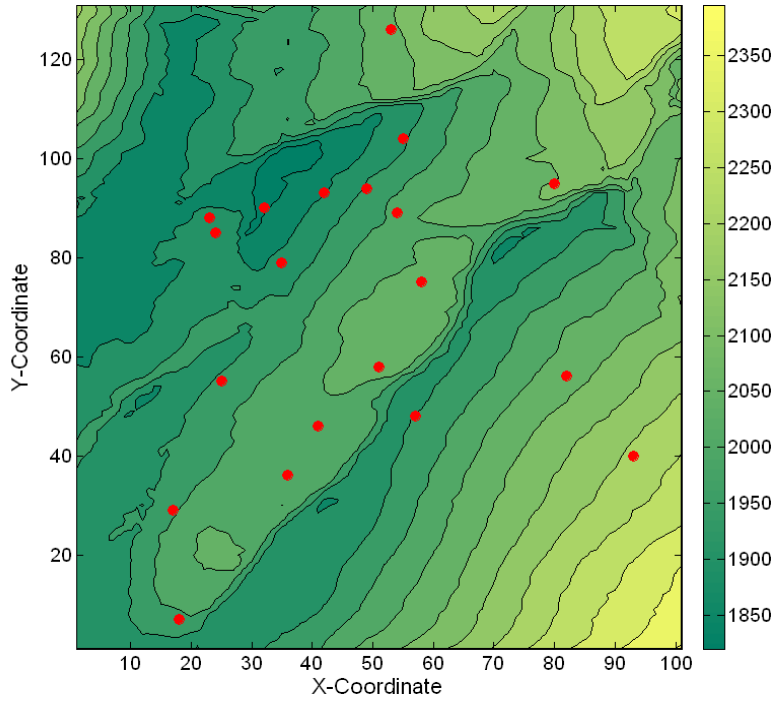


Figure 6-4: Contour map of H2 layer depth in Hekla field with showing the distribution of twenty well locations. The depths are in meters.

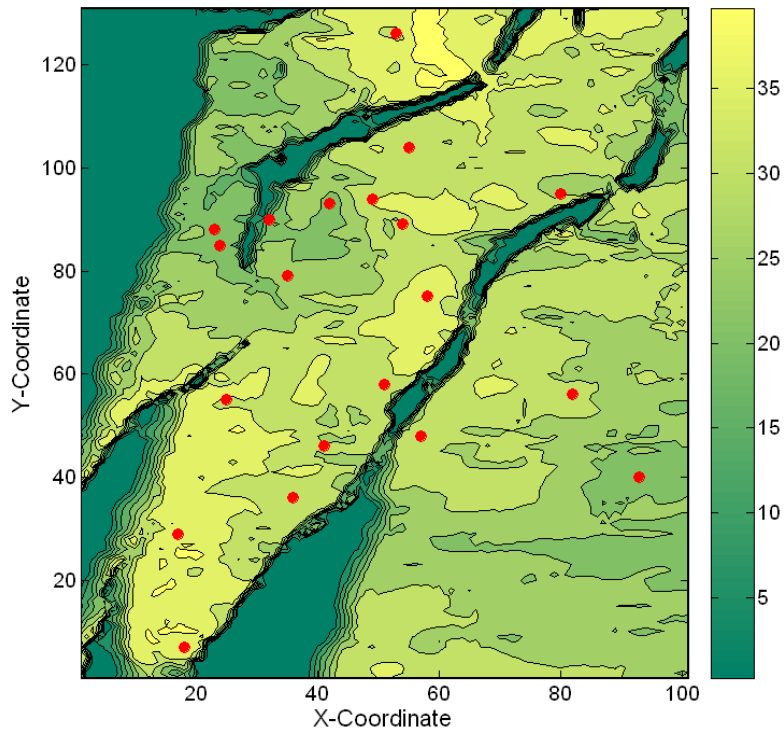


Figure 6-5: Contour map of H1 layer thickness in Hekla field with showing the distribution of twenty well locations. The thickness is in meters.

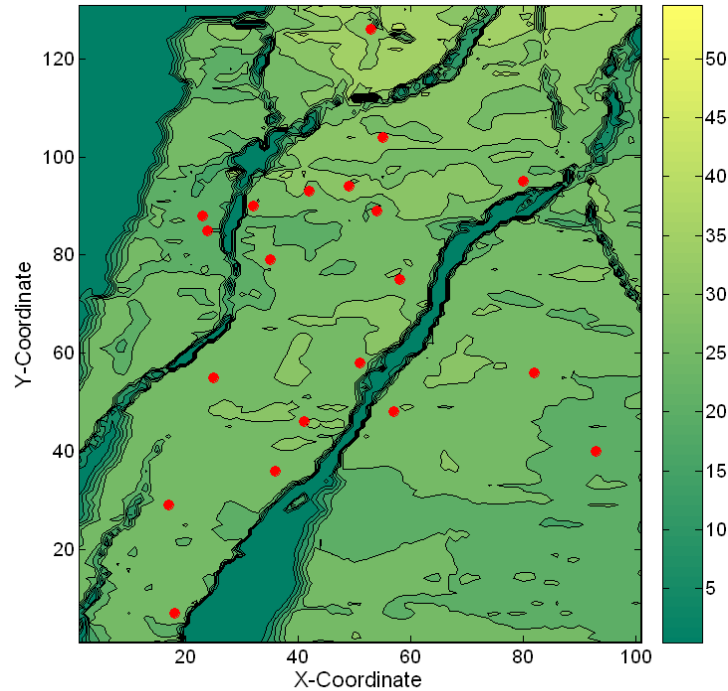


Figure 6-6: Contour map of H2 layer thickness in Hekla field with showing the distribution of twenty well locations. The thickness is in meters.

two faults. And to ensure that there are two faults, cross-sectional views are plotted at different sections of the field, see Figures 6-7 and 6-8. The views in these two figures, from top to bottom, represent the cross sectional views from West to East and South to North, respectively.

By analyzing the well data file, there are twenty existing wells. Table 6-2 summarizes well locations, depth of top structure of each layer (H1, H2, and H3), and thickness of the two layers (H1 and H2) for all wells while Well No. 8 was eliminated from the data since it is a horizontal well with length of about 1000 m. Therefore, the thickness found doesn't reflect the actual vertical thickness in the layers especially H2 layer since H3 top structure is unknown. So, the study will be based on data of 19 wells only.

The histograms for all top structure depths from logs/well data were generated for the three top structures, H1, H2, and H3 layers. Figure 6-9 shows

the results of those six histograms. As seen, that there are two populations in the histograms and they have the log-normal shape. The reason of the two populations might be the faults available in the field. There were no data about any fluid contacts levels; therefore, it was assumed that the reservoir is oil bearing with no Gas Cap while the Oil Water Contact (OWC) was assumed to be at 2150m depth as a base case.

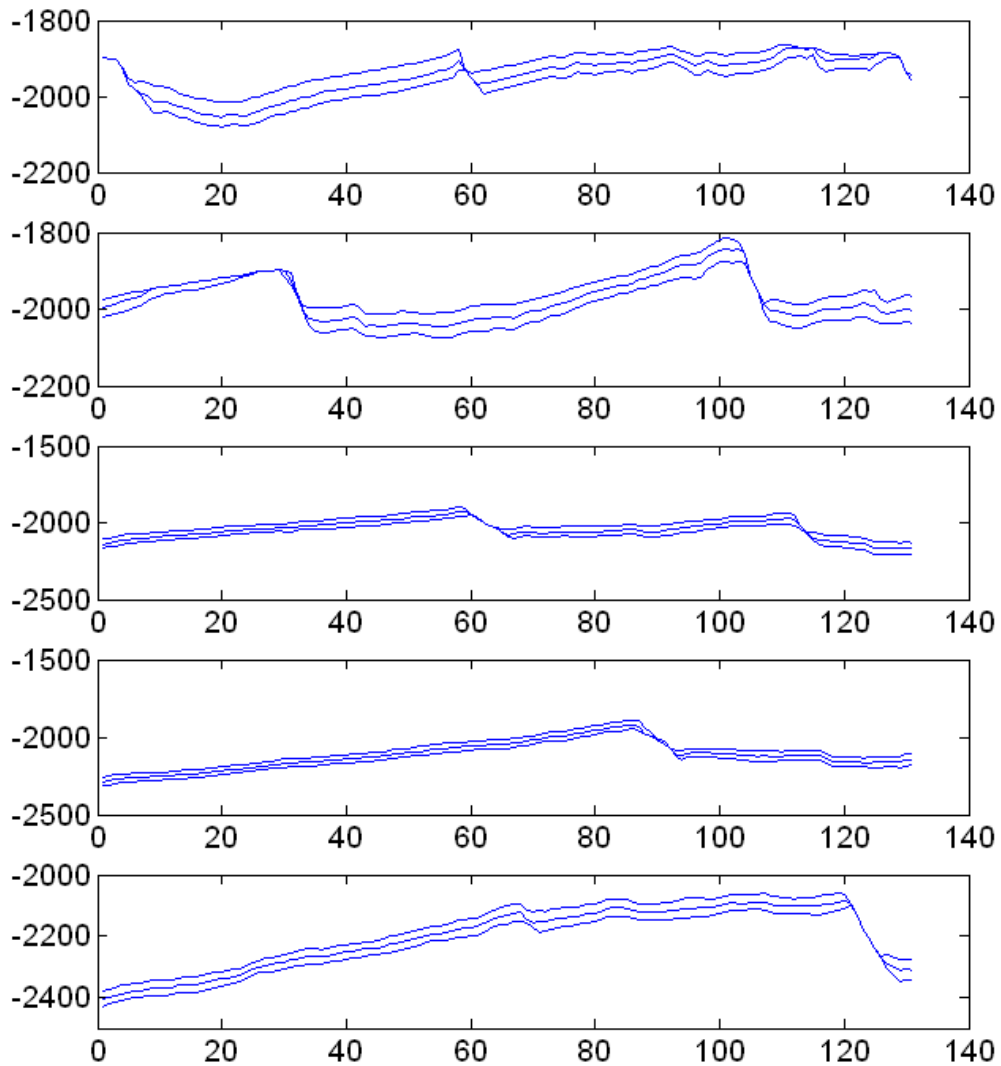


Figure 6-7: Cross Sectional views along Y-axes at different X values (X = 21, 41, 61, 81, and 101). The views from top to bottom represent the cross sectional views from west to east. The depths are in meters.

It is common to find the porosity cutoff based on a correlation between permeability and porosity, where cutoff porosity corresponds to the minimum permeability judged to be commercial. In this study, it was assumed that 10% was the porosity cutoff since it needs some works in the laboratory to be determined and it is not the aim of this study.

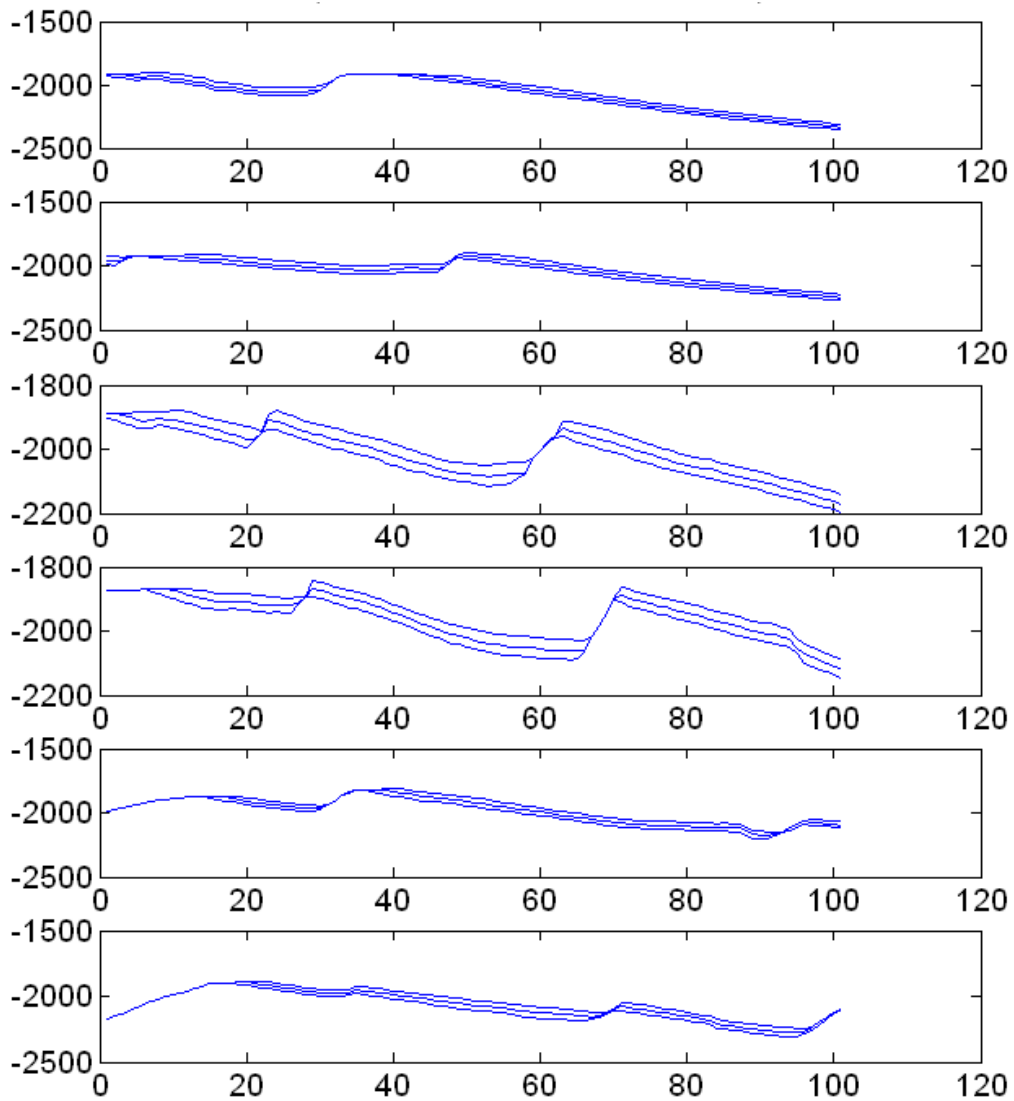


Figure 6-8: Cross Sectional views along X-axes at different Y values (Y = 21, 41, 61, 81, 101, and 121). The views from top to bottom represent the cross sectional views from south to north. The depths are in meters.

Well number	X-Coor.	Y-Coor.	Depth of Top H1	Depth of Top H2	Depth of Top H3	Thickness H1	Thickness H2
1	2618.6	6257.0	2044.2	2078.3	2110.8	34.1	32.5
2	2433.9	4679.5	1924.1	1958.3	1988.2	34.2	29.9
3	2021.5	2257.5	2012.3	2043.7	2073.5	31.4	29.8
4	4055.8	2759.5	2043.3	2075.9	2105.3	32.6	29.4
5	2667.0	4445.5	1986.7	2018.6	2046.3	31.9	27.7
6	2073.8	4630.0	1875.4	1897.4	1926.0	22.0	28.6
7	1197.0	4248.0	1889.7	1919.9	1943.3	30.2	23.4
9	3998.3	4748.0	2072.7	2103.5	2130.8	30.8	27.3
10	1747.9	3914.0	1890.5	1917.5	1943.8	27.0	26.3
11	2893.0	3733.0	2023.9	2060.9	2088.7	37.0	27.8
12	1223.8	2709.0	1928.2	1959.8	1983.3	31.6	23.5
13	2841.6	2387.5	1919.1	1954.9	1986.9	35.8	32.0
14	1797.3	1752.0	2006.4	2040.1	2067.6	33.7	27.5
15	4607.4	1990.0	2185.3	2214.2	2242.5	28.9	28.3
16	893.9	342.5	1953.0	1981.5	1987.7	28.5	6.2
17	841.8	1433.5	1957.7	1996.3	2023.6	38.6	27.3
18	2702.6	5165.0	1916.0	1950.1	1982.8	34.1	32.7
19	1583.1	4488.0	1821.6	1838.3	1862.6	16.7	24.3
20	2549.1	2889.5	2038.9	2070.9	2097.2	32.0	26.3

Table 6-2: Summary of Well Locations, Depth of Top Structure of Each Layer (H1, H2, and H3), and Thickness of the Two Layers (H1 and H2). All units are in meters.

Porosity cutoff is really effective parameter since it has a lot of effects on average porosity and net-to-gross. As porosity cutoff value increases, as average values of porosity at well locations increase and values of NTG decrease, but this relationship does not mean that average porosity and NTG are negatively correlated. Spreadsheet was used in this step to find average porosity and NTG values at well locations based on the assumed porosity cutoff. Table 6-3 shows NP, NTG, and average porosity for both layers at well locations. It is obvious that means of thickness, NP, NTG, and porosity for H1 layer are higher than those for H2 layer.

Layer 2 at well-16 is the only layer that has no pay zone detected from well logs, so its NTG is zero. Figure 6-10 shows distributions of NTG and average porosity for both H1 and H2 layers at well locations. More analysis and

comparison between those data were conducted, Figures 6-11 through 6-13 show H2 vs. H1 layer data for each well. The results show that NP and NTG in most of the wells have higher values in H1 layer, but porosity was different, where some wells have better H1 layer porosities than H2 layer ones and some wells have better H2 layer porosities than those for H1 layer.

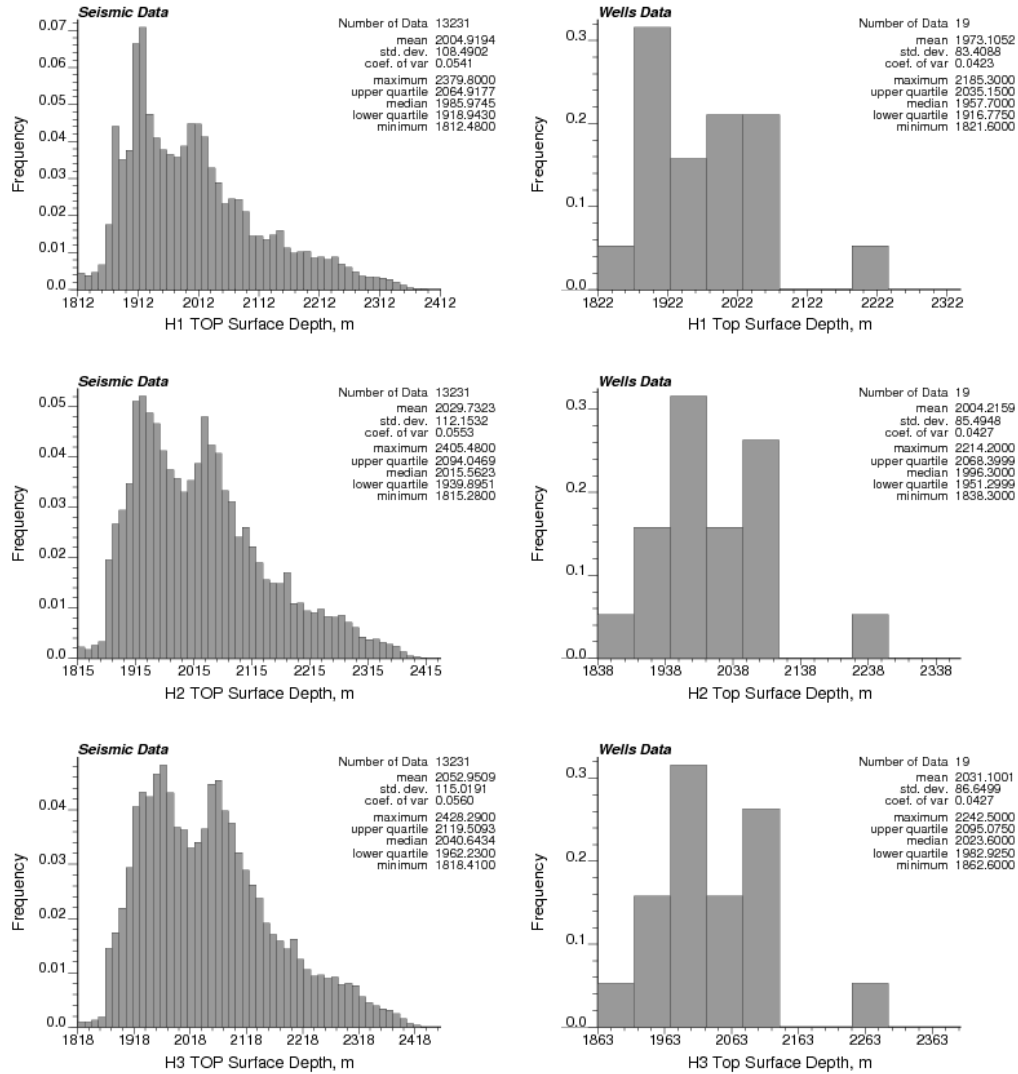


Figure 6-9: Histograms for surface structure depth for H1, H2, and H3 layers from top to bottom, respectively, and using seismic data on the left and well data on the right.

Well number	Thickness H1 (m)	Thickness H2 (m)	NP1 (m)	NP2 (m)	NTG for H1 (%)	NTG for H2 (%)	Av. Poro. H1	Av. Poro. H2	Std.Dev. Porosity-H1	Std.Dev. Porosity-H2
1	34.1	32.5	18.4	13.6	54.0	41.8	0.1898	0.1701	0.0523	0.0487
2	34.2	29.9	30.8	15.3	90.1	51.2	0.2214	0.2018	0.0637	0.0636
3	31.4	29.8	26.2	11.2	83.4	37.6	0.2032	0.2101	0.0662	0.0670
4	32.6	29.4	22.8	11.9	69.9	40.5	0.1987	0.1642	0.0613	0.0644
5	31.9	27.7	14.7	1.1	46.1	4.0	0.2381	0.1609	0.0521	0.0289
6	22.0	28.6	12.7	12.9	57.7	45.1	0.2142	0.2509	0.0686	0.0592
7	30.2	23.4	8.8	4.3	29.1	18.4	0.2116	0.1504	0.0579	0.0524
9	30.8	27.3	16.9	11.8	54.9	43.2	0.2266	0.2183	0.0614	0.0522
10	27.0	26.3	12.7	12.6	47.0	47.9	0.2625	0.1789	0.0857	0.0671
11	37.0	27.8	15.2	11.4	41.1	41.0	0.2248	0.2015	0.0587	0.0586
12	31.6	23.5	10.9	6.4	34.5	27.2	0.2074	0.2518	0.0751	0.0582
13	35.8	32.0	12.7	14.3	35.5	44.7	0.2245	0.2530	0.0855	0.0542
14	33.7	27.5	19.7	10.0	58.5	36.4	0.2558	0.2429	0.0789	0.0774
15	28.9	28.3	0.2	7.1	0.7	25.1	0.1116	0.1725	0.0066	0.0455
16	28.5	6.2	11.4	0.0	40.0	0.0	0.2546	0.0000	0.0596	NA
17	38.6	27.3	3.5	4.4	9.1	16.1	0.1914	0.1925	0.0682	0.0590
18	34.1	32.7	21.4	3.1	62.8	9.5	0.2596	0.1539	0.0528	0.0205
19	16.7	24.3	1.6	12.6	9.6	51.9	0.1308	0.1826	0.0236	0.0557
20	32.0	26.3	15.2	8.3	47.5	31.6	0.2542	0.1980	0.0586	0.0601
Minimum	16.7	6.2	0.2	0	0.7	0.0	0.1116	0.0000	0.0066	0.0205
Maximum	38.6	32.7	30.8	15.3	90.1	51.9	0.2625	0.2530	0.0857	0.0774
Mean	31.1105	26.8842	14.5158	9.0684	45.8607	32.2658	0.2148	0.1871	0.0598	0.0552
Std.Dev.	5.1155	5.6834	7.9049	4.6557	23.5292	15.9817	0.0404	0.0563	0.0189	0.0134

Table 6-3: Summary of Each Layer Thickness, Net Pay, Net-to-Gross, Average Porosity, and Porosity Standard Deviation in All 19 Wells Based on 10 % Porosity Cutoff.

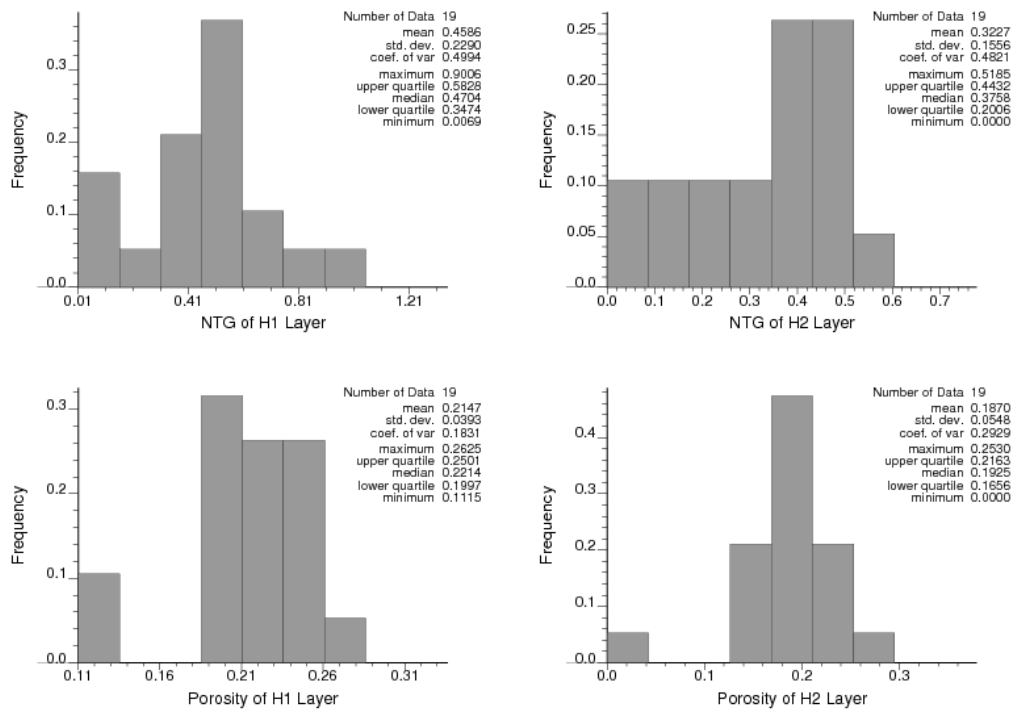


Figure 6-10: Histograms of NTG and Porosity for H1 and H2 layers obtained from well data logs.

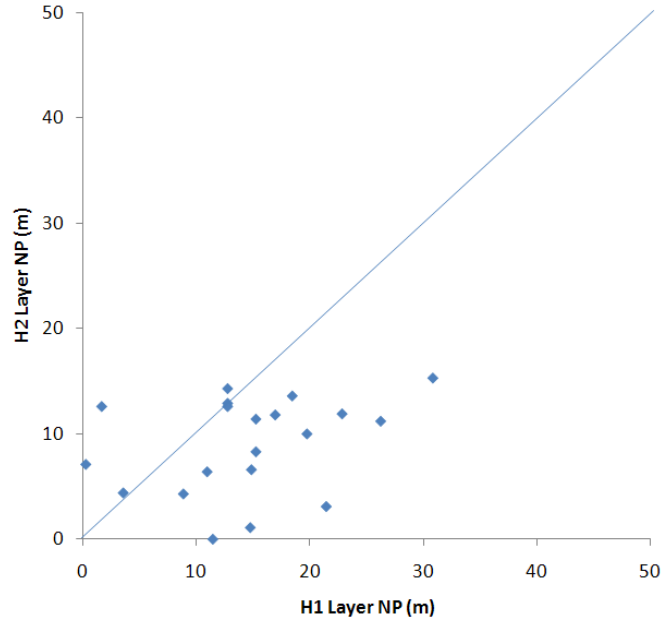


Figure 6-11: Net Pay Data at well locations: H2 layer vs. H1 layer. Most of the wells have more net pay from H1 layer.

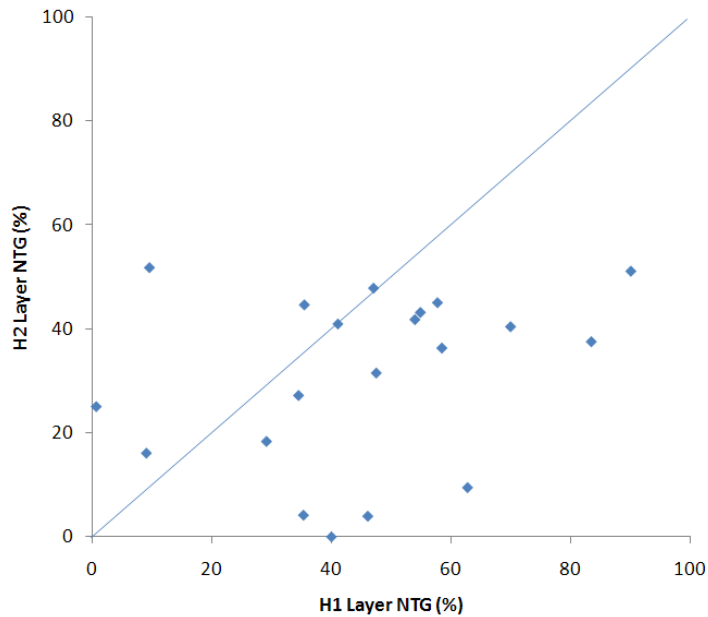


Figure 6-12: Net-to-Gross Data at well locations: H2 layer vs. H1 layer. Most of the wells have more NTG from H1 layer.

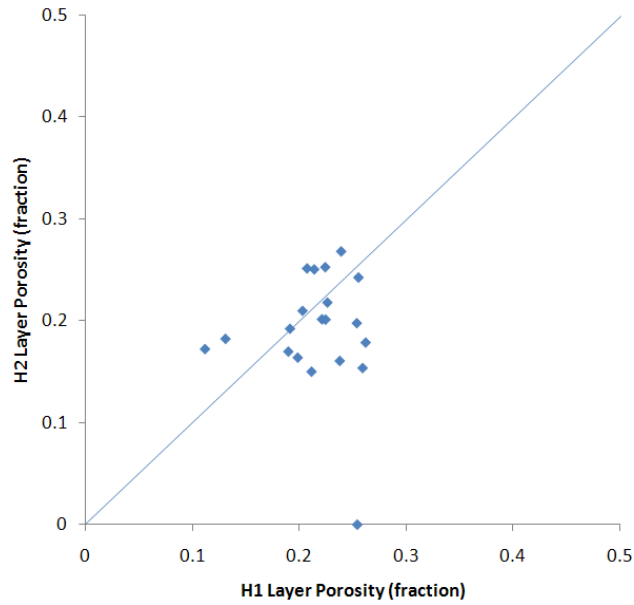


Figure 6-13: Porosity Data at well locations: H2 layer vs. H1 layer. Most of the wells have average porosity close to each other for both layers.

Correlation Coefficient matrix for some parameters in the two layers was generated to show the relationship among those variables, see Figure 6-14. Some of these correlation coefficients are used in cosimulating technique and also to know how these parameters are related.

In this study, four scenarios are conducted. First scenario assesses uncertainty in HIIP without parameter uncertainty. The other three scenarios assess uncertainty in HIIP with parameter uncertainty. Each scenario uses different parameter uncertainty distribution obtained from using BS, SBS, or CFD approach.

In each scenario, uncertainty of eight parameters and their effects on HIIP are investigated individually and combined all together in a ninth case. First three cases investigate the effects of uncertainty in structural surfaces on HIIP. The effects of fluid contacts level uncertainty are studied in the fourth case. Cases five to eight investigate HIIP uncertainty due to uncertainty in petrophysical properties. The last case combines the effects of all parameter uncertainties on HIIP.

Correlation Matrix

Top Elevation H3	1.00	0.46	0.11	0.02	-0.20	1.00	0.24	0.00	-0.08	0.02	1.00
Porosity H2	-0.03	0.10	0.12	0.12	-0.10	-0.02	0.70	0.60	0.61	1.00	0.02
NTG_H2	-0.10	-0.24	0.23	0.26	-0.22	-0.11	0.46	0.98	1.00	0.61	-0.08
Net Pay H2	-0.03	-0.12	0.32	0.34	-0.18	-0.04	0.53	1.00	0.98	0.60	0.00
Thickness H2	0.16	0.30	0.33	0.27	-0.15	0.16	1.00	0.53	0.46	0.70	0.24
Top Elevation H2	1.00	0.44	0.09	0.00	-0.20	1.00	0.16	-0.04	-0.11	-0.02	1.00
Porosity H1	-0.22	0.34	0.52	0.53	1.00	-0.20	-0.15	-0.18	-0.22	-0.10	-0.20
NTG_H1	-0.01	0.22	0.97	1.00	0.53	0.00	0.27	0.34	0.26	0.12	0.02
Net Pay H1	0.07	0.38	1.00	0.97	0.52	0.09	0.33	0.32	0.23	0.12	0.11
Thickness H1	0.39	1.00	0.38	0.22	0.34	0.44	0.30	-0.12	-0.24	0.10	0.46
Top Elevation H1	1.00	0.39	0.07	-0.01	-0.22	1.00	0.16	-0.03	-0.10	-0.03	1.00
	Top Elevation H1	Thickness H1	Net Pay H1	NTG_H1	Porosity H1	Top Elevation H2	Thickness H2	Net Pay H2	NTG_H2	Porosity H2	Top Elevation H3

Figure 6-14: Correlation Coefficient matrix for some parameters in the two layers to show the relationship among those variables.

In case of conducting sensitivity analysis, different realizations of a variable of interest are used with one fixed realization (selected randomly) of the remaining variables of interest; while in case of full uncertainty, all realizations of all variables of interest are used to calculate HIIP and get its distribution.

There are no water saturation data; therefore, it is assumed to be fixed in this case study at 20%. If water saturation data are available then its uncertainty can be investigated using the same technique used with uncertainty in NTG and porosity.

6.2. HIIP without Parameter Uncertainty

Uncertainty in HIIP without parameter uncertainty in the mean is investigated in this section. Eight cases study the effects of the following parameters uncertainty on HIIP individually. The parameters are top and bottom surfaces, H1 layer thickness, H2 layer thickness, OWC, H1 layer NTG, H2 layer NTG, H1 layer porosity, and H2 layer porosity.

6.2.1. HIIP with Uncertainty in Structural Surfaces

Structure and thickness uncertainty must be assessed in all reservoir uncertainty studies. A basic assumption is that the top and bottom surfaces from seismic interpretation were considered as reference surfaces, which have been fitted to well data. Away from well locations, there exist uncertainties in the reference surfaces. The deviations from the reference surfaces are assumed to follow a Gaussian distribution. The deviation will be zero at the well locations and increase away from the well locations. Such deviations are simulated by a SGS with conditioning data at the well locations to be zeros. Then the deviations are added to the reference surfaces/layer thicknesses. Such simulation provides alternative scenarios, which quantifies the uncertainty in the HIIP and provides us with a distribution of HIIP.

Three structural surface variables are investigated in this section, top and bottom surfaces, H1 layer thickness, and H2 layer thickness. The methodology described in Section 5.1.1 is followed in this section.

First case investigates the effects of Layers structures, top and bottom surfaces uncertainties on HIIP. *GSLIB* software was used first in the method to generate the variogram of the well data using a *gamv2004* code for the top structure of H1 Layer (Gringarten and Deutsch; 1999). The variograms were calculated in the omnidirection due to sparse data. Then the *vmodel* code was used

to obtain a spherical model that was the best variogram model fitting the variogram result trends (Wilde and Deutsch; 2005). The equation of the H1 Top Surface variogram model, as shown in Figure 6-15, is:

$$\gamma(h) = 0.001 + 0.999 * sph \tag{6-1}$$

$$a_v = 1$$

$$a_{h1} = 2400$$

$$a_{h2} = 2400$$

By getting the variogram model parameters, the conditional Gaussian simulation was ran using a *sgsim* code with conditioning data at the well locations to be zeros. 100 realizations were generated where each realization gives a Gaussian distribution with a mean of zero and a standard deviation of one. The results then were analyzed with a new code, called *OOIP* created in this study (see Appendix A). The code can multiply the results with some standard deviations then add the new results to the reference data as in Equation 5-3. The

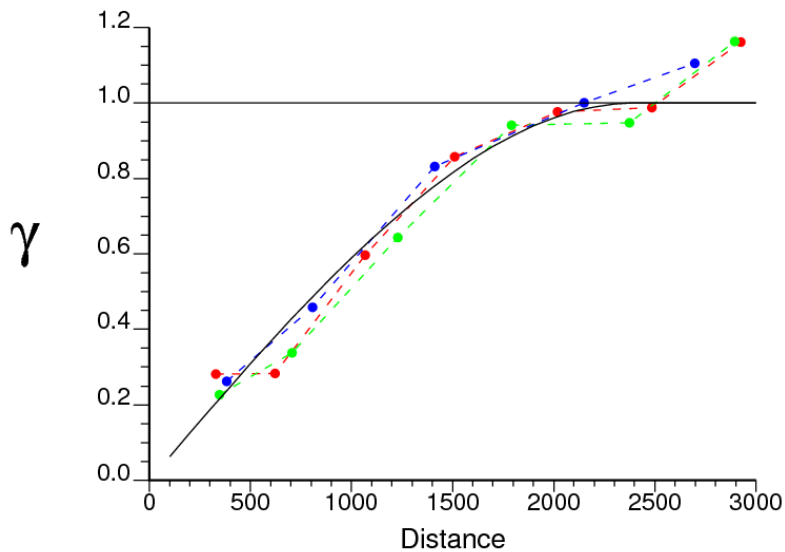


Figure 6-15: Case 1: Experimental variograms in the omnidirection and best fitted model for Top Surface of H1 Layer using data from 19 wells in Hekla Field; a Gaussian model was used with a nugget effect of 0.001 and a range of 2400m.

standard deviation of the distributions should be estimated by referring to seismic interpretation, and it was assumed to be 15 meters for the reference top and bottom surfaces in this study. Finally, the uncertainty in HIIP without parameter uncertainty was estimated by calculating the HIIP of each realization and generating a distribution plot. The results of HIIP distribution were obtained as shown in Figure 6-16. The mean and standard deviation of the HIIP were 92.8086 and 0.7745 Mm³, respectively.

OWC level was assumed to be at 2150 m if there is no uncertainty in its level. In reality, OWC should be determined by logs or should be assumed at the lowest known hydrocarbon level, if not detected. The impact of OWC level uncertainty on the calculations is investigated in section 6.2.2 since calculating HIIP relies not only on the top and bottom surfaces, but also on OWC level.

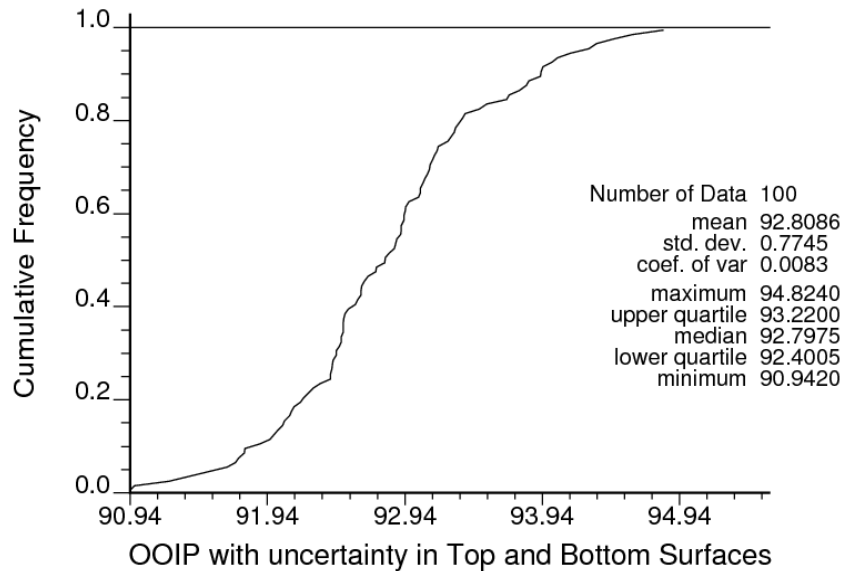


Figure 6-16: Case 1: The impacts of the uncertainty of top and bottom surfaces on the HIIP without parameter uncertainty. The deviations in the top and bottom uncertainty were assumed to have a standard deviation of 15m, the results are in millions m³.

In the second case, the effects of H1 layer thickness uncertainty on HIIP are investigated. Simulated thicknesses are obtained for each layer by adding the reference thicknesses and normally distributed deviations. Similarly to what have been done in investigating the top/bottom surfaces structures, the deviations can be generated by a *sgsim* code with zero values at well locations. The problem in running this case is that the variogram model could not be generated due to a decreasing trend of the experimental variograms obtained from H1 layer thicknesses at well locations, see Figure 6-17. Therefore, the variogram model obtained from top surface structure, as in equation (6-1), was used in case-2 to generate the SGS with conditioning data to be zeros at well locations, since the correlation coefficient between H1 layer thickness and its top surface depth is 0.39 that is the highest compared to other correlation coefficients with the remaining parameters of H1 layer.

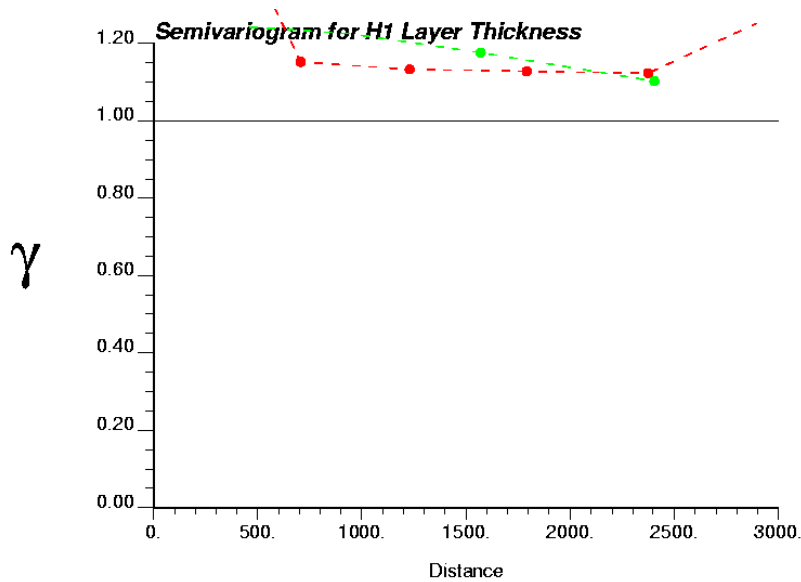


Figure 6-17: Case 2: Experimental variograms in the omnidirection for thickness of H1 layer using data from 19 wells in Hekla Field; no model was able to be generated due to no spatial relationship between the data.

100 realizations were generated by using conditional SGS to simulate the uncertainty realizations in the thickness. Then the standard deviation for H1 layer thickness was assumed to be 3m. After nonstandardizing the realizations, the results were used to get the HIIP distributions as shown in Figure 6-18. The mean and the standard deviation of HIIP were 93.1718 and 0.8546 MMm³, respectively.

The effects of H2 layer thickness uncertainty on HIIP was investigated in the third case. The process was similar to that was conducted in the case-2, but the variogram model used in this case was generated using H2-Layer thickness data at all well locations, see the second plot in Figure 6-19; where the H2 Thickness variogram model is a spherical model with the following equation:

$$\gamma(h) = 0.001 + 0.999 * sph \tag{6-2}$$

$$a_v = 1$$

$$a_{h1} = 4000$$

$$a_{h2} = 4000$$

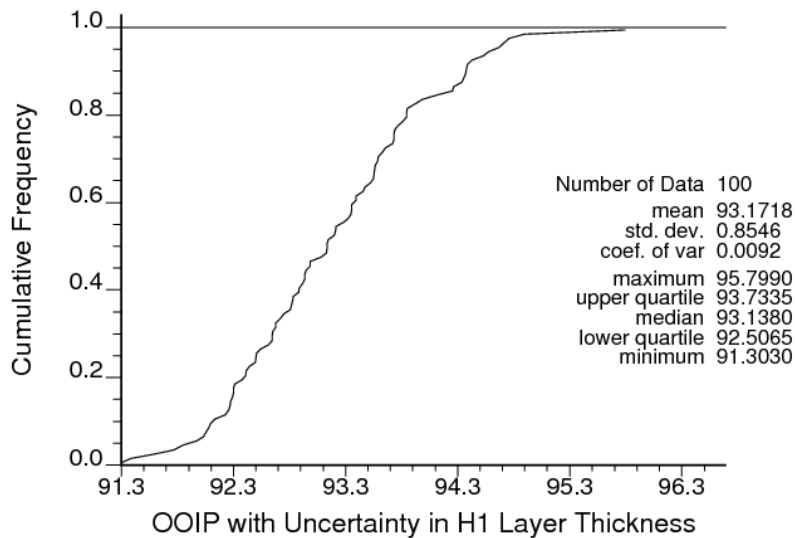


Figure 6-18: Case 2: The impacts of the uncertainty of H1 layer thickness on the HIIP without parameter uncertainty. The deviations in the H1 layer thickness uncertainty were assumed to have a standard deviation of 3m, the results are in millions m³.

Then the deviations were generated by a *sgsim* code with a zero mean value and a standard deviation of one and conditioning data at well locations to be zeros. The standard deviation was assumed in this case to be 3m; and by generating 100 realizations, the HIIP distribution was obtained as shown in Figure 6-20. The mean and the standard deviation of HIIP were 92.9618 and 0.4405 MMm^3 , respectively.

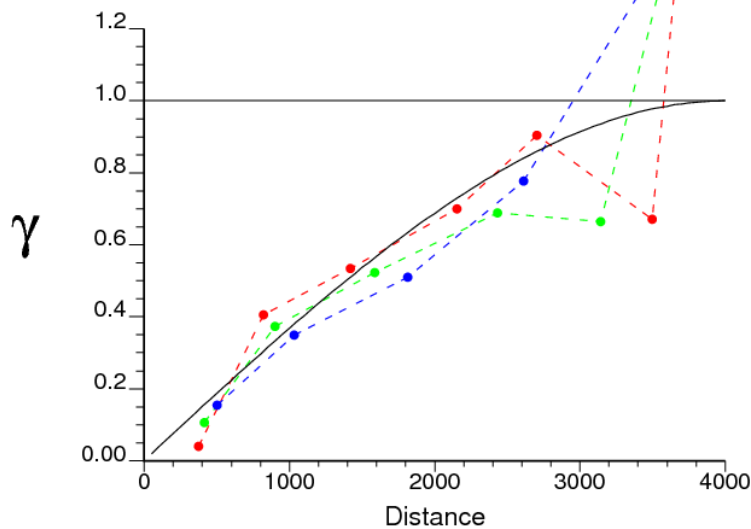


Figure 6-19: Case 3: Experimental variograms in the omnidirection and best fitted model for H2 layer thickness using data from 19 wells in Hekla Field; a Gaussian model was used with a nugget effect of 0.001 and a range of 4000m.

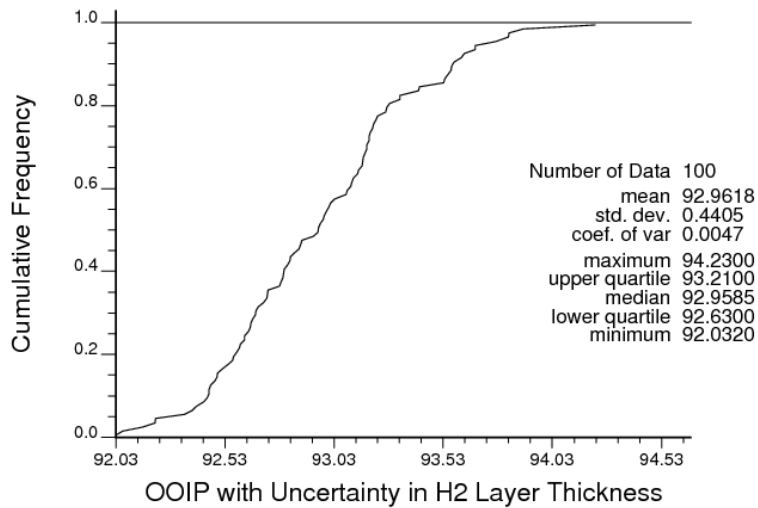


Figure 6-20: Case 3: The impacts of the uncertainty of H2 layer thickness on the HIIP without parameter uncertainty. The deviations in the H2 layer thickness uncertainty were assumed to have a standard deviation of 3m, the results are in millions m^3 .

6.2.2. HIIP with Uncertainty in Fluid Contacts Level

It was assumed that there is no gas cap in this case study; therefore, only one case was needed to investigate the uncertainty in OWC level by determining the OWC minimum, maximum and most likely levels, and then 100 realizations were generated using *mcs* code assuming a triangular distribution with changing the seed number, see Section 5.1.2. These realizations were used to get the HIIP distributions above OWC as shown in Figure 6-21. The mean and the standard deviation of HIIP were 92.9115 and 0.0048 MMm³, respectively.

6.2.3. HIIP with Uncertainty in Petrophysical Properties

Four cases investigate the effects of uncertainty in H1 layer NTG, H2 layer NTG, H1 layer porosity, and H2 layer porosity on HIIP. Uncertainty in water saturation can be investigated using the same technique used for NTG and porosity, but it was assumed that water saturation was fixed at 20% in all realizations as mentioned formerly.

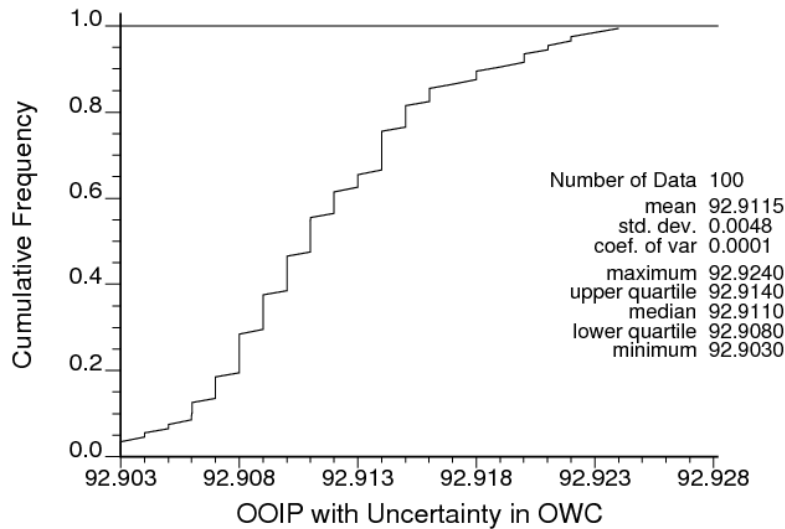


Figure 6-21: Case 4: The impacts of the uncertainty of OWC on the HIIP without parameter uncertainty. The OWC uncertainty was assumed to follow a triangular distribution with a minimum of 2148m, a mode of 2150m, a maximum of 2152m, the results are in millions m³.

The porosity cutoff was assumed to be at 10% in this study, as mentioned before. The NP and NTG for each layer in all 19 wells were calculated based on this cutoff. According to the methodology described in section 5.1.3, the next step is to obtain the best variogram model fitting the experimental variogram result for variables of interest. The experimental variograms for NTG and porosity of H1 layer were generated in the omnidirection, as shown in Figures 6-22 and 6-23. Gaussian models were selected to fit the experimental variograms with a nugget effect of 0.001 and a range of 800m for the two variables. The equation of the variogram models is the same one as follows:

$$\gamma(h) = 0.001 + 0.999 * Gau \tag{6-3}$$

$$a_v = 1$$

$$a_{h1} = 800$$

$$a_{h2} = 800$$

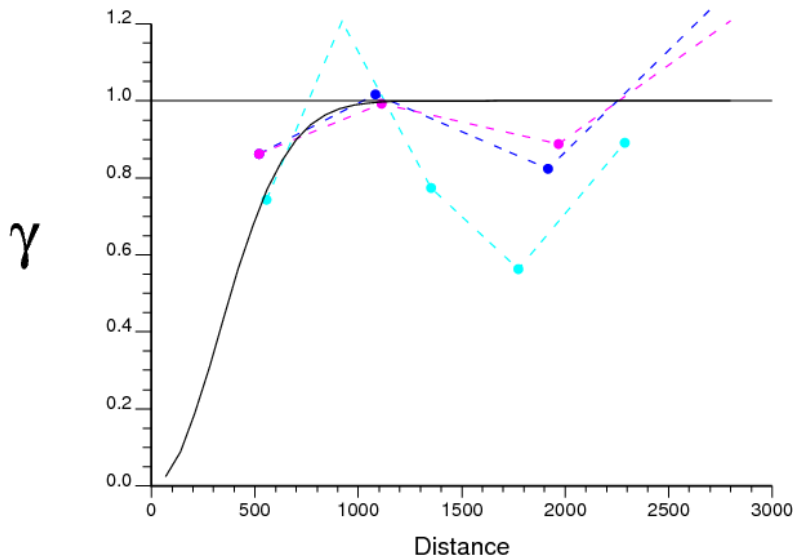


Figure 6-22: Case 5: Experimental variograms in the omnidirection and best fitted model for NTG of H1 layer using data from 19 wells in Hekla Field; a Gaussian model was used with a nugget effect of 0.001 and a range of 800m.

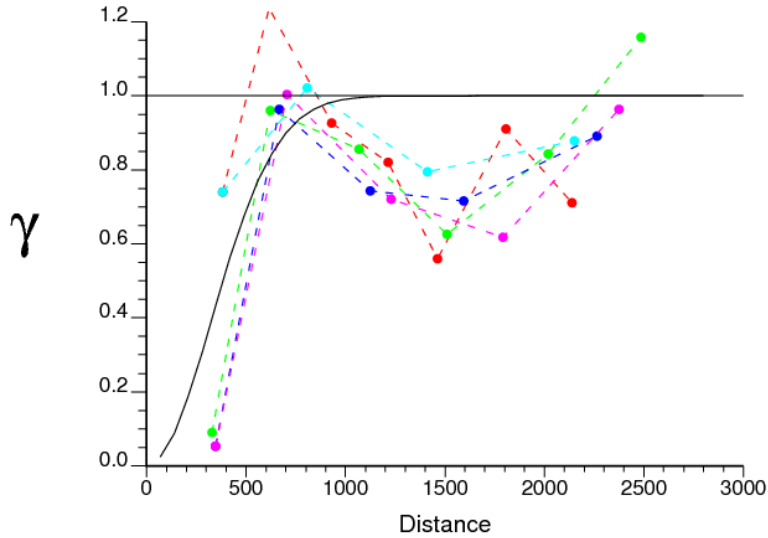


Figure 6-23: Case 7: Experimental variograms in the omnidirection and best fitted model for Porosity of H1 layer using data from 19 wells in Hekla Field; Gaussian model was determined to fit the experimental results with a nugget effect of 0.001 and a range of 800m.

The correlation coefficients among NTG, porosity and thickness for H1 layer were used to generate NTG and porosity realizations simultaneously. The *ultimate_sgsim* code was used with the original data as reference distributions to simulate 100 realizations for each case. All NTG realizations were used with the first porosity realization in case 5, while all porosity realizations were used with the first NTG realization in case 7. The results were used to calculate HIIP realizations and obtain its distribution, as shown in Figures 6-24 and 6-25. The mean and the standard deviation of HIIP were 90.8410 and 0.3374 MMm³ with uncertainty in H1 layer NTG, and 90.8585 and 0.2242 MMm³ with uncertainty in H1 layer porosity, respectively.

In cases 6 and 8, the effects of uncertainty in NTG and porosity of H2 layer on HIIP were investigated individually. The experimental variograms in the omnidirection were generated. It seems that there is no relationship between the NTG data of H2 layer since there is no clear spatial correlation between the data. Therefore, the model fitting the experimental variograms of porosity for H2 layer

was used for both NTG and porosity of H2 layer since the correlation coefficient between them is 0.61 that is the highest value compared to the other correlation coefficients between NTG and other parameters of H2 layer, see Figure 6-14.

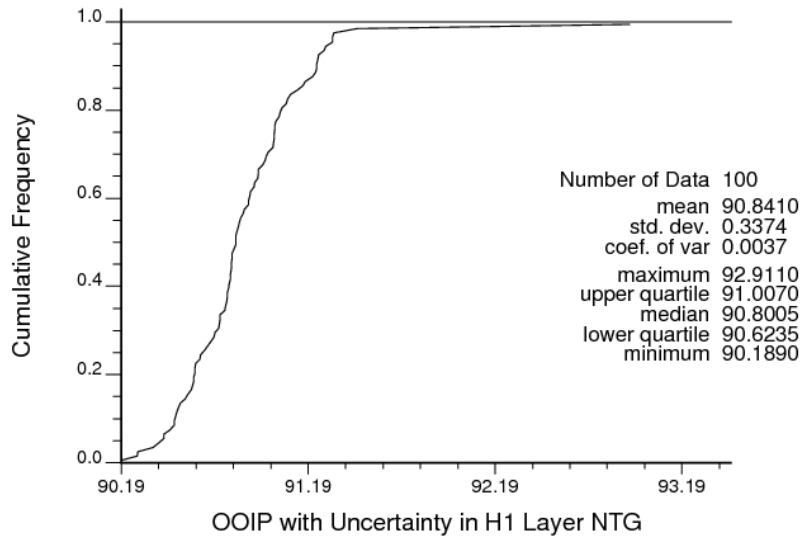


Figure 6-24: Case 5: The impacts of the uncertainty of H1 layer NTG on the HIIP without parameter uncertainty, the results are in millions m³.

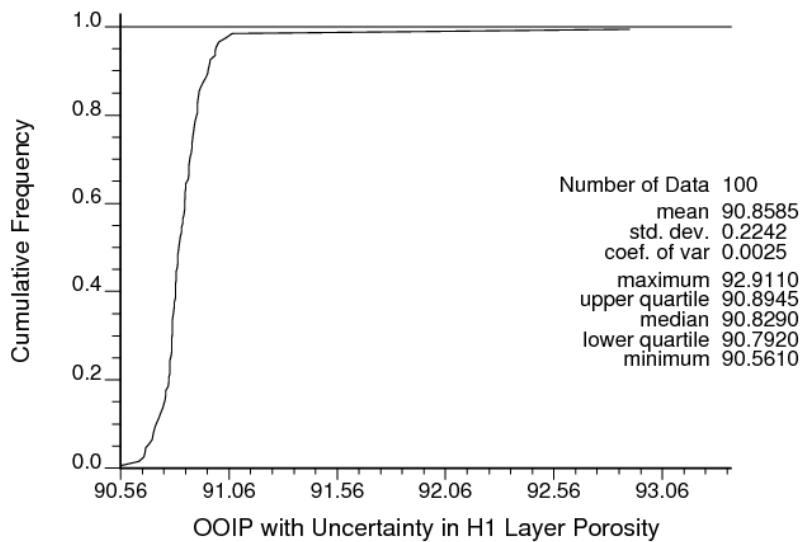


Figure 6-25: Case 7: The impacts of the uncertainty of H1 layer porosity on the HIIP without parameter uncertainty, the results are in millions m³.

As Figures 6-26 and 6-27 show, Gaussian models were selected to fit the experimental variograms with a nugget effect of 0.001 and a range of 500m for the porosity of H2 layer. The equation of the variogram model is as follows:

$$\gamma(h) = 0.001 + 0.999 * Gau \tag{6-3}$$

$$a_v = 1$$

$$a_{h1} = 500$$

$$a_{h2} = 500$$

NTG and porosity realizations were generated simultaneously by cosimulating NTG and porosity with thickness obtained from seismic data by using an *ultimate_sgsim* code with the same variogram model for the variables in interest, NTG and porosity of H2 layer. 100 realizations were generated for each case. The results were used to calculate HIIP and obtain the HIIP distribution for each case as shown in Figures 6-28 to 6-29. The mean and the standard deviation of HIIP were 91.4682 and 0.2131 MMm³ with uncertainty in H2 layer NTG, and 91.4708 and 0.1555 MMm³ with uncertainty in H2 layer porosity, respectively.

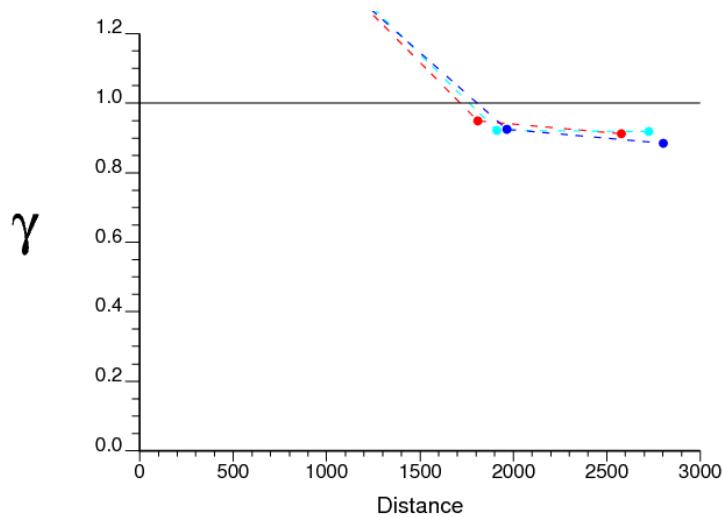


Figure 6-26: Case 6: Experimental variograms in the omnidirection for NTG of H2 Layer using data from 19 wells in Hekla Field; no model was able to be generated due to no spatial relationship between the data.

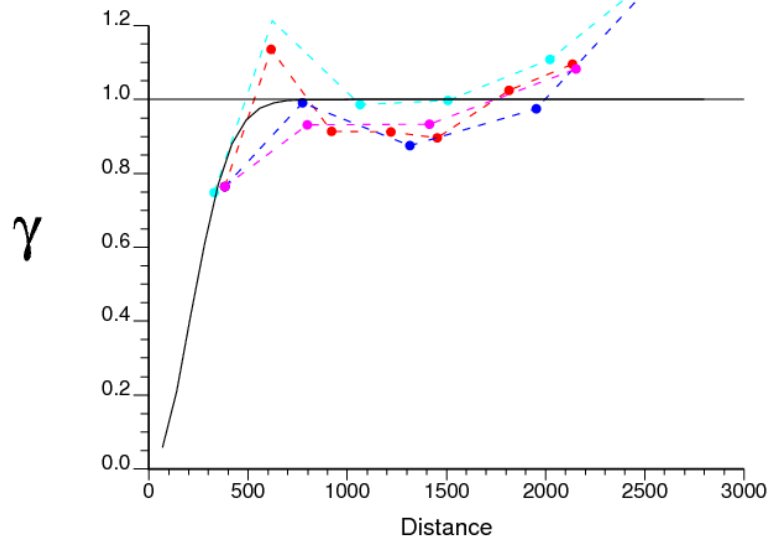


Figure 6-27: Case 8: Experimental variograms in the omnidirection and best fitted model for Porosity of H2 Layer using data from 19 wells in Hekla Field; a Gaussian model was determined to fit the experimental results with a nugget effect of 0.001 and a range of 500m.

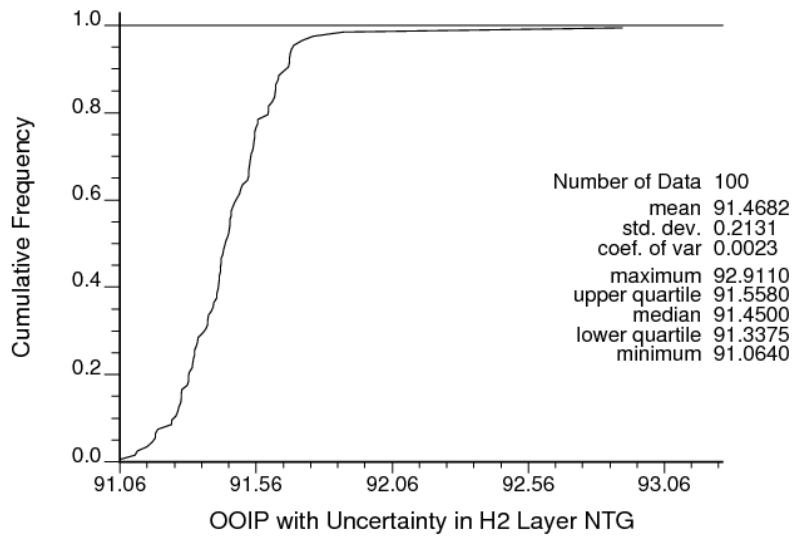


Figure 6-28: Case 6: The impacts of the uncertainty of H2 layer NTG on the HIIP without parameter uncertainty, the results are in millions m³.

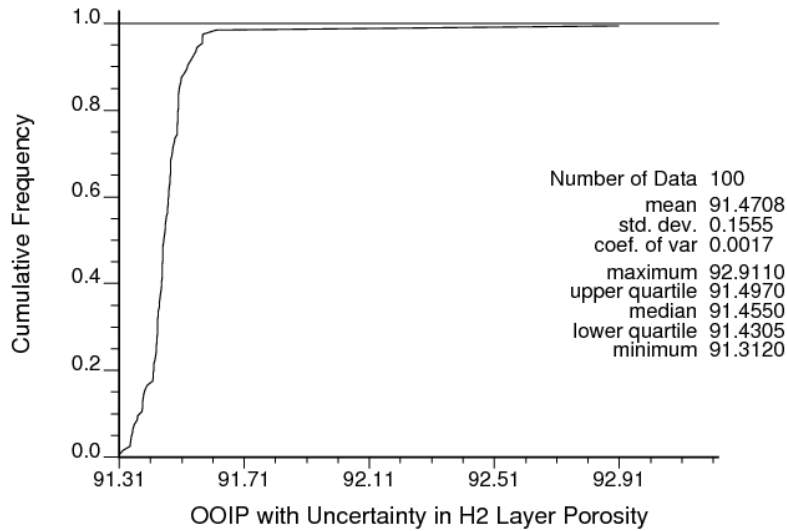


Figure 6-29: Case 8: The impacts of the uncertainty of H2 layer porosity on the HIIP without parameter uncertainty, the results are in millions m³.

6.2.4. HIIP with Full Uncertainty

In this case, multiple realizations should be drawn with uncertainty attached to all parameters, top and bottom surfaces, layer thicknesses, OWC levels, NTG, and Porosity for each layer. The deviations were generated without parameter uncertainty in the mean for all parameters. The standard deviations of 15m for top and bottom surfaces uncertainty and 3m for thickness uncertainty of each layer were used. 100 realizations were generated to get the HIIP distribution above OWC level of 2150m as shown in Figure 6-30. The mean and the standard deviation of HIIP with full uncertainty were 93.0990 and 1.1415 MMm³, respectively.

Uncertainty in HIIP was assessed with assuming a fixed uncertainty in the parameter mean. To account for parameter uncertainty distribution, a parameter uncertainty approach has to be used. Chapter 3 described three different approaches that can be used. In the next section, those three different approaches

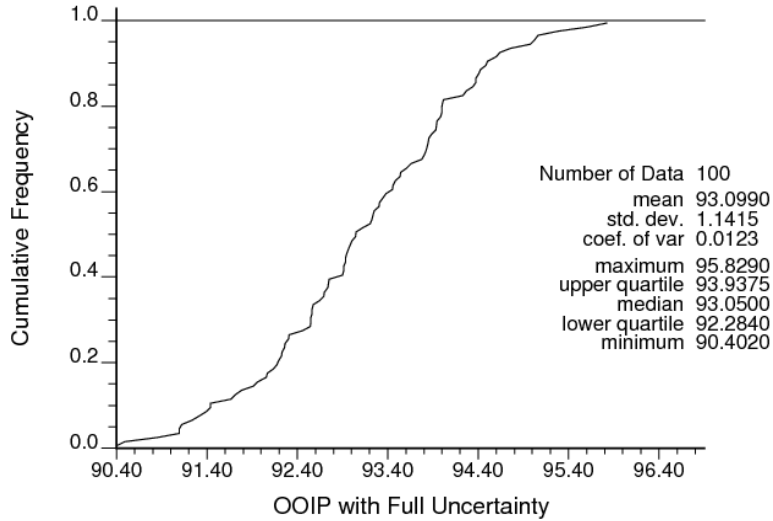


Figure 6-30: Case 9: The impacts of the uncertainty of all variables on the HIIP without parameter uncertainty, the results are in millions m^3 .

are used and their results are compared with the results of this section to assess the uncertainty in HIIP with and without parameter uncertainty.

6.3. HIIP with Parameter Uncertainty

It is important to account for parameter uncertainty in the mean since ignoring it might lead to less uncertainty that might not reflect the real uncertainty available with the known collected data. Parameter uncertainty has to be incorporated in assessing the uncertainty of HIIP.

6.3.1. Parameter Uncertainty Distributions

The parameter uncertainty in the means of the variables of interest were quantified using the three different approaches described in Chapter 3, conventional bootstrap (BS), spatial bootstrap (SBS), and conditional finite domain (CFD). The parameters investigated in the last section 6.2 were investigated again in this section but with parameter uncertainty in the mean. The

parameters were top and bottom surfaces, H1 layer thickness, H2 layer thickness, H1 layer NTG, H2 layer NTG, H1 layer porosity, and H2 layer porosity.

The uncertainty in the mean of H1 top surface was quantified as shown in Figure 6-31. The mean of the parameter distribution with using SBS and CFD were 1962.2m and 1964.05m, respectively. They were lower than 1972.5m, the mean obtained with BS approach. The standard deviation of the parameter uncertainty with using SBS was 26.9m and higher than 18.8m and 15.79m obtained with BS and CFD, respectively.

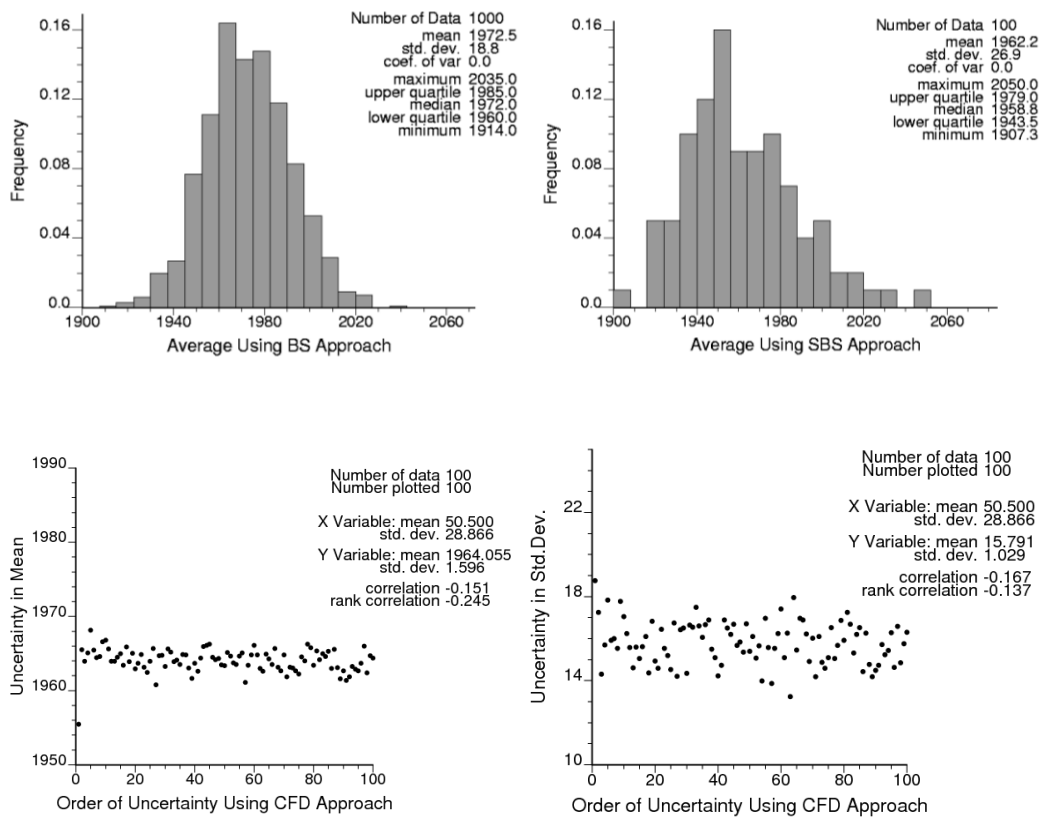


Figure 6-31: Case 1: Parameter uncertainty distributions for H1 layer top surface (top left: results of using BS approach, top right: results of using SBS approach, bottom left: uncertainty in the mean using CFD approach, and bottom right: uncertainty in the standard deviation using CFD approach). The units are in meters.

The parameter uncertainty in the mean of H1 layer thickness with SBS approach showed a lower value in the mean, 30.6m and higher one in the standard deviation, 1.6m compared to those obtained with using BS and CFD, see Figure 6-32. For case 3 investigating H2 layer thickness uncertainty, using SBS and CFD approaches gave lower means, 26.4m and 26.38m, respectively. The standard deviation was high with SBS approach, 1.9m as shown in Figure 6-33.

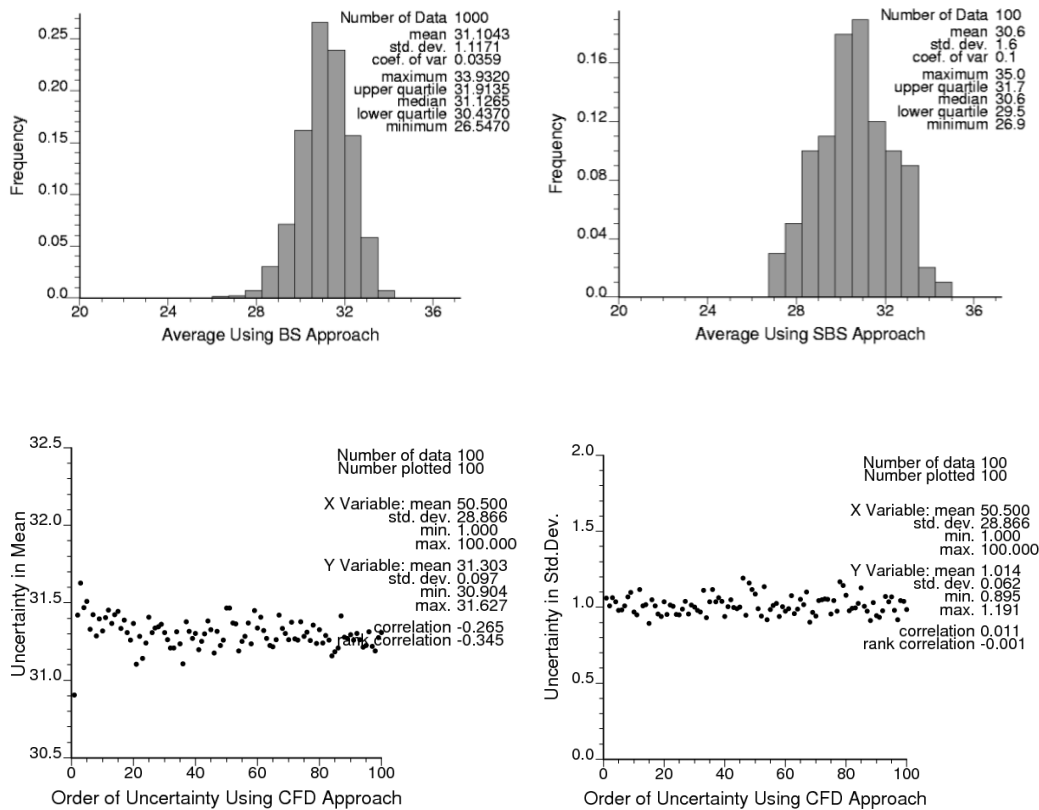


Figure 6-32: Case 2: Parameter uncertainty distributions for H1 layer thickness (top left: results of using BS approach, top right: results of using SBS approach, bottom left: uncertainty in the mean using CFD approach, and bottom right: uncertainty in the standard deviation using CFD approach). The units are in meters.

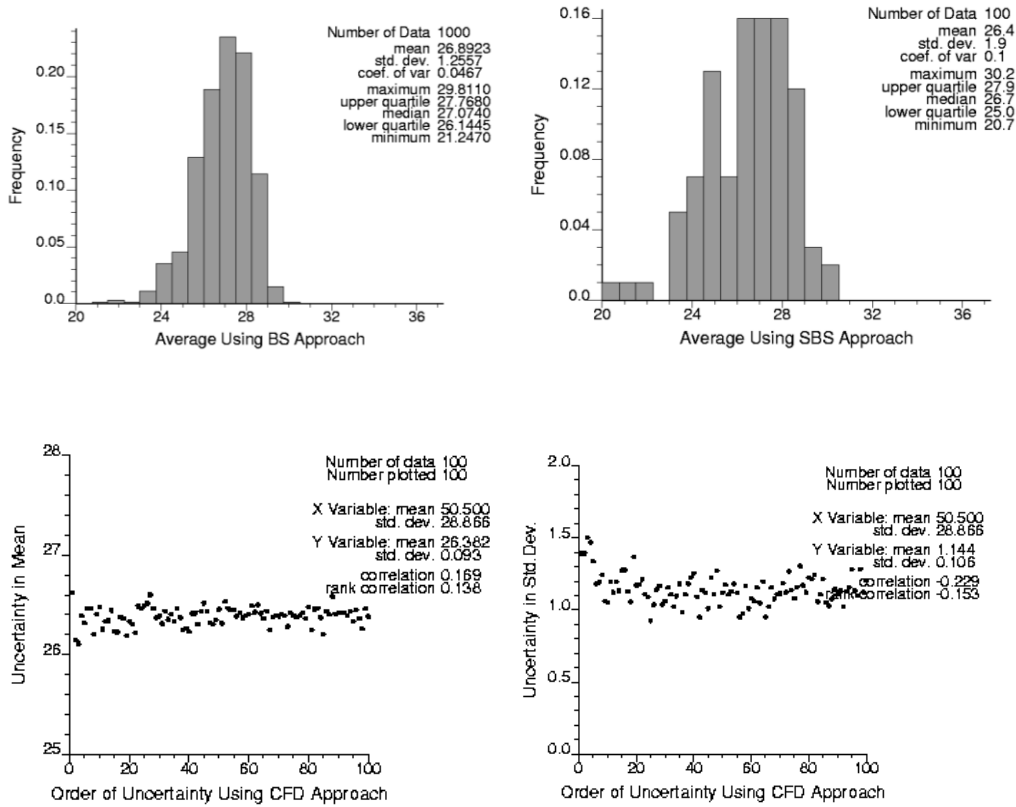


Figure 6-33: Case 3: Parameter uncertainty distributions for H2 layer thickness (top left: results of using BS approach, top right: results of using SBS approach, bottom left: uncertainty in the mean using CFD approach, and bottom right: uncertainty in the standard deviation using CFD approach). The units are in meters.

Quantifying the parameter uncertainty for NTG of H1 layer, as shown in Figure 6-34, gave a lower mean and a higher standard deviation using SBS approach (0.4333, 0.0558) compared to the results obtained using BS approach (0.4577, 0.0512), while CFD approach gave the lowest standard deviation (0.4431, 0.0402) compared to other approaches.

The results of quantifying the parameter uncertainty for NTG of H2 layer are shown in Figure 6-35. Using SBS approach gave a lower mean (0.3078, 0.0356) while using CFD approach gave a lower standard deviation (0.3284, 0.029) compared to the results of using BS approach (0.3219, 0.035).

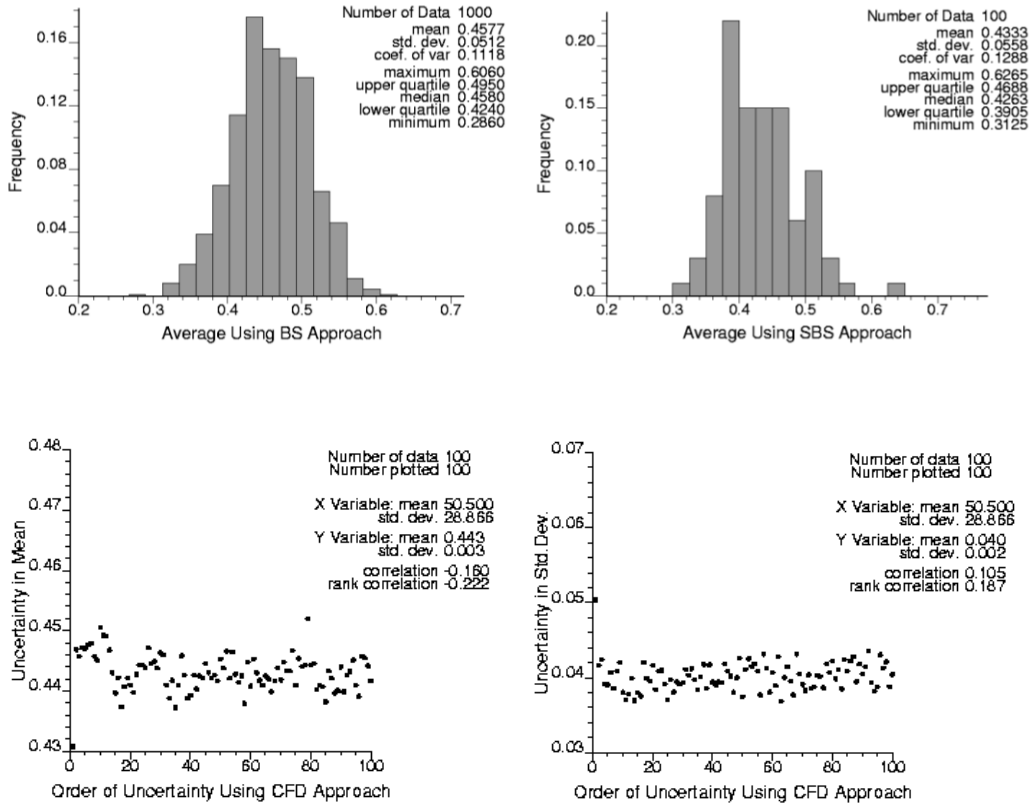


Figure 6-34: Case 5: Parameter uncertainty distributions for H1 layer NTG in fractions (top left: results of using BS approach, top right: results of using SBS approach, bottom left: uncertainty in the mean using CFD approach, and bottom right: uncertainty in the standard deviation using CFD approach).

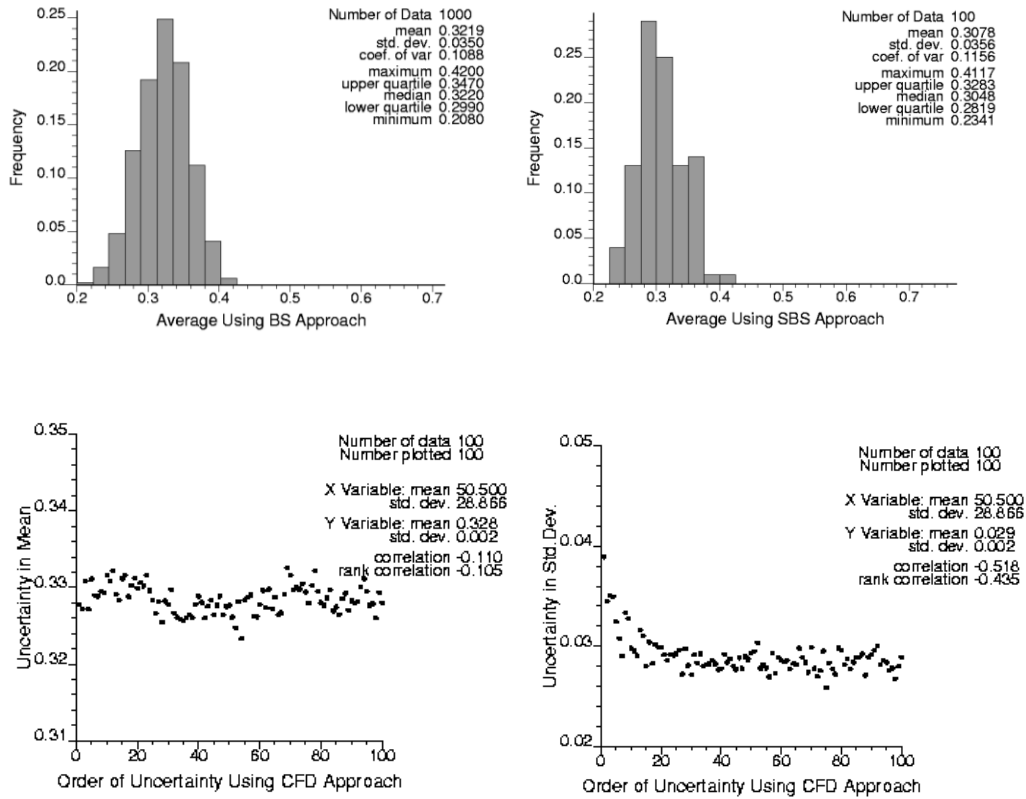


Figure 6-35: Case 6: Parameter uncertainty distributions for H2 layer NTG in fractions (top left: results of using BS approach, top right: results of using SBS approach, bottom left: uncertainty in the mean using CFD approach, and bottom right: uncertainty in the standard deviation using CFD approach).

The parameter uncertainty for porosity of H1 layer was quantified for case 7 as shown in Figure 6-36. The standard deviation was higher with using SBS approach (0.2107, 0.0101) and lower with using CFD approach (0.2159, 0.0070) than that obtained from BS approach (0.2147, 0.0089).

In case 8 investigating the uncertainty in the porosity of H2 layer, the parameter uncertainty was quantified and gave a lower mean and a higher standard deviation using SBS approach (0.1803, 0.0134) and a higher mean and a lower standard deviation using CFD approach (0.1902, 0.0105) compared to the results obtained from using BS approach (0.187, 0.0124), see Figure 6-37.

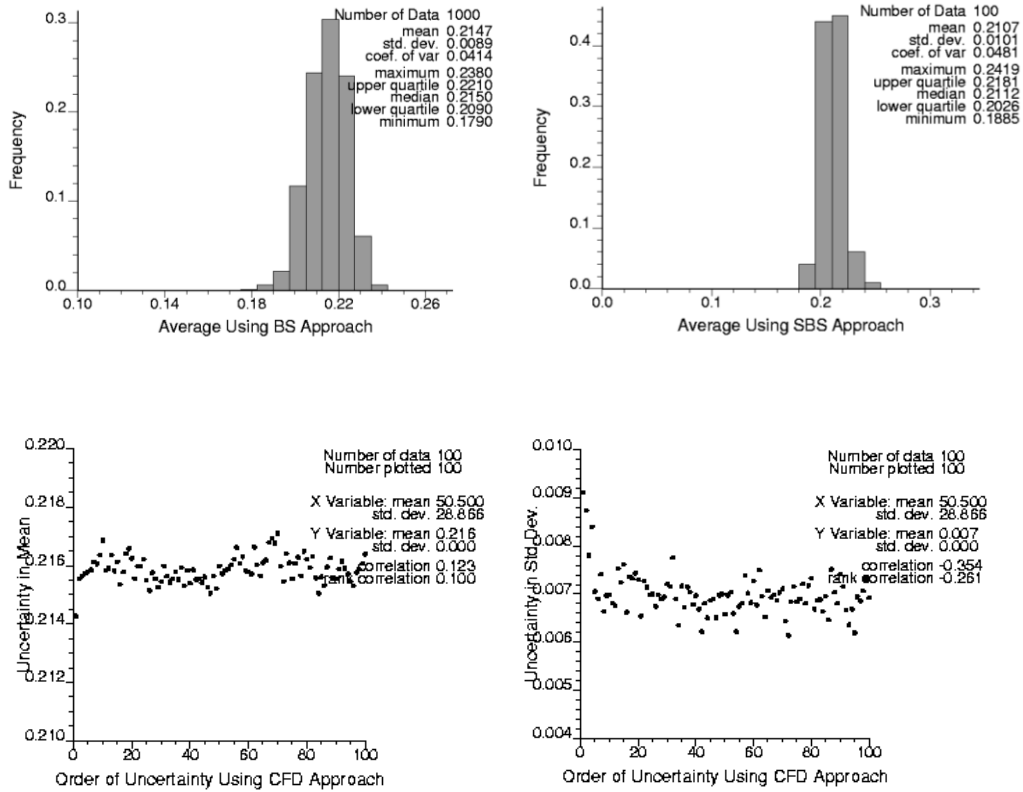


Figure 6-36: Case 7: Parameter uncertainty distributions for H1 layer porosity in fractions (top left: results of using BS approach, top right: results of using SBS approach, bottom left: uncertainty in the mean using CFD approach, and bottom right: uncertainty in the standard deviation using CFD approach).

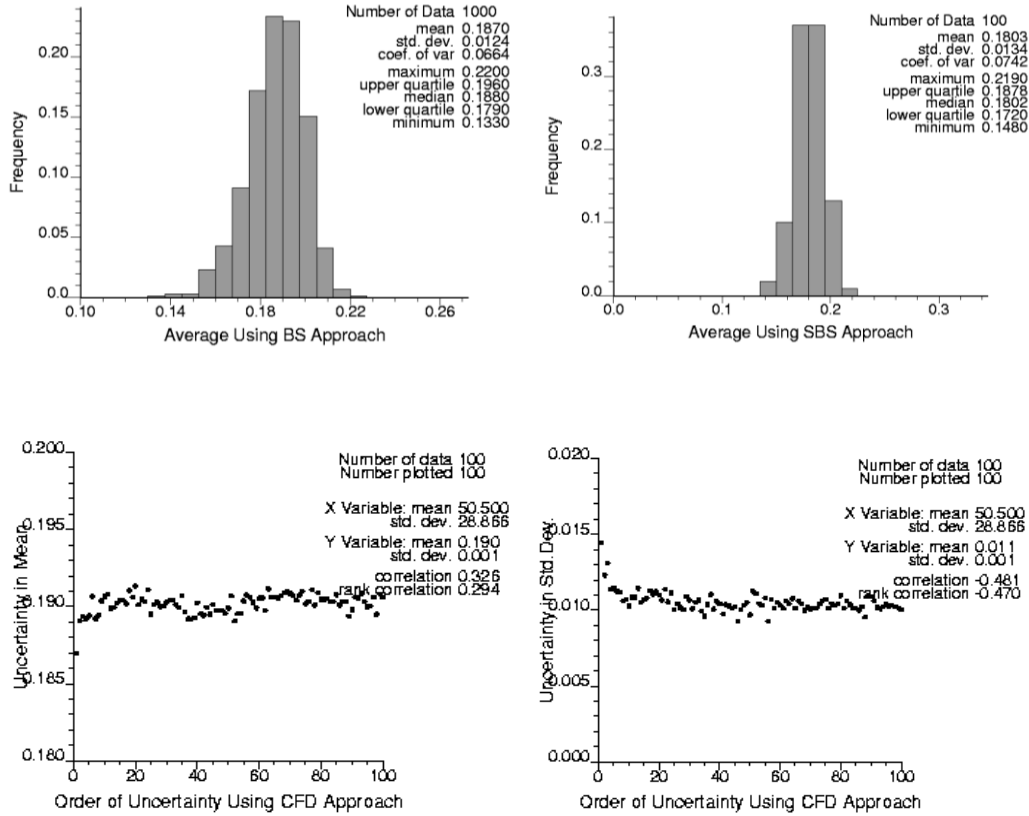


Figure 6-37: Case 8: Parameter uncertainty distributions for H2 layer porosity in fractions (top left: results of using BS approach, top right: results of using SBS approach, bottom left: uncertainty in the mean using CFD approach, and bottom right: uncertainty in the standard deviation using CFD approach).

It was noticed that the variograms used in cases 5 through 8 have low ranges, which made the results of the parameter uncertainty using SBS and CFD approaches have standard deviations close to those results obtained from BS approach. Therefore, another run was conducted to quantify the parameter uncertainty using SBS and CFD with a higher arbitrary range, 2500m. Figure 6-38 shows the parameter uncertainty results of using SBS and CFD approaches for NTG of each layer individually. The results of quantifying the porosity uncertainty in the mean using SBS and CFD approaches with the arbitrary high range (2500m) are shown in Figure 6-39.

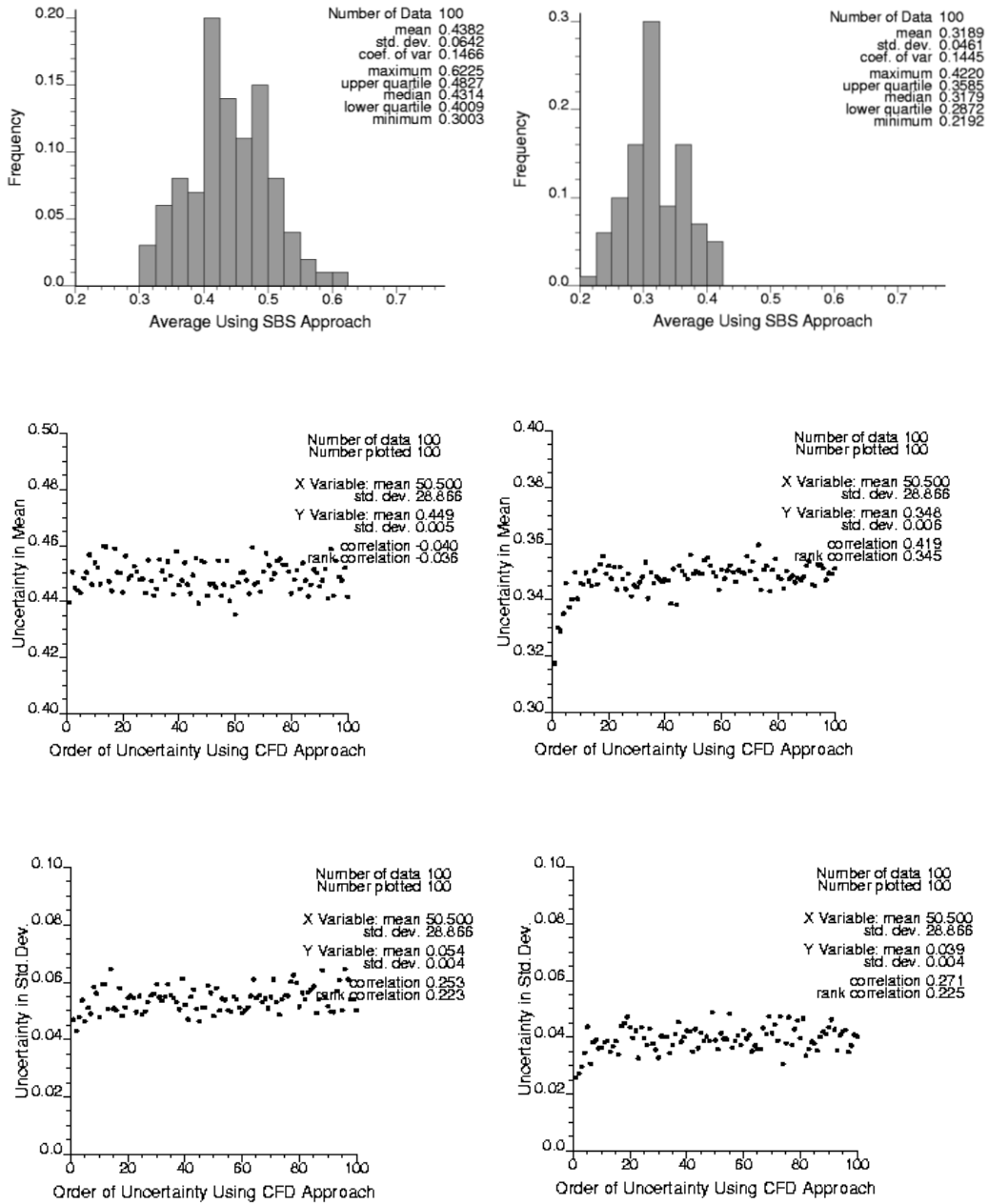


Figure 6-38: Cases 5 & 6: Parameter uncertainty quantification with high arbitrary range, 2500m for NTG (fractions) of each layer (top left: results of using SBS approach for NTG of H1 layer, top right: results of using SBS approach for NTG of H2 layer, mid left: uncertainty in the mean for NTG of H1 layer using CFD approach, mid right: uncertainty in the mean for NTG of H2 layer using CFD approach, bottom left: uncertainty in the standard deviation for NTG of H1 layer using CFD approach, and bottom right: uncertainty in the standard deviation for NTG of H2 layer using CFD approach).

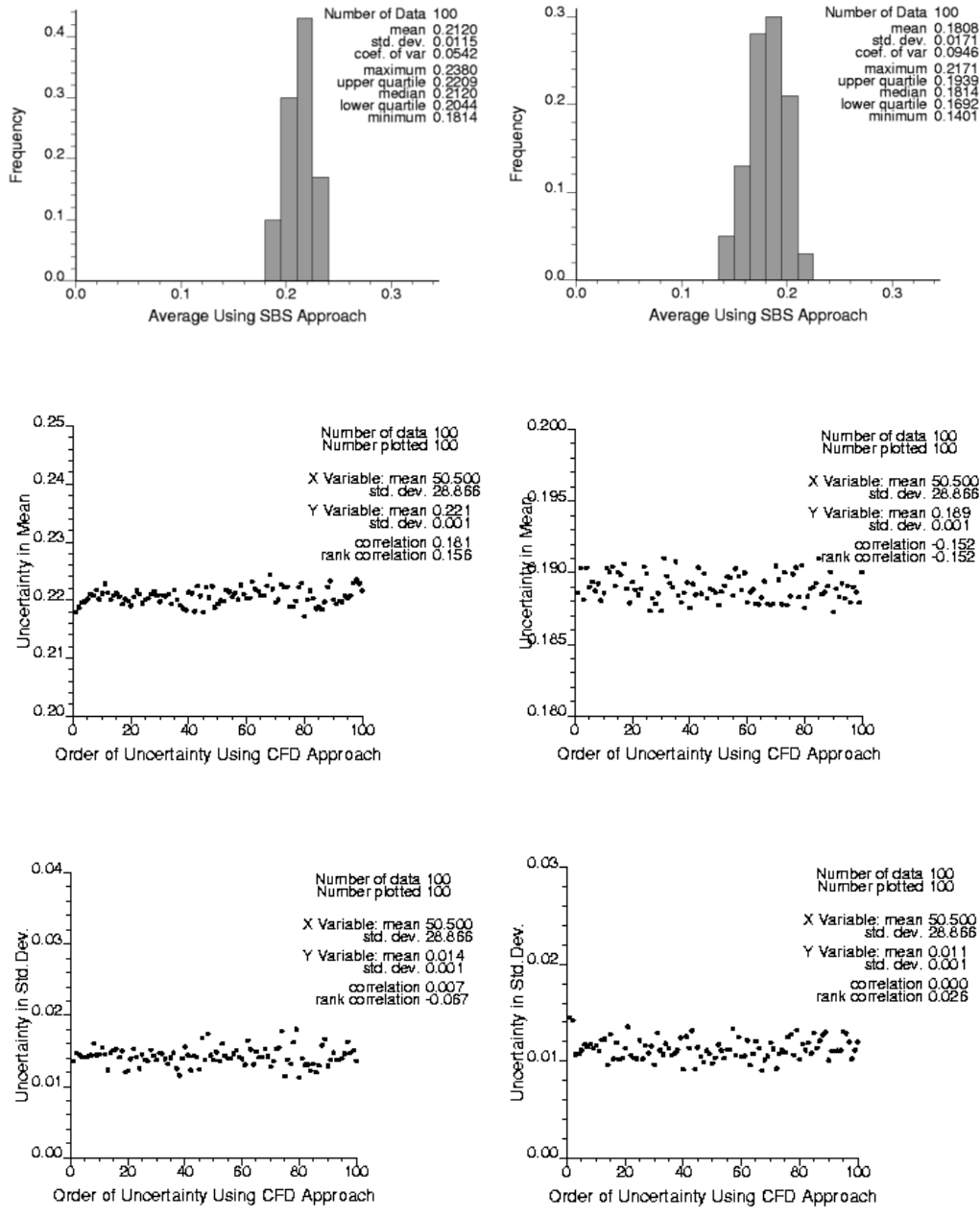


Figure 6-39: Cases 7 & 8: Parameter uncertainty quantification with high arbitrary range, 2500m for porosity (fractions) of each layer (top left: results of using SBS approach for porosity of H1 layer, top right: results of using SBS approach for porosity of H2 layer, mid left: uncertainty in the mean for porosity of H1 layer using CFD approach, mid right: uncertainty in the mean for porosity of H2 layer using CFD approach, bottom left: uncertainty in the standard deviation for porosity of H1 layer using CFD approach, and bottom right: uncertainty in the standard deviation for porosity of H2 layer using CFD approach).

Parameters	Layer	Original Data		BS		Variogram Range	SBS		CFD	
		Mean	σ	Mean	σ		Mean	σ	Mean	σ
Top	H1	1973.1	83.4	1972.5	18.8	2400	1962.2	26.9	1964.1	15.8
Thickness	H1	31.1105	4.9791	31.1043	1.1171	2400	30.6000	1.6000	31.3034	1.0141
Thickness	H2	26.8842	5.5318	26.8923	1.2557	4000	26.4000	1.9000	26.3825	1.1440
NTG	H1	0.4586	0.2290	0.4577	0.0512	800	0.4333	0.0558	0.4431	0.0402
						2500	0.4382	0.0642	0.4490	0.0540
NTG	H2	0.3227	0.1556	0.3219	0.0350	500	0.3078	0.0356	0.3284	0.0290
						2500	0.3189	0.0461	0.3476	0.0393
Porosity	H1	0.2147	0.0393	0.2147	0.0089	800	0.2107	0.0101	0.2159	0.0070
						2500	0.2120	0.0115	0.2206	0.0136
Porosity	H2	0.1870	0.0548	0.1870	0.0124	500	0.1803	0.0134	0.1902	0.0105
						2500	0.1808	0.0171	0.1890	0.0113

Table 6-4: Comparison between means and standard deviations obtained from using different parameter uncertainty approaches.

The results of using the three approaches on all eight parameters, even with the arbitrary high variogram range, are summarized in Table 6-4. The next step was to incorporate those parameter uncertainty distributions into the process of quantifying HIIP with those uncertainties as described in section 5.2. The same eight parameters investigated without parameter uncertainty were investigated again but with parameter uncertainty. Eight cases study the effects of these parameters uncertainty on HIIP individually and the ninth case studies the effects of full uncertainty on HIIP with parameter uncertainty. The scenario of estimating HIIP and its sensitivity analysis has to be run three times. In each scenario, the results of using one of the parameter uncertainty approaches are incorporated.

6.3.2. HIIP with Uncertainty in Structural Surfaces

Three different scenarios were conducted with a different parameter uncertainty approach incorporated in each scenario. Cases 1 to 3 investigated uncertainty in the top and bottom surfaces, the H1 layer thickness, and the H2 layer thickness, respectively. The methodology described in section 5.2.2 was followed to simulate 100 realizations using a SGS method for each case. First step was to find the variogram model fitting the generated experimental variograms of H1 top surface and thickness of H1 and H2 layers for cases 1 to 3. The spherical

variogram models were already determined in cases 1 to 3 without parameter uncertainty and used in these cases with parameter uncertainty.

Preparing the input file was the next step by adding 100 columns. Each column was used to simulate one realization. The dx values were used as conditioning data at well locations and calculated by using equation (5-9). They had one value in each column and varied from column to column as $m_{p,l}(i)$ changed and determined by drawing from parameter uncertainty distribution. $m_{p,l}(i)$ is calculated based on equation (6-4) for each i simulation. Then the corresponding value of $m_{p,l}$ is determined by using the parameter mean distribution at the calculated probability (i). *input_mp* code is a code created in this study (see Appendix A) to print out the values of $m_{p,l}$ required in the simulation.

$$m_{p,l}(i) = (i - 0.5) / \text{nsim} \quad (6-4)$$

where $m_{p,l}$ = parameter mean at location l .

$$i = 1, 2, \dots, \text{nsim}.$$

nsim = number of simulation.

The next step was to add ($-dx$) to the results of SGS simulation to reset the values at well locations to be zero then non-standardize the realizations by multiplying them with the assumed standard deviation σ_{Δ} , 15m. So, the results are uncertainty realizations with means of ($mean(i) = \sigma_{\Delta} * m_{p,l}(i) = 15 * m_{p,l}(i)$) and 15m standard deviation. The results were added to the base reference surfaces obtained from seismic data (to the top and bottom surfaces to quantify uncertainty in top and bottom surfaces and only to the bottom surface to quantify uncertainty in layer thickness).

The uncertainty realizations were used to calculate HIIP realizations and obtain the HIIP distribution. The effects of the uncertainty in top and bottom surfaces on HIIP using the three parameter uncertainty approaches were shown in

Figure 6-40. For cases 2 and 3, the standard deviation was assumed to be 3m for thickness of layers H1 and H2. The effects of the uncertainty in thickness of H1 and H2 layers on HIIP were shown in Figures 6-41 and 6-42 using the three parameter uncertainty approaches.

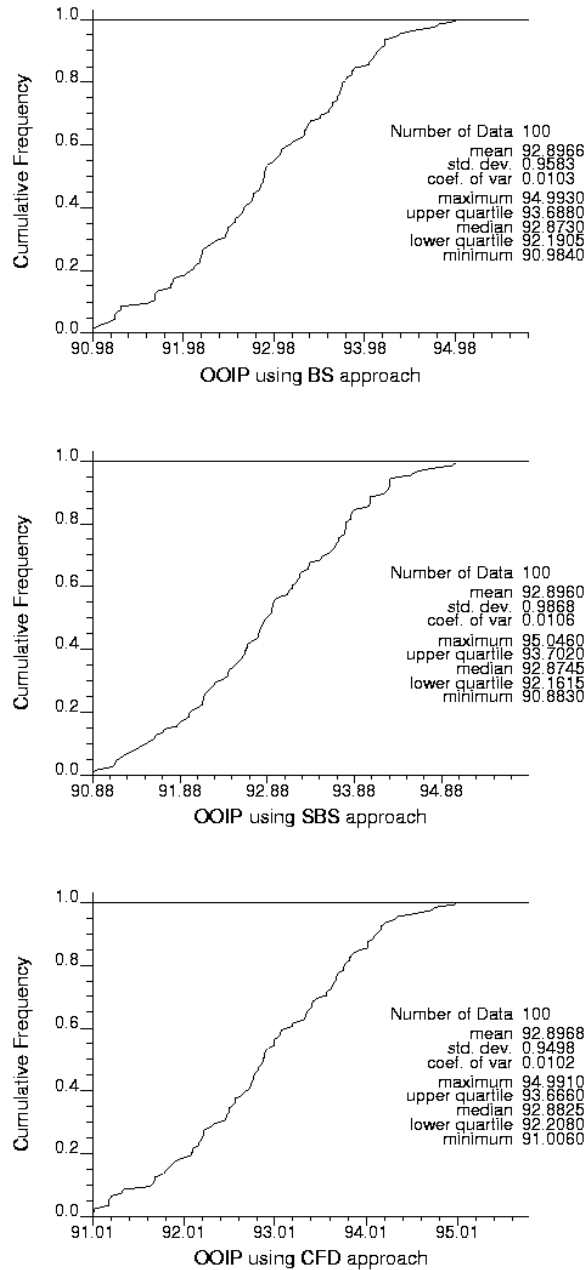


Figure 6-40: Case 1: The impacts of the uncertainty of top and bottom surfaces on the HIIP with parameter uncertainty. The deviations in the top and bottom uncertainty were assumed to have a standard deviation of 15m. The plots from top to bottom are the results of using BS, SBS, and CFD approaches, respectively; the results are in millions m³.

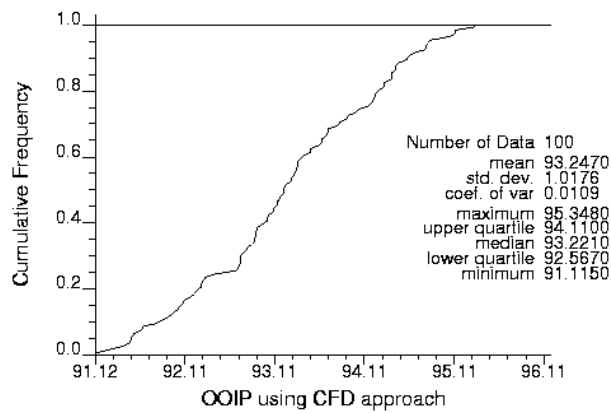
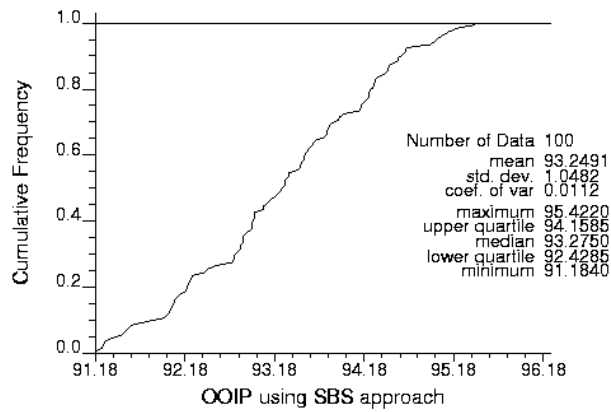
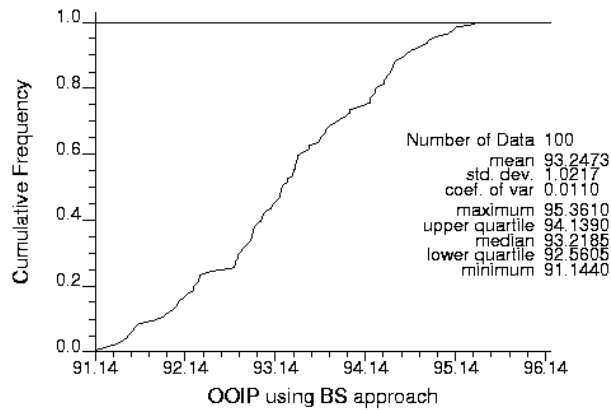


Figure 6-41: Case 2: The impacts of the uncertainty of H1 layer thickness on the HIIP with parameter uncertainty. The deviations in the H1 layer thickness uncertainty were assumed to have a standard deviation of 3m. The plots from top to bottom are the results of using BS, SBS, and CFD approaches, respectively; the results are in millions m³.

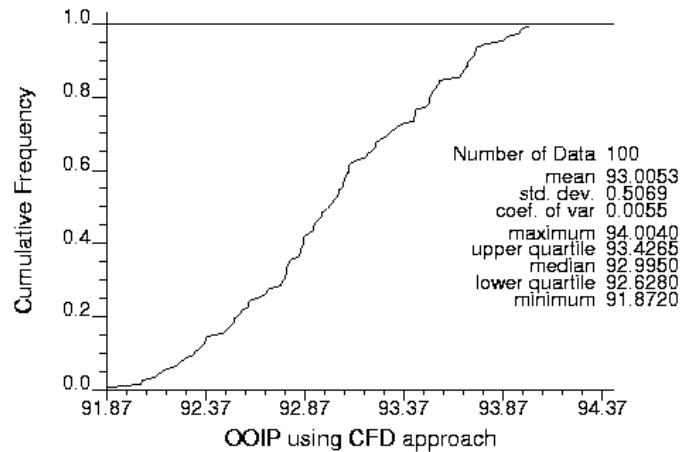
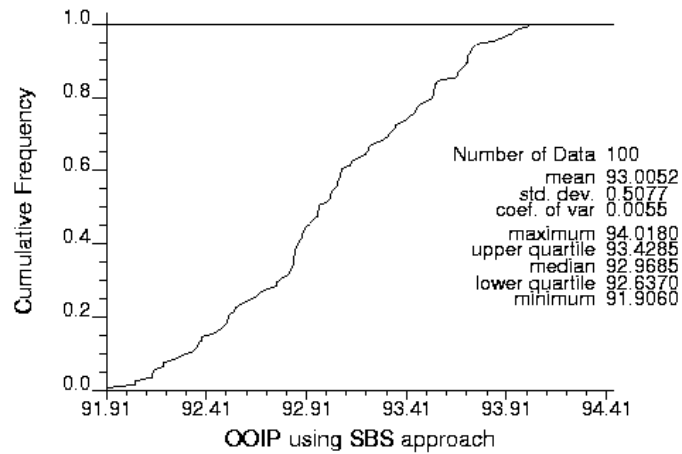
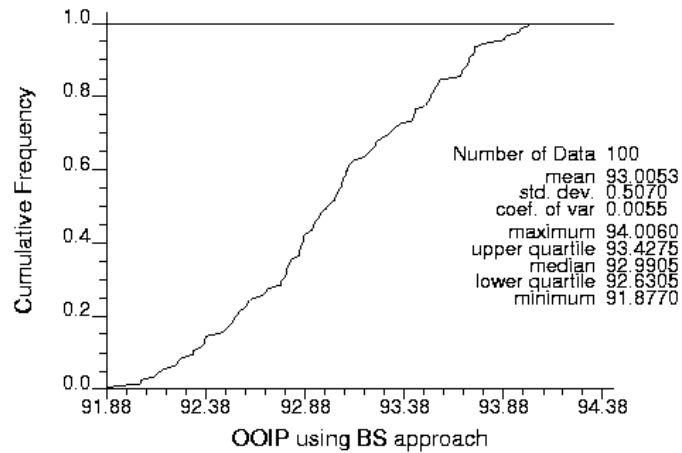


Figure 6-42: Case 3: The impacts of the uncertainty of H2 layer thickness on the HIIP with parameter uncertainty. The deviations in the H2 layer thickness uncertainty were assumed to have a standard deviation of 3m. The plots from top to bottom are the results of using BS, SBS, and CFD approaches, respectively. The results are in millions m³.

6.3.3. HIIP with Uncertainty in Fluid Contacts Level

The same assumptions in the scenario without parameter uncertainty were assumed in these scenarios with parameter uncertainty. It was assumed that there is no gas cap; therefore, only OWC uncertainty had to be investigated. The OWC levels uncertainty was assumed to have a triangular distribution shape. The OWC level uncertainty distribution can be determined by the minimum, maximum and most likely levels of OWC.

In this study, there is no uncertainty in the minimum and maximum OWC levels, while the most likely levels of OWC, the mode was variable in each realization. 100 realizations were generated using *mcs* code assuming a triangular distribution with a variable mode, see Section 5.2.3. These realizations were used to get the HIIP distributions above OWC as shown in Figure 6-43. The mean and the standard deviation of HIIP were 92.9180 and 0.0644 MMm³, respectively.

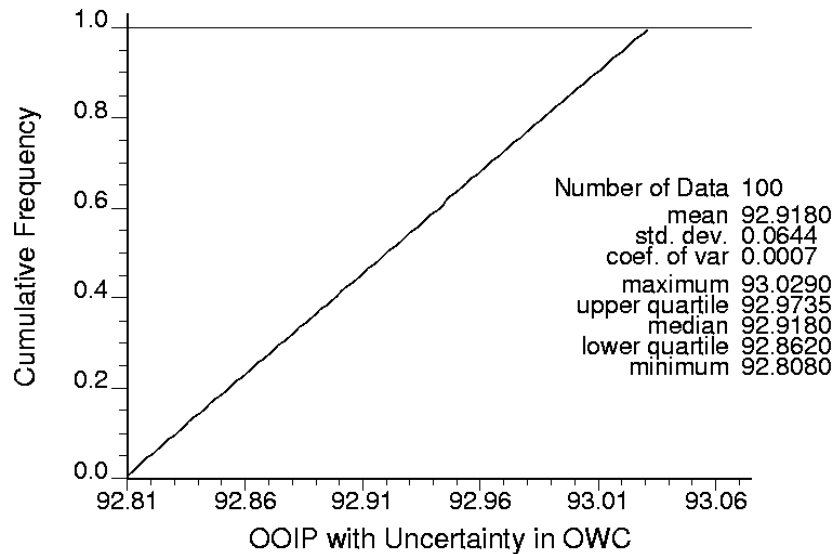


Figure 6-43: Case 4: The impacts of the uncertainty of OWC levels on the HIIP with parameter uncertainty. The deviations in the OWC levels were assumed to have a triangular distribution with a variable mode and fixed limits, minimum and maximum levels. The results are in millions m³.

6.3.4. HIIP with Uncertainty in Petrophysical Properties

Uncertainties in petrophysical properties with parameter uncertainty in the mean were assessed in four cases. Cases 5 through 8 investigate the uncertainty in H1 layer NTG, H2 layer NTG, H1 layer porosity, and H2 layer porosity, individually and respectively. The four cases were conducted three times each. The parameter uncertainty approach was changed in each scenario to compare the three different approaches, BS, SBS, and CFD. The parameter uncertainty distributions obtained in section 6.3.1 were incorporated in the methodology of estimating HIIP with parameter uncertainty as described in section 5.2.4.

In each scenario, a parameter uncertainty distribution was used to generate 100 input reference distributions by shifting the original reference distribution to have a new mean drawn from the parameter uncertainty distribution. A *shift_pdf* code was created for this purpose in this study (see Appendix A). Then 100 realizations were generated for each variable by cosimulating NTG and Porosity of each layer simultaneously with thickness using an *ultimate_sgsim* code. The HIIP distributions were obtained for the four cases in each scenario.

The impacts of the NTG uncertainty for H1 layer on the HIIP with parameter uncertainty were shown on Figure 6-44 using the different parameter uncertainty approaches, BS, SBS, and CFD. In case 5, the HIIP distribution with parameter uncertainty had a mean and a standard deviation of 93.3908 and 6.3876 MMm³ using BS approach 90.3157 and 6.9903 MMm³ using SBS approach and 91.5688 and 5.0388 MMm³ using CFD approach.

The same methodology was followed in case 6 to investigate the impacts of the NTG uncertainty for H1 layer on the HIIP with parameter uncertainty using BS, SBS, and CFD approaches. The results are shown in Figure 6-45. The HIIP distribution with parameter uncertainty had a mean and a standard deviation of

94.1744 and 3.8429 MMm³ using BS approach 92.6174 and 3.9092 MMm³ using SBS approach and 94.8937 and 3.1845 MMm³ using CFD approach.

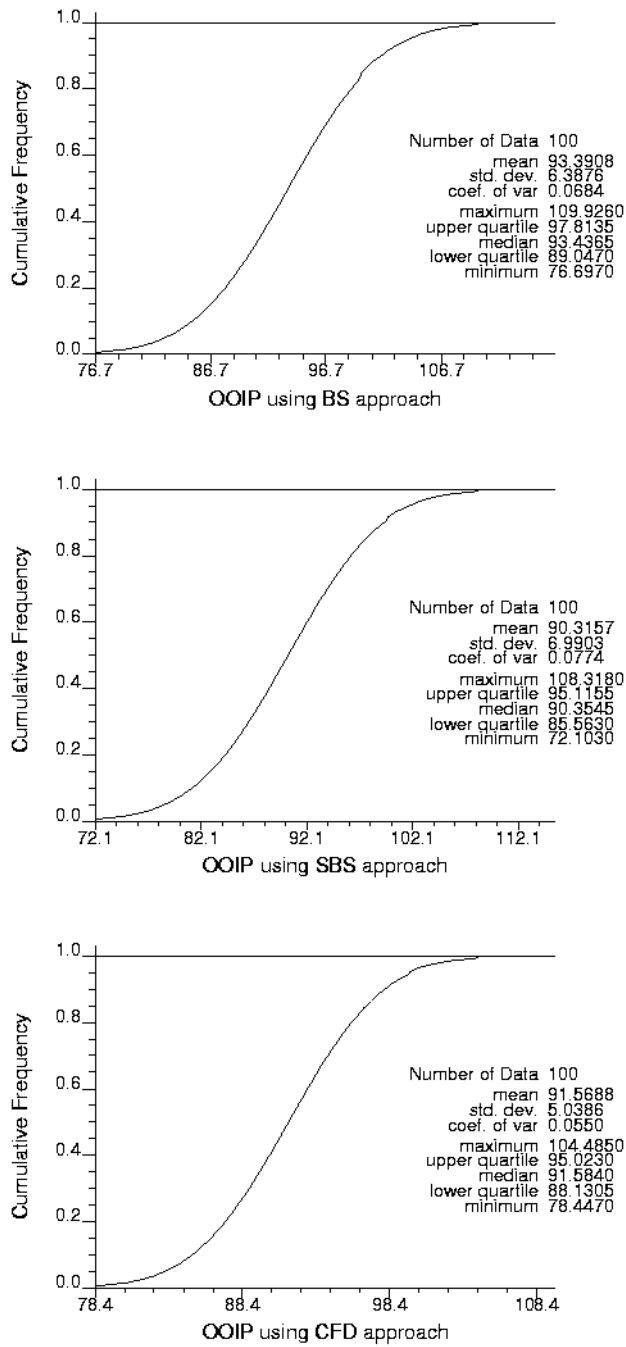


Figure 6-44: Case 5: The impacts of the uncertainty of H1 layer NTG on the HIIP with parameter uncertainty. The plots from top to bottom are the results of using BS, SBS, and CFD approaches, respectively. The results are in millions m³.

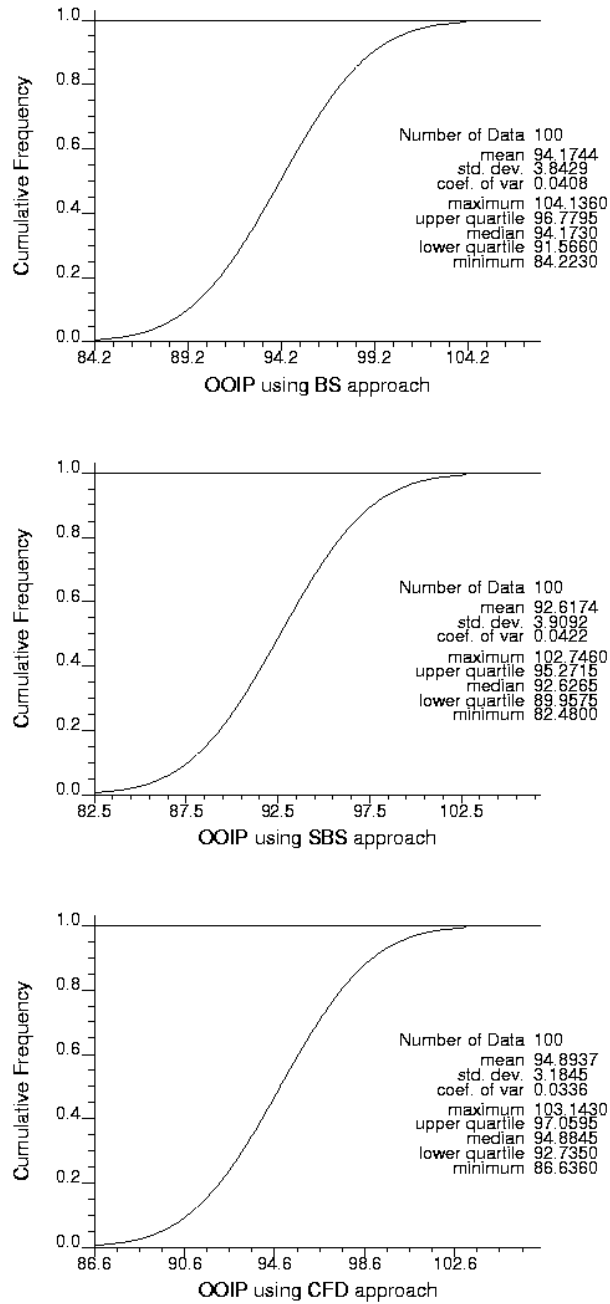


Figure 6-45: Case 6: The impacts of the uncertainty of H2 layer NTG on the HIIP with parameter uncertainty. The plots from top to bottom are the results of using BS, SBS, and CFD approaches, respectively. The results are in millions m³.

Cases 7 and 8 were conducted to investigate the impacts of the porosity uncertainty for H1 and H2 layers on the HIIP with parameter uncertainty using BS, SBS, and CFD approaches. The results of case 7 are shown in Figure 6-46 for

the HIIP distribution with parameter uncertainty with a mean and a standard deviation of 92.8095 and 2.3520 Mm³ using BS approach 91.7472 and 2.6676 Mm³ using SBS approach and 93.1311 and 1.6491 Mm³ using CFD

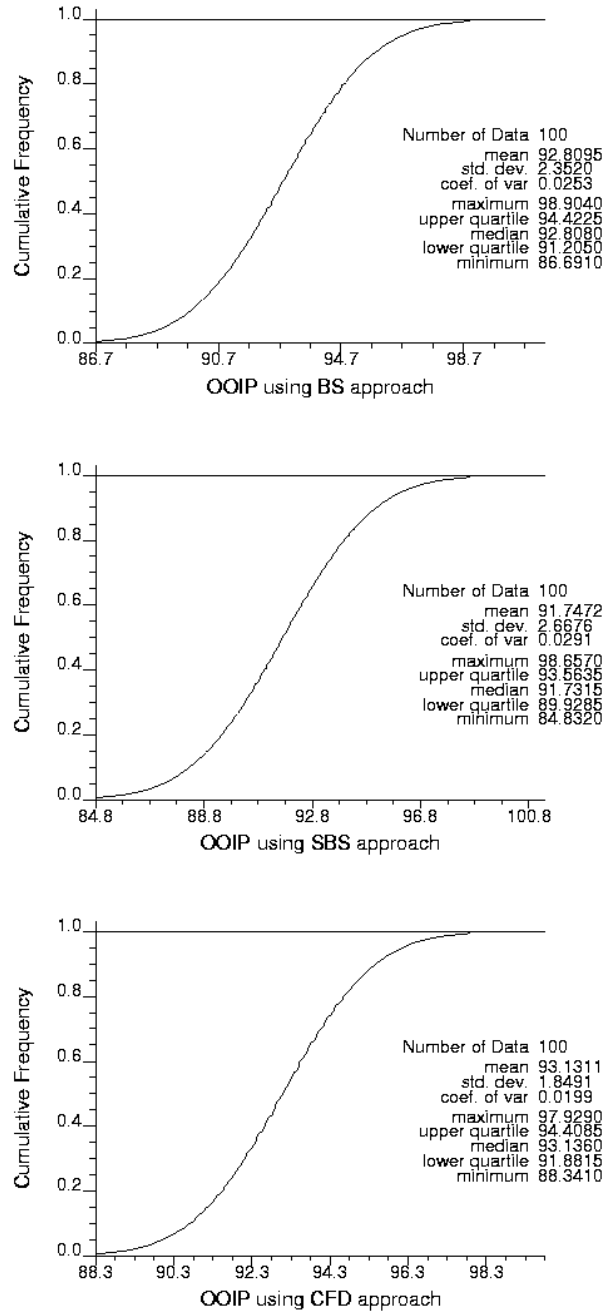


Figure 6-46: Case 7: The impacts of the uncertainty of H1 layer porosity on the HIIP with parameter uncertainty. The plots from top to bottom are the results of using BS, SBS, and CFD approaches, respectively. The results are in millions m³.

approach. Figure 6-47 shows the results of case 8, the HIIP distributions with a mean and a standard distribution of 92.3249 and 2.2224 MMm³ using BS approach 91.1167 and 2.4022 MMm³ using SBS approach and 92.9032 and 1.8826 MMm³ using CFD approach.

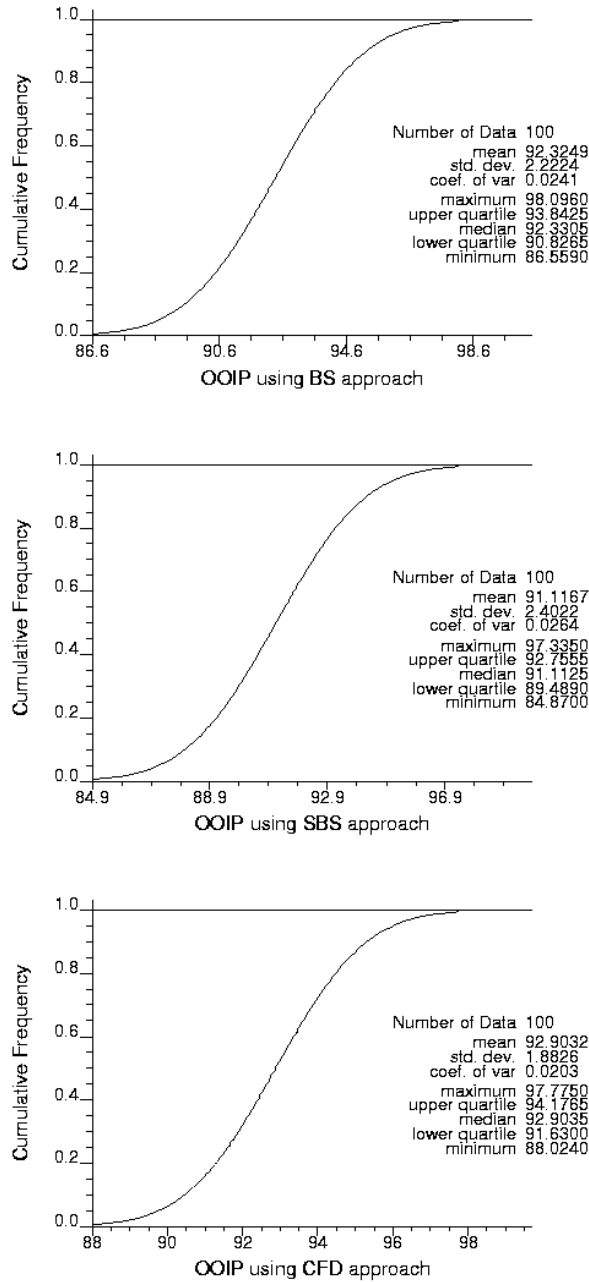


Figure 6-47: Case 8: The impacts of the uncertainty of H2 layer porosity on the HIIP with parameter uncertainty. The plots from top to bottom are the results of using BS, SBS, and CFD approaches, respectively. The results are in millions m³.

6.3.5. HIIP with Full Uncertainty

Quantifying the uncertainties in estimating the reserve/resource volumes with parameter uncertainty is the main aim of this research. The Multivariate Parameter Uncertainty technique is used in this case to quantify the full uncertainty in HIIP with parameter uncertainty. It is based on incorporating the correlation coefficients among all variables of interest to determine the means of parameter uncertainty. Those means are used to simulate different uncertainty realizations for parameters of interest.

This case shows the results of the novel scenario developed in this research to incorporate a parameter uncertainty in the mean that can be obtained from using a parameter uncertainty approach. All four techniques described in section 5.2 were used in this case to assess HIIP uncertainty with parameter uncertainty in all parameters of interest. The four techniques are Multivariate Parameter Uncertainty, SGS, MCS, and Cosimulating with Super Secondary data. Three scenarios were conducted with the three parameter uncertainty approaches, BS, SBS, or CFD individually.

First technique was MVPU that accounts for the correlation coefficients between all variables of interest. The *nscore* code was used first to generate transformation tables for all variables of interest (Deutsch and Cullick; 2002). In this study, transformation tables were obtained for seven variables in each scenario. Next step was to generate random normal score values (0,1) by running *mcs* code. There were 100 values in each column as the number of uncertainty realizations needed to be generated. Then, the *correlate* code was used to incorporate the correlation coefficients between the variables of interest. The results had to be back transformed to the real units using the transformation tables. The *backtr* code developed by CCG was used for such purpose. The results are the values that would be used as means for the uncertainty realizations. The correlation coefficients were checked by running *corrmat* code (Neufeld and

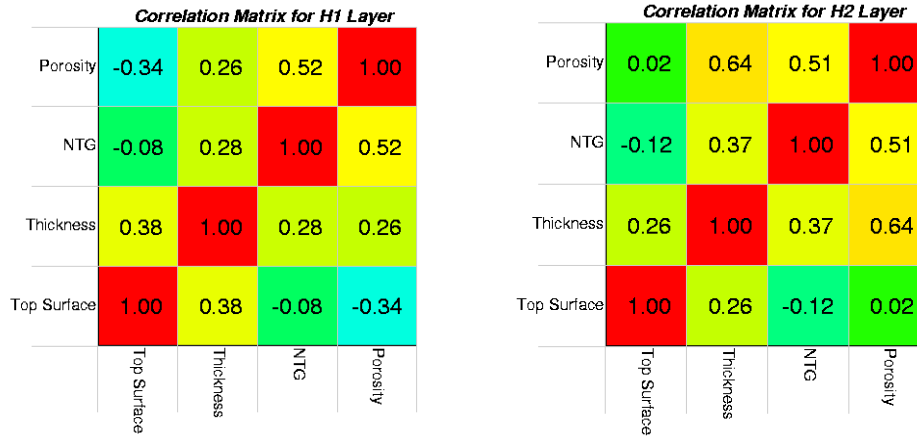


Figure 6-48: Correlation coefficient matrix between the mean values obtained from MVPU technique for all variables of interest in the two layers.

Deutsch; 2006) to generate the correlation coefficients between the results and compare the coefficients to those were obtained between the original well data, see Figure 6-48.

After obtaining the mean values, they were used to find the values of dx , the conditioning values at well locations used in SGS to quantify the uncertainties in the structural surfaces variables. The standard deviations of 15m for top and bottom surfaces uncertainty and 3m for thickness uncertainty of each layer were also used. The MVPU results were also used to generate the input reference distributions that were used in the cosimulation technique with super secondary data to quantify the uncertainties in the petrophysical properties, NTG and porosity for both layers, H1 and H2. The uncertainty in the OWC level was quantified by using MCS technique.

The uncertainty realizations were obtained for all variables of interest and combined to calculate the 100 HIIP realizations and generate its distribution as shown in Figure 6-49. The HIIP distributions with parameter uncertainty were with a mean and a standard deviation of 94.7320 and 15.0209 MMm³ using BS approach 87.9839 and 15.6295 MMm³ using SBS approach and 94.3674 and

12.2283 MMm³ using CFD approach. Next section compares and discusses the results of quantifying HIIP uncertainty with/without parameter uncertainty using the three different approaches.

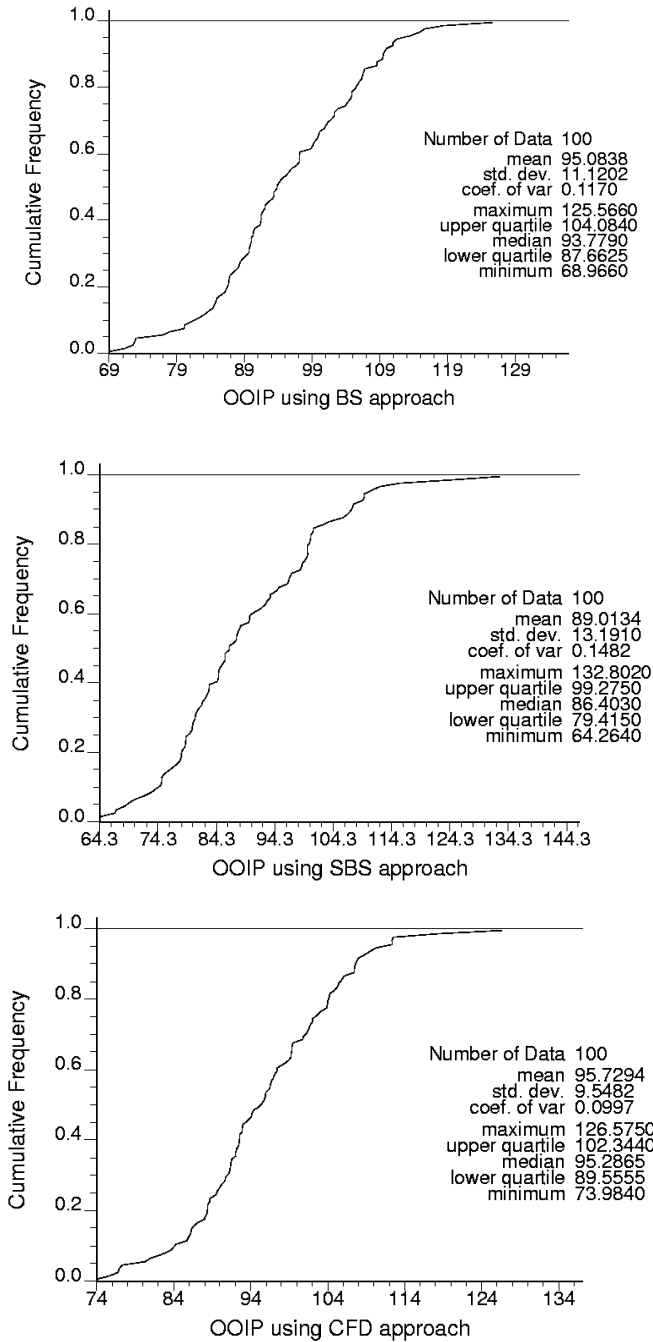


Figure 6-49: Case 9: The impacts of the full uncertainty of all parameters on the HIIP with parameter uncertainty. The plots from top to bottom are the results of using BS, SBS, and CFD approaches, respectively. The results are in millions m³.

6.3.6. HIIP with Uncertainty in Petrophysical Properties Using High Variogram Ranges

It was noticed that the variogram range for NTG and porosity of both layers, 500 to 800m were too small compared to the field size 5000 x 6500m, which made the standard deviation of using SBS and CFD not far away from those obtained from BS approach. Therefore, it was assumed that the variogram range was arbitrary high to be about 2500m to see the effects of increasing the variogram range on the HIIP uncertainty. The four cases 5 through 8 were repeated to investigate the impacts of each variable of interest on the HIIP with parameter uncertainty. They were also repeated for the three scenarios using different parameter uncertainty approaches. Of course, the parameter uncertainty distributions for those variables were already generated with the arbitrary high variogram range as shown in Figure 6-38 and 6-39.

The effects of NTG uncertainty for H1 layer on HIIP distribution with parameter uncertainty were quantified as shown in Figure 6-50. The HIIP distributions with parameter uncertainty were with a mean and a standard deviation of 93.3908 and 6.3876 MMm³ using BS approach 90.9277 and 8.0360 MMm³ using SBS approach and 92.2973 and 6.7492 MMm³ using CFD approach.

The HIIP cumulative distributions, investigating the H2 layer NTG uncertainty with parameter uncertainty, were shown on Figure 6-51. They were with a mean and a standard deviation of 94.1744 and 3.8429 MMm³ using BS approach 93.8443 and 5.0619 MMm³ using SBS approach and 97.0139 and 4.3152 MMm³ using CFD approach.

Figure 6-52 showed the HIIP cumulative distributions with parameter uncertainty in H1 layer porosity were with a mean and a standard deviation of

94.1744 and 3.8429 MMm³ using BS approach 93.8443 and 5.0619 MMm³ using SBS approach and 97.0139 and 4.3152 MMm³ using CFD approach.

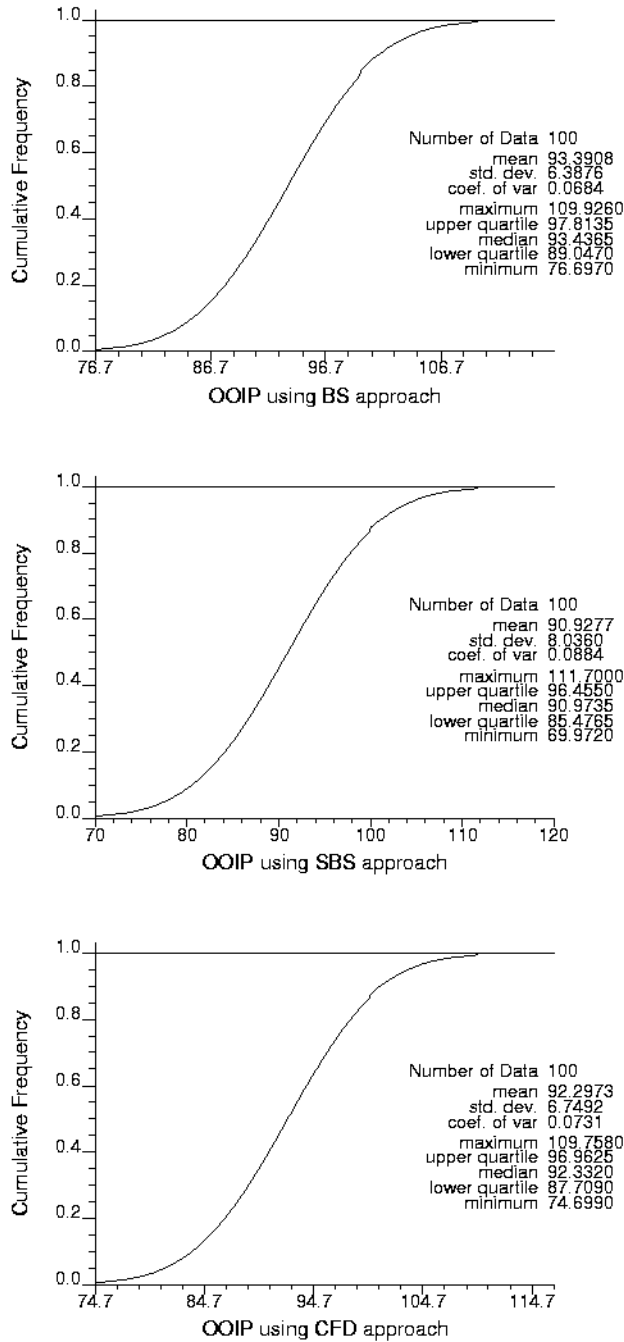


Figure 6-50: Case 5: The impacts of the uncertainty of H1 layer NTG on the HIIP with parameter uncertainty. The plots from top to bottom are the results of using BS, SBS, and CFD approaches and with arbitrary high variogram range, 2500m, respectively. The results are in millions m³.

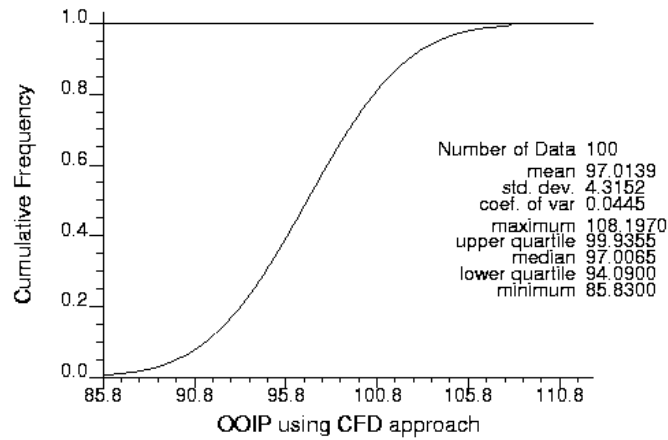
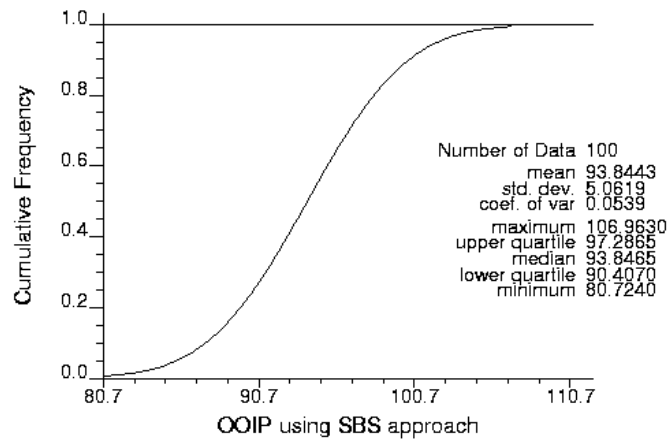
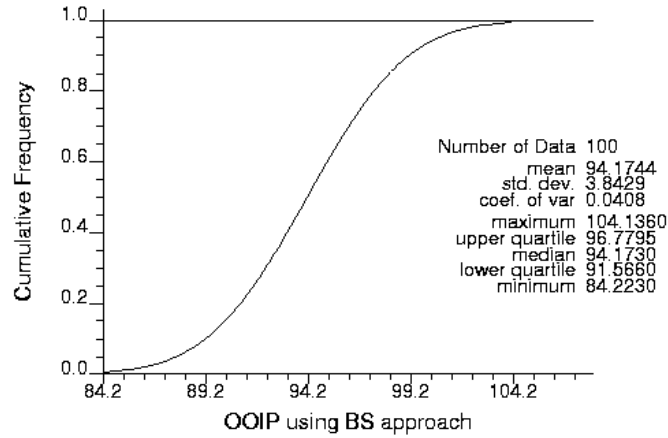


Figure 6-51: Case 6: The impacts of the uncertainty of H2 layer NTG on the HIIP with parameter uncertainty. The plots from top to bottom are the results of using BS, SBS, and CFD approaches and with arbitrary high variogram range, 2500m, respectively. The results are in millions m³.

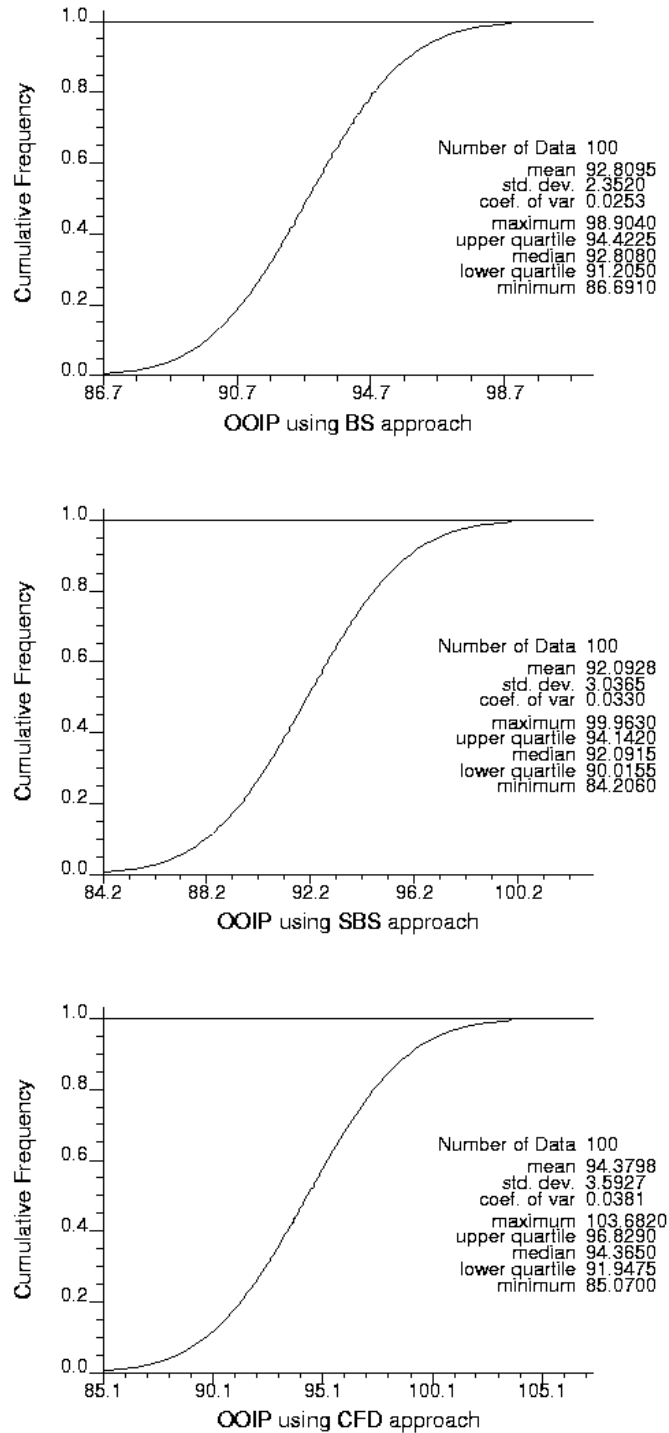


Figure 6-52: Case 7: The impacts of the uncertainty of H1 layer porosity on the HIIP with parameter uncertainty. The plots from top to bottom are the results of using BS, SBS, and CFD approaches and with an arbitrary high variogram range, 2500m, respectively. The results are in millions m³.

For case 8, the effects of porosity uncertainty for H2 layer on HIIP distributions with parameter uncertainty were shown on Figure 6-53. The HIIP distributions were with a mean and a standard distribution of 92.3249 and 2.2224 MMm³ using BS approach 91.2068 and 3.0622 MMm³ using SBS approach and 92.6851 and 2.0242 MMm³ using CFD approach.

6.3.7. HIIP with Full Uncertainty Using High Variogram Ranges

The HIIP uncertainty with parameter uncertainty in all variables of interest was investigated. Case 9 as in section 6.3.5 was repeated but with the arbitrary high variogram range, 2500m. The HIIP distributions with parameter uncertainty were shown in Figure 6-54 and were with a mean and a standard deviation of 95.0838 and 11.1202 MMm³ using BS approach 91.5967 and 15.7863 MMm³ using SBS approach and 100.5689 and 13.5197 MMm³ using CFD approach, respectively.

6.4. Comparing Results and Discussion

All HIIP distributions were obtained for all nine cases in the four scenarios, without parameter uncertainty and with parameter uncertainty using different parameter uncertainty distributions. Some statistical analysis were conducted on those distributions and summarized in Table 6-5. Spider charts and tornado charts were used to compare the uncertainty effects of each parameter on HIIP estimation with/without parameter uncertainty using all different approaches. They were also used to investigate the key parameters that play a major role in the HIIP uncertainty in each scenario.

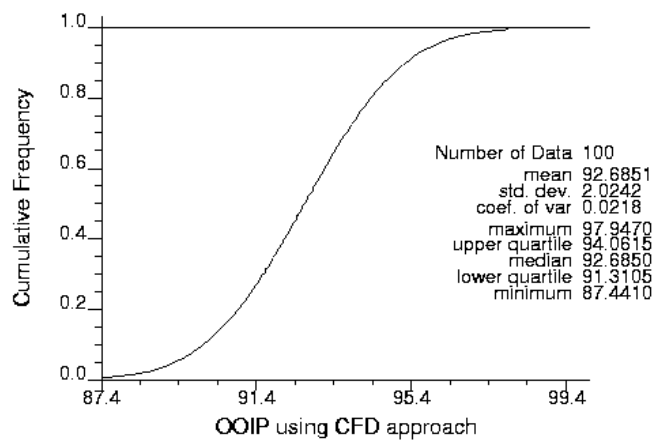
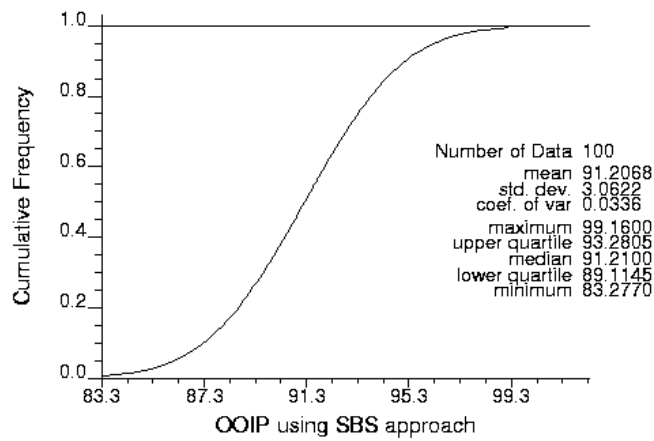
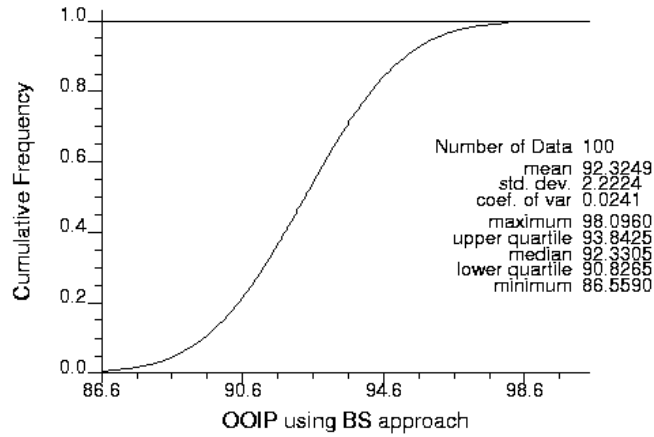


Figure 6-53: Case 8: The impacts of the uncertainty of H2 layer porosity on the HIIP with parameter uncertainty. The plots from top to bottom are the results of using BS, SBS, and CFD approaches and with an arbitrary high variogram range, 2500m, respectively. The results are in millions m³.

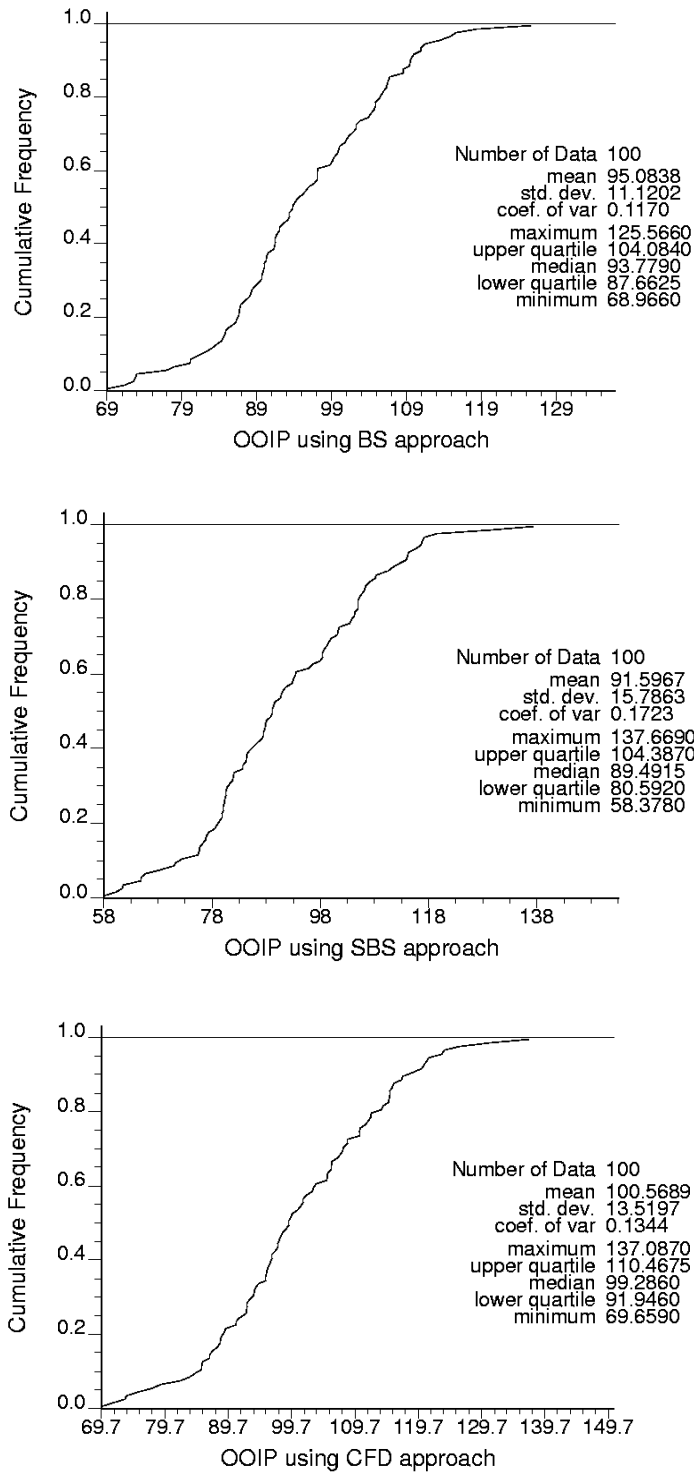


Figure 6-54: Case 9: The impacts of the full uncertainty of all parameters on the HIIP with parameter uncertainty. The plots from top to bottom are the results of using BS, SBS, and CFD approaches and with an arbitrary high variogram range, 2500m, respectively. The results are in millions m³.

Statistics of Both Layers OoIP with/without Parameter Uncertainty											
Case#	PU Approach	Mean	Std	Minimum	Maximum	P90	P50	P10	P90-Mean	P50-Mean	P10-Mean
1 - Uncertainty in Top Structures	No PU	92.8086	0.7745	90.9420	94.8240	93.9310	92.7975	91.8315	1.1224	-0.0111	-0.9771
	BS	92.8966	0.9583	90.9840	94.9930	94.1325	92.8730	91.6285	1.3239	0.0644	-1.1801
	SBS	92.8960	0.9868	90.8830	95.0460	94.2360	92.8745	91.4965	1.4274	0.0659	-1.3121
	CFD	92.8968	0.9498	91.0060	94.9910	94.1205	92.8825	91.6505	1.3119	0.0739	-1.1581
2 - Uncertainty in H1 Thickness	No PU	93.1718	0.8546	91.3030	95.7990	94.3780	93.1380	92.1180	1.5694	0.3294	-0.6906
	BS	93.2473	1.0217	91.1440	95.3610	94.5880	93.2185	91.8395	1.7794	0.4099	-0.9691
	SBS	93.2491	1.0482	91.1840	95.4220	94.5925	93.2750	91.8495	1.7839	0.4664	-0.9591
	CFD	93.2470	1.0176	91.1150	95.3480	94.5960	93.2210	91.8285	1.7874	0.4124	-0.9801
3 - Uncertainty in H2 Thickness	No PU	92.9618	0.4405	92.0320	94.2300	93.5755	92.9585	92.4540	0.7669	0.1499	-0.3546
	BS	93.0053	0.5070	91.8770	94.0060	93.7040	92.9905	92.3140	0.8954	0.1819	-0.4946
	SBS	93.0052	0.5077	91.9060	94.0180	93.7100	92.9685	92.3125	0.9014	0.1599	-0.4961
	CFD	93.0053	0.5069	91.8720	94.0040	93.7020	92.9950	92.3150	0.8934	0.1864	-0.4936
4 - Uncertainty in OWC	No PU	92.9115	0.0048	92.9030	92.9240	92.9185	92.9110	92.9060	0.1099	0.1024	0.0974
	PU in the mode	92.9180	0.0644	92.8080	93.0290	93.0075	92.9180	92.8290	0.1989	0.1094	0.0204
5 - Uncertainty in H1 NTG	No PU	90.8410	0.3374	90.1890	92.9110	91.2345	90.8005	90.4765	-1.5741	-2.0081	-2.3321
	BS	93.3908	6.3876	76.6970	109.9260	101.5115	93.4365	85.1200	8.7029	0.6279	-7.6886
	BS with high range	93.3908	6.3876	76.6970	109.9260	101.5115	93.4365	85.1200	8.7029	0.6279	-7.6886
	SBS	90.3157	6.9903	72.1030	108.3180	99.4270	90.3545	81.2595	6.6184	-2.4541	-11.5491
	SBS with high range	90.9277	8.0360	69.9720	111.7000	101.1200	90.9735	80.5245	8.3114	-1.8351	-12.2841
	CFD	91.5688	5.0386	78.4470	104.4850	98.1170	91.5840	85.0455	5.3084	-1.2246	-7.7631
	CFD with high range	92.2973	6.7492	74.6990	109.7580	100.7715	92.3320	83.5590	7.9629	-0.4766	-9.2496
6 - Uncertainty in H2 NTG	No PU	91.4682	0.2131	91.0640	92.9110	91.6740	91.4500	91.2620	-1.1346	-1.3586	-1.5466
	BS	94.1744	3.8429	84.2230	104.1360	99.1265	94.1730	89.2195	6.3179	1.3644	-3.5891
	BS with high range	94.1744	3.8429	84.2230	104.1360	99.1265	94.1730	89.2195	6.3179	1.3644	-3.5891
	SBS	92.6174	3.9092	82.4800	102.7460	97.6600	92.6265	87.5760	4.8514	-0.1821	-5.2326
	SBS with high range	93.8443	5.0619	80.7240	106.9630	100.3770	93.8465	87.3130	7.5684	1.0379	-5.4956
	CFD	94.8937	3.1845	86.6360	103.1430	99.0100	94.8845	90.7785	6.2014	2.0759	-2.0301
	CFD with high range	97.0139	4.3152	85.8300	108.1970	102.5865	97.0065	91.4500	9.7779	4.1979	-1.3586
7 - Uncertainty in H1 Porosity	No PU	90.8585	0.2242	90.5610	92.9110	90.9635	90.8290	90.7245	-1.8451	-1.9796	-2.0841
	BS	92.8095	2.3520	86.6910	98.9040	95.8545	92.8080	89.7740	3.0459	-0.0006	-3.0346
	BS with high range	92.8095	2.3520	86.6910	98.9040	95.8545	92.8080	89.7740	3.0459	-0.0006	-3.0346
	SBS	91.7472	2.6677	84.8320	98.6570	95.2010	91.7315	88.3045	2.3924	-1.0771	-4.5041
	SBS with high range	92.0927	3.0365	84.2060	99.9630	96.0270	92.0915	88.1635	3.2184	-0.7171	-4.6451
	CFD	93.1311	1.8491	88.3410	97.9290	95.5255	93.1360	90.7595	2.7169	0.3274	-2.0491
	CFD with high range	94.3798	3.5927	85.0700	103.6820	99.0225	94.3650	89.7470	6.2139	1.5564	-3.0616
8 - Uncertainty in H2 Porosity	No PU	91.4708	0.1555	91.3120	92.9110	91.5300	91.4550	91.3780	-1.2786	-1.3536	-1.4306
	BS	92.3249	2.2224	86.5590	98.0960	95.1970	92.3305	89.4610	2.3884	-0.4781	-3.3476
	BS with high range	92.3249	2.2224	86.5590	98.0960	95.1970	92.3305	89.4610	2.3884	-0.4781	-3.3476
	SBS	91.1167	2.4022	84.8700	97.3350	94.2050	91.1125	88.0110	1.3964	-1.6961	-4.7976
	SBS with high range	91.2068	3.0622	83.2770	99.1600	95.1500	91.2100	87.2585	2.3414	-1.5986	-5.5501
	CFD	92.9032	1.8826	88.0240	97.7750	95.3275	92.9035	90.4690	2.5189	0.0949	-2.3396
	CFD with high range	92.6851	2.0242	87.4410	97.9470	95.3010	92.6850	90.0685	2.4924	-0.1236	-2.7401
9 - Full Uncertainty	No PU	93.0990	1.1415	90.4020	95.8290	94.4935	93.0500	91.4405	1.6849	0.2414	-1.3681
	BS	95.0838	11.1202	68.9660	125.5660	109.5415	93.7790	81.6240	16.7329	0.9704	-11.1846
	BS with high range	95.0838	11.1202	68.9660	125.5660	109.5415	93.7790	81.6240	16.7329	0.9704	-11.1846
	SBS	89.0134	13.1910	64.2640	132.8020	107.3660	86.4030	74.3275	14.5574	-6.4056	-18.4811
	SBS with high range	91.5967	15.7863	58.3780	137.6690	113.5846	89.4915	72.3795	20.7760	-3.3171	-20.4291
	CFD	95.7294	9.5482	73.9840	126.5750	107.6170	95.2865	84.1300	14.8084	2.4779	-8.6786
	CFD with high range	100.5689	13.5197	69.6590	137.0870	117.9896	99.2860	84.9505	25.1810	6.4774	-7.8581

Table 6-5: Statistical analysis for all HIIP distributions from all cases in all scenarios; The results are in millions m³.

6.4.1. Comparing uncertainty effects of individual parameters in each scenario

It is important to investigate the uncertainty effects of individual parameters on HIIP estimations. Figure 6-55 shows the tornado chart and spider plot for uncertainty effects of individual parameters on HIIP estimations without parameter uncertainty. It is obvious that H1 layer thickness uncertainty was the most effective parameter on estimating HIIP, followed by top and bottom surfaces uncertainty then H2 layer thickness. So, the surface structural parameters were more effective on HIIP uncertainty than petrophysical properties. The uncertainty in OWC was the least effective parameter on HIIP.

The uncertainty effects of individual parameters in HIIP estimations with parameter uncertainty using BS approach were compared as shown in the tornado chart and spider plot of Figure 6-56. Petrophysical properties became more effective on HIIP estimation than structural surfaces parameters and H1 layer NTG was the most effective parameter followed by H2 layer NTG. Then the porosity of both layers H1 and H2 had almost the same effects. Then the remaining structural parameters were less effective. Finally, the uncertainty in OWC was the least effective parameter on HIIP.

The tornado chart and spider plot of Figure 6-57 compared the uncertainty effects of individual parameters in HIIP estimations with parameter uncertainty using SBS approach. The order of the most effective parameters on HIIP estimation with parameter uncertainty using SBS approach was as same as that obtained by using BS approach. H1 layer NTG was the most effective parameter followed by H2 layer NTG, and the uncertainty in OWC was the least effective parameter on estimating HIIP. Using CFD approach made a little change on the order of the effective parameters. The results had the same order except the porosity of layers H1 and H2 were exchanged; even though, they were close to each other, see Figure 6-58.

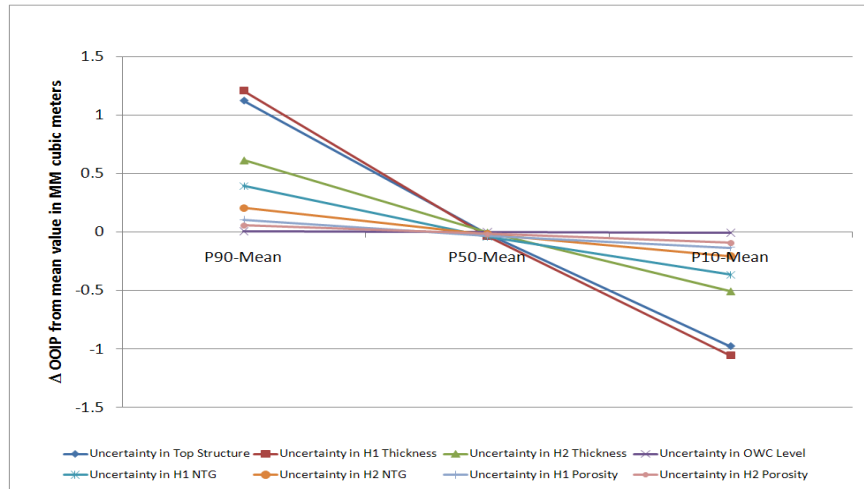
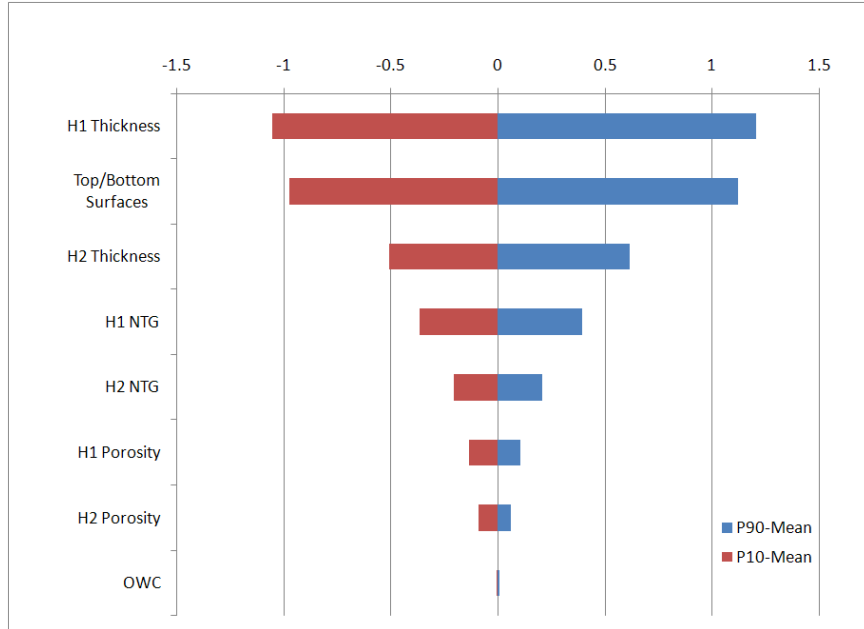


Figure 6-55: Sensitivity analysis for quantifying HIIP without parameter uncertainty; the results are in millions m^3 .

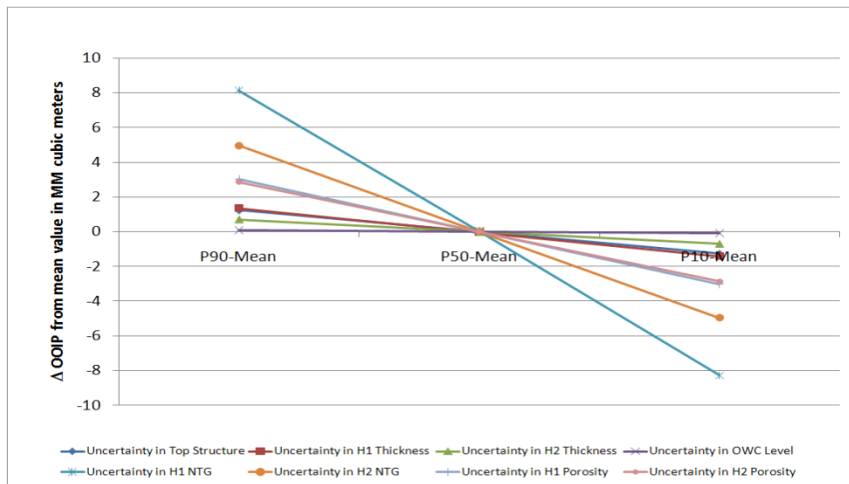
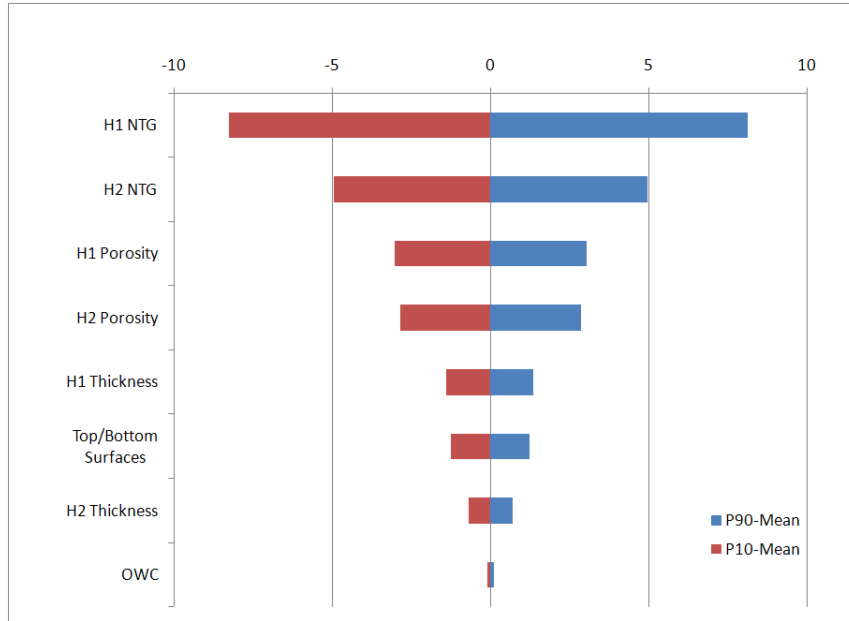


Figure 6-56: Sensitivity analysis for quantifying HIIP with parameter uncertainty using BS approach; the results are in millions m³.

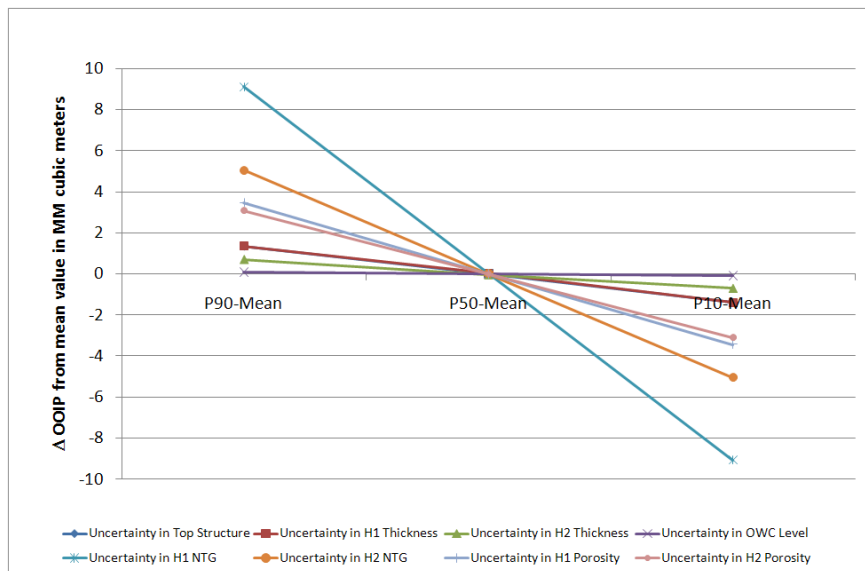
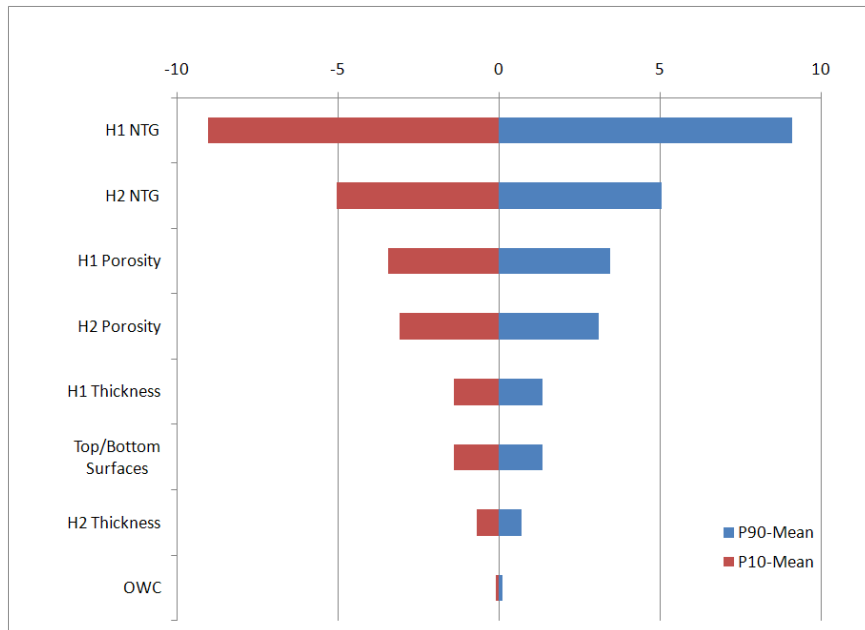


Figure 6-57: Sensitivity analysis for quantifying HIIP with parameter uncertainty using SBS approach; the results are in millions m^3 .

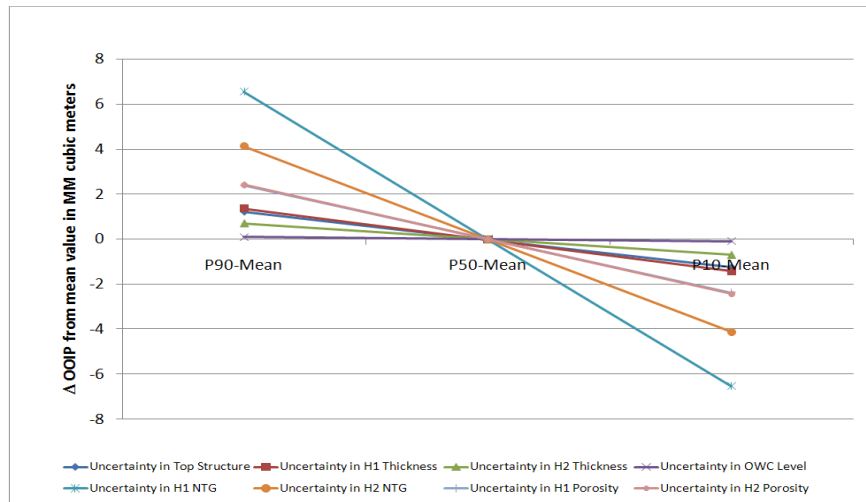
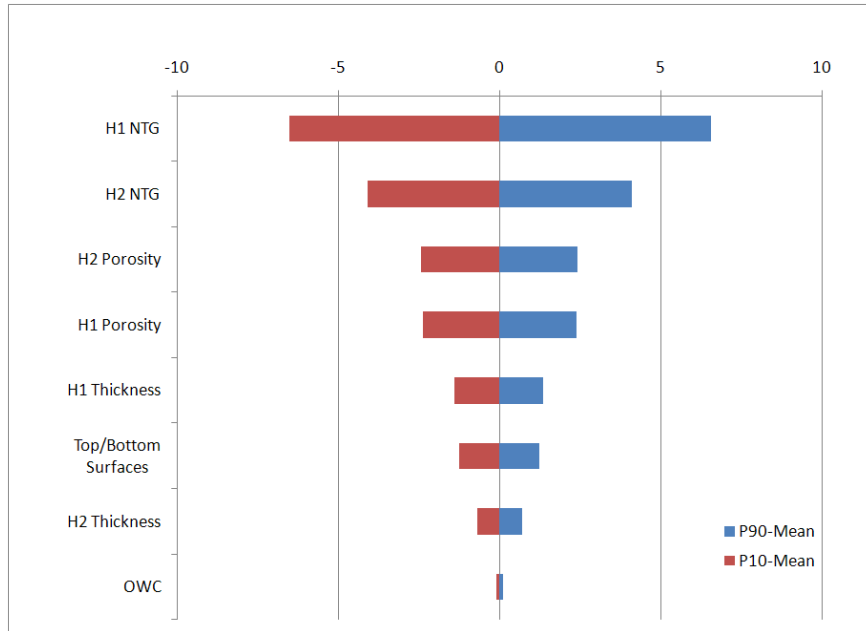


Figure 6-58: Sensitivity analysis for quantifying HIIP with parameter uncertainty using CFD approach; the results are in millions m^3 .

The three scenarios using different parameter uncertainty approaches were repeated with the arbitrary high variogram range of 2500m. The order of the parameters affecting HIIP distribution was almost the same as those obtained with low variogram ranges except the porosity of both layers H1 and H2 that sometimes had been exchanged; see Figures 6-59 to 6-61.

The orders of the parameters affecting HIIP uncertainty from the most effective parameter to the least effective one were summarized for all seven scenarios in Table 6-6. Two observations can be inferred from the comparison between those results. First, quantifying the uncertainty in HIIP without parameter uncertainty was more sensitive to structural surfaces parameters, then petrophysical properties, and last to the OWC. The other six scenarios quantifying the uncertainty in HIIP with parameter uncertainty were more sensitive to petrophysical properties, then structural surfaces parameters, and last to the OWC.

Second observation was about the order of the parameters in the six scenarios quantifying the uncertainty in HIIP with parameter uncertainty. It was almost the same except the porosity of H1 and H2 layers that were exchanged in those six scenarios because their effects on the HIIP uncertainty were almost close to each other.

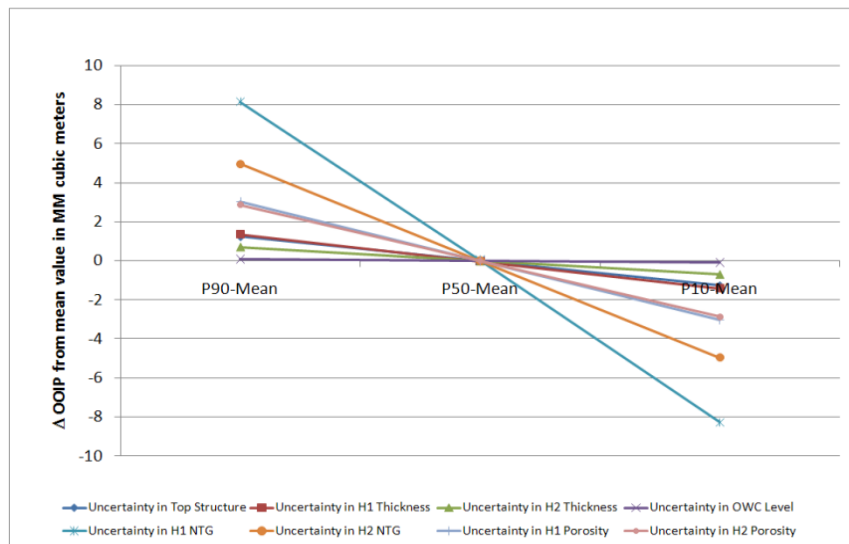
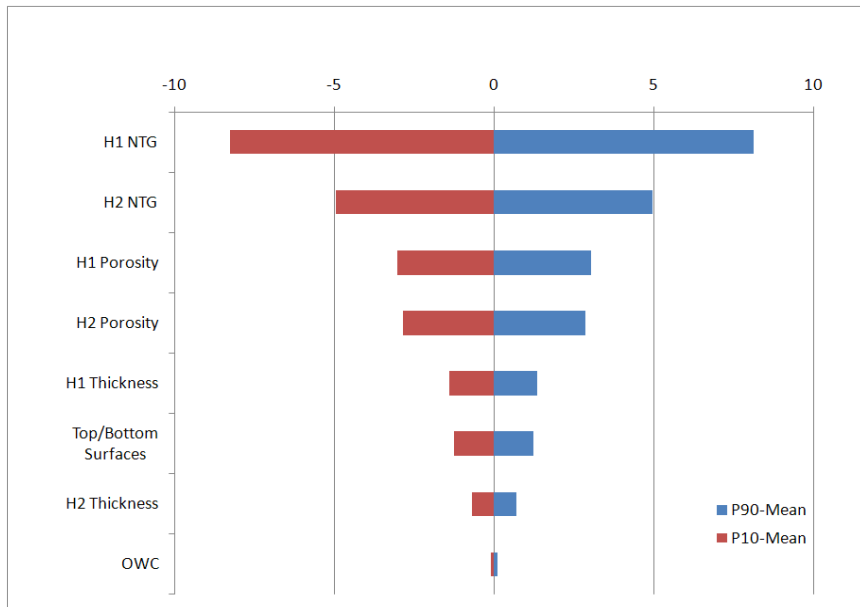


Figure 6-59: Sensitivity analysis for quantifying HIIP with parameter uncertainty using BS approach and high arbitrary variogram range of 2500m; the results are in millions m^3 .

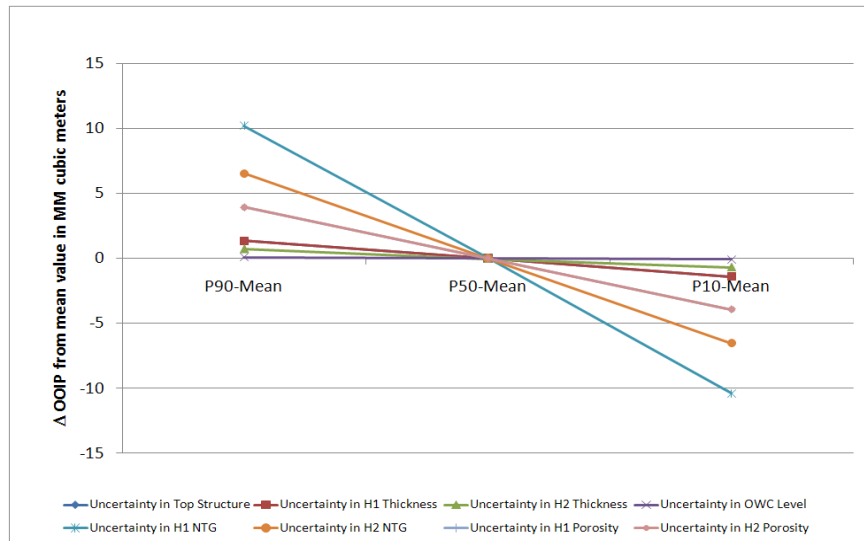
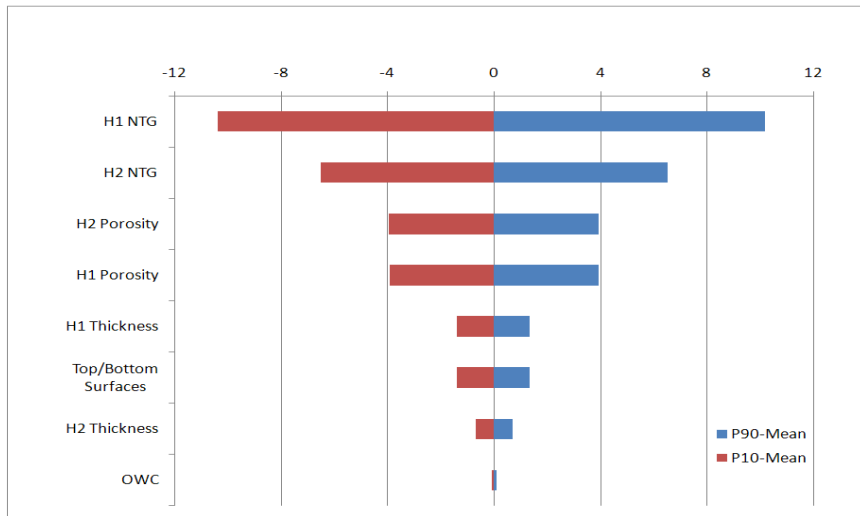


Figure 6-60: Sensitivity analysis for quantifying HIIP with parameter uncertainty using SBS approach and high arbitrary variogram range of 2500m; the results are in millions m^3 .

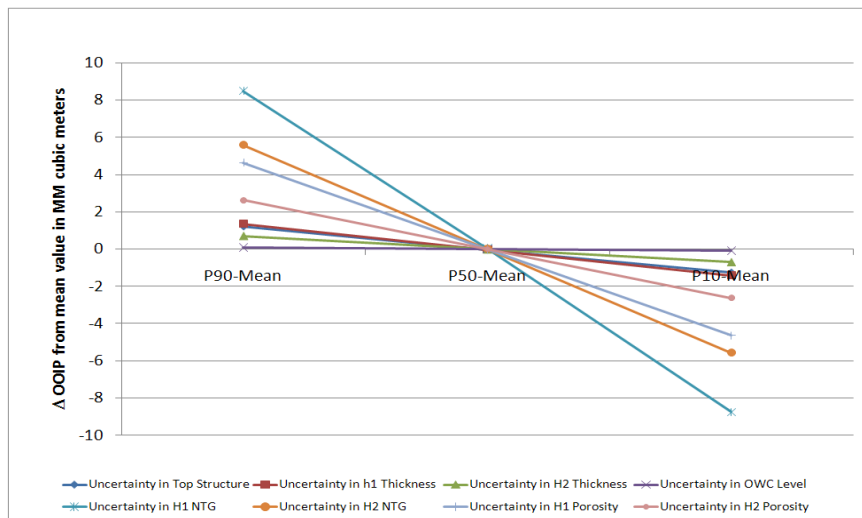
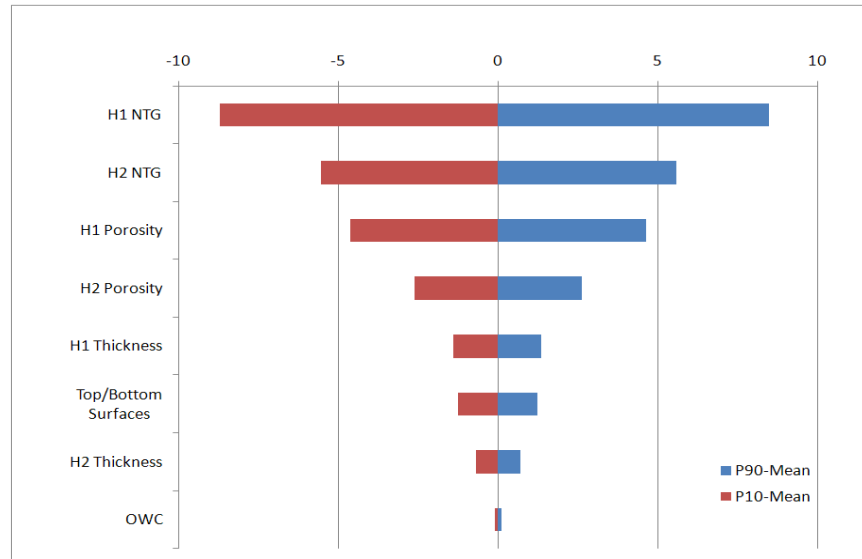


Figure 6-61: Sensitivity analysis for quantifying HIIP with parameter uncertainty using CFD approach and high arbitrary variogram range of 2500m; the results are in millions m³.

Scenarios	Order of parameters affecting on HIIP distribution from the most effective parameter to the least effective one in all seven scenarios.							
	Most effective parameters				Less effective parameters			
No PU	Thickness of H1	Top&bottom surfaces	Thickness of H2	NTG of H1	NTG of H2	Porosity of H1	Porosity of H2	OWC
BS	NTG of H1	NTG of H2	Porosity of H1	Porosity of H2	Thickness of H1	Top&bottom surfaces	Thickness of H2	OWC
SBS	NTG of H1	NTG of H2	Porosity of H1	Porosity of H2	Thickness of H1	Top&bottom surfaces	Thickness of H2	OWC
CFD	NTG of H1	NTG of H2	Porosity of H2	Porosity of H1	Thickness of H1	Top&bottom surfaces	Thickness of H2	OWC
BS with high range	NTG of H1	NTG of H2	Porosity of H1	Porosity of H2	Thickness of H1	Top&bottom surfaces	Thickness of H2	OWC
SBS with high range	NTG of H1	NTG of H2	Porosity of H2	Porosity of H1	Thickness of H1	Top&bottom surfaces	Thickness of H2	OWC
CFD with high range	NTG of H1	NTG of H2	Porosity of H1	Porosity of H2	Thickness of H1	Top&bottom surfaces	Thickness of H2	OWC

Table 6-6: Order of parameters affecting on HIIP distribution from the most effective parameter to the least effective one in all seven scenarios.

6.4.2. Comparing effects of uncertainty in individual parameters from different scenarios

The effects of changing parameter uncertainty approach on all parameters were investigated. Four scenarios investigated the effects of the uncertainty in top and bottom surfaces on HIIP estimation as shown in Figure 6-62 for case 1. The results of using parameter uncertainty approaches had more uncertainty compared to the scenario without parameter uncertainty. Using the SBS approach had the

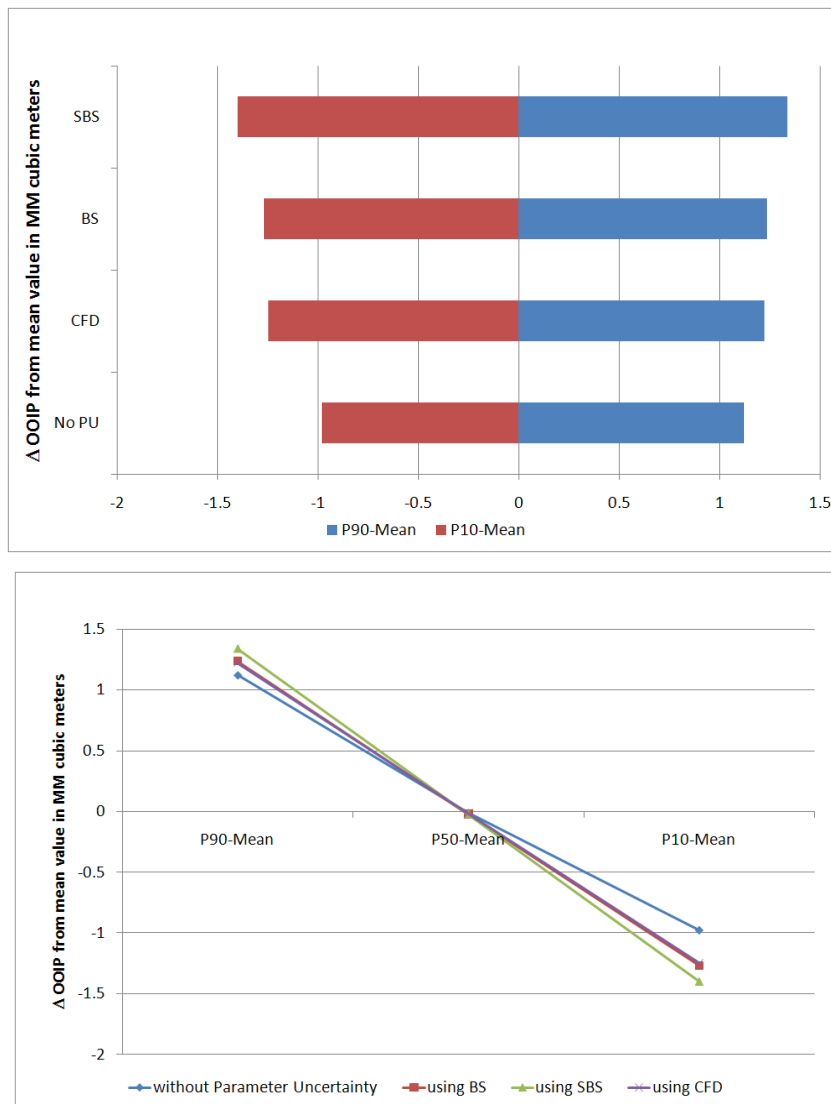


Figure 6-62: Case1: Sensitivity analysis to compare different parameter uncertainty approaches when calculating HIIP with uncertainty in Top/Bottom Structure Surfaces.

most uncertain HIIP distribution. Using the CFD approach gave narrower distribution than that obtained from using BS approach. All the three scenarios using parameter uncertainty approaches had similar HIIP distributions.

Case 2 investigated the effects of the uncertainty in H1 layer thickness on HIIP distribution using different approaches, see Figure 6-63. The results showed wider HIIP distribution with using parameter uncertainty approaches. The order

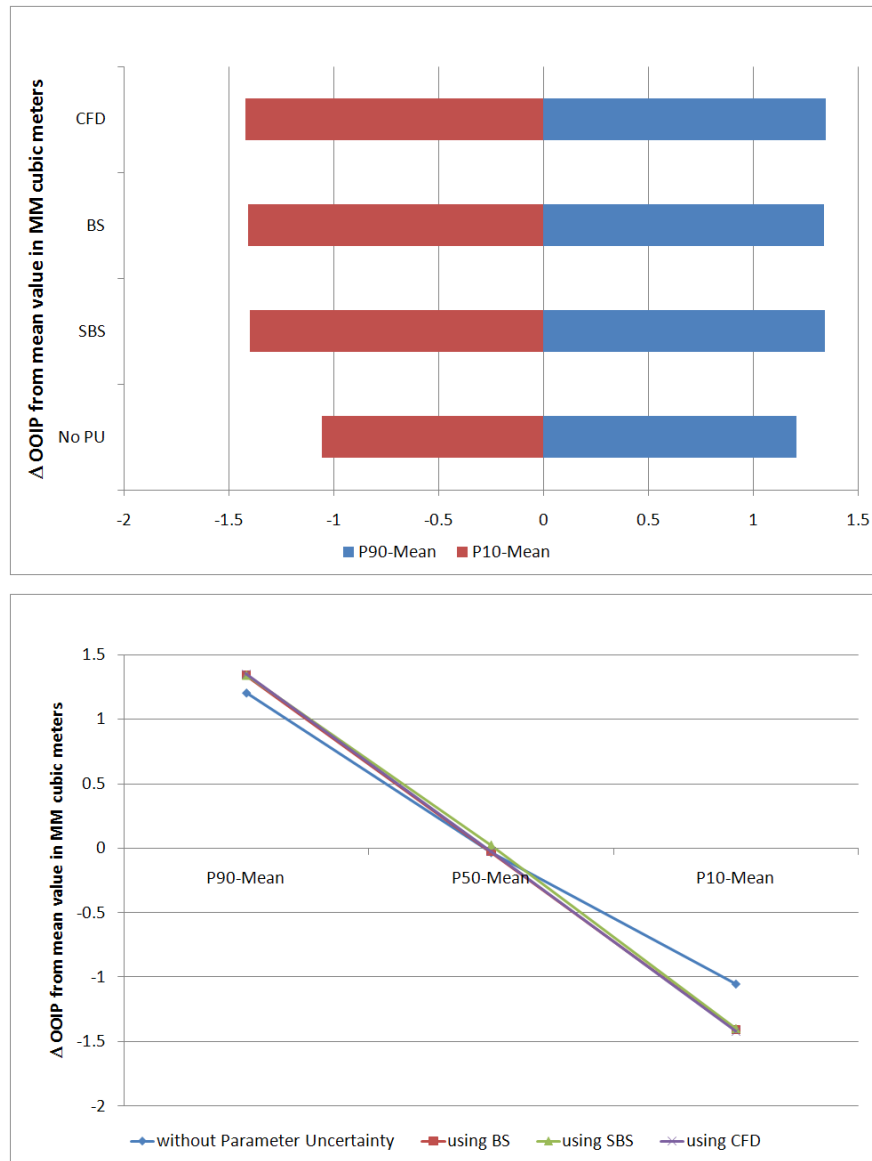


Figure 6-63: Case2: Sensitivity analysis to compare different parameter uncertainty approaches when calculating HIIP with uncertainty in thickness of H1 layer.

of approaches from more uncertain distributions to less uncertain distributions is CFD, BS, and SBS; although, the results were close to each other.

The effects of the uncertainty in H2 layer thickness on HIIP distributions using different approaches were investigated in case 3. The results in Figure 6-64 showed similar results to those obtained in case 2, but with different order of the parameter uncertainty approaches since the three approaches had almost the same effects on HIIP distributions.

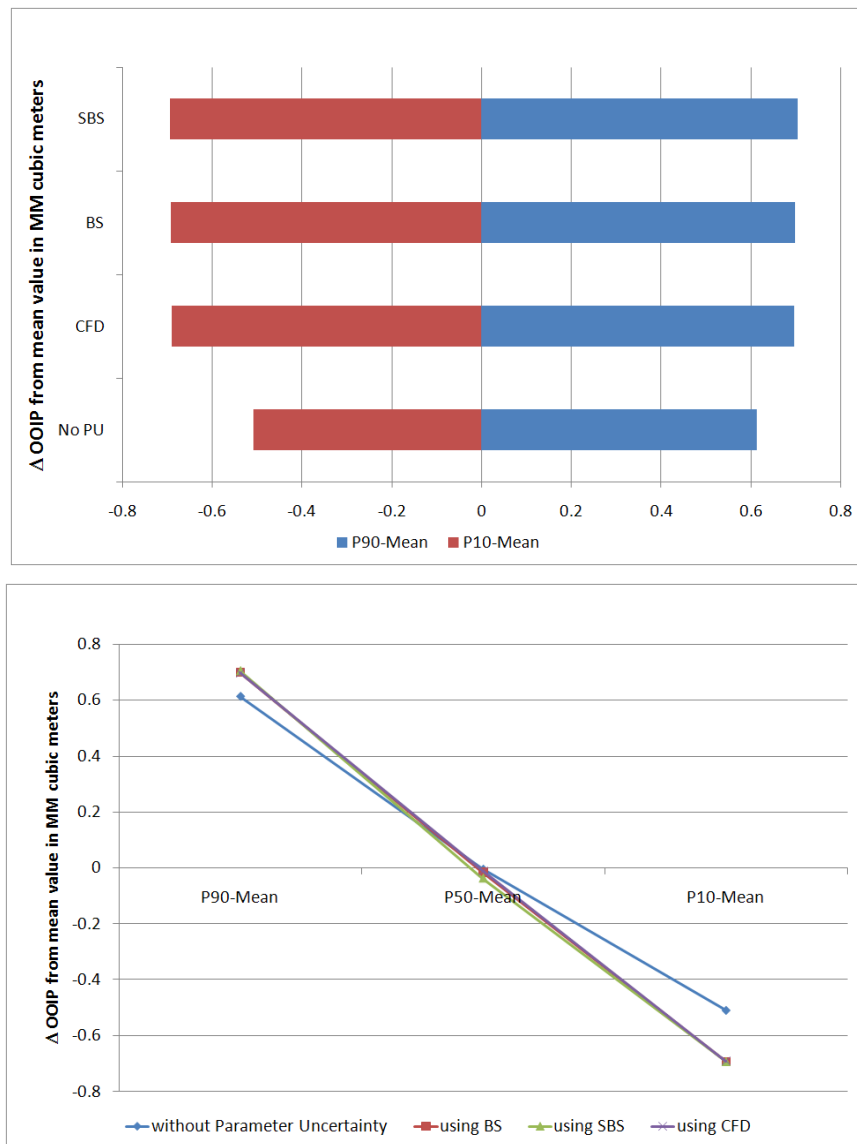


Figure 6-64: Case3: Sensitivity analysis to compare different parameter uncertainty approaches when calculating HIIP with uncertainty in thickness of H2 layer.

In case 4, the effects of the uncertainty in OWC on HIIP distributions were investigated by assuming a variable mode in the triangular distribution for OWC levels. Figure 6-65 shows the comparison results without/with parameter uncertainty in the OWC levels. Using the parameter uncertainty in the mode of the triangular distribution of the OWC levels had more uncertain HIIP distributions compared to that obtained without parameter uncertainty.

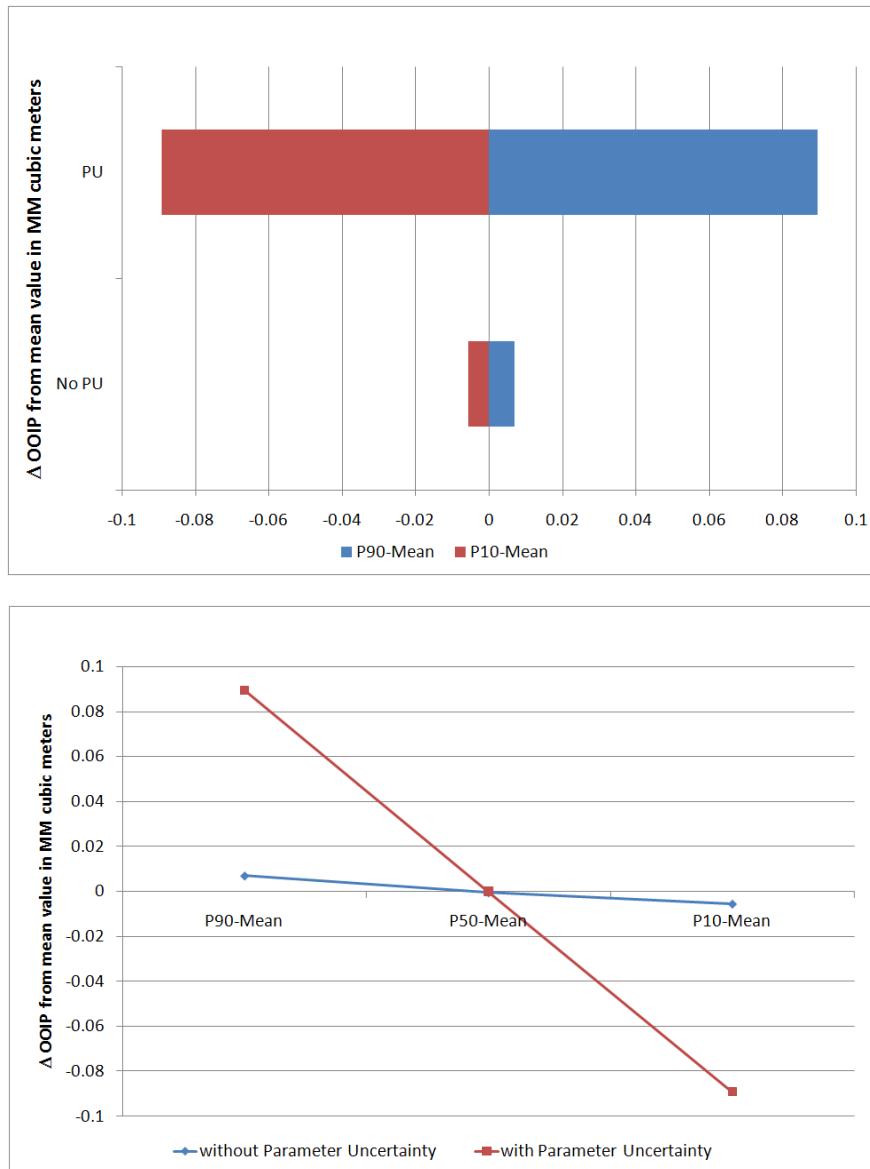


Figure 6-65: Case4: Sensitivity analysis to compare effects of OWC on HIIP with/without parameter uncertainty.

In cases 5 to 8, the effects of uncertainty in petrophysical properties on HIIP distributions were investigated. Figure 6-64 shows the comparison results of investigating the effects of uncertainty for H1 layer NTG on HIIP. SBS approach had the most uncertain HIIP distribution regardless the amount of the variogram range. It is obvious how important is to account for parameter uncertainty due to the narrow HIIP distribution without parameter uncertainty that might lead to HIIP underestimation. The results of using SBS or CFD approaches were sensitive to variogram range not as those obtained from using BS approach.

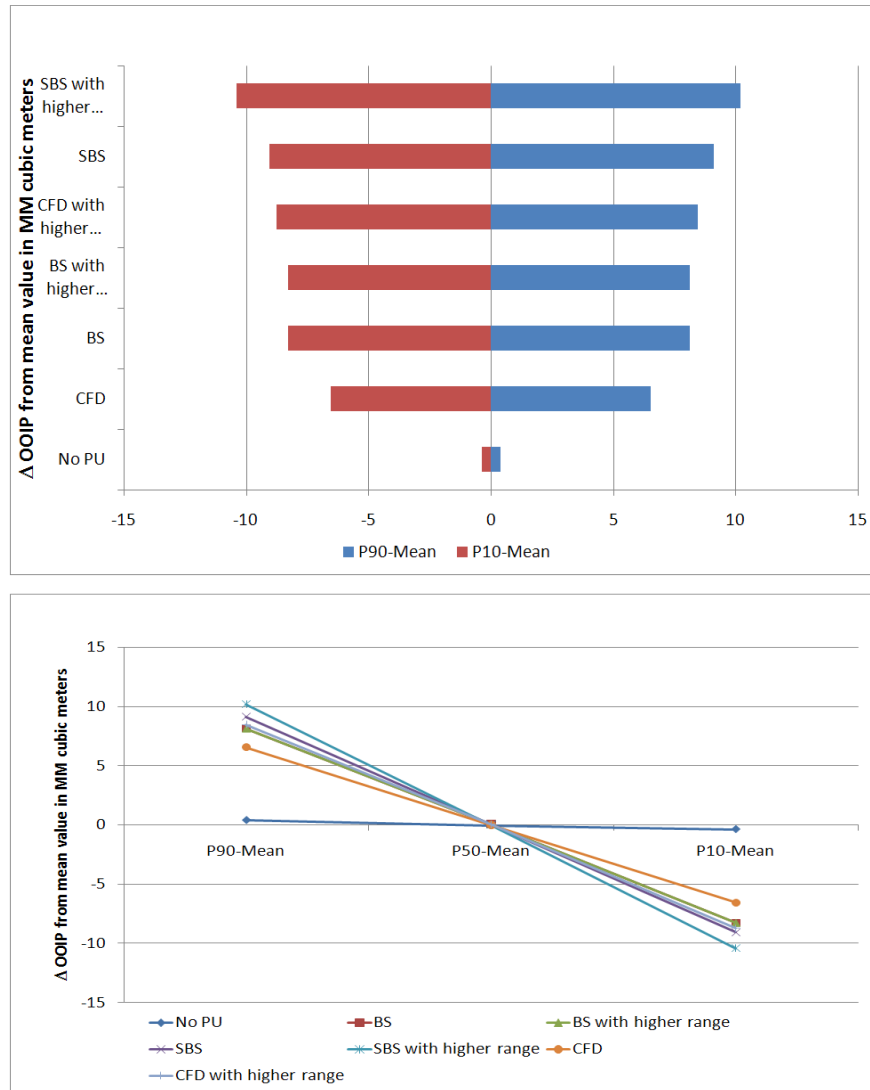


Figure 6-66: Case5: Sensitivity analysis to compare different parameter uncertainty approaches when calculating HIIP with uncertainty in NTG of H1 layer.

Case 6 investigated the effects of uncertainty in H2 layer NTG on HIIP distributions. The results were compared as shown in Figure 6-67. Similar to case 5, SBS approach had the most uncertain HIIP distribution regardless the amount of the variogram range. The narrowest HIIP distribution was obtained from the scenario ignored the parameter uncertainty. Increasing the variogram range had almost no effect on the case using BS approach, but its effect was clear on the scenarios using SBS or CFD approaches.

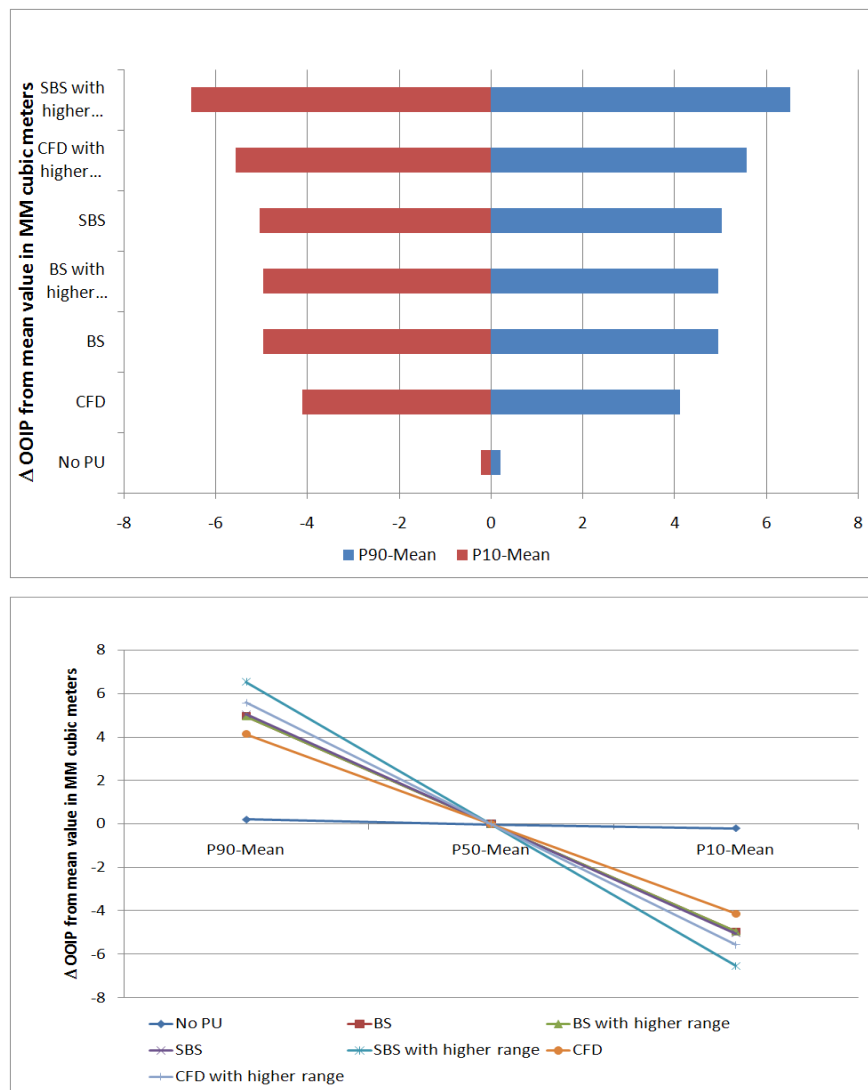


Figure 6-67: Case6: Sensitivity analysis to compare different parameter uncertainty approaches when calculating HIIP with uncertainty in NTG of H2 layer.

Figure 6-68 shows the comparison between the results investigating the effects of the individual uncertainty in H1 layer porosity on HIIP distributions (case 7). Of course as in the previous cases, estimating HIIP without parameter uncertainty had the narrowest distribution. Using SBS approach gave the most uncertain distribution compared to BS and CFD approaches. Increasing the variogram range to 2500m made the HIIP to have more uncertainty using the CFD compared to those obtained from using BS and SBS with the high variogram ranges. The BS approach results were almost the same with low/high variogram ranges.

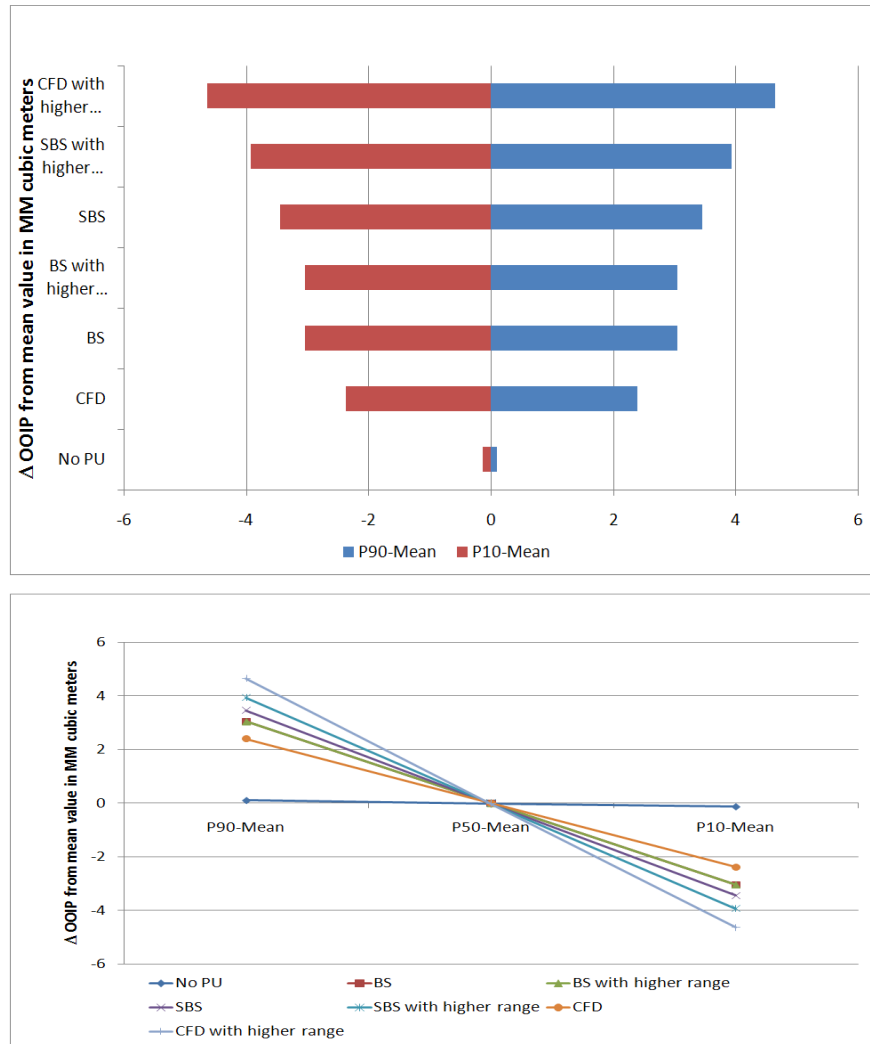


Figure 6-68: Case7: Sensitivity analysis to compare different parameter uncertainty approaches when calculating HIIP with uncertainty in porosity of H1 layer.

Case 8 investigated the effects of the individual uncertainty in H2 layer porosity on HIIP distributions. The results of using different parameter uncertainty approaches were compared and shown in Figure 6-69. The narrowest HIIP distribution was obtained from estimating HIIP without parameter uncertainty. Using SBS approach gave the most uncertain distribution with a low/high variogram range compared to those obtained from using BS or CFD approaches. The BS approach results were almost the same with low/high variogram ranges. Although using CFD approach with high variogram range made the HIIP distribution getting more uncertainty, but the standard deviation was still smaller than that obtained from using the BS approach.

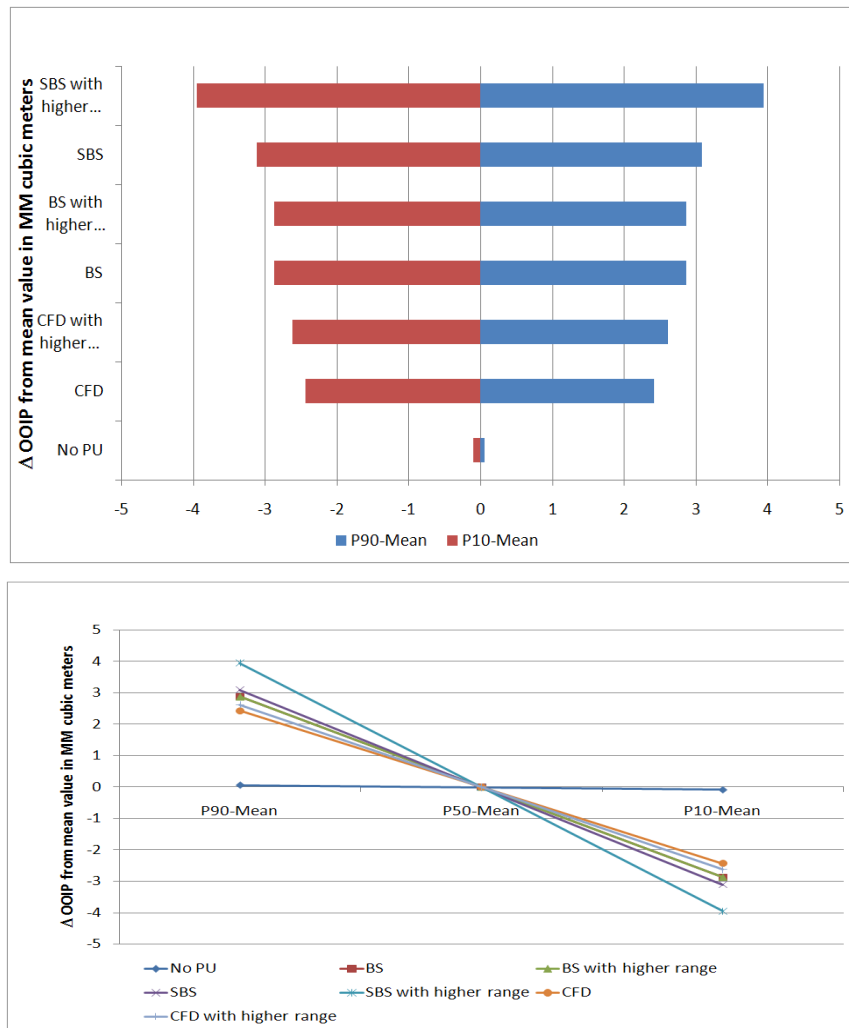


Figure 6-69: Case8: Sensitivity analysis to compare different parameter uncertainty approaches when calculating HIIP with uncertainty in porosity of H2 layer.

The order of different parameter uncertainty approaches was summarized in Table 6-7 based on the HIIP distribution uncertainty. In all cases, it was obvious that ignoring parameter uncertainty gives always the narrowest HIIP distribution. By comparing the results of using different parameter uncertainty approaches, the order of the approaches was SBS, BS, and CFD as the results had more uncertainty distribution to less uncertainty distribution except case-2 where the order was reversed, CFD, BS, and SBS. The effects of using different parameter uncertainty approaches were almost the same in cases 1 to 3, but cases 5 to 8 showed a significant difference between the HIIP distributions.

In cases 5 to 8, increasing the variogram range affected on the HIIP distributions with using SBS and CFD approaches, while the results with using the BS approach were almost the same because SBS and CFD are based on the spatial correlation between the data but BS approach is based on the independency assumption between the data.

The standard deviations of the HIIP distributions obtained from using parameter uncertainty approaches were related to the standard deviations of the parameter uncertainty distributions used. For example in case 1, the order of the

Case No.	Parameters to be investigated	More Uncertainty Distribution ←				→ Less Uncertainty Distribution			
1	Top & Bottom surfaces	SBS		BS		CFD		No PU	
2	Thickness – H1	CFD		BS		SBS		No PU	
3	Thickness – H2	SBS		BS		CFD		No PU	
4	OWC	With PU				No PU			
5	NTG – H1	SBS-2	SBS	CFD-2	BS-2	BS	CFD	No PU	
6	NTG – H2	SBS-2	CFD-2	SBS	BS-2	BS	CFD	No PU	
7	Porosity – H1	CFD-2	SBS-2	SBS	BS-2	BS	CFD	No PU	
8	Porosity – H2	SBS-2	SBS	BS-2	BS	CFD-2	CFD	No PU	

Table 6-7: Order of parameter uncertainty approaches used to quantify HIIP uncertainty due to uncertainty of individual parameters. No. 2 stands for using high variogram range.

standard deviations of HIIP distributions was SBS, BS, CFD, descendingly. As the order of the standard deviations of the parameter uncertainty was SBS (26.9m), BS (18.8m), and CFD (15.79m) as shown in Table 6-4. This comment was applied for all cases.

6.4.3. Comparing effects of full parameter uncertainty using different approaches

The HIIP distributions with full uncertainty (case 9) were obtained in seven scenarios. The first scenario estimated the HIIP without parameter uncertainty as shown in Figure 6-30. Three scenarios estimated HIIP distributions with parameter uncertainty using BS, SBS, or CFD as shown in Figure 6-49. The last three scenarios estimated HIIP distributions with parameter uncertainty using BS, SBS, or CFD with high variogram range, 2500m as shown in Figure 6-54.

The results of using different parameter uncertainty approaches were compared using the tornado chart and the spider plot and shown in Figure 6-70. The narrowest HIIP distribution was obtained from estimating HIIP without parameter uncertainty. Using SBS approach gave the most uncertain distribution with a low/high variogram range compared to those obtained from using BS or CFD approaches. The BS approach results were almost the same with low/high variogram ranges. The result of using CFD approach was narrower than those obtained with using BS and SBS approaches but with high variogram range, the result of using BS approach became the narrowest compared to those obtained from using SBS and CFD approaches.

The probability distribution frequency of HIIP with full uncertainty were plotted together, see Figure 6-71. It is obvious that the HIIP distribution using SBS approach was the most uncertain distribution compared to those obtained from using BS and CFD approaches, which produced distributions similar to each other.

The cumulative distribution frequencies of HIIP with full uncertainty were compared as shown in Figure 6-72. It is noticed that using BS approach produced more uncertainty in the HIIP estimates compared to the result without parameter uncertainty but BS approach was ignoring the spatial correlation between the data. Using SBS approach considered the spatial correlation between the data and produced more uncertainty in the HIIP distribution with high standard deviation compared to all other approaches. The CFD approach considered the correlation between the input data and the conditioning data, so it can more realistic; even though, it is not such well known and popular as SBS approach.

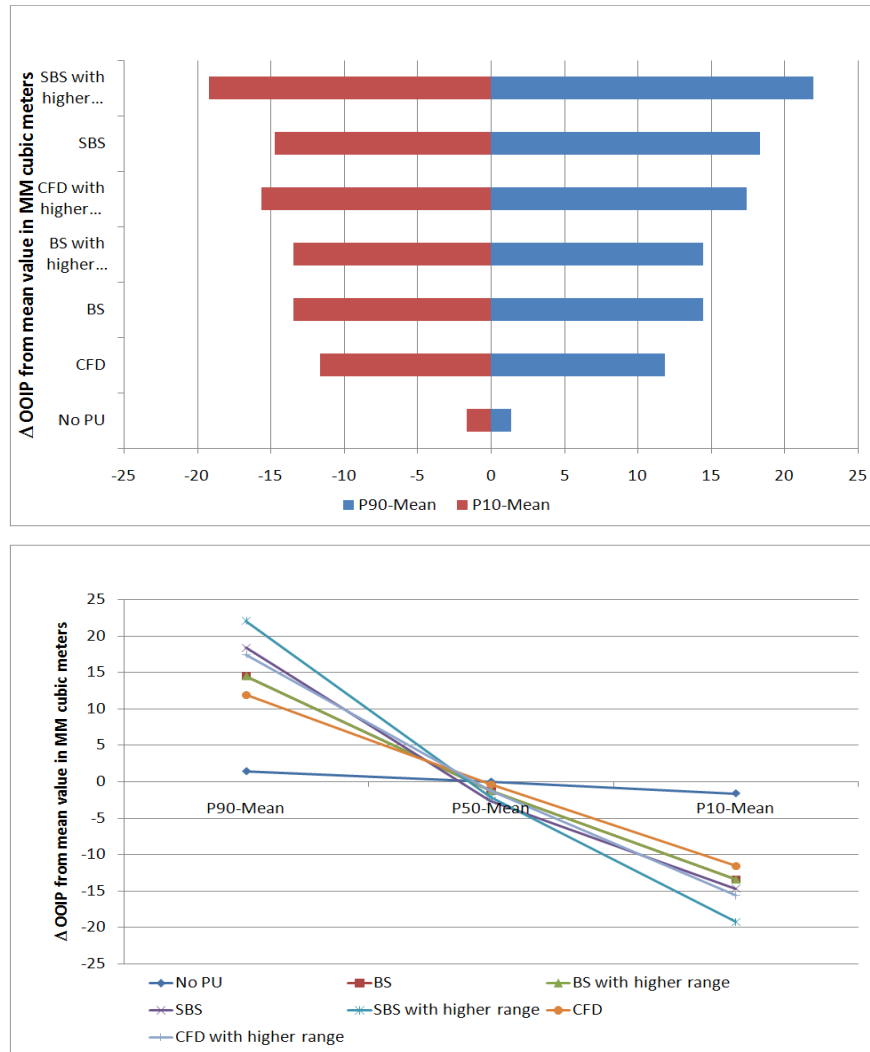


Figure 6-70: Case9: Sensitivity analysis to compare different parameter uncertainty approaches when calculating HIIP with full uncertainty.

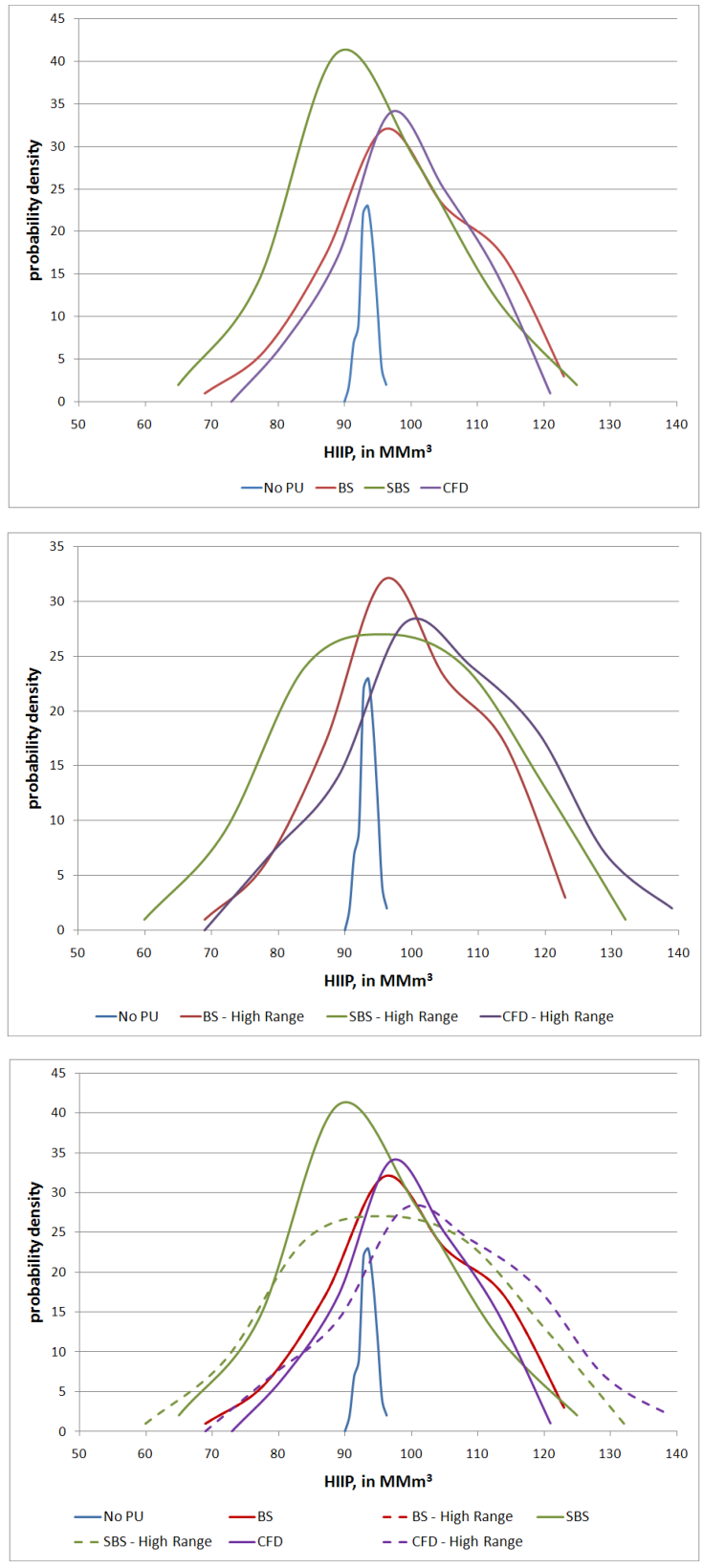


Figure 6-71: Case9: Probability Distributions for HIIP with full uncertainty using different parameter uncertainty approaches.

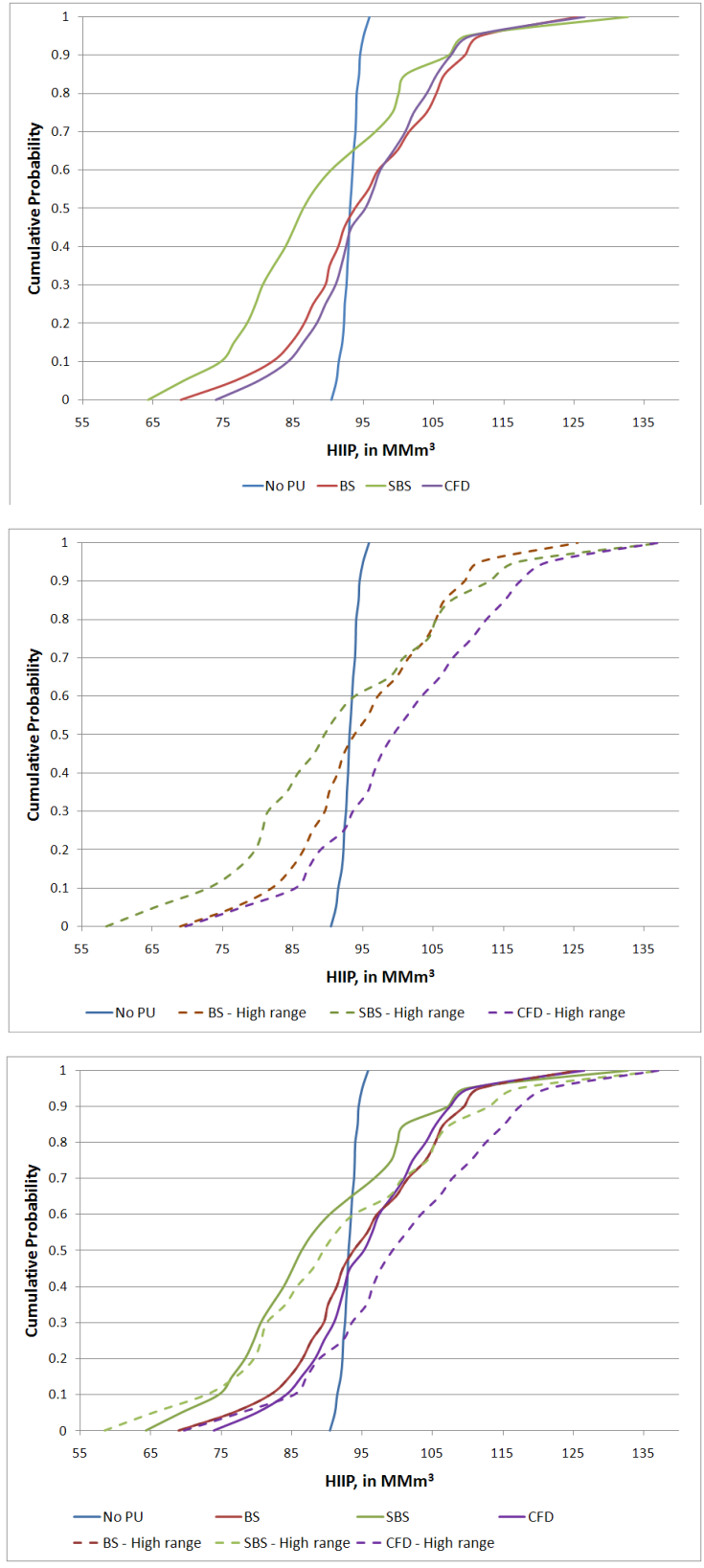


Figure 6-72: Case9: Cumulative Probability Distributions for HIIP with full uncertainty using different parameter uncertainty approaches.

BS approach might be recommended in the early stages of the reservoir life because of its simplicity. CFD approach might give the same results in that stage of the reservoir life plus it will give more realistic results as more data are gathered. The only disadvantage of using the CFD is the significant time required to generate a parameter uncertainty that might reach to a few hours depending on the input data and the CPU and this time is unwanted to make quick decisions.

As mentioned previously, increasing the variogram range affected the HIIP distribution with using SBS and CFD approaches. It can be noticed from Figures 6-71 and 6-72 that the expansion in the distributions was to right. In another word, P10 estimates were close to each other in values but P90 had a significant change in the values.

2-D vs. 0-D and 3-D MODELING

Reservoir heterogeneity characterization is a big challenge. There is no way to assess the true heterogeneity, but models can be created to mimic the important features of variability. It is important to select the appropriate modeling scale to get a fair global uncertainty of resource volumes. Chapter 2 discussed the difference between different scale modeling and their applications. A methodology of 2-D modeling with parameter uncertainty was set up in this research and used in the case study in chapter 6 to compare different parameter uncertainty approaches. In this chapter, the results of using BS approach in the 2-D modeling are compared with the results of using 0-D modeling using the same input data of the case study. In addition, the parameter uncertainty of one the variables of interest, porosity of H1 layer is quantified by 3-D modeling and compared to the results obtained from 2-D data with different parameter uncertainty.

7.1 Comparison between 2-D and 0-D Modeling

In early stages of a reservoir life, there is no choice sometimes but to use 0-D modeling to estimate the resource volumes due to short time to make some quick decisions and/or unavailable data to apply different modeling scale. In the 0-D modeling, the variables of interest are represented by probability distributions that are used to calculate resource volumes by drawing values for those variables according to their specified probability distribution. There are several fast and friendly programs that can be used to simulate realizations of the resource

volume. Some of them ignore the correlation between the input parameters, which is not realistic. In this study, GSLIB-like programs and spreadsheets were used to quantify uncertainty in HIIP. Many scenarios were conducted using 0-D modeling to investigate the effects of accounting for the correlation coefficients between the variables of interest and obtaining the thickness probability distribution from well data or seismic data. Accounting for the correlation coefficients between the variables of interest showed no significant change from the results obtained with ignoring the correlation coefficients since the data were not strongly correlated. Therefore, only the results with accounting for the correlation coefficients are presented in this study.

7.1.1 0-D Modeling with Thickness Data Obtained from Seismic

The resource volumes calculation in the 0-D modeling is based on drawing a value for each variable of interest involved from its representative distribution then multiplying those values with each other as shown in the following equation:

$$\text{HIIP} = \text{Area} * \text{Thickness} * \text{NTG} * \text{porosity} * (1 - \text{Sw}) \quad 7-1$$

The thickness data in this scenario were obtained from Seismic. Figure 7-1 shows the distributions of H1 and H2 layer thicknesses obtained from Seismic data. To assess the uncertainty in the thickness of each layer, n values were drawn randomly from thickness distribution in Gaussian space as one realization. This process was repeated L times. The average of each realization was determined in original units. These averages represent the uncertainty in the means of the thickness, see Figure 7-2. BS approach was used to assess the uncertainty in the means of NTG and porosity similar to those obtained with 2-D modeling, see Figure 7-3. Random values for all variables of interest had to be drawn in Gaussian space and correlated using the correlation coefficients between those variables. The uncertainty in HIIP was calculated by multiplying the correlated

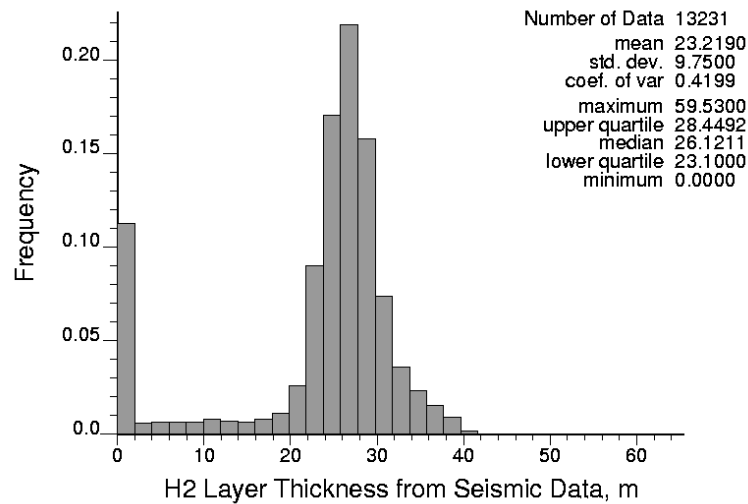
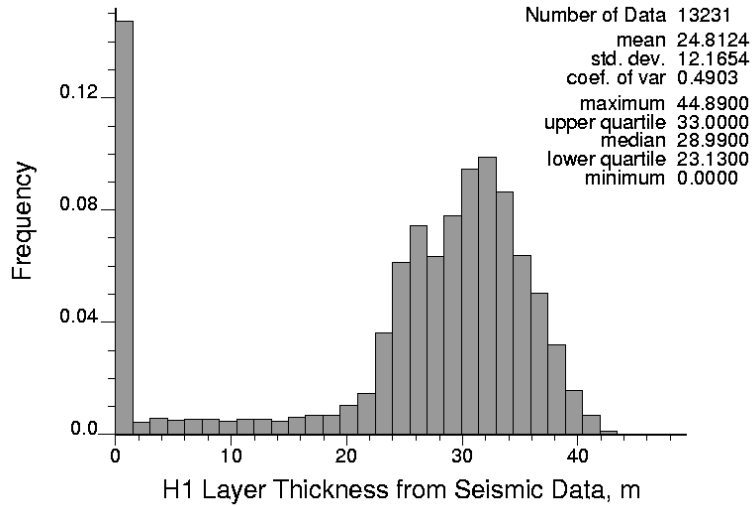


Figure 7-1: Histograms for H1 and H2 layer thicknesses obtained from Seismic Data. Top: H1 layer thickness. Bottom: H2 layer thickness.

values but in their original units. As in 2-D modeling, water and oil saturations were assumed to be fixed at %20 and %80, respectively because their data were unavailable. The following steps describe in details the methodology followed in 0-D modeling using Seismic data with accounting for correlation coefficients between the variables on interest:

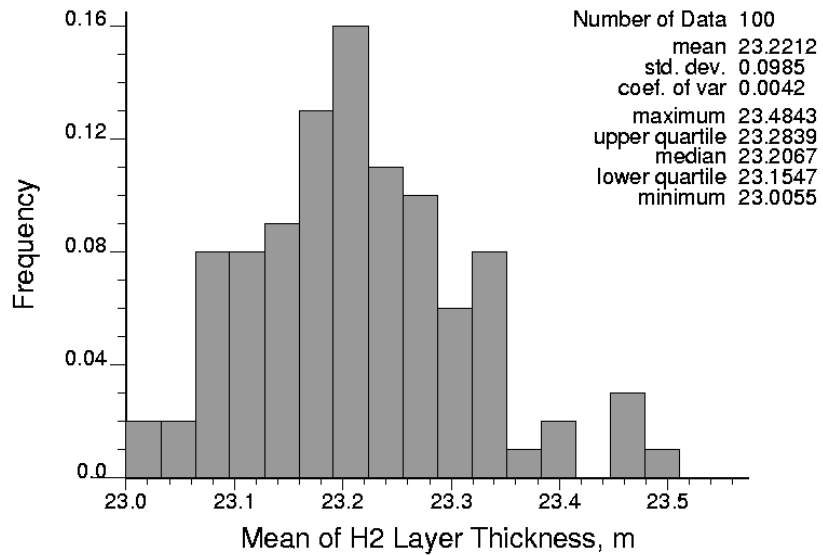
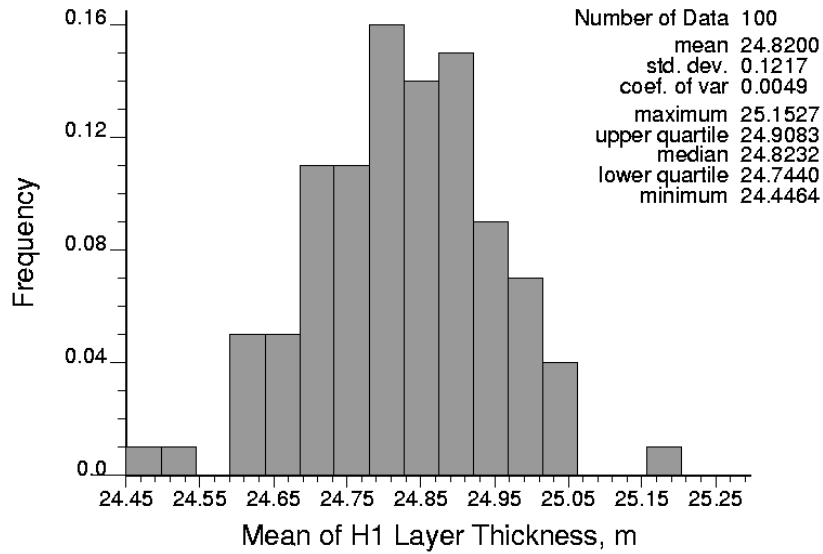


Figure 7-2: Parameter Uncertainty in the means of H1 and H2 layer thicknesses obtained from Seismic Data.

1. normal score the thickness data obtained from Seismic to get the transformation tables for H1 layer thickness by running *nscore* program.
2. generate L realizations by using *mcs* program, each realization has n values in Gaussian space to represent H1 layer thickness data (let $L = 100$ and $n = 10000$ in this study).

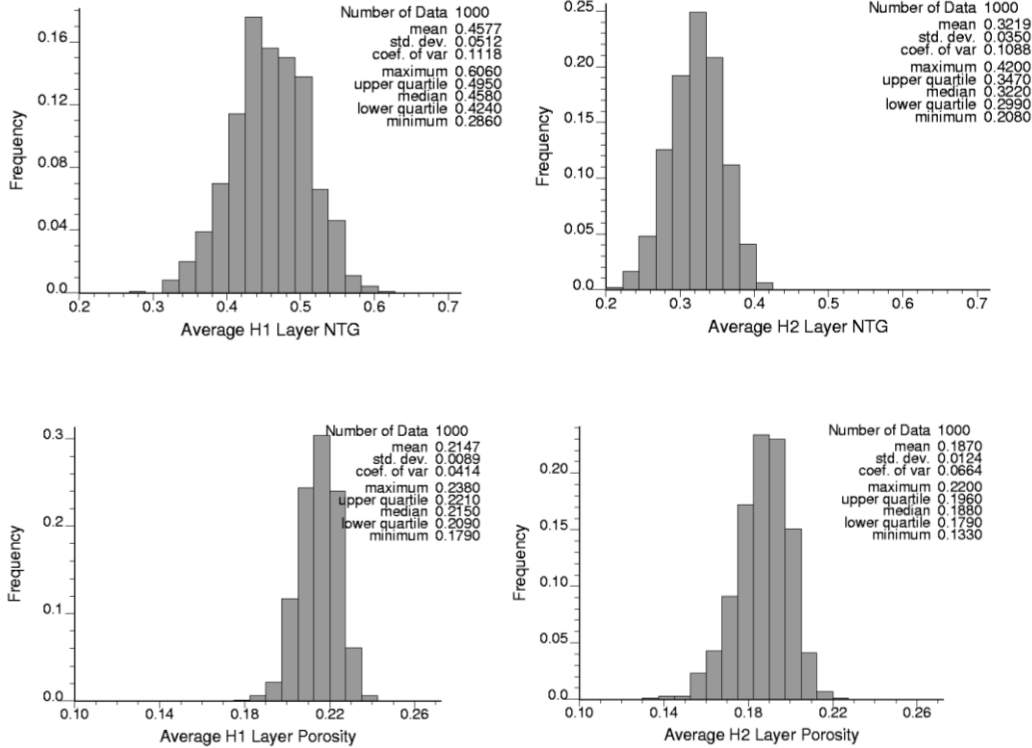


Figure 7-3: Parameter Uncertainty in the means of NTG and porosity of H1 and H2 layers using BS approach. The units are in fractions.

3. back transform the realizations data using the transformation table obtained from step 1 for H1 layer thickness.
4. calculate average H1 layer thickness in each realization using *AvgVr* program. The results represent the uncertainty in the mean of H1 layer thickness.
5. repeat steps 1 through 4 for H2 layer thickness.
6. use a parameter uncertainty approach to assess the uncertainty in NTG and porosity for each layer of H1 and H2 (BS approach was used in this study).
7. normal score the data obtained for all variables of interest from steps 4 through 6 to get the transformation tables for the variables by running *nscore* program.
8. draw L values from normal distribution (0,1) for each variable of interest by using *mcs* program (let L = 100 in this study). Each value in each column

represents a mean for one of the variables of interest (Average thickness, NTG, or porosity).

9. use the correlation coefficients between the variables to correlate those mean values by using *correlate* program.
10. back transform the means data using the transformation tables obtained from step 7 for all variables of interest.
11. calculate HIIP in each layer by multiplying the first realizations of all variables to get the first realization of HIIP in that layer and so on to the L realization. Then calculate HIIP for all layers by adding the individual layer results as in the following equation:

$$HIIP = \sum_{i=1}^{nl} HIIP_i = \sum_{i=1}^{nl} h_i * NTG_i * \phi_i * (1 - Sw_i) \quad 7-2$$

where nl = number of layers.

12. get HIIP distribution and assess its uncertainty.

HIIP was calculated using 0-D modeling with accounting for correlation coefficients. The results were presented in Figure 7-4 as probability distribution frequency and cumulative probability frequency. The mean and standard deviation of HIIP were 102.1249 and 10.9210 m³, respectively. The P-10 and P-90 were 88.7681 and 116.2502 m³, respectively.

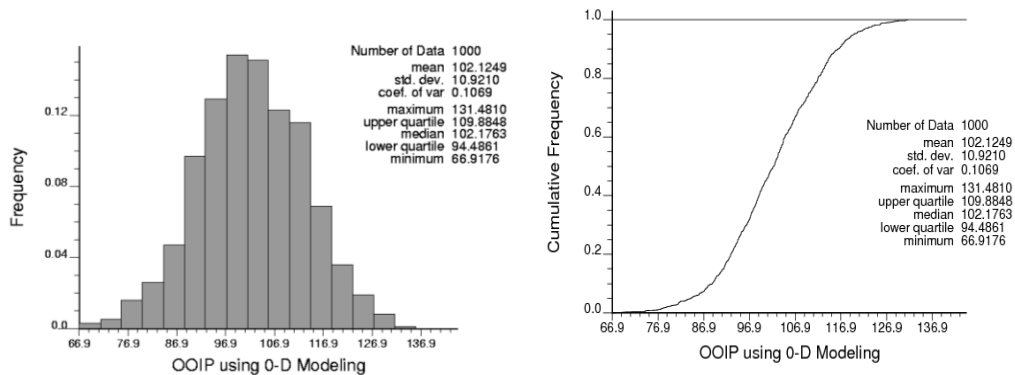


Figure 7-4: HIIP using 0-D modeling with the correlation coefficients between the variables of interest. The results are in million cubic meters.

In this case, the seismic data was used to assess the uncertainty in the layers thicknesses in order to have a fair comparison of the results of using 0-D modeling against those obtained from using 2-D modeling.

7.1.2 0-D Modeling with Thickness Data obtained from Well Logs

This scenario was conducted to investigate the effects of assessing the thickness uncertainty using well data with BS approach on HIIP instead of using seismic data and show the importance of seismic data to get better evaluation of the resource/reserve volumes. The thickness of each layer from well data was used to assess the uncertainty in the mean of that layer thickness. Figure 7-5 shows the parameter uncertainty in the means of thickness using BS approach for H1 and H2 layers. The parameter uncertainty in NTG and porosity for H1 and H2 layers are similar to those used in previous scenario, see Figure 7-3.

The procedure of estimating the HIIP using 0-D modeling is based on Monte Carlo simulation. As mentioned earlier, considering correlation coefficients between the variables of interest didn't have a major effect on the HIIP results. So, only the results of considering correlation coefficients were presented in this study because it is more realistic than ignoring these coefficients. The procedure steps were as follows:

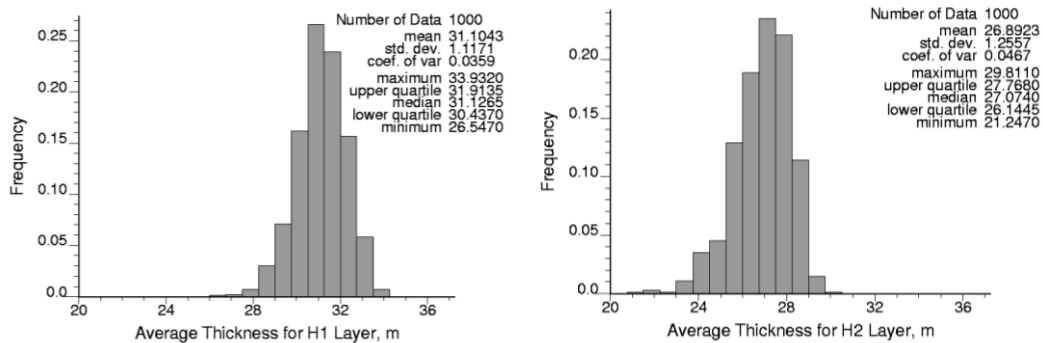


Figure 7-5: Parameter Uncertainty in Thickness of H1 and H2 layers using BS approach. Left: H1 layer. Right: H2 layer.

1. quantify the parameter uncertainty in the mean for all variables of interest (BS approach was used in this scenario).
2. normal score the data obtained for all variables of interest from step 1 to get the transformation tables for the variables by running *nscore* program.
3. draw L values from normal distribution (0,1) for each variable of interest by using *mcs* program (let L = 100 in this study). Each column represents one of the variables of interest (Average thickness, NTG, or porosity) and each value in the column represents a mean for one realization of that variable.
4. use the correlation coefficients between the variables to correlate those mean values by using *correlate* program.
5. back transform the means data using the transformation tables obtained from step 2 for all variables of interest.
6. calculate HIIP in each layer by multiplying the first realizations of all variables to get the first realization of HIIP in that layer and so on to the L realization. Then calculate HIIP for all layers by adding the individual layer results as in equation (7-2).
7. get HIIP distribution and assess its uncertainty.

The uncertainty in HIIP of Hekla field was estimated using 0-D modeling with thickness obtained from well log data. The mean and standard deviation of the results were 124.6272 and 14.7800 m³, respectively. Figure 7-6 shows the probability and cumulative distribution frequencies.

A comparison between the three scenarios of estimating HIIP, one scenario using 2-D modeling with BS approach and two scenarios using 0-D modeling with thickness data obtained from either seismic or well logs. The results were summarized in Table 7-1. Figure 7-7 compared the results of the three scenarios using spider plot and tornado chart. The standard deviations were similar except with 0-D modeling with thickness obtained from well logs, which had a higher standard deviation than others by about %32.

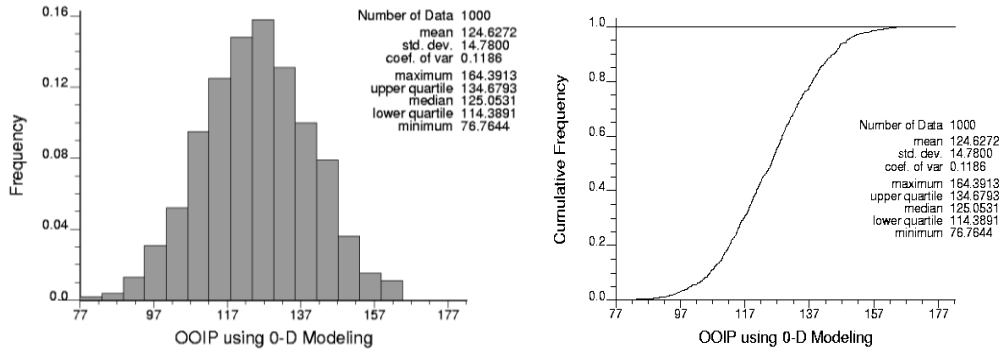


Figure 7-6: HIIP using 0-D modeling with thickness obtained from well data the correlation coefficients between the variables of interest. The results are in million cubic meters.

2D vs. 0D Modelling Results			
Dimension	2-D	0-D with Sies.&corre.	0-D with corre.
Mean	95.0838	102.2947	124.6272
Std	11.1202	11.1925	14.78
Minimum	68.966	66.0694	76.7644
Maximum	125.566	132.1702	164.3913
P90	109.5415	116.6759	144.2652
P50	93.779	102.5044	125.0532
P10	81.624	88.5083	105.9197
P90-Mean	14.4577	14.3812	19.638
P50-Mean	-1.3048	0.2097	0.426
P10-Mean	-13.4598	-13.7864	-18.7075

Table 7-1: 2-D vs. 0-D modeling: Comparison between three scenarios estimating HIIP. First scenario used 2-D modeling with parameter uncertainty approach. The other two scenarios used 0-D modeling with accounting for correlation coefficients between the variables of interest; the thickness was obtained in one scenario from seismic and in the other from well logs. The results are in million cubic meters.

Figure 7-8 presents the probability and cumulative distribution frequencies for the three scenarios. It was obvious that using 0-D modeling overestimated the HIIP volumes especially the scenario that used thickness obtained from well logs, which increased the mean by about %31. Using thickness from well logs with 0-D modeling could reduce the overestimating from %31 to less than 8% compared to 2-D modeling.

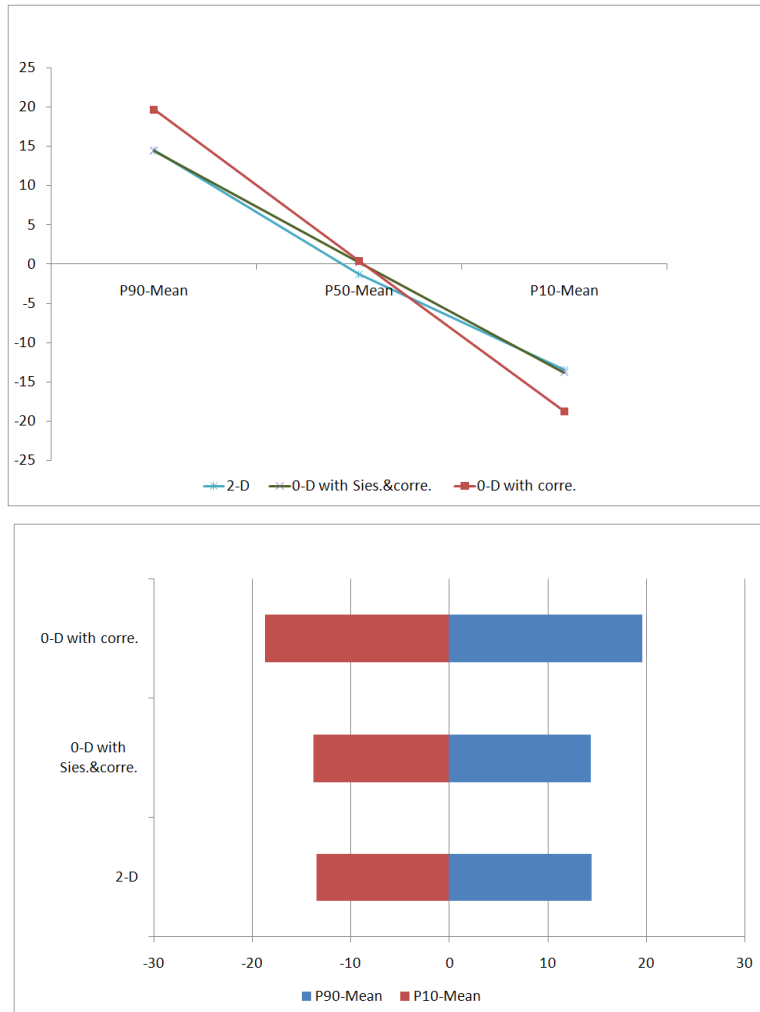


Figure 7-7: 2-D vs. 0-D modeling: a spider plot and tornado chart to compare between the three different models, 2-D modeling with parameter uncertainty approach, 0-D modeling with thickness data obtained from Seismic, and 0-D modeling with thickness data obtained from well logs. The results are in million cubic meters.

As mentioned earlier in chapter 2, using 2-D modeling has many advantages. It is based on geological mapping, which make it easy to see the results and check them by mapping the results and checking them locally, but using 0-D modeling can not be checked. It just gives the distribution of the resource/reserve volumes. Figure 7-9 shows some examples of the HIIP realizations obtained from using 2-D modeling with BS approach. The better the local HIIP estimates are, the more confidence the global results have. In addition, HIIP realizations can be ranked based on the HIIP volumes, thickness, NTG,

average porosity, or any variable of interest. Then the realizations that represent P-90 and P-10 can be used to make some decisions about the optimum location(s) to drill new wells.

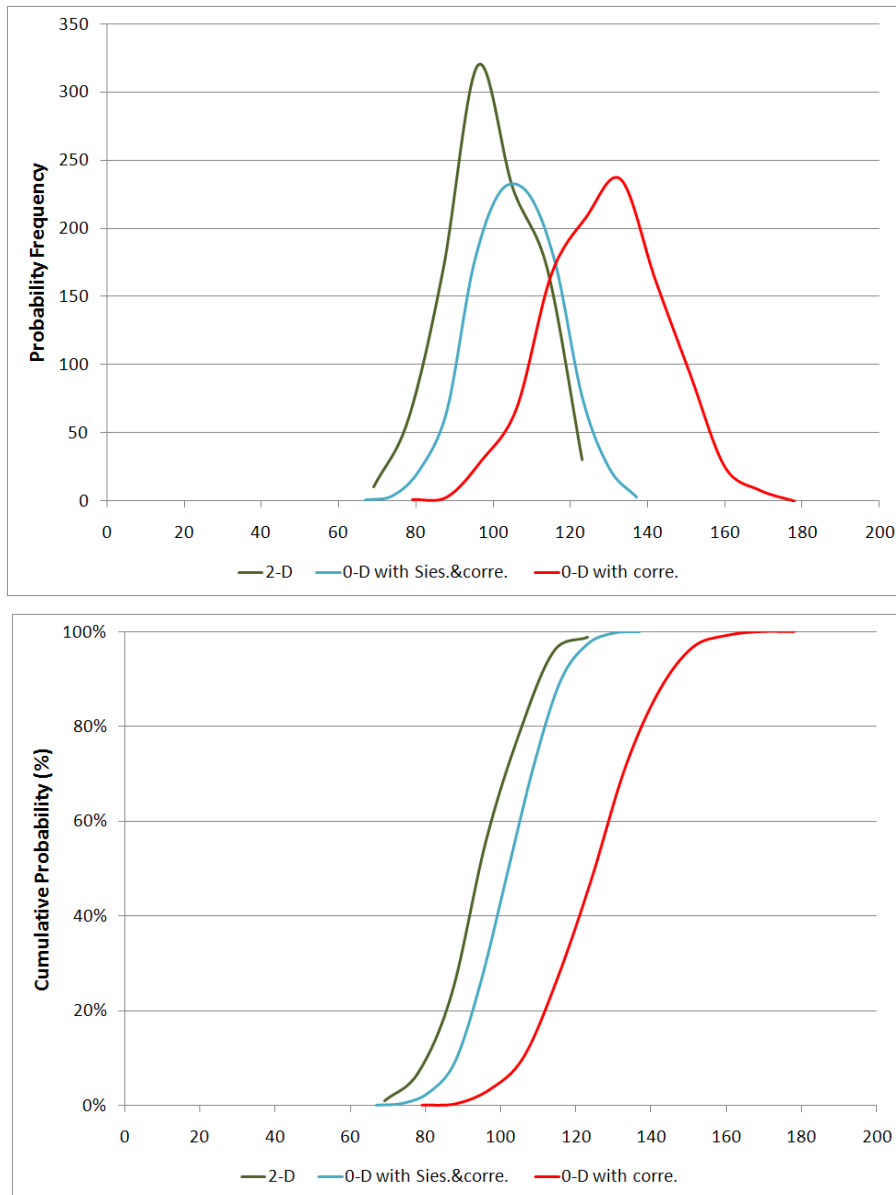


Figure 7-8: 2-D vs. 0-D modeling: a comparison between the probability and cumulative distribution frequencies of HIIP volumes estimated by different modeling. Top: probability distribution frequencies of HIIP volumes. Bottom: cumulative distribution frequencies of HIIP volumes. The models are 2-D modeling with parameter uncertainty approach, 0-D modeling with thickness data obtained from Seismic, and 0-D modeling with thickness data obtained from well logs. The results are in million cubic meters.

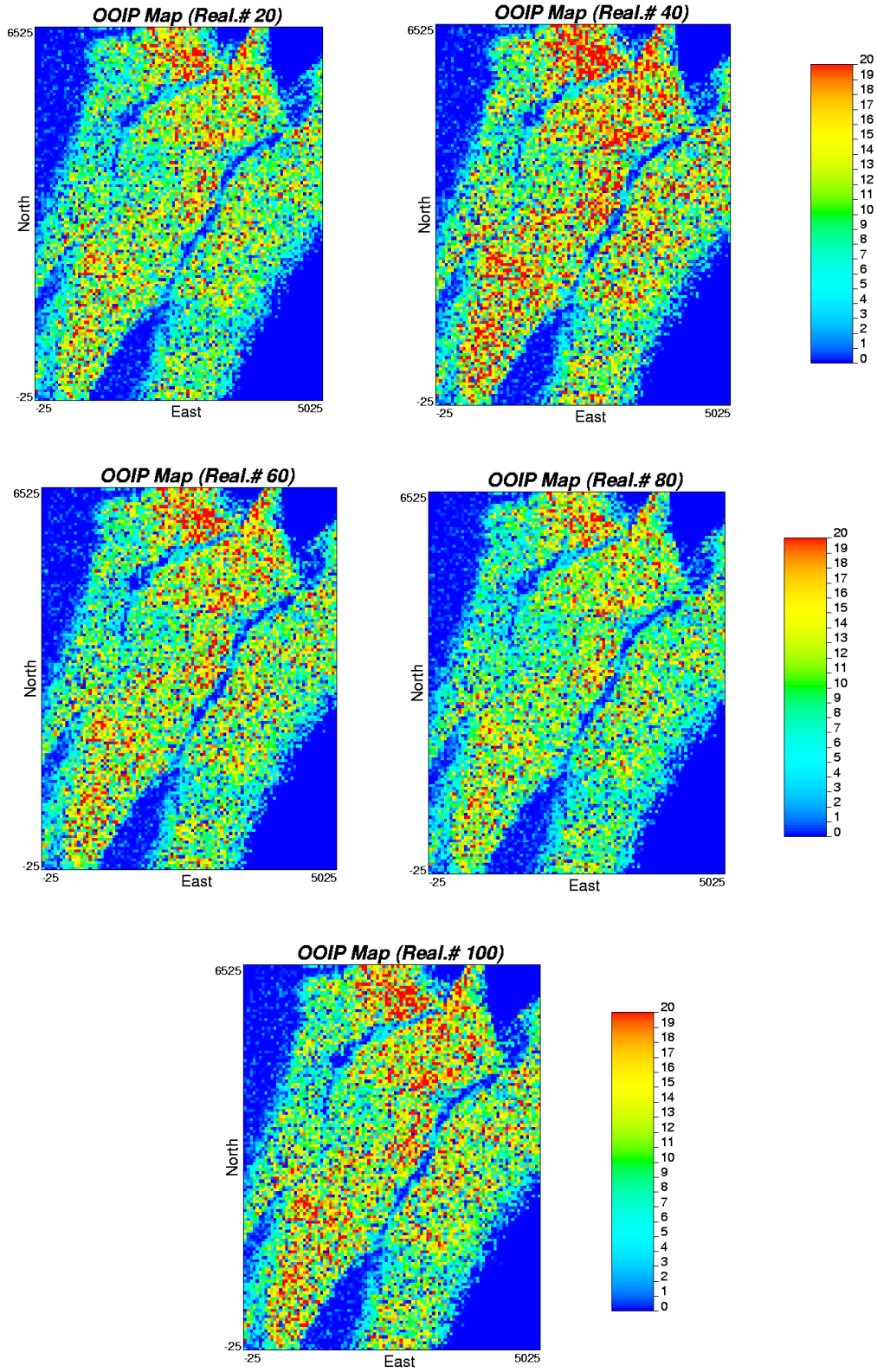


Figure 7-9: 2-D HIIP Maps for different realizations. These maps were obtained from using 2-D modeling with BS approach to quantify the parameter uncertainty in the variables of interest.

7.2 Comparison between 2-D and 3-D Modeling

It is good to have a model describing the field of interest in a high resolution, but it is important to account for the parameter uncertainty in the variables of interest. In the early stages of the reservoir life, 3-D models are rarely used to calculate the resource/reserve volumes for many reasons. The most important reasons are the significant time, CPU, and capacity required to run such high resolution models and the little data available at that time. In this section, the parameter uncertainty of H1 layer porosity will be quantified using 3-D modeling to be compared with the quantified average porosity for H1 layer using 2-D data and different parameter uncertainty approaches.

In order to quantify the parameter uncertainty in H1 layer porosity, it is important to get a better 3-D variogram model that represents the continuity in the existing layer. Therefore, calculating proportional stratigraphic coordinate systems based on depth is the first step in order to capture original continuity of petrophysical properties and preserving this continuity within the existing layer structure (McLennan, 2004). The proportional coordinates Z_{PROP} can be calculated as the relative distance between the existing top and bottom depths (in percentage), see Figure 7-10. The coordinate transformations in equation (7-3) can be calculated using Wells-1, 2, and 3 in depth coordinates:

$$Z_{PROP}(\mathbf{u}_i) = \frac{z_s(\mathbf{u}_i) - Z_{top}(\mathbf{u}_i)}{Z_{base}(\mathbf{u}_i) - Z_{top}(\mathbf{u}_i)} \cdot 100 \quad 7-3$$

Where Z_{PROP} = proportional coordinates

Z_{top} = existing top layer surface

Z_{bottom} = existing bottom layer surface

z_s = elevation data

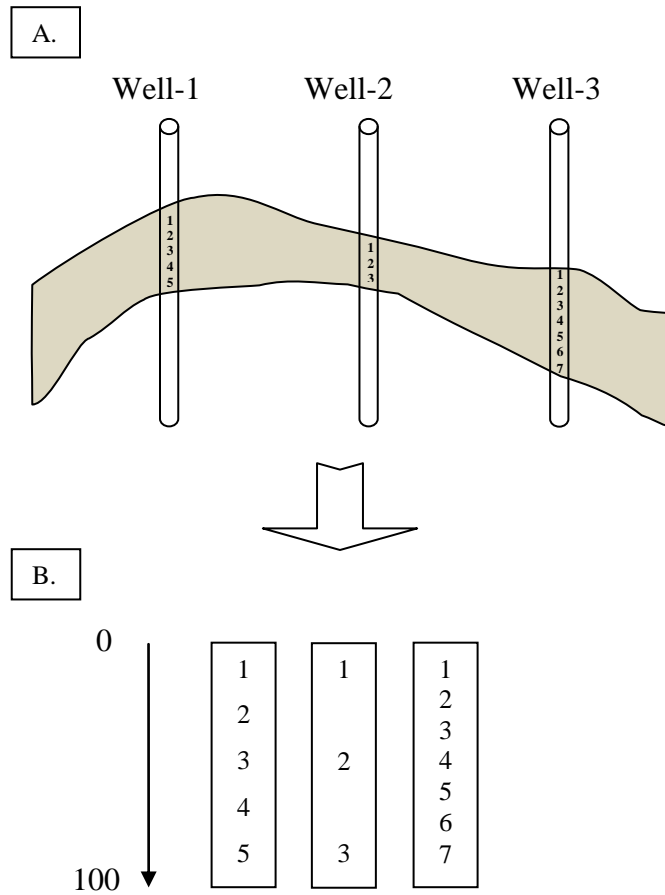


Figure 7-10: (a) A schematic reservoir, the shaded portion of Wells-1, 2, and 3 are extracted. (b) Proportional coordinates are calculated and shown. The shaded composites represent horizontal variogram calculation pairs.

The results of proportional stratigraphic coordinate systems for 19 wells of Hekla field were used to generate the 3-D experimental variograms to capture the major directions of continuity for H1 layer porosity. The *gamv2004* program was used because the data are irregularly spaced. The experimental variograms in two main horizontal directions of continuity were found to be at (45 and 135 degrees). They were calculated with lag distance of 300m and 200m lag tolerance, while the experimental variogram in the vertical direction was calculated with lag distance of 2m and 0.3m lag tolerance. Table 7-2 summarizes the Parameters used to calculate the experimental variograms for H1 layer porosity in Hekla field. A

spherical model was used to fit the experimental results. Figure 7-11 shows the best 3-D experimental variograms and their best fit models. Top plot shows the experimental variogram and its best fit model in the major and minor horizontal direction at 45 and 135 degrees, respectively. Bottom plot shows the experimental variogram and its best fit model in the vertical direction. The 3-D variogram model equation for H1 layer porosity in Hekla field is as follow:

$$\gamma(h) = 0.001 + 0.999 * sph \quad 7-4$$

$$av = 18$$

$$ahl = 1200$$

$$ah2 = 500$$

A good variogram model is essential step required to get better simulation results. 100 different 3-D realizations for H1 layer porosity were sampled using Sequential Gaussian simulation with changing the seed number in each realization. A big capacity in the memory is required to store these realizations. As the reservoir has higher resolution as the memory needs more capacity. To quantify the parameter uncertainty in H1 layer porosity, the average porosity was calculated from each realization above the assumed porosity cutoff, %10.

Direction	Major Horizontal	Minor Horizontal	Vertical
Azimuth	45	135	0
Azimuth Tolerance	30	30	30
Bandwidth horizontal	1000	1000	10
Dip	0	0	90
Dip tolerance	30	30	30
Bandwidth vertical	10	10	10
Number of lags	6	6	15
Lag distance	300	300	2
Lag tolerance	200	200	1

Table 7-2. Experimental variograms parameters for H1 layer porosity in Hekla field.

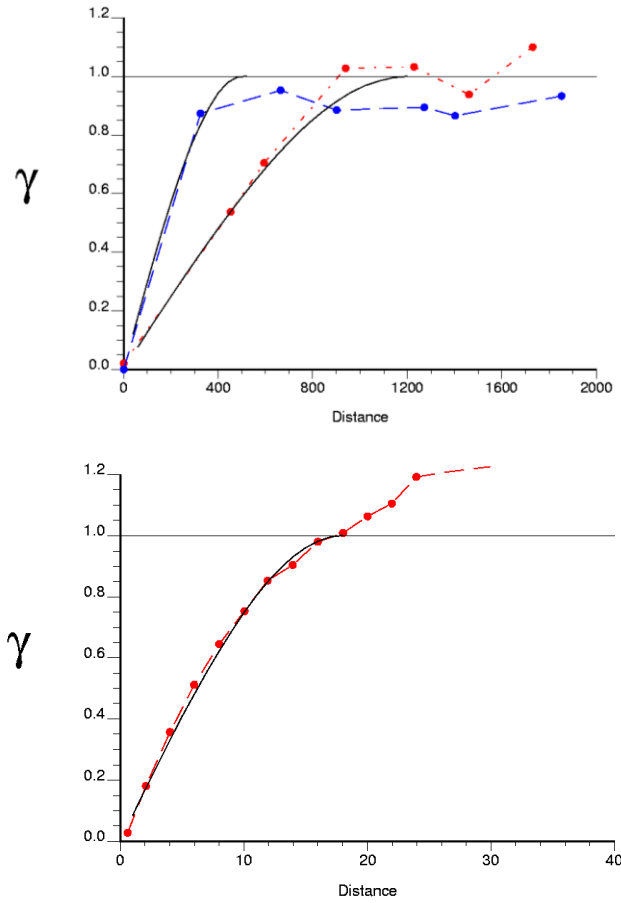


Figure 7-11: 3-D Experimental variograms for H1 layer porosity. Top plot shows the variograms in the two main directions with their best fit model. Bottom plot shows the variogram in the vertical direction with its best fit model. The distance units are in meters.

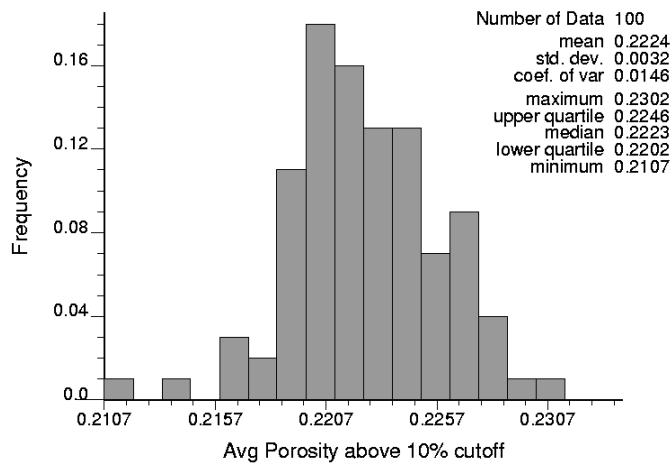


Figure 7-12: Parameter uncertainty in H1 layer porosity using 3-D modeling. The porosity cutoff was 10%.

The following steps summarized the steps required to quantify the parameter uncertainty of H1 layer porosity using 3-D model:

1. calculate proportional stratigraphic coordinate systems based on elevation.
2. generate 3-D experimental variograms and find the best fit model for H1 layer porosity.
3. generate L realizations of H1 layer porosity using Sequential Gaussian simulations with changing the seed number in each realization.
4. calculate the average porosity above porosity cutoff for each realization and obtain a distribution for H1 layer porosity.

A comparison between the results of the parameter uncertainty for H1 layer porosity using 3-D modeling and 2-D modeling was conducted. Figure 7-13 shows the parameter uncertainty in H1 layer porosity using 3-D and 2-D modeling with different parameter uncertainty approaches. It is obvious that 3-D modeling did not capture wide uncertainty as 2-D modeling did. The CPU time required to quantify the parameter uncertainty using 3-D modeling and the memory allocation

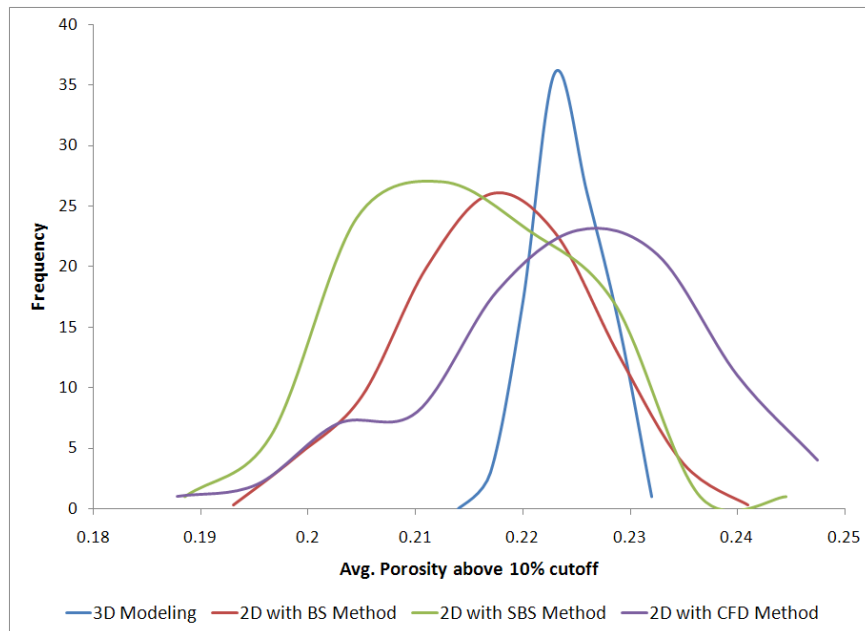


Figure 7-13: 2-D vs. 3-D Modeling: Parameter uncertainty in H1 layer porosity. The porosity cutoff was 10%.

needed for previously simulated nodes are significantly more than those required for quantifying parameter uncertainty using parameter uncertainty approaches and 2-D modeling. Based on the reservoir grid definition used in this study, more than one gigabyte was needed to simulate 100 realizations and get the parameter uncertainty in the porosity using 3-D modeling. On the other hand, the amount of memory required for quantifying the parameter uncertainty of H1 layer porosity were about few kilobytes for BS approach, about a hundred for SBS approach, and more than ten megabytes for CFD approach; even though, the data required for the post process were just few kilobytes not like the results of the 3-D models where all realizations are required for the post process to estimate the resource/reserve volumes.

A complete study quantifying uncertainty in HIIP with full uncertainty and using 3-D models will need really a huge computer memory in order to store the simulation realizations for so the variables of interest.

CONCLUSIONS AND FUTURE WORK

We would wish for the lowest uncertainty possible. However, too narrow uncertainty due to ignoring the uncertainty in the present geology leads to a false confidence in reserves and resources. Our aim is to obtain a realistic and fair measure of uncertainty. Decisions of stationarity and a modeling methodology are the most important factors in determining output uncertainty in any practical modeling study.

8.1 Summary of Contributions

In this study, a methodology for the assessment of uncertainty in the structure surfaces of a reservoir, fluid contacts levels, and petrophysical properties was developed and investigated. A complete setup was considered with accounting for parameter uncertainty in order to get a fairly global uncertainty. There is no question that uncertainty in the input histogram main parameter, such as the mean, must be considered for realistic global uncertainty characterization. There are several techniques for calculating parameter uncertainty in a required input histogram. These techniques include conventional bootstrap (BS), spatial-bootstrap (SBS), and Condition finite-Domain (CFD).

Any of the three techniques can be applied to quantify the uncertainty in the mean of each variable. Uncertainty in the mean is of primary importance; the details of the histogram are of second order importance compared to the mean.

Uncertainty in the variogram is sometimes considered; however, it is also of second order importance. Uncertainty in the mean of each parameter was quantified with the three techniques mentioned above. The results of uncertainty in HIIP distribution with/without parameter uncertainty were analyzed and assessed to show the importance of accounting for parameter uncertainty in estimating HIIP and choose the optimum technique for quantifying full uncertainties in HIIP with parameter uncertainty for this case study.

Techniques used in this research were described how they work, what variables to be used with, and how to be implemented with/without parameter uncertainty. There were three main techniques used to quantify uncertainty in the variables of interest. The techniques are conditional Sequential Gaussian Simulation (SGS), Monte Carlo Simulation (MCS), and cosimulation with super secondary data; while MVPU technique was used in assessing HIIP with parameter uncertainty in all variables of interest.

Reservoir scenario defined by the reference top and bottom surfaces is only one possible estimate of the reality. Although this scenario matches the reality at well locations, there might be uncertainties in the area away from the well locations. Therefore, estimating HIIP cannot be treated as unambiguous results. Conditional SGS is the best choice to simulate different realizations quantifying the uncertainty in the structural surfaces parameters.

A cosimulation technique with super secondary data was used to quantify the uncertainty in petrophysical properties such as NTG, ϕ , and Sw because these parameters had some relationship with thickness and a relation between each other. Many realizations of those petrophysical properties were generated simultaneously by using this technique.

The Multivariate Parameter Uncertainty technique is a stochastic approach that was used to quantify full uncertainty HIIP with parameter uncertainty. It is

based on incorporating the correlation coefficients among variables of interest to determine the means of parameter uncertainty to eliminate the aggregation problem.

There are a lot of parameters that play key factors in reserve estimations. The parameters and their sources should be known to do more investigations in order to reduce uncertainties. First sensitivity analysis was to investigate the orders of the parameters affecting HIIP uncertainty from the most effective parameter to the least effective one in all seven scenarios, without parameter uncertainty, with parameter uncertainty using BS, SBS, and CFD approaches with low and high variogram ranges each. Quantifying the uncertainty in HIIP without parameter uncertainty was more sensitive to structural surfaces parameters, then petrophysical properties, and last to the OWC. The other six scenarios quantifying the uncertainty in HIIP with parameter uncertainty were more sensitive to petrophysical properties, then structural surfaces parameters, and last to the OWC. In addition, the order of the parameters in the six scenarios quantifying the uncertainty in HIIP with parameter uncertainty was almost the same except the porosity of H1 and H2 layers that were exchanged in those six scenarios because their effects on the HIIP uncertainty were almost close to each other.

The standard deviations of the HIIP distributions obtained from using parameter uncertainty approaches were positively correlated to the standard deviations of the parameter uncertainty distributions used.

By comparing the cumulative distribution frequencies of HIIP with full uncertainty, the results of using BS approach had more uncertainty in the HIIP estimates compared to those results without parameter uncertainty. The problem of using BS approach was to ignore the spatial correlation between the data. Therefore, SBS approach was used to consider the spatial correlation between the data, but its results had more uncertainty in the HIIP distributions than those results obtained from using all other approaches. The CFD approach considered

the correlation between the input data and the conditioning data, so it should be more realistic; even though, it is not such well known and popular as SBS approach. The disadvantage of using the CFD is the significant time required to generate a parameter uncertainty that might reach to a few hours depending on the input data and the CPU.

A comparison between 2-D modeling with BS approach and 0-D modeling with thickness data obtained from either seismic or well logs was conducted. The 0-D modeling overestimated the HIIP volumes especially the scenario that used thickness obtained from well logs. Using seismic data for thickness in 0-D modeling reduced the overestimating of HIIP compared to the results obtained from 2-D modeling. One of the disadvantages of using 0-D modeling is that it can not be checked, while 2-D is based on geological mapping and can be checked locally. The better the local HIIP estimates are, the more confidence the global results have. But sometimes in early stages of a reservoir life, there is no choice but to use 0-D modeling to estimate the resource volumes due to short time to make some quick decisions and/or unavailable data to apply different modeling scale.

The parameter uncertainty in the thickness of H1 layer was quantified using 3-D modeling. The results using 3-D modeling was much narrower than that obtained from using 2-D modeling. The CPU time required to quantify the parameter uncertainty using 3-D modeling and the memory allocation needed for previously simulated nodes are significantly more than those required for quantifying parameter uncertainty using parameter uncertainty approaches and 2-D modeling. A complete study quantifying uncertainty in HIIP with full uncertainty and using 3-D models will need really a huge computer memory in order to store the simulation realizations for so the variables of interest.

8.2 Future Work

There is some additional work that may be considered in the development of geostatistical techniques that allow for the improved integration of assessing uncertainty in resource/reserve volumes estimations. The following are some ideas for future research in points:

- Effects of increasing number of wells can be investigated by increasing it in steps to evaluate the effects of increasing available data on HIIP uncertainty.
- Different standard deviation values should be used in the undulation generation for the top and bottom surfaces and layers thickness to assess the sensitivity of HIIP volumes with the standard deviation of the uncertainty in the structural parameters.
- Uncertainty in fluid contact levels was assessed by changing the mode in each realization, while its uncertainty can be assessed by varying the limits with the mode in each realization or assuming different distribution shape. It depends on the available data.
- Formation volume and recovery factors can be added to the evaluation to estimate stock tank HIIP and recoverable reserves.
- A complete study often studies the effects of 20 to 30 variables. Hydrocarbon resources or reserves are calculated as a combination of these variables. In this research, only few geologic factors and petrophysical properties were considered, even though the procedure might be extended to study the effects of other parameters such as other geologic factors, economic conditions, and engineering conditions.

Bibliography

Abrahamsen, P.; Hauge, R.; Hegglund, Knut; and Mostad, Petter (1998) Uncertain Cap Rock Geometry, Spill Point, Gross Rock Volume. Paper SPE-49286 was prepared to be presented at the SPE Annual Technical Conference.

Babak, O. and Deutsch, C.V. (2006) A Conditional Finite-Domain (CFD) Approach to Parameter Uncertainty. 8th Annual CCG Meeting.

Babak, O. and Deutsch, C.V. (2007) Merging Multiple Secondary Data for Collocated Cokriging (recall of super secondary variable). 9th Annual CCG Meeting.

Behrenbruch, P.; Turner, G.J.; and Bachhouse, A.R. (1985, Sep.10-15) Probabilistic Hydrocarbon Reserves Estimation: A Novel Monte Carlo Approach. Paper SPE 13982 presented at Offshore Europe 1985, Aberdeen.

Berteig, V.; Halvorsen, K.B.; More, H.; Hof., A.K.; Jorde, K.; and Steinle, O.A. (1988, Oct.2-5) Prediction of Hydrocarbon Pore Volume With Uncertainties. Paper SPE 18325 was prepared to be presented at the 63rd Annual Technical Conference and Exhibition of the SPE held in Houston, TX.

Deutsch, Clayton V. (2002) Geostatistical Reservoir Modeling. *Oxford University Press*, New York.

Deutsch, Clayton V. (2004) A Statistical Resampling Program for Correlated Data: Spatial_Bootstrap. 6th Annual CCG Meeting.

Deutsch, Clayton V. and Cullick, A.S. (2002) Short Note: MultiGaussian Model for Uncertainty in a Non-Spatial Context. 4th Annual CCG Meeting.

Deutsch, Clayton V. and Journel, A.G. (1998) GSLIB: Geostatistical Software Library: and User's Guide. *Oxford University Press*, New York, 2nd Ed.

Deutsch, Clayton V. and Zanon, Stefan (2002) UltimateSGSIM: Non-Stationary Sequential GaussianCosimulation by Rock Type. 4th Annual CCG Meeting.

Efron, B. (1979) Bootstrap Methods: Another Look at The Jackknife. *The Annals of Statistics*, Vol. 7, No. 1, p. 1-26.

Etherington, John; Pollen, Torbjorn; and Zuccolo, Luca (Mapping Subcommittee) (2005, December) Oil and Gas Reserves Committee (OGRC): Comparison of Selected Reserves and Resources Classifications and Associated Definitions. www.spe.org.

Garb, Forrest A. (1988, June) Assessing Risk in Estimating Hydrocarbon Reserves and in Evaluating Hydrocarbon-Producing Properties. *Journal of Petroleum Technology*. Also as SPE paper 15921.

Gringarten, E. and Deutsch, C.V. (1999) Methodology for Improved Variogram Interpretation and Modeling for Petroleum Reservoir Characterization. 1st Annual CCG Meeting.

Hall, P. (1985) Resampling A Coverage Pattern. *Stochastic Processes and Their Applications*, 20, 231-246.

Hall, P.; Horowitz, J.L.; and Jing, B. (1995) On Blocking Rules for the Block Bootstrap with Dependent Data. *Biometric*, 82, 561-574.

Jornel, A.G. (1993) Resampling from stochastic simulations. *Environmental and Ecological Statistics*, 1:63-83.

Kunsch, H.R. (1989) The Jackknife and The Bootstrap for General Stationary Observations. *Annals of Statistics*, 17, p. 1217-1261.

Liu, R.Y. and Singh, K. (1992) Moving Blocks Jackknife and Bootstrap Capture Weak Dependence. In Exploring the Limits of Bootstrap (R. Lepage and L. Billard, eds.) 225-248. *John Wiley*, New York.

McLennan, Jason A. (2004) Using the Variogram to Establish the Stratigraphic Correlation Structure. 6th Annual CCG Meeting.

Mishra, S. (1996, Sep.27-30) Alternatives to Monte-Carlo Simulation for Probabilistic Reserves Estimation and Production Forecasting. SPE-49313 was prepared for presentation at the SPE Annual Technical Conference and Exhibition held in New Orleans, Louisiana.

Murtha, J.A. (1997, April) Monte Carlo Simulation: Its Status and Future. *Journal of Petroleum Technology*, 361. Also presented as paper SPE 37932 at the SPE Annual Technical Conference and Exhibition, San Antonio, Oct. 5-8; 1997.

Neufeld, Chad and Deutsch, Clayton V. (2006) A Short Note on Fixing the Correlation Matrix. 8th Annual CCG Meeting.

Neufeld, Chad and Deutsch, Clayton V. (2007) CCG Software Catalogue. 9th Annual CCG Meeting.

Neufeld, Chad and Leuangthong, Oy (2005) Recoverable Reserves. 7th Annual CCG Meeting.

Norris, R.; Massonat, G.; and Alabert, F. (1993) Early Quantification of Uncertainty in the Estimation of Oil-in-Place in a trubidite reservoir. Paper SPE 26490 presented in SPE Annual Technical Conference and Exhibition.

Peng, Cheong Y. and Gupta, R. (2003, Sep.9-11) Experimental Design and Analysis Methods for Assessing Volumetric Uncertainties. Paper SPE 80537 was first presented at the 2003 SPE Asia Pacific Oil and Gas Conference and Exhibition, Jakarta, Indonesia.

Ren, Weishan; Leuangthong, Oy; and Deutsch, Clayton V. (2004) Geostatistical Reservoir Characterization of McMurray Formation by 2-D Modeling. 6th Annual CCG Meeting.

Samson, P.; Dubrule, O.; and Euler, N. (1996, Apr.16-17) Quantifying the Impact of Structural Uncertainties on Gross-Rock Volume Estimates. Paper SPE 35535 was prepared to be presented at the European 3-D Reservoir Modeling Conference held in Stavanger, Norway.

Solow, A.R. (1985) Bootstrapping Correlated Data. *Journal of the International Association for Mathematical Geology*, 17, p. 769-775.

Wilde, Brandon and Deutsch, Clayton V. (2005) A New Approach to Calculate a Robust Variogram for Volume Variance Calculations and Kriging. 7th Annual CCG Meeting.

Xie, YuLong and Deutsch, Clayton (1999) A Short Note on Surface-Based Modelling for Integration of Stratigraphic Data in Geostatistical Reservoir Models. 1st Annual CCG Meeting.

Zanon, Stefan and leuangthong, Oy (2003) Selected Implementation Issues with Sequential Gaussian Simulation. 5th Annual CCG Meeting.

Appendix A

DOCUMENTATION

GSLIB software package (Deutsch and Journel, 1998) is used for the preparation of the research. There are some new GSLIB-type FORTRAN programs created for the techniques developed in this dissertation including *OOIP* to calculate hydrocarbon initially-in-place (HIIP) with full uncertainty in all parameters of interest, *input_mp* to calculate the values of the parameter means, *shift_pdf* to shift any original reference distribution to a new mean, and *combine_1col* to combine multiple columns from multiple files into one column. This appendix documents those programs created for quantifying uncertainty in HIIP with parameter uncertainty. Their parameter files were presented as an example then described. The source codes are not listed because of length considerations.

The first program *OOIP* is to calculate hydrocarbon initially-in-place with uncertainty in one/multi parameter(s). The program takes the realizations generated for parameters of interest to calculate HIIP for each grid (in details) and realization (in brief). The second program *input_mp* is to calculate the values of the parameter means. It draws parameter means with equal probability distance between the data. The third program *shift_pdf* is used to shift any distribution to a new mean using a multiplication or addition approach. The fourth program *combine_1col* is to combine the data from multiple columns from multiple files into one column. Any number of columns can be read from any number of files. This program was required to combine the realizations of any parameter of interest into one file when generating these realizations had to be conducted in separate runs.

Parameters for OOIP

```

Line  START OF PARAMETERS:
1     OOIP.out           -file with output data
2     OOIP_details.out  -file with detail output data
3     100                - number of realizations
4     50 0.5 1.0        - nx,xmn,xsiz
5     50 0.5 1.0        - ny,ymn,ysiz
6     seismic.dat       -file for seismic data
7     3 4                - columns of top and bottom surface data
8     -1.0 1.0e21      - trimming limits
9
10    START OF PARAMETERS (Top Structure Uncertainty):
11    1                  - consider uncertainty in Top Surface data (0=no,1=yes)
12    2000.0 15.0       - mean and standard deviation for Top Surface means if yes
13    Top_PU_means.dat  - PU file for Top/Bottom Structure in normal scored values
14    1                  - column no. for PU means of top/bottom surfaces
15    1                  - Standard Deviation in original Top Surface data (if yes)
16    1                  - Standard Deviation of Uncertainty in Top Surface means (if yes)
17    TopUncertainty.dat -file for uncertainty in Top Surface data (if yes)
18    1                  - column no. for uncertainty in top and bottom surfaces
19
20    START OF PARAMETERS (Thickness Uncertainty):
21    0                  - consider uncertainty in Thickness (0=no,1=yes)
22    20.0 3.0          - mean and standard deviation for Thickness means if yes
23    Thick_PU_means.dat - PU file for Thickness in normal scored values
24    1                  - column no. for PU means of thickness
25    1                  - Standard Deviation in original Thickness data (if yes)
26    1                  - Standard Deviation of Uncertainty in Thickness means (if yes)
27    ThicknessUncertainty.dat -file for uncertainty in Thickness (if yes)
28    1                  - column no. for uncertainty in thickness
29
30    START OF PARAMETERS (OWC Uncertainty):
31    0                  - =iOWC, consider uncertainty in OWC (0=no,1=yes)
32    2000               - OWC level (if no)
33    OWCUncertainty.dat -file for uncertainty in OWC, (if yes)
34    1                  - column no. for uncertainty in OWC
35
36    START OF PARAMETERS (NTG Uncertainty):
37    0                  - =iNTG, consider uncertainty in NTG (0=no,1=yes)
38    1                  - specify realization no. to be used, if iNTG=0
39    NTGUncertainty.dat -file for NTG realizations
40    1                  - column no. for uncertainty in NTG
41
42    START OF PARAMETERS (Porosity Uncertainty):
43    0                  - =iporo, consider uncertainty in Porosity (0=no,1=yes)
44    1                  - specify realization no. to be used, if iporo=0
45    PoroUncertainty.dat -file for Porosity realizations
46    1                  - column no. for uncertainty in Porosity
47
48    START OF PARAMETERS (Sw Uncertainty):
49    0                  - =iSw, consider uncertainty in Sw (0=no,1=yes)
50    1                  - specify realization no. to be used, if iSw=0
51    SwUncertainty.dat  -file for Water Saturation realizations
52    1                  - column no. for uncertainty in Sw
  
```

Figure A-1: An example parameter file for OOIP program.

Figure A-1 presents an example of the parameter file for *OOIP* program. The output files are specified on **Lines 1 and 2**. The first file gives the HIIP for all realizations and the second file gives more details output by listing all parameter values including HIIP for all grids in all realizations. The number of realizations is given on **Line 3**. The grid definition is given on **Lines 4 and 5**. The input file for seismic data is specified on **Line 6**. The column numbers for the top and bottom surface data are given on **Line 7**. The trimming limits are given on **Line 8** for the data of the top and bottom surface depths.

Parameters required for uncertainty in top structure start on **Line 10**. **Line 11** gives the option to consider the uncertainty in top and bottom surfaces (0 for no and 1 for yes). If the value is 1, then **Lines 12 to 18** become active. The mean and standard deviation for top surface using a parameter uncertainty approach such as BS, SBS, or CFD are specified on **Line 12**. The input file for the means of the uncertainty realizations in the top and bottom surfaces in normal score values is specified on **Line 13**. The column number for the mean values is given on **Line 14**. The standard deviation of the original data is given on **Line 15**. The standard deviation in the uncertainty realizations is given on **Line 16**. The input file with uncertainty realizations obtained from conditional SGS is specified on **Line 17**. The column number for the uncertainty realizations is given on **Line 18**.

Parameters required for uncertainty in thickness start on **Line 20**. **Line 21** gives the option to consider the uncertainty in thickness (0 for no and 1 for yes). If the value is 1, then **Lines 22 to 28** become active. The mean and standard deviation for thickness using a parameter uncertainty approach are specified on **Line 22**. The input file for the means of the uncertainty realizations in the thickness in normal score values is specified on **Line 23**. The column number for the mean values is given on **Line 24**. The standard deviation of the original data is given on **Line 25**. The standard deviation in the uncertainty realizations is given on **Line 26**. The input file with uncertainty realizations obtained from conditional

SGS is specified on **Line 27**. The column number for the uncertainty realizations is given on **Line 28**.

Parameters required for uncertainty in OWC start on **Line 30**. **Line 31** gives the option to consider the uncertainty in OWC ($i\text{OWC} = 0$ for no and 1 for yes). If $i\text{OWC}$ is 0, **Line 32** becomes active to give the OWC level. If $i\text{OWC}$ is 1, **Lines 33 and 34** become active. The file for the uncertainty in OWC is specified on **Line 33**. The column number for uncertainty realizations in OWC is given on **Line 34**.

Parameters required for uncertainty in NTG start on **Line 36**. **Line 37** gives the option to consider the uncertainty in NTG. ($i\text{NTG} = 0$ for no and 1 for yes). If $i\text{NTG}$ is 0, **Line 38** becomes active to give the realization number required to be used in calculating all OOIP realizations. The file for the NTG realization(s) is specified on **Line 39**. The column number for NTG realizations is given on **Line 40**.

Parameters required for uncertainty in porosity start on **Line 42**. **Line 43** gives the option to consider the uncertainty in porosity. ($i\text{poro} = 0$ for no and 1 for yes). If $i\text{poro}$ is 0, **Line 44** becomes active to give the realization number required to be used in calculating all OOIP realizations. The file for the porosity realization(s) is specified on **Line 45**. The column number for porosity realizations is given on **Line 46**.

Parameters required for uncertainty in water saturation start on **Line 48**. **Line 49** gives the option to consider the uncertainty in porosity. ($i\text{poro} = 0$ for no and 1 for yes). If $i\text{Sw}$ is 0, **Line 50** becomes active to give the realization number required to be used in calculating all HIIP realizations. The file for the Sw realization(s) is specified on **Line 51**. The column number for Sw realizations is given on **Line 52**.

```

Parameters for Input_mp
*****

Line  START OF PARAMETERS:
1   Top_PU.dat      -file with output data
2   100             - number of realizations
3   18.8           - Standard Deviation of parameter means
4   83.4           - Standard Deviation of original data

```

Figure A-2: An example parameter file for *input_mp* program.

Figure A-2 presents an example of the parameter file for *input_mp* program. The output file is specified on **Line 1**. The number of realizations is given on **Line 2**. The standard deviation obtained from parameter uncertainty approach is given on **Line 3**. The standard deviation obtained from parameter original data is given on **Line 4**.

```

Parameters for shifting distribution
*****

Line      START OF PARAMETERS:
1         ../data/input.dat    - file with input data
2         shift_pdf.out       - file with output data
3         shift_pdf.dbg       - file for debugging output
4         1                   - column for variable
5         100                 - number of data
6         -900.0  1.0e21      - trimming limits
7         50.0                - targeted parameter mean
8         1                   - use shifting approach: 1=Multiplying or 2=Adding

```

Figure A-3: An example parameter file for *shift_pdf* program.

Figure A-3 presents an example of the parameter file for *shift_pdf* program. The input file is specified on **Line 1**. The output file is specified on **Line 2**. The debugging file output is specified on **Line 3**. The column number of the input data needed to be shifted on **Line 4**. The number of data is given on **Line 5**. The trimming limits for the data are given on **Line 6**. The new mean, that the data mean has to be shifted to, is given on **Line 7**. **Line 8** is to specify the approach

option that will be used to shift the data (1 for multiplying approach or 2 for adding approach).

```
Parameters for COMBINE
*****

Line  START OF PARAMETERS:
1  combine.out      -file for output
2  4                - number of columns to be combined
3  firstfile.dat   -first file
4  1                - column of interest
5  secondfile.dat  -second file
6  1                - column of interest
7  secondfile.dat  -third file
8  2                - column of interest
9  thirdfile.dat   -fourth file
10 1                - column of interest
```

Figure A-4: An example parameter file for *combine_1col* program.

Figure A-4 presents an example of the parameter file for *combine_1col* program. The output file is specified on **Line 1**. The number of columns needed to be combined in one is given on **Line 2**. The name of the input file for the first column to be combined is specified on **Line 3**. The column number of the first data needed to be combined in one column is given on **Line 4**. The name of the input file for the second column to be combined is specified on **Line 5**. The column number of the second data needed to be combined in one column is given on **Line 6**. The name of the input file for the third column to be combined is specified on **Line 7**. The column number of the third data needed to be combined in one column is given on **Line 8**. The name of the input file for the fourth column to be combined is specified on **Line 9**. The column number of the fourth data needed to be combined in one column is given on **Line 10**.

Appendix B

ALPHABETICAL LISTING OF PROGRAMS USED

backtr	normal scores back transformation
boot_avg	Bootstrap resampling for the average
combine_1col	combines as many columns from different files into one column
correlate	correlates random values based on input correlation coefficients
corrmat	generates correlation coefficients matrix
corrmat_plot	PostScript plot of corrmat
gamv2004	computes variograms of irregularly spaced data
histplt	Postscript plot of histogram with statistics
input_mp	Draw values from parameter uncertainty distribution based on equally distanced probabilities
manip	Manipulate columns
mcs	Monte Carlo simulation
nscore	Normal scores transformation
OOIP	Calculate hydrocarbon initially-in-place with parameter uncertainty
plotem	Combine PostScript plots onto a single page
quantile	Calculate quantiles/CDF from non-parametric distribution
scatplt	Postscript plot of scattergram with statistics
sgsim	sequential Gaussian simulation

sgsim00	Conditional finite domain
shift_pdf	Shift probability distribution to a new targeted mean
spatial_bootstrap	Spatial bootstrap resampling for the average
vargplt	PostScript plot of variogram
ultimatesgsim	Ultimate sGs
vmodel	variogram file from model

Appendix C

ACRONYMS AND NOTATIONS

A	Area
a	range parameter
a_v	range parameter in the vertical direction
a_{h1}	range parameter in the major horizontal direction
a_{h2}	range parameter in the minor horizontal direction
Bo	Formation volume factor
BS	Bootstrap
CFD	Conditional Finite Domain
CIM	Canadian Institute of Mining
Cov	covariance
CPU	Central processing unit
D	Dimensions
Fz	Cumulative distribution function of a random variable Z
Fz^{-1}	Inverse cumulative distribution function
GOC	Gas oil contact

GRV	Gross rock volume
GWC	Gas water contact
h	Thickness
HIIP	Hydrocarbon initially in place
K	Number of data combinations
k	order of uncertainty
L	Number of Realizations
LU	Lower and upper triangular matrices
Max.	Maximum
MCS	Monte Carlo Simulation
Min.	Minimum
MVPU	Multivariate Parameter Uncertainty
m_p^l	l th realization of parameter mean
m_o	Parameter mean for the original data
m_z	Experimental mean
n	Number of data
NP	Net Pay
NTG	Net-to-Gross
OWC	Oil Water Contact

P	Probability
PU	Parameter uncertainty
PVT	Pressure, volume, and temperature
SBS	Spatial Bootstrap
SGS	Sequential Gaussian simulation
SPE	Society of Petroleum Engineers
sph	spherical equation
So	Oil saturation
Sw	Average water saturation
Swi	Connate water saturation
TD	Time-to-depth
TI	Time interpretation
u	Location vector in A
Y	Transform function
$y^l(\mathbf{u})$	l th realization of variable y at location \mathbf{u} .
Z	generic random variable
$z_b(\mathbf{u})$	depth from the base structure at location \mathbf{u} .
$\Delta^l(\mathbf{u})$	l th realization of Uncertainty at location \mathbf{u} .

σ	Standard deviation
σ_o	Standard deviation of the original data
σ_{Δ}	Standard deviation in uncertainty
σ_{TI}	Standard deviation in time interpretation
σ_{Δ}	Standard deviation in time-to-depth
ϕ	Average porosity
$\gamma(\mathbf{h})$	Stationary semivariogram between any two random variables $Z(\mathbf{u})$ and $Z(\mathbf{u}+\mathbf{h})$ separated by lag vector \mathbf{h} .